

ANNUAL RESEARCH REPORT

2022-2023



Programme Leader
Dr. M.A. Monayem Miah, cse



Bangladesh Agricultural Research Institute
Agricultural Statistics and ICT Division
Gazipur 1701

October 2023

ANNUAL RESEARCH REPORT 2022-2023

Programme Leader

Dr. M. A. Monayem Miah
Chief Scientific Officer & Head



Agricultural Statistics and ICT Division
Bangladesh Agricultural Research Institute
Gazipur-1701

October 2023

Annual Research Report 2022-23

Compiled & Edited by

Dr. M. A. Monayem Miah, CSO & Head
MohammadMukhlesur Rahman, SO
Nur Mohammad, SO
Dr. ZobaerAkond, SO
Kazi Saidur Rahman, SO
Istiak Ahmed, SO



Agricultural Statistics and ICT Division
Bangladesh Agricultural Research Institute
Gazipur-1701, Bangladesh

How to cite

Agricultural Statistics and ICT Division (2023). *Annual Research Report 2022-2023*. Bangladesh Agricultural Research Institute, Gazipur-1701.

© Agricultural Statistics and ICT Division, Bangladesh Agricultural Research Institute, Gazipur-1701

All rights are reserved. No part of this publication may be reproduced or transmitted in any form or by any means without prior permission in writing from the publisher. Any person who does any unauthorized act in relation to this publication may be liable to criminal prosecution and civil claims for damages.

Editorial Committee

Dr. M. A. Monayem Miah, CSO & Head
MohammadMukhlesur Rahman, SO
Nur Mohammad, SO
Dr. ZobaerAkond, SO
Kazi Saidur Rahman, SO
Istiaq Ahmed, SO

Compilation

Dr. M. A. Monayem Miah, CSO & Head
Nur Mohammad, SO

Cover Design

MohammadMukhlesur Rahman, SO
Nur Mohammad, SO
Istiaq Ahmed, SO

Published by

Dr. M. A. Monayem Miah
Chief Scientific Officer & Head
Agricultural Statistics and ICT Division
Bangladesh Agricultural Research Institute,
Gazipur-1701, Phone: +88-0249270129
E-mail: csو.asict@bari.gov.bd
Website: www.bari.gov.bd
www.baripmis.org/web/asict

Published on

October 2023

List of Contributors

Dr. M. A. Monayem Miah, CSO & Head
MohammadMukhlesur Rahman, SO
Nur Mohammad, SO
Dr. ZobaerAkond, SO
Kazi Saidur Rahman, SO
Istiak Ahmed, SO
Mohammad Rasel, SO
Jamila Khatun Prioty, SO
Md. Shakil Hossain, SO

PREFACE

The application of Information and Communications Technology (ICT) in agriculture is increasingly becoming important. The ICT revolution has brought huge implications for both social and economic development in the world and obviously in Bangladesh as well. The use of ICT in agriculture ranges from advanced modern technologies, such as GPS navigation, satellite communication, earth observation satellites (EOSs), unmanned aerial vehicles (UAVs), agricultural robots, internet of things (IoTs), data science, machine learning, cloud computing, and mobile & web-based apps to older technologies such as radio and television. However, the stakeholders still lack basic communication infrastructure in accessing crucial information to make timely decisions. The application of ICT in agriculture generates possibilities to resolve problems of stakeholders and also to promote agricultural production by providing scientific information timely and directly to farmers.

The importance of ICT was rightly recognized by BARI and a dedicated cell was constituted with competent scientists from different disciplines. Later, the Agricultural Statistics section was separated from the Agricultural Economics Division and renamed as the Agricultural Statistics and ICT (ASICT) section to take overall responsibilities of the ICT Cell. Finally, ASICT Division evolved in 2012 through the implementation of the project entitled “strengthening of information and communication technology (ICT) and biometrical facilities at BARI”.

ASICT Division has been active both in support services and research dimensions since its inception. For ICT service and modern ICT-related research and development, the ASICT division is maintaining partial network connectivity, e-governance, e-agricultural, and different laboratories (MIS Lab, biometry lab, etc.) to ensure clients’ (scientists and end-users) services. The agro-environmental remote sensing and modeling (ARSAM) laboratory of this division is performing applied research to harness the power of modern remote sensing and geospatial technologies in promoting sustainable cropping intensification. The award-winning BARI mobile and interactive web application কৃষিক্ষেত্রিকিডাওয়ার has been playing a vital role in disseminating modern agricultural technologies to the doorsteps of farmers. GeoMango, a semi-automated satellite-based mango orchard mapping system for the greater Rajshahi region developed at ARSAM Lab shows the power and potential of satellite-based crop mapping and monitoring opportunities for Bangladesh.

Indeed, I am happy to see that the Annual Research Report 2022-23 of the ASICT Division has been published. This report covers the activities of research, outreach, and ICT services rendered inside BARI and to other stakeholders.

I gratefully acknowledge the contribution of all the scientists and staff in conducting research and other activities and successfully preparing the report.

Dr. M. A. Monayem Miah

Chief Scientific Officer and Head
Agricultural Statistics and ICT Division

Contents

Sl. No.	Topics	Page No.
Research Report 2022-23		
1.	Assessment of Rabi crops for sustainable intensification in drought-prone ecosystem using remote sensing and geospatial modeling	1
2.	Growth and instability analysis in area and production of major pulses in Bangladesh	44
3.	Forecasting onion yield by using satellite-based remote sensing technique in Bangladesh	67
4.	Yield prediction of mustard crop by using satellite based remote sensing technique in Bangladesh	82
5.	Potato yield forecasting using satellite images and crop simulation model under changing climate	94
6.	Bioinformatic analysis of Dicer-like (DCL), Argonaute (AGO), and RNA-dependent RNA polymerase (RDR) genes and their associated regulatory elements in brassica species (<i>Brassica Rapa L.</i>)	108
7.	Development of online-based BARI vehicle management and requisition system	126
Services Report 2022-23		
	Services of the Agricultural Statistics and Information & Communication Technology Division 2022-2023	133
1.	<i>Self-evaluated annual report of APA work plan 2022-23</i>	140
	<i>Appendix I: Scientists Working at ASICT Division 2022-2023</i>	143
	<i>Appendix II: Supporting Staff Working at ASICT Division 2022-2023</i>	143
	<i>Appendix III: Labour Working at ASICT Division 2022-2023</i>	143
	<i>Appendix IV: List of Publications 2022-2023</i>	144
	<i>Appendix IV: Rapporteur's Report</i>	145

Agricultural Statistics and Information & Communication Technology (ASICT) Division at a Glance

The ASICT division initially served as a Statistical Section of the Agricultural Economics Division of Bangladesh Agricultural Research Institute (BARI) since 2007. Afterward, the section worked as a new name titled “Information and Communication Technology (ICT) section under the Training and Communication Wing up to February 18, 2008. Once more, BARI authority changed this section to Agricultural Statistics and Information & Communication Technology (ASICT) Section by issuing an order on 19th February 2008. Finally, the ASICT section had been updated to a new division as per the decision of the 49th Board of Management meeting of BARI on 9th April 2012. Currently, the division performs its activities under the Training and Communication Wing of BARI.

ASICT division comprises two parts: Agricultural Statistics and ICT. The division is headed by a Chief Scientific Officer (CSO) who is assisted by a number of Senior Scientific Officers (SSO), Scientific Officers (SO), System Analyst, Programmer, Assistant Programmer, Assistant Maintenance Engineer, and supporting staff. Concerned scientists of both parts conduct different types of researches relevant to Agricultural Statistics and ICT. In addition, the scientists of both parts are providing agricultural statistics and ICT-related support services to BARI scientists in order to facilitate agricultural research and development. However, ASICT is constantly keeping its vital role for BARI as a whole.

ASSESSMENT OF RABI CROPS FOR SUSTAINABLE INTENSIFICATION IN DROUGHT-PRONE ECOSYSTEMS USING REMOTE SENSING AND GEOSPATIAL MODELING

MOHAMMAD MUKHLESUR RAHMAN¹, DR. MD. GOLAM MAHBOOB², DR. AFM TARIQUL ISLAM², MD. HASNAIN AHMED¹, MD. HASAN RASHID¹, SADIQ MUBASHSIR KHAN¹, SUMAN BISWAS³

¹ASICT DIVISION, BARI, GAZIPUR 1701, BANGLADESH

²BANGLADESH AGRICULTURAL RESEARCH COUNCIL (BARC), DHAKA 1215, BANGLADESH

³DEPARTMENT OF STATISTIC, ISLAMIC UNIVERSITY, KUSHTIA, BANGLADESH

Abstract

Bangladesh Government has given high priority to sustaining groundwater use for irrigation. Hence, it is important to conduct agricultural land use and cropping patterns analysis and their implication to foster sustainable intensification (SI) strategies in the drought-prone regions of Bangladesh. Remote sensing and geospatial modeling can play a vital role to assess the cropping patterns and availability of natural resources on the ground and allocate them to the judiciary for SI in agriculture. Geospatial modeling can help allocate an appropriate cropping pattern based on the best judicial use of available natural resources. Hence, to facilitate sustainable cropping intensification in the agro-environments of Bangladesh, the current research project has been initiated to carry out in the drought-prone agro-ecosystems prevailing in the Barind Tract region of Bangladesh. During the project period (2018-2023), a total of seven extensive surveys were conducted for collecting necessary ground data from the study area. These reference data were pre-processed in the GIS domain and split into 70:30 ratios to train and validate the algorithms for crop type mapping. A crop inventory for the entire Barind Tract region was prepared in previous years according to the methodological framework. Six major crop types, predominant in the area, were chosen for delineation from satellite image classification namely: maize, lentil, mustard, potato, Boro rice, and wheat. Sentinel-2A images were collected through Google Earth Engine during the dry months (Oct-Mar) of each cropping season. Although the cloud was masked out, these images were filtered to ensure the cloud percent was less than or equal to 20 percent. After resampling all the bands into 10 meters, visible, NIR, Red edge, and short-wave IR bands were used to classify crop types along with two vegetation indices NDVI and EVI. Seasonal composite (Oct-Mar) of these bands and indices were derived in GEE based on median statistics. Three machine learning algorithms (Random Forest, CART, and Support Vector Machine) along with different band combinations were experimented with during this reporting period to improve the classification algorithm. Among several experimental trials, Random Forest with scheme 5 band combinations was found to be the best model to classify the crop type of the study area. The classification result showed that the area covered by rice, 22253.46 ha (45.17%), was relatively better than other classified crop fields initially during 2020-21 cropping season, but over time it gradually dropped and replaced with significant portion of the maize field which occupied 2296.02 ha (9.31%), 6033 ha (12.38%), and 13247 ha (26.89%) during 2020-21, 2021-22, 2022-23 cropping season accordingly. Concerning the reference data, the overall accuracy and Kappa coefficient of the classified map were found to be around 86%, 91% and 89%, and 0.81, 0.89, and 0.86 during the 2020-21, 2021-22, 2022-23 cropping season accordingly indicating satisfactory results. The F1 score for all crop types was also satisfactory in RF and scheme 5. Area coverage of the classified crop type map was also compared to the DAE area dataset for each cropping season. Besides, a set of agro-environmental resources geo-database was developed including the digital elevation model, slope map, aspect map, soil map, topsoil texture, soil reaction, soil consistency and land type of the Godagari Upazila to be used as input data in further analysis towards achieving final objective location-specific cropping pattern modeling in GIS environment. To obtain sustainable cropping pattern, crops suitability analysis for major rabi crops by integrating Analytic Hierarchy Process (AHP) and geographic information system (GIS) technique with multiple factors, which are initially developed for geo-database development, The highest two crops that occupied S1 (Highly Suitable) class were Wheat with 5243.6 ha (10.67 %) and Potato with 4389.25 ha (8.9%) of the study area. In S2 (Moderately Suitable) class, Wheat with 30304.16 ha (61.71%) and Lentils with 29654.53 ha (60.39%) of the total study area occupied respectively. The lowest suitability areas in the study areas N (Not Suitable) class were occupied by mustard and potatoes, with 8128.52 ha (16.55%) and 6534.55 ha (13.30%), respectively. The results revealed that the integration of Remote sensing, geospatial modeling for crop type mapping, and crop suitability analysis made an appropriate approach for the evaluation of suitable cropping patterns of this area for optimized land use planning

Introduction

Food security is a global concern with rapidly increasing consequences (Wahlqvist *et al.* 2012). Global food demand is projected to increase at least until 2050. The ability to produce sufficient food will be challenged by the increasing competition for land, water, and energy, and will also be affected by the urgent requirement to reduce the impact of the food system on the environment (Godfray *et al.*, 2010). Bangladesh, with a population density of 1,016 people per km² (in 2011) faces a great challenge to ensure food security for its ever-growing population from its shrinking agricultural lands (Mainuddin and Kirby, 2015; Timsina *et al.*, 2018). Sustainable intensification (SI) aims to augment land productivity by increasing resource use efficiency while minimizing environmental trade-offs (Pretty and Bharucha, 2014) and has been proposed as an alternative approach to area expansion (Godfray *et al.*, 2010; Garnett *et al.*, 2013) to ensure food security in Bangladesh (Schulthess *et al.*, 2015; Krupnik *et al.*, 2017). For effective research in unfavorable ecosystems, a systems approach is necessary where new technology must be carefully designed to fit a location-specific combination of climatic, physical, and socioeconomic constraints (Riches *et al.*, 2008).

Barind Tract lies in the driest part of Bangladesh. High and medium highlands of the area used to be largely dependent on rain-fed agriculture that permitted cropping once a year. However, major parts of this region have been turning into year-round multiple cropping areas since the introduction of modern crop varieties and facilities to pump groundwater for irrigation in the late eighties (Fujita and Hossain, 1995). This mass facilitation of tube wells for groundwater pumping for irrigation is credited with such attainment. The northwest region, where 96.5% of groundwater is used for irrigation (Shahid, 2010), is of the greatest concern over falling groundwater levels (Kirby *et al.*, 2013), which leads to a lack of access to water for drinking (Haq, 2013) and irrigation in some areas. The falling groundwater level, within the Barind Tract area in the northwest region, is a result of excessive pumping for irrigation (Kirby *et al.*, 2013). Access to adequate irrigation has the greatest influence on Boro rice yield during the dry season (Bell *et al.*, 2015). Continuous depletion of groundwater levels in the northwestern region has been evident to be an effect of excessive withdrawals for irrigation for dry-season agriculture particularly for irrigated Boro-rice cultivation (Shahid, 2011; Ahmad *et al.*, 2014). The Bangladesh Government has also given high priority to sustaining groundwater use for irrigation in this region. Hence, it is important to conduct agricultural land use and cropping patterns analysis and their implication to foster sustainable intensification strategies in the drought-prone regions of Bangladesh.

Remote sensing and geospatial modeling can play a vital role to assess cropping patterns and the availability of natural resources on the ground and allocate them to the judiciary for SI in agriculture. However, the classification of agricultural lands (crop types) of smallholding farms has been challenging in this region particularly due to their smaller plot sizes and huge variability over time and space. The unavailability of year-round multispectral satellite data due to monsoon cloud coverage is another constraint to analyzing sequential cropping practices or cropping patterns. Free access to historical archived data and recent multi-sensor high spatial and temporal resolution satellite imagery offers an enormous opportunity to analyze historical dry-season and current year-round agricultural practices in this region at a minimal cost. Current advancements in image classification algorithms, free open-source software tools, and increments in high computing performances can be utilized to realize such an opportunity for a developing nation like Bangladesh. A big share of the remote sensing data analysis is involved in collecting reliable ground reference data, which could again be minimized by employing a controlled crowdsourcing approach. Recent provisions of access to high-performance cloud servers (e.g., Google Earth Engine) for large volume (i.e., up to planetary-scale) remote sensing image analysis, offer time and a cost-saving mechanism by providing analytical algorithms and ground-referenced data (Moore and Hansen, 2011; Gorelick, 2012). National agricultural research institutes (e.g., BARI, BRRI) have developed a range of modern crop varieties and technology options (e.g., management practices, farm machinery) for water and other resources conservation which could fit well in area-specific cropping patterns to achieve SI goals in different areas in

the drought and saline-prone ecosystem of Bangladesh. Geospatial modeling can help allocate an appropriate cropping pattern based on the best judicial use of available natural resources. Hence, to facilitate sustainable crop intensification in the problem agro-environments of Bangladesh, the current research project has been proposed to carry out in the drought-prone agro-ecosystems prevailing in the Barind Tract region of Bangladesh. In this study, the dry season cropping pattern has been suggested because this season is the critical season as many irrigated crops are grown in this season and most of the water withdrawal is needed to grow them. Therefore, a multi-year dry-season cropping pattern can assist in planning the sustainable intensification of crop production. Moreover, this season is usually cloud-free, which enables optical sensors to get cloud-free images for cropping pattern mapping.

Crop suitability is the process of determining the appropriateness or ability of a given type of land based on the growing conditions of a specific crop (Singh *et al.*, 2018; Halder, 2013). The suitability analysis for crop production is one of the most important tools for ensuring sustainable agriculture and for attaining the present global food security goal by the Sustainable Development Goals (SDGs) of the United Nations (Akpoti, Kabo-bah and Zwart, 2019). To meet the growing food demands brought on by population growth, environmental contamination, and climate change, agricultural suitability must be determined (Kumbhar *et al.*, 2014; Shaloo *et al.*, 2022). The analysis enables decision-makers to develop a crop management system for increasing land productivity by identifying the main limiting factors of specific crop production. According to the FAO, "suitability is a function of crop requirements and land characteristics, and it is a measure of how well the qualities of a land unit will match the requirements of a particular form of land use" (FAO, 1976). Cropland suitability analysis is required to maximize the use of available land resources for agricultural production sustainably. The best possible use of the available land resources for sustainable agricultural production requires a crop-land suitability analysis. Improving agricultural land management and cropping patterns is very important and urgent in Bangladesh to increase agricultural production with efficient use of land resources (Perveen *et al.*, 2005).

At the moment, Commonwealth Scientific and Industrial Research Organization (CSIRO), Australia is conducting a multi-stakeholder study (Sustainable Development Investment Portfolio, SDIP Phase-II) entitled "Sustaining groundwater irrigation for food security in the Northwest Region of Bangladesh". Scientists involved in this proposed project are also a part of the CSIRO project (SDIP Phase II). Activities of this proposed project can complement the other project (SDIP II) and increase the output in a synergistic way for mutual interests.

Specific objectives

- i.** To develop dry season crop type maps in the study areas using remote sensing image analysis.
- ii.** To develop agro-environmental resources and constraints geo-database from remote sensing image analysis and secondary data acquisition.
- iii.** To suggest location-specific suitable cropping patterns for sustainable intensification by geospatial modeling.

Methodology

Study Area

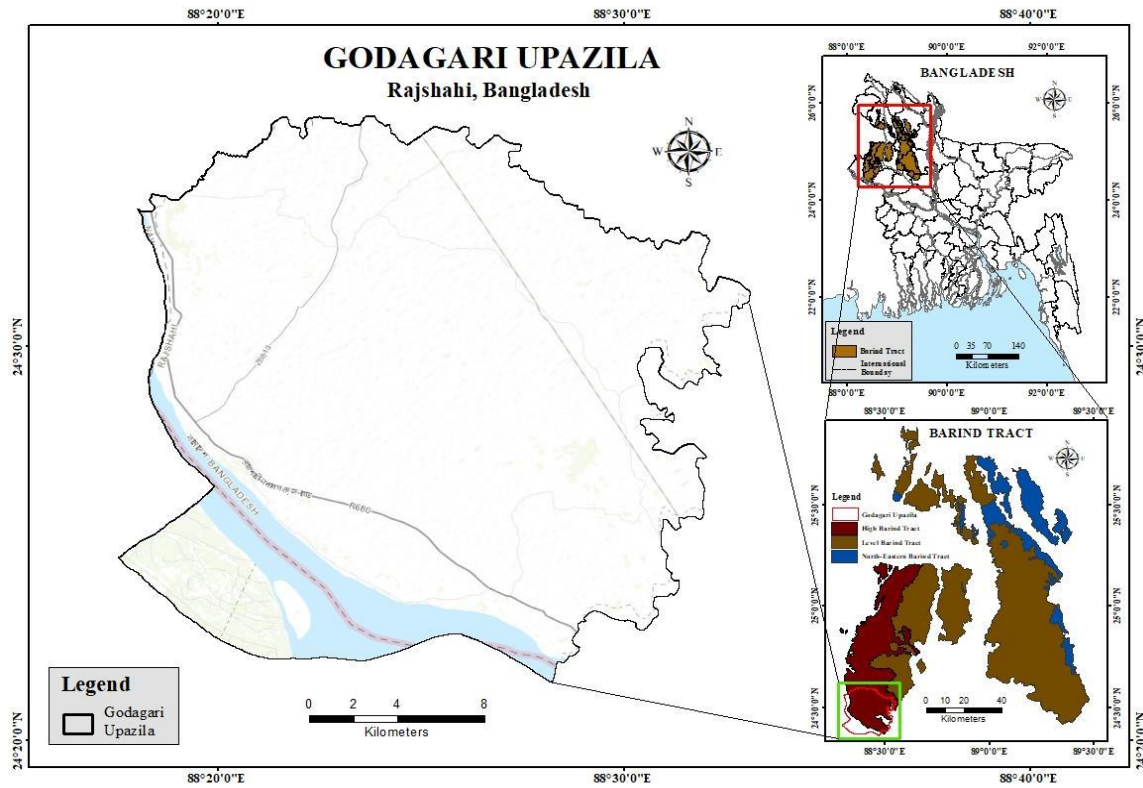


Figure 1. Location of the study area

The project was initiated to carry out in the drought-prone agro-ecosystems prevailing in seven selected Upazilas namely Godagari, Gomastapur, Nachole, Niamatpur, Porsha, Sapahar, and Tanore of High-Barind Tract region under Rajshahi, Chapainawabgonj and Naogaon districts, where the pilot project carried out on Godagari Upazila (Fig. 1) for further detail research. The study area is surrounded by rivers; the Ganges (Padma) in the south, Mohananda in the west, and Sib in the east. The Sib River flows from north to south, and its tributaries form the drainage network of Tanore. The tributaries of Sib River, and partly of Mohananda River mainly drain Godagari Upazilla. The study area comprises various types of lithology components. Within the study area, agricultural land comprises the homestead, natural vegetation, garden, pond, and forest cover; also, agricultural practice varies with the elevation, soil characteristics, water availability, and wide range of crop variety that is also related to the recharge processes. Another factor that influences recharge potentiality is the bund that stores water for a few days in the rainy season and ultimately contributes to water percolation.

Materials

During the project period (April 2018-March 2023), a crop inventory for the entire Barind Tract region was prepared as per the methodological framework. Six major crop types were chosen for classification such as maize, lentil, mustard, potato, Boro rice, and wheat along with another common class namely Others based on collected crop production, agricultural information briefly of Godagari Upazila, open table discussion with Upazila Agricultural Officers (UAOs), Agriculture Extension Officers (AEOs) and Sub-Assistant Agriculture Officer's (SAAOs) and crop inventory.

Table 1. Major crops and their dominant varieties.

S/L	Class Name	Dominant varieties
1	Rice	BRRI- 28 & 63
2	Wheat	BARI Gom 25, 26 & 28
3	Maize	981, Super 45, Pinal 92
4	Lentil	BARI Moshur 4, 6 & 8
5	Mustard	Torry 7/BARI Sharisha 14
6	Potato	Diamant & Asterix
7	Others	Chickpea, Onion, Mixed crop (Malta/Guava/Papaya/ Jujube/Mango/Lichi, etc.), Waterbody, River, Sand, Road, etc.

The characteristics of all seven classes are illustrated in Table 1. Remote sensing data specifications and secondary data specifications both spatial and non-spatial were prepared according to project interest, availability, applicability, suitability, established literature, scientific journals, and expert opinion (Table 2 and Table 3).

Eleven criteria including temperature, rainfall, DEM, slope, aspect, soil type, soil texture, soil reaction, soil consistency, soil moisture, land type, and land use & land cover data were considered to determine suitable land for cultivation.

Sentinel-2A Data

The Sentinel-2 for Agriculture project funded by the European Space Agency aims at fully exploiting the unprecedented Sentinel-2 observational capabilities for agricultural monitoring through the development of open-source processing chains capable of large-scale production (Inglada *et al.*, 2015). Sentinel-2 10 m resolution from the EU Copernicus Programme is ideal for monitoring at a small scale (Gumma, 2022). In this study, we use Sentinel-2 data, which provides composite images at 10 m spatial resolution. Sentinel-2 products include blue, green, red, near-infrared, and mid-infrared bands. The data are described in greater detail in the Scientific Data set documentation for Sentinel-2 (Xiong *et al.*, 2017).

Meteorological Data

The National Centers for Environmental Prediction (NCEP), the Weather Research Forecast (WRF) model community and the Air Force Weather Agency have all made extensive use of the Noah LSM, which has a long history of development through multi-institutional cooperation. (Niu *et al.*, 2011) For our study, we selected the Surface Radiative Temperature set which has a temporal resolution of one month and a spatial resolution of 0.1° or 11.1km. Note that this is the actual surface temperature and might be different than the air temperature above the surface especially during warm and sunny days.

The NOAA (National Oceanic and Atmospheric Administration) team at SSEC (Space Science and Engineering Center) developed this land-sea mask in the 1980s. It was first created with a resolution of 1/6 degrees and regrided for use in GPCP, TMPA, and IMERG precipitation products. Version 2 was developed in May 2019 to address errors found in coastal areas. For this study, GPM IMERG Land/Sea Mask data was used with a spatial resolution of 0.1° or 11.1km.

Table 2. Specifications of data used for the study.

No	Data	Description	Source
1	Sentinel 2A	MSI, 10m, 13 bands	GEE
2	Temperature	NOAH land Surface Model, 0.1°/11.1km	Earth Data
3	Rainfall	GPM, 0.1°/11.1km	Global Precipitation Measurement

4	DEM	SRTM 30m	USGS (United States Geological Survey)
5	Slope	SRTM 30m	USGS (United States Geological Survey)
6	Aspect	SRTM 30m	USGS (United States Geological Survey)
7	Soil Type	-	BARC
8	Soil Texture	HYSOGs250m	Earth Data
9	Soil Reaction	-	BARC
10	Soil Consistency	-	BARC
11	Soil Moisture	NOAH land Surface Model, 0.1°/11.1km	Earth Data
12	Land Type	-	BARC
13	LULC	Near real-time global 10m LULC mapping	Dynamic World

Land and Soil Constraints

The space shuttle Endeavour carried out the Shuttle Radar Topography Mission (SRTM) from February 11 to 22, 2000. The first nearly global collection of land elevations has been produced using radar data that the National Aeronautics and Space Administration (NASA) and the National Geospatial-Intelligence Agency (NGA) acquired as part of an international effort.

The elevation data used for this study is the SRTM 1 Arc-Second Global elevation data. With a resolution of 1 arc-second (30 meters), it provides worldwide coverage of void-filled data and makes this high-resolution global data set available for free. There could still be voids in some tiles. The acquired data was then processed to map out the digital elevation model, slope, and aspect of the designated study area.

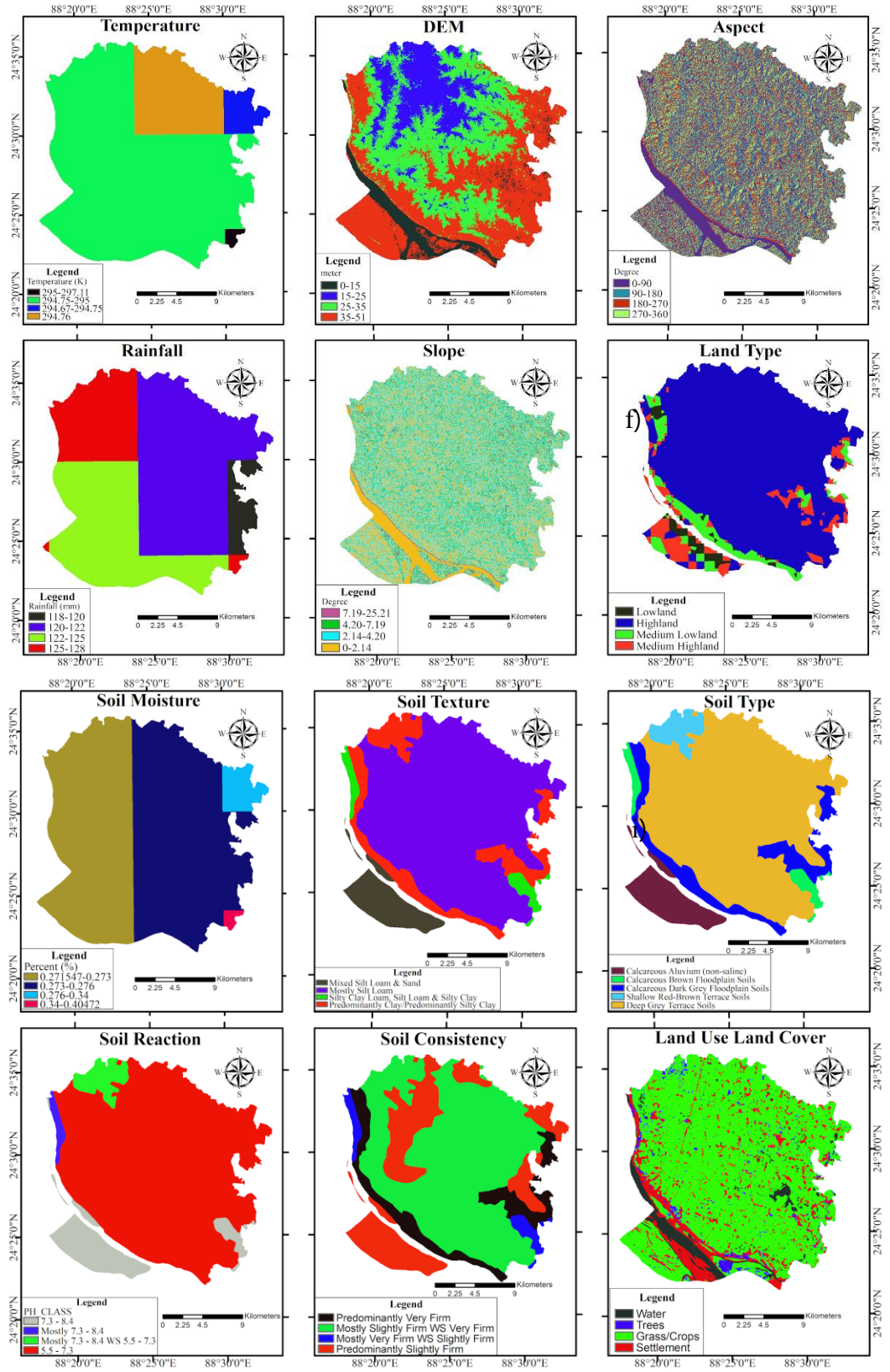


Figure 2: Processed data to develop geo-database for Godagari Upazila

Soil and land type data were acquired from CZIS (Crop Zoning Information System). CZIS was developed through a joint project by (Bangladesh Agricultural Research Council (BARC), Soil Resource Development Institute (SRDI), and Institute of Water Modelling (IWM). Their soil characteristics maps are based on

Bangladesh. It is best suited for this study due to the detailed shape file that can be found corresponding to the study area. Only the soil moisture data was acquired from the NOAA land surface model with a resolution of 0.1° or 11.1km. Dynamic World is a global land use and covers dataset with a 10m resolution, created using deep learning, and made accessible for free under an open license. It is the outcome of a collaboration between Google and the World Resources Institute to create a dynamic dataset of the Earth's surface's physical composition.

Ground Truth data

After the successful completion of the inception workshop, the first reconnaissance survey was conducted in March/2019 and the second one in July/2019 to identify the potential unmanned aerial vehicle (UAV) operational research fields; to observe the pros/cons analytically as per the rules and regulations provided by the Civil Aviation Authority of Bangladesh (CAAB) regarding UAV flying. Afterward, an extensive ground survey (second) was conducted in October/2019 to collect the ground truth (GT)/ground reference sample points from different crop fields to train satellite imagery classification algorithms and validation purposes using GARMIN GPS and two satellite-enabled-GPS cameras (Sony Cyber-shot and NIKON COOLPIX-AW110) were used to collect location information and to capture field photographs. A total of 900 geotagged field photographs were taken using GPS embedded digital camera; and 89 ground sample points (Figure 3) were taken including cereals, pulses, oilseeds, fruits sugarcane, mixed crops, and fallow land, river, wetland, etc.

Table 3. Specifications of spatial & non-spatial data

S/L	Data type	Source
1	Demographic data	BBS, MoF, WB & World Population Review
2	Upazila level crop census data	UAO, BARI, DAE, BADC, BARC, DAM etc.
3	Thematic layer <i>i.e.</i> , administrative boundary, road, tidal layer, etc.	SoB, BADC, BARC, IWM, BIWTA etc.
4	Meteorological data	Bangladesh Meteorological Department (BMD)
5	Soil Maps	BARC & ORNL-DAAC HYSOGs250m

The 3rd field survey was conducted afterward in February/2020 over the entire Godagari Upazila. A total of 54-points data were collected for crop inventory (Fig. 4). All the collected GT data were further classified into 6 distinct crop types chosen classification of maize, lentil, mustard, potato, Boro rice, and wheat along with another common class namely others. The characteristics of all seven (7) classes are illustrated in Table 1.

From 2020-2021, two massive fieldworks (4th and 5th field surveys) were planned and successfully executed over the study area in February and March 2021 (Figure 5A). These visits were divided into two parts i) Interviews with UAOs and SAAOs; ii) Collection of pre-defined structured GT points. A total of 660-point data were collected for crop inventory (Fig. 5A), which was further filtered into 580- points divided into a 70:30 ratio as truth point (70%) and checkpoint (30%) as shown in Figures 6A, 6B. All of the collected GT data were further classified into seven (7) classes as illustrated earlier. In this fieldwork, a total of 2693 geo-tag photos were also collected using two satellite-enabled-GPS cameras (Sony Cyber-shot and NIKON COOLPIX-AW110). The data was later processed and organized in the GIS platform.

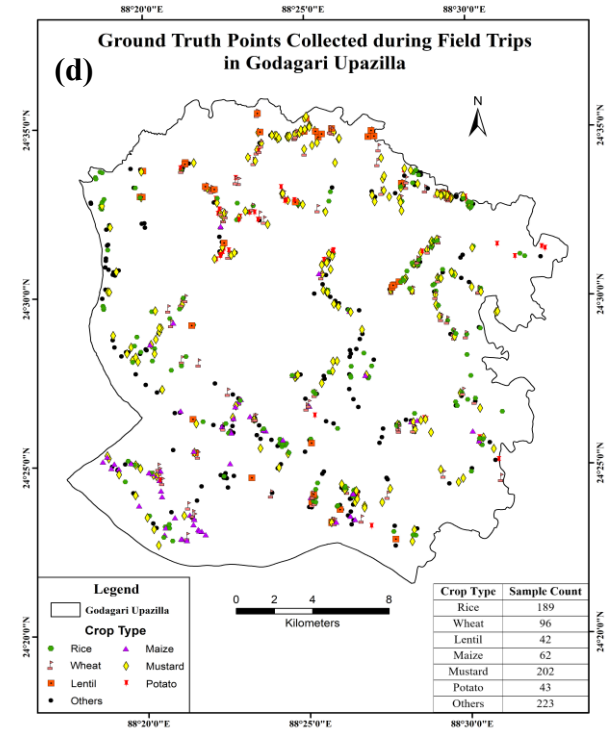
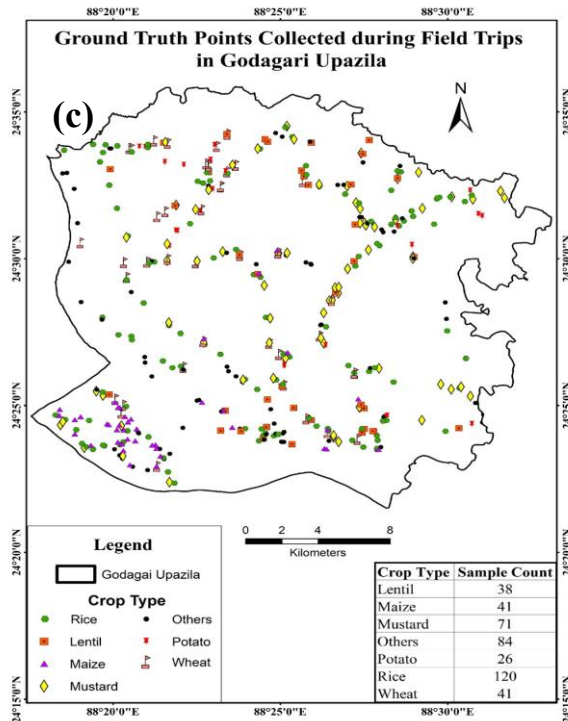
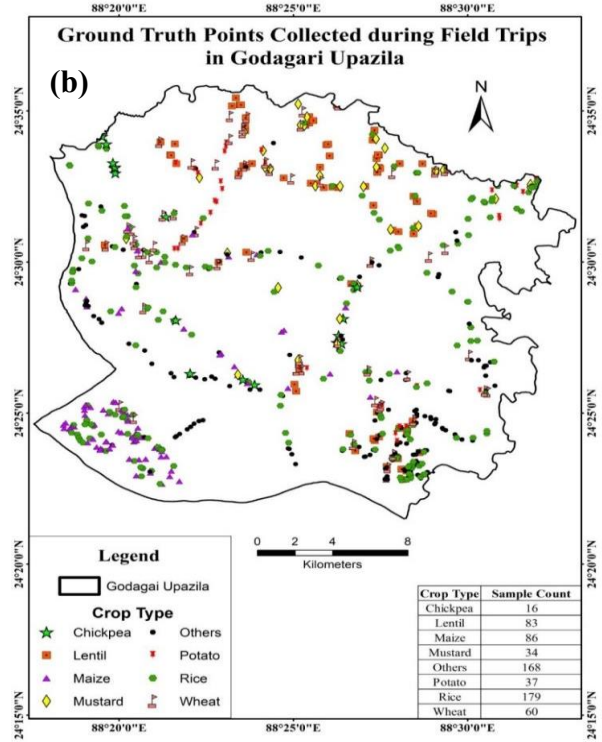
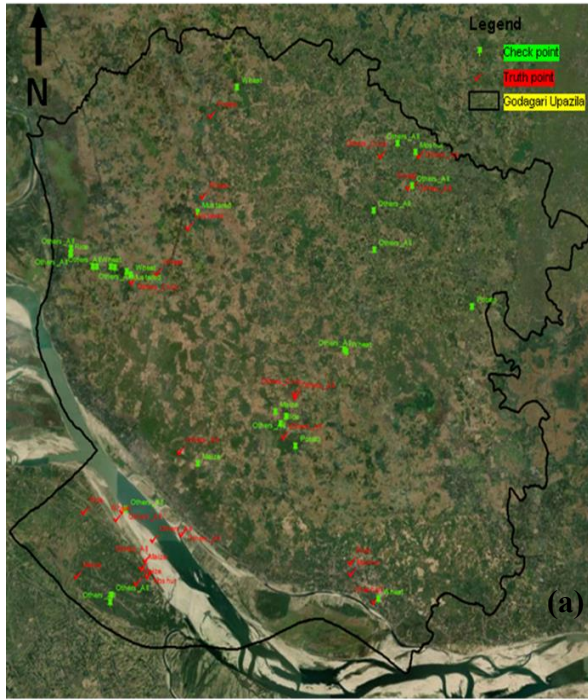


Figure 3. GCPs on 6 crop types and others during field visits in the (a) 2019-20, (b) 2020-21, (c) 2021-22, and (d) 2022-23 dry Season

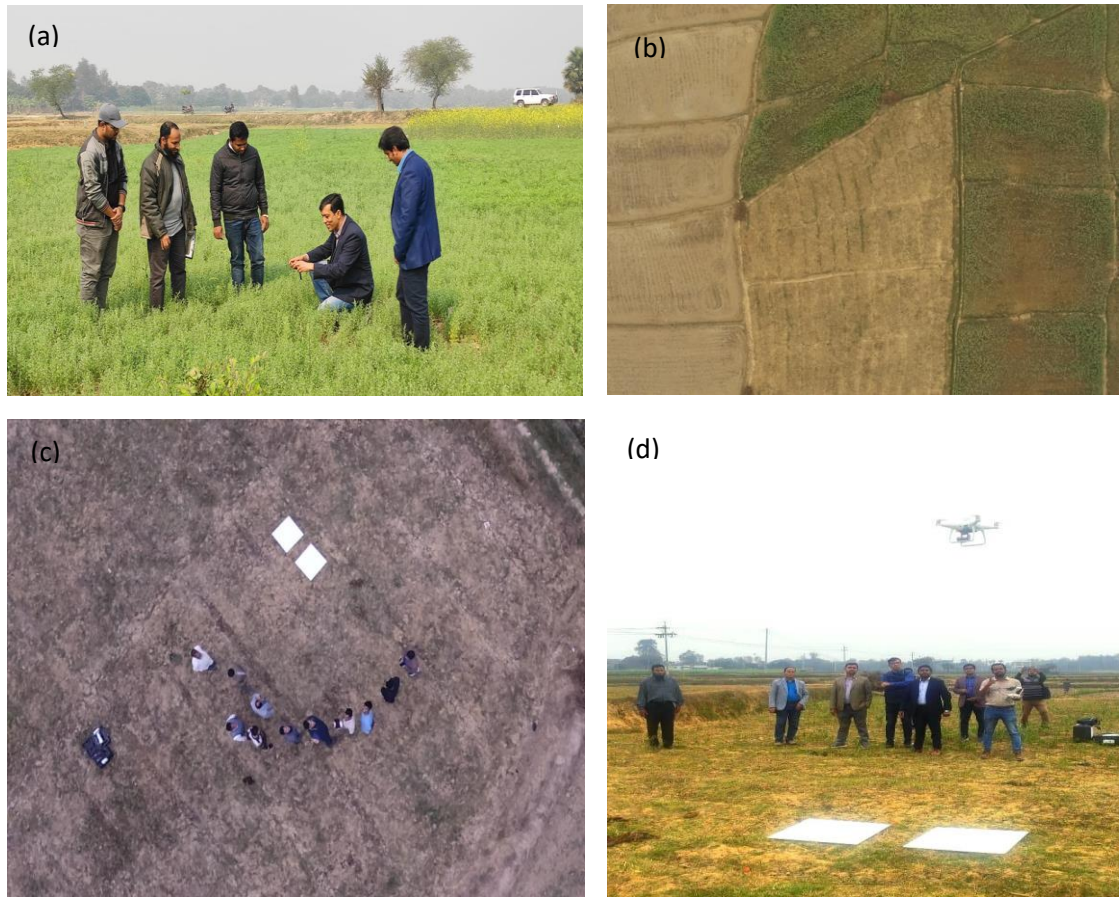


Figure 4. Ground truth point collection (a) during the 2021-2022 dry season; (b), (c), and (d) drone images during 2022-23 season

In the same period (2020-2021), we worked on the methodology to a great extent and enhanced; prepared necessary thematic geo-datasets for location-specific suitable cropping patterns identification by geospatial modeling; developed reliable real-time field data collection scheme using KoboCollect open data kit; time-series remotely sensed satellite data collection, processing, extract necessary vegetation indices (VIs) and analyze accordingly focusing objectives of the project. Moreover, with prior approval, the UAV and relevant geospatial items are under procurement through CGP. Two Research Assistants have been recruited. Besides, demo field data collection was conducted on 09 February 2021 using KoboCollect Apps; data collection from the KoboCollect server, post-processing, visualization, overlay on Sentinel 2B RGB and NDVI imagery (acquisition date 05 February 2021), and data quality was assessed.

The 6th field survey was in February/2022 over the entire Godagari Upazila as per previous ones. Before the fieldwork, the target training sample was designed consciously taking care of previous experience, crop types, expected crop types, possible special features, possible mixed features, possible confusion, accessibility, possible accessible distance from the roadside, and many other aspects.

The 7th field survey was arranged from 28th January to 3rd February 2023 in the pilot study area from 2022-2023. Samples were collected following the previous methods using Garmin GPS and smartphones. A total of 999 ground reference points were collected using KoboCollect apps as well a total of 999 geo-tag photos were collected using 14 satellite-enabled GPS cameras and smartphones.

Methods

The study has adopted a robust methodology (Fig. 5) to achieve the project goal and objectives. The methodological approach has been updated incorporating Machine Learning Algorithms as well as different band combinations. The framework of this research is shown in Figure 5 using the flow chart diagram. In general, the methodology is separated into four parts: (1) data collection; (2) data processing and analysis; (3) crop type classification and mapping; and (4) cropping pattern identification and analysis.

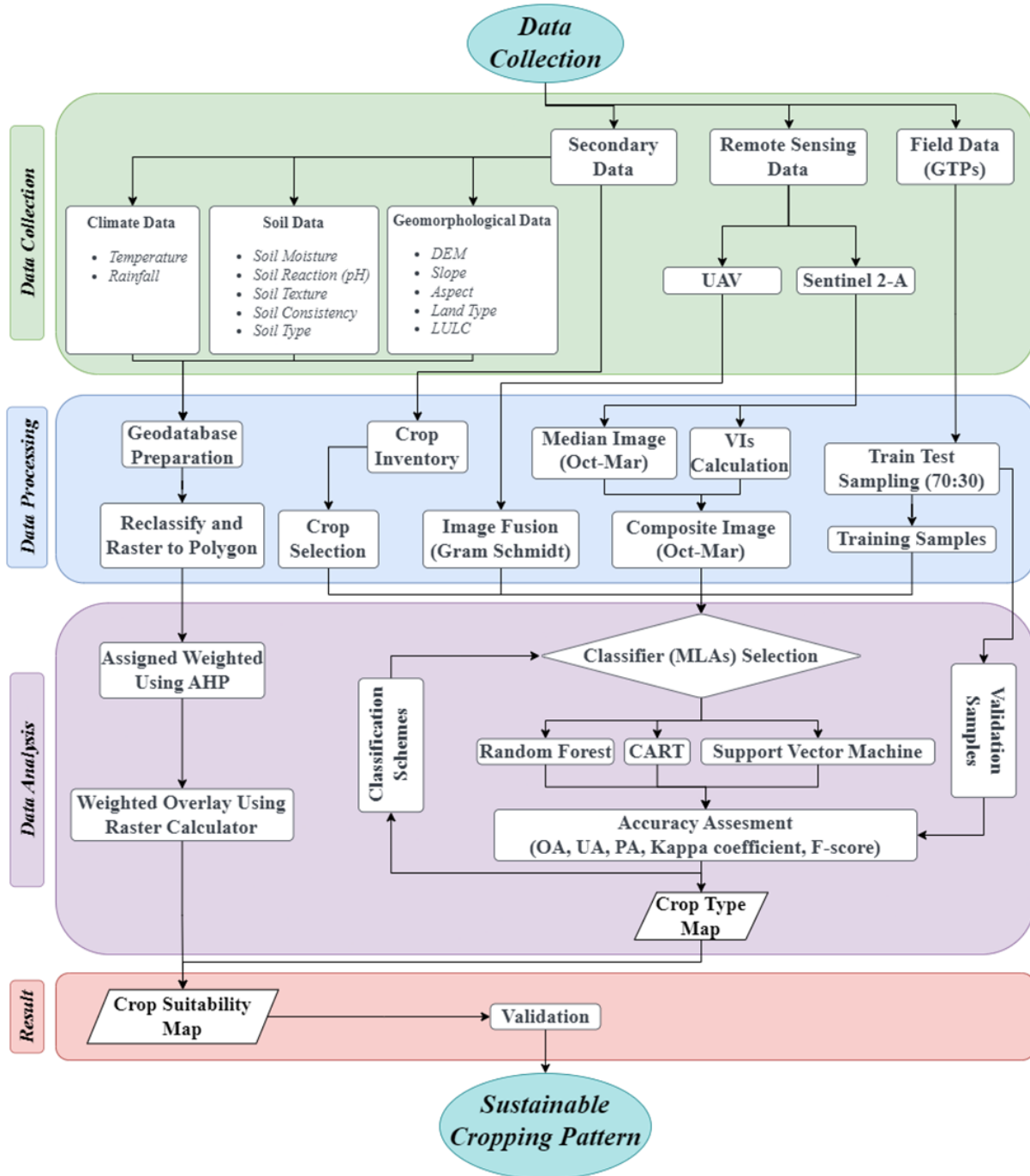


Figure 5. Methodological flow chart

Reference/field data processing

This updated methodology was applied based on GCPs collected during field visits in dry season. Firstly, ground reference points were filtered manually and the quality of the data was ensured based on field experiences and expert perception. Among collected GTPs from field, after screening some GTPs were selected for crop type classification which represented raw GPS data collected from field visits using KoboCollect. The crop fields were ensured with the dimension of 30*30 meters at least while collecting GPS data as we have been planning to use Sentinel-2 satellite images.

Table 4: Collected data on 6 crop types and others during field visits in the 2019-20, 2020-21, 2021-22, and 2022-23 dry Season

Crops	2019-2020				2020-2021				2021-2022				2022-2023			
	Geo-Tagged Photos	GTPs	Training	Validation	Geo-Tagged Photos	GTPs	Training	Validation	Geo-Tagged Photos	GTPs	Training	Validation	Geo-Tagged Photos	GTPs	Training	Validation
Rice	900	54	26	28	664	179	125	54	956	120	84	36	1052	189	132	57
Wheat						60	42	18		41	29	12		96	67	29
Lentil						83	58	25		38	27	11		42	29	13
Maize						86	60	26		41	29	12		62	43	19
Mustard						34	24	10		71	50	21		202	141	61
Potato						37	26	11		26	18	8		43	30	13
Others						168	118	50		84	59	25		223	156	67

Based on these selected GTPs, sample polygons were generated (Kussul *et al.*, 2017; Cai *et al.*, 2018; Rao *et al.*, 2021). These polygons were digitized in ArcGIS 10.8 based on the concurrent available sentinel-2 images and field experiences so that fields can be identical to the point observations. The boundary line of the crop fields was avoided while drawing polygons so that mixed pixels can be avoided. Hereafter these polygons were split into 70:30 ratios to train and validate the ML models.

Satellite Image Processing

During the project period (2018-2023), crop type classification for each cropping season (Oct-Mar) was executed using machine learning algorithms. Sentinel-2 MSI: Multispectral Instrument, Level-2A data was used in this approach. 45, 52, and 48 images were available with a cloud coverage of less than or equal to twenty percent comprising the study area from October to March of 2020-21, 2021-22, and 2022-23 seasons respectively. All the images were masked using the Sentinel-2 cloud masking function. The Red Edge ('B5', 'B6', 'B7', 'B8A') and Short Wave ('B11', 'B12') bands were resampled from 20 meters to 10 meters spatial resolution using resample (default) and project function in GEE. Median image of these Sentinel-2 products from October to March each cropping season was derived in Google Earth Engine (GEE). Median NDVI and EVI were also derived in GEE to prepare a median composite image having the following 12 bands: 'B2', 'B3', 'B4', 'B8', 'B5', 'B6', 'B7', 'B8A', 'B11', 'B12', 'NDVI', 'EVI'.

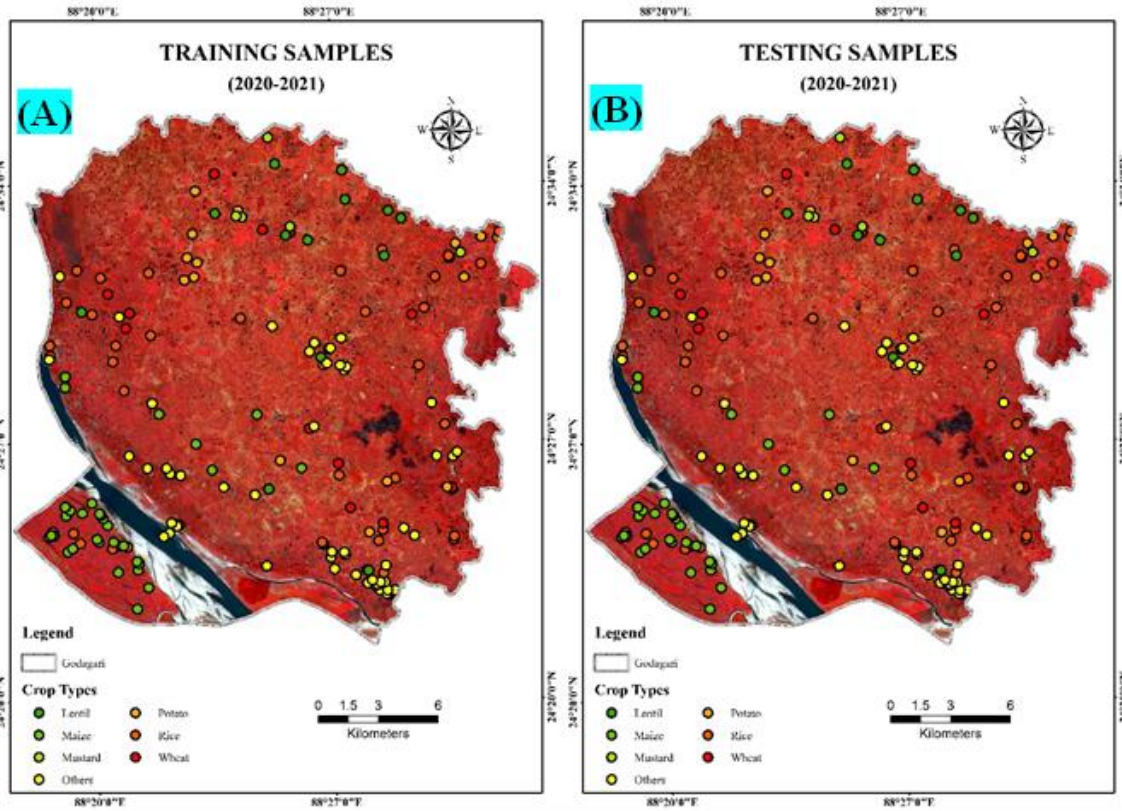


Figure 6. Splitting GTPs into (A) training and (B) testing samples for 2020-21.

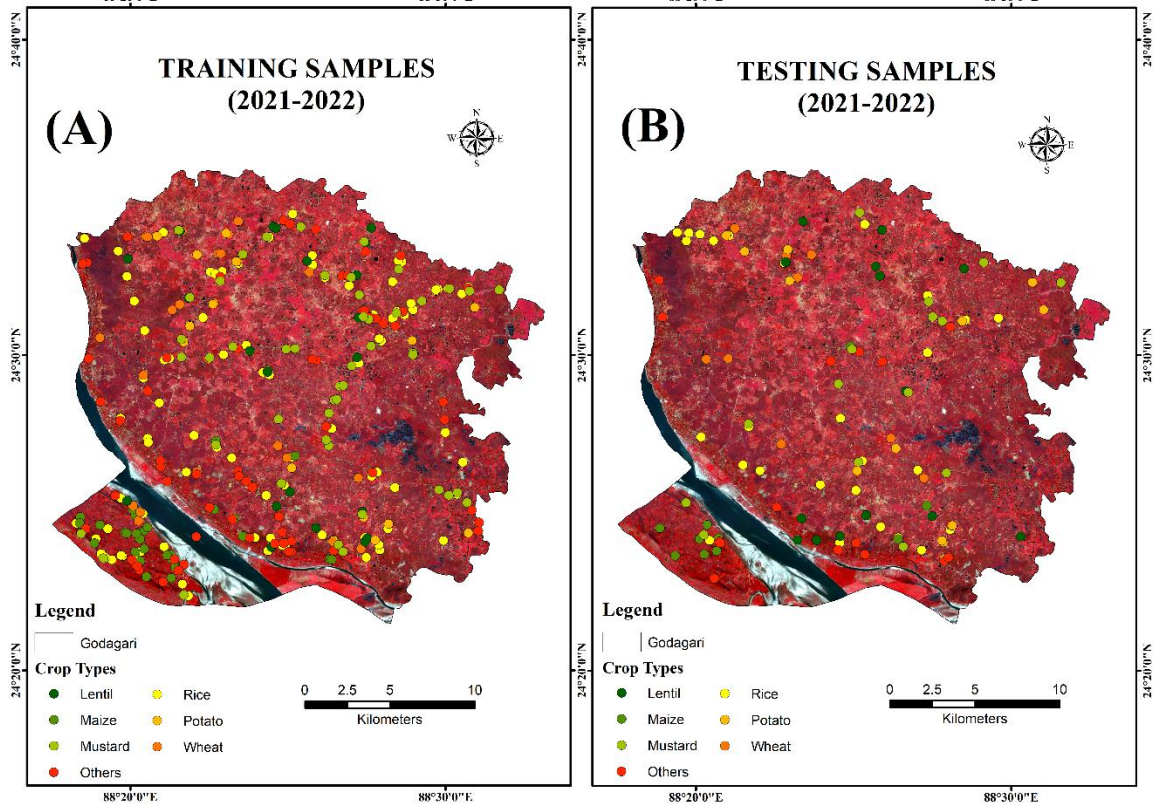


Figure 7. Splitting GTPs into (A) training and (B) testing samples for 2021-22

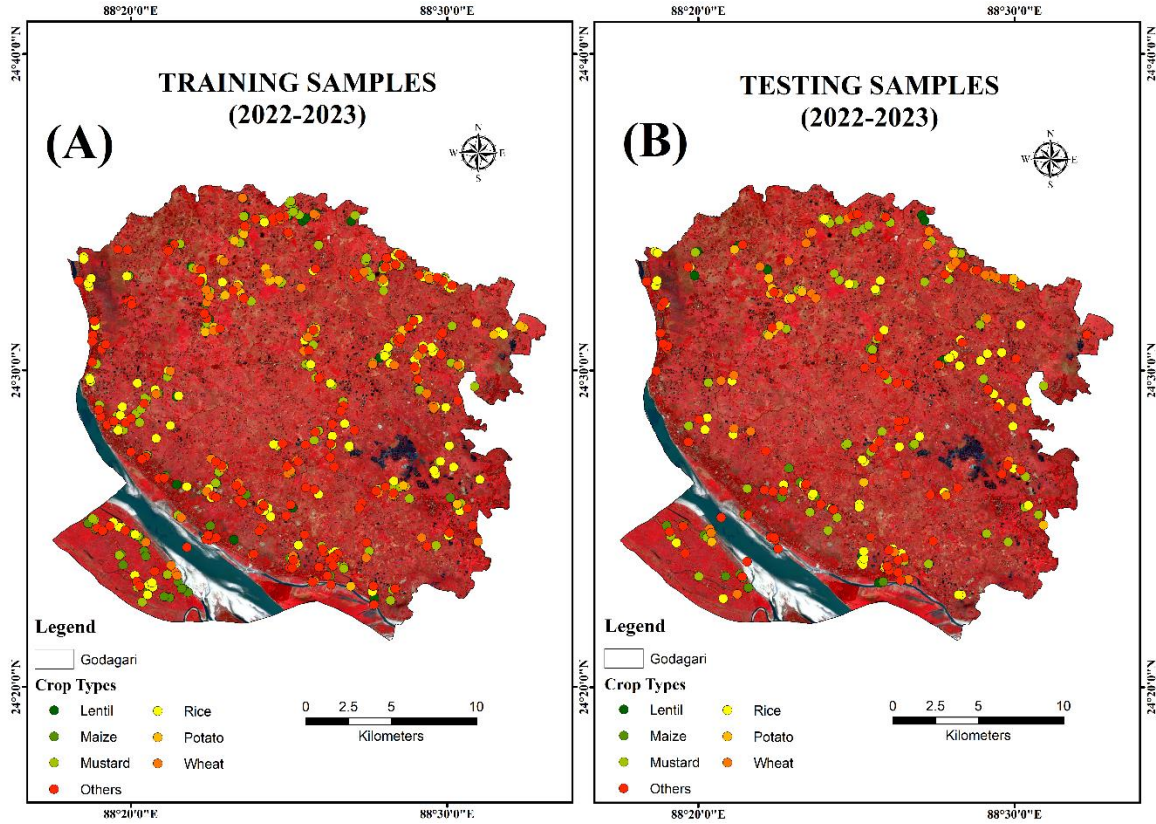


Figure 8. Splitting GTPs into (A) training and (B) testing samples for 2022-23

Image Classification

Experimental Design

According to LUO *et al.* (2021), we evaluated several experiments based on different band combinations as well as MLAs. Firstly, we consider the bands into the following categories: visible bands ('B2', 'B3', 'B4'), NIR band ('B8'), red-edge bands ('B5', 'B6', 'B7', 'B8A'), and short-wave bands ('B11', 'B12'). We designed five experimental schemes using these band compositions and derived vegetation indices.

Table 5. Experimental schemes using different band combinations.

Schemes	Sentinel-2A Bands	Bands Combination (s)
Scheme 1	'B2', 'B3', 'B4', 'B8'	VIS + NIR
Scheme 2	'B2', 'B3', 'B4', 'B8', 'B5', 'B6', 'B7', 'B8A'	VIS + NIR + Red Edge
Scheme 3	'B2', 'B3', 'B4', 'B8', 'B11', 'B12'	VIS + NIR + SWIR
Scheme 4	'B2', 'B3', 'B4', 'B8', 'NDVI', 'EVI'	VIS + NIR + Vegetation Indices
Scheme 5	'B2', 'B3', 'B4', 'B8', 'B5', 'B6', 'B7', 'B8A', 'B11', 'B12', 'NDVI', 'EVI'	VIS + NIR + Red Edge + SWIR + Vegetation Indices

To evaluate the differences in classification results, all the above schemes were tested on a seasonal median image composite. Therefore, this experiment includes around 80 trials.

Train-test Splitting

Based on the reference dataset, the training and testing (validation) points and polygons were prepared in Google Earth Engine (GEE) considering the seven distinct classes throughout the study area (Figure 9). Both training and testing samples were split into 70:30 ratios which cover around on average 189.92 ha and 83.24 ha accordingly. The crop-wise area coverage in both training and testing samples was represented in Table 5.

Classifier Selection

Remote sensing has made extensive use of machine learning (Lary *et al.*, 2016). Decision Trees (DTs), Random Forest (RF), Neural Networks (NN), and Support Vector Machines are some of the most frequently applied machine learning techniques (Al-doski *et al.*, 2013; Lary *et al.*, 2016). In this research, three machine learning algorithms (Random Forest, CART, and Support Vector Machine) have been investigated for mapping the crop types accurately.

(a) Random Forest

Random Forest is a popular machine learning algorithm that belongs to the supervised learning technique. RF is an ensemble and non-parametric algorithm that has been much used for crop classification and yield prediction (Tatsumi *et al.*, 2016; Neetu Andray, 2019). It is a classifier that contains several decision trees on various subsets of the given dataset and takes the average to improve the predictive accuracy of that dataset. Instead of relying on one decision tree, the random forest takes the prediction from each tree, and based on the majority votes of predictions, it predicts the final output. The greater number of trees in the forest leads to higher accuracy and prevents the problem of over fitting. In this study, the number of trees ($n = 100$) was used after several optimizations keeping other parameters as default.

(b) CART

Although CART is the predecessor of the Random Forest algorithm, it is an advanced technique based on the Decision Tree (DT) classifier, which is built from a set of training data. Classification and regression trees are machine-learning methods for constructing prediction models from data. The models are obtained by recursively partitioning the data space and fitting a simple prediction model within each partition. As a result, the partitioning can be represented graphically as a decision tree. Classification trees are designed for dependent variables that take a finite number of unordered values, with prediction error measured in terms of misclassification cost. Regression trees are for dependent variables that take continuous or ordered discrete values, with prediction error typically measured by the squared difference between the observed and predicted values. (Loh, 2011). In this study, all parameters were kept at default while using this algorithm.

(c) Support Vector Machine

Support Vector Machine or SVM is one of the most popular Supervised Learning algorithms, which is used for Classification as well as Regression problems. In support vector machines the classification problems are solved through the concept of margin, which is defined as the smallest distance between the decision boundary and any of the samples. The decision boundary is chosen to be the one for which the margin is maximized. In this case, the margin is the perpendicular distance between the decision boundary and the closest of the data points. Support vectors are the data points, which determine the location of this boundary (Bishop, 2006; Breiman, 2001). There are several kernels available under this algorithm (RBF, polynomial, linear, etc.) but only the RBF kernel was used in this study for classification purposes.

Accuracy Assessment and Validation

Accuracy assessments essentially determine the quality of the information derived from remotely sensed data. In these assessments, we compare map data with reference or ground truth data. Accuracy is important because remotely sensed data are often used for mapping and developing environmental models that are used for management and decision-making purposes. There are a few matrices available for evaluating supervised classification problems. Among them often used Kappa coefficient and F1 score along with the Overall Accuracy, Producer Accuracy, and User Accuracy matrices were used in this study.

Overall Accuracy (OA)

The overall accuracy is calculated by summing the number of correctly classified values and dividing by the total number of values. The correctly classified values are located along the upper-left to the lower-right diagonal of the confusion matrix. The total number of values is the number of values in either the truth or predicted-value arrays.

$$OA = \frac{\text{Number of correctly classified samples}}{\text{Number of reference samples}} \times 100 \dots \dots \dots (1)$$

Producer's Accuracy (PA)

The producer's Accuracy is the map accuracy from the point of view of the map maker (the producer). It is also the number of reference sites classified accurately divided by the total number of reference sites for that class.

$$PA = \frac{\text{Number of correctly classified pixels of a particular class}}{\text{Number of reference pixels of the same class}} \times \dots \dots \dots (2)$$

User's Accuracy (UA)

The User's Accuracy is the accuracy from the point of view of a map user, not the map maker. The User's accuracy essentially tells us how often the class on the map will be present on the ground. This is referred to as reliability. The User's Accuracy is calculated by taking the total number of correct classifications for a particular class and dividing it by the row total.

$$UA = \frac{\text{Number of correctly classified pixels of a particular class}}{\text{Number of classified pixels in the class}} \times 10 \dots \dots (3)$$

Kappa Coefficient

The Kappa Coefficient is generated from a statistical test to evaluate the accuracy of classification. Kappa essentially evaluates how well the classification performed as compared to just randomly assigning values, i.e., did the classification do better than random. The Kappa Coefficient can range from -1 to 1. A value of 0 indicated that the classification is no better than a random classification. A negative number indicates the classification is significantly worse than random. A value close to 1 indicates that the classification is significantly better than random.

The kappa coefficient is computed as follows:

$$\kappa = \frac{N \sum_{i=1}^n m_{i,i} - \sum_{i=1}^n G_i C_i}{N^2 - \sum_{i=1}^n G_i C_i} \dots \dots \dots (4)$$

Where,

i is the class number.

N is the total number of classified values compared to truth values.

$m_{i,i}$ is the number of values belonging to the truth class i that have also been classified as class i (i.e., values found along the diagonal of the confusion matrix).

C_i is the total number of predicted values belonging to class i .

G_i is the total number of truth values belonging to class i .

F1 Score

One of the often-used metrics to evaluate a classifier's effectiveness is the F1 score (Baeldung, 2020) also known as F-score. It is usually used to assess binary classification systems (Wood, 2022). When using classification models in machine learning, a common metric used to assess the quality of the model is the F1 Score. We do not determine an overall F1 score for a multi-class classification problem. Instead, we use a one-vs-rest method to determine the F1 score for each class. With this method, we evaluate the effectiveness of each class independently, as if there were different classifiers for each class (Baeldung, 2020). The F1 score is a way to combine the model's precision and recall. It is the harmonic mean of the model's precision and recall. Precision is the proportion of true positive examples among the examples that the model classified as positive. On the other hand, the proportion of examples classified as positive out of all examples classed as positive is known as recall, also known as sensitivity.

This metric is calculated as:

$$Precision = \frac{TP}{TP + FP} \dots \dots \dots (5)$$

$$Recall = \frac{TP}{TP + FN} \dots \dots \dots (6)$$

$$F1\ Score = 2 \times \frac{Precision \times Recall}{Precision + Recall} \dots \dots \dots (7)$$

Where,

TP: True-Positive.

FP: False-Positive.

FN: False-Negative.

The highest possible value of an F-score is 1.0, indicating perfect precision and recall, and the lowest possible value is 0 if either the precision or the recall is zero.

Modeling on cropping patterns

Historical land use/cover change analysis would be conducted for dry season cropping practices mostly by using Landsat data archives for the years 2001, 2011 and 2021. To assess present crop types and cropping pattern mapping, Sentinel 2 imagery from the year 2015 to date was collected, processed, and analyzed in both the desktop-based geospatial domain and GEE platform. Very high-resolution (VHR) UAV data (optical & multispectral) would be collected and used as a reference for training/validating algorithms for the classification of satellite imagery. An open-source crowdsourcing geo-visual web interface was developed to collect ground reference data and validate map outputs with multi-stakeholder involvement. The potential workforce in such a crowd-sourcing platform may include the distributed research facilities of BARI offices across the agroecological zones and trained technologically advanced local youth and stakeholders active in the study area.

The AHP uses pairwise comparisons as a fundamental component. These comparisons may be established utilizing true measurements or a fundamental scale that represents how strongly different preferences and emotions are expressed (Saaty, 1987). The AHP is particularly concerned about changes in measurement, dependencies within and between groups of structural components, and departures from consistency (Saaty, 1987).

The Analytical Hierarchy Process was used to determine how important or weighted the criteria were compared to one another. The information obtained from specialists is then combined with logic to create a pairwise comparison matrix (PWCM). A pairwise comparison matrix with n rows and n columns (n is the number of parameters) helps quantify the findings. Here for our research, 11 parameters were selected showing the relationship between the criteria.

The magnitude of the row I indicator to column j is indicated by the a_{ij} element when $a_{ij} > 0$ (Table 7). The elements of the pairwise comparison medium's primary diagonal values are given a fixed value of 1. Given the square-symmetric pairwise comparison matrix, just the upper triangular medium's element needs to be identified, from there, the lower triangular medium is obtained by applying the opposite. Then determine the weight for each criterion based on the pairwise comparison matrix. To obtain the most accurate information on the final priorities of the options, summarize the top priorities of each alternative.

Table 7: Pairwise Comparison Matrix

Criteria	X1	X2	...	Xn
X1	1	a_{12}	...	a_{1n}
X2	a_{21}	1	...	a_{2n}
...
Xn	a_{n1}	a_{n2}	...	1

The sum of each column in PWCM is represented as follows:

$$a_{ij} = \sum_{i=1}^n a_i \dots \dots \dots (8)$$

Eigen value: Take the mean of the consistency vector to calculate the maximum eigenvalue (λ_{max}):

$$\lambda_{max} = \frac{\sum_{i=1}^n a_i}{n} \dots \dots \dots (9)$$

Consistency index: Calculate the consistency index (CI), the index measuring the degree of consistency deviation, determined by the formula:

$$CI = (\lambda_{max} - n) / (n - 1) \dots \dots \dots (10)$$

Consistency ratio: Calculate the consistency ratio (CR):

$$CR = CI / RI \dots \dots \dots (11)$$

Here, RI is a random index determined from the lookup table proposed by Saaty (1994)

Table 8: RI (random index) value

n	1	2	3	4	5	6	7	8	9	10	11
RI	0.00	0.00	0.52	0.89	1.11	1.25	1.35	1.4	1.45	1.49	1.51

If the CR value is $\leq 10\%$, then the expert's judgment is consistent and the weight set is accepted. On the contrary, if the CR value is $> 10\%$, it is necessary to conduct discussions with experts to re-evaluate the weight of the criteria using pairwise comparison.

Suitability Analysis

After computing the weight of each criterion relative to the crops and the generation of thematic layers of input parameters, the suitability models were developed for each crop by using the model builder module of ArcGIS 10.8 software (Figure 10). The crop-wise thresholds for input parameters were prepared based on the NBSS & LUP crop-suitability manual [43]. Each criterion was reclassified into four groups, namely, S1 represents land that is highly appropriate for crops with no limiting factors, S2 denotes land that is moderately suitable with some limiting factors, S3 denotes land that is marginally ideal for crops with severe limiting factors, and N indicates land unsuitable for agriculture. After that, suitability maps for each crop were obtained by integrating all the reclassified thematic layers, including LU/LC map (Figure 10) with corresponding weights derived from AHP using the weighted overlay analysis (WOA) technique, as follow:

$$S = \sum_{j=1}^n w_j \cdot x_j \quad \text{where, } \sum_{j=1}^n w_j = 1 \dots \dots \dots (12)$$

Where, w_j is the weight of criterion j , x_j is the obtained score of criterion j , n is the total number of criteria, and S is the suitability score corresponding to each crop, from the complete target region.

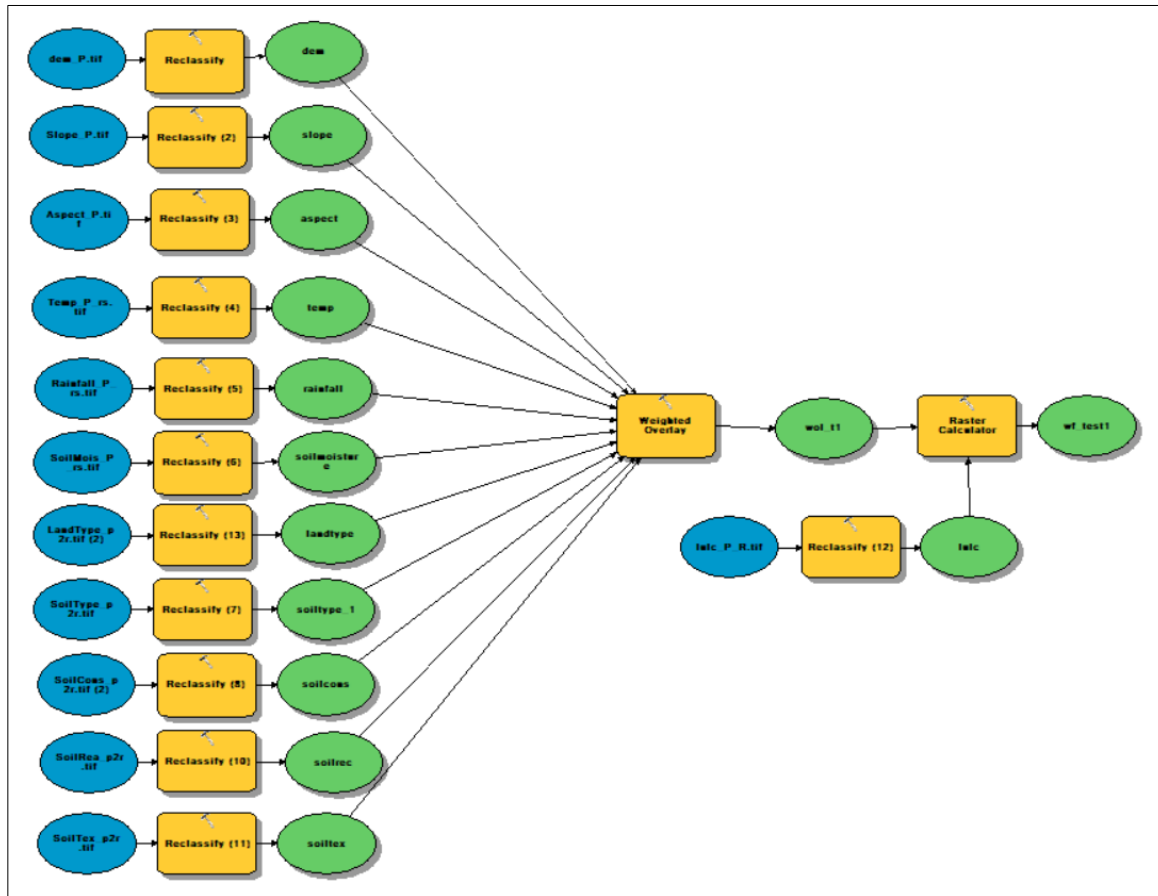


Figure 9: Suitability model based on GIS environment

Results and Benefits

Crop type mapping

During the project period, an algorithm was developed to delineate dry season crops using Sentinel-2 imageries in the Godagari Upazila. Several machine learning algorithms were employed in Google Earth Engine to classify the seasonal median composite image. Firstly, the monthly median, seasonal composites and NDVI were investigated (Fig. 10-15) for 2020-21, 2021-22, and 2022-23 dry season.

**MONTHLY MEDIAN COMPOSITE OF SENTINAL-2A
IMAGERY IN GODAGARI UPAZILA**

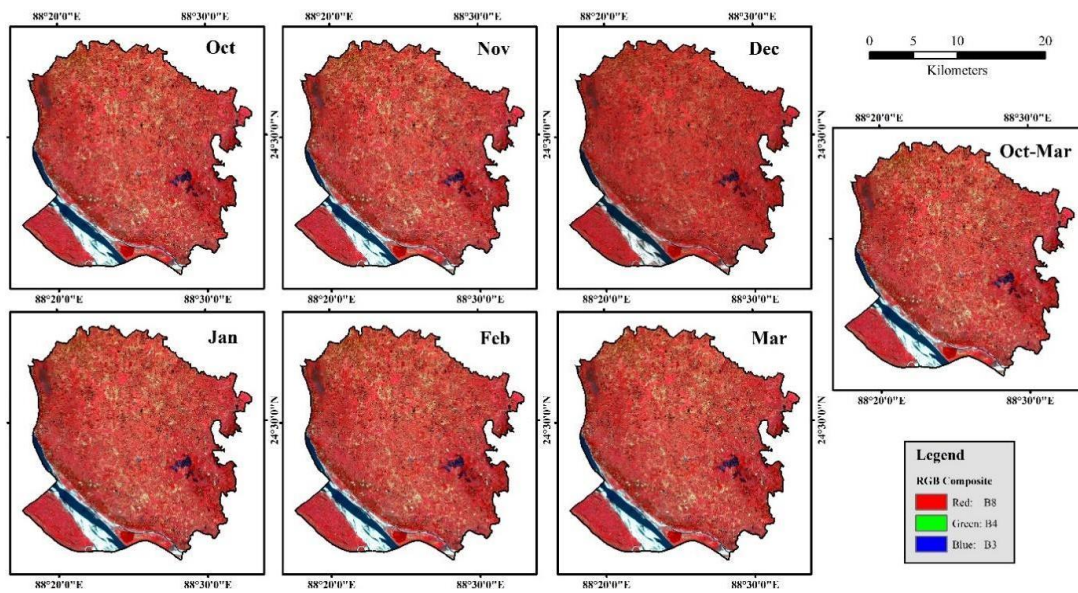


Figure 10. Median monthly and seasonal (RGB) composites of Sentinel-2A images (2020-21).

**MONTHLY MEDIAN COMPOSITE OF
SENTINAL-2A IMAGERY (2021-2022)
GODAGARI UPAZILLA**

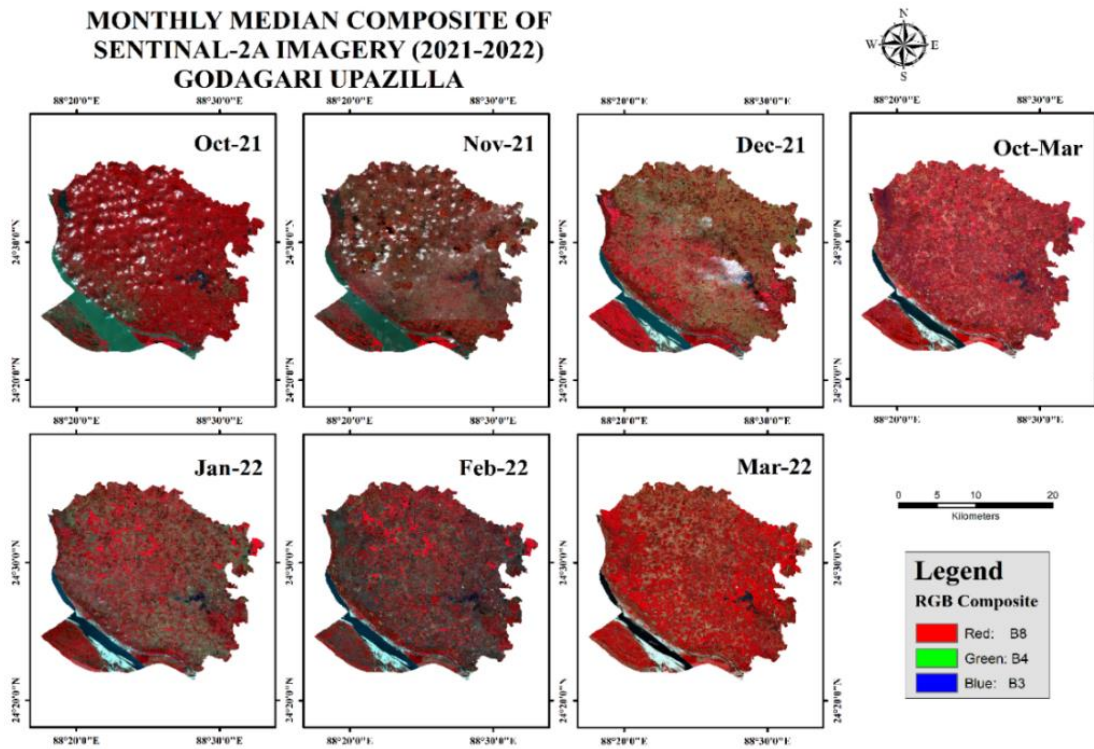


Figure 11. Median monthly and seasonal (RGB) composites of Sentinel-2A images (2021-22).

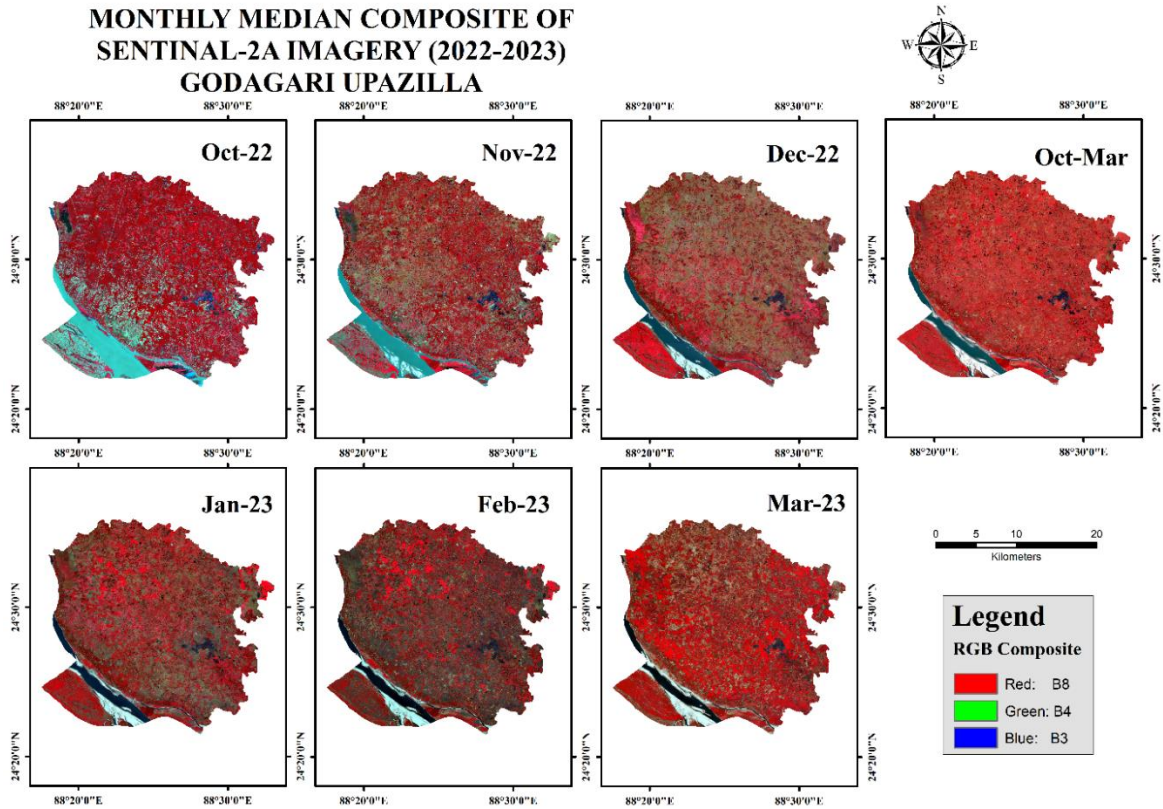


Figure 12. Median monthly and seasonal (RGB) composites of Sentinel-2A images (2022-23).

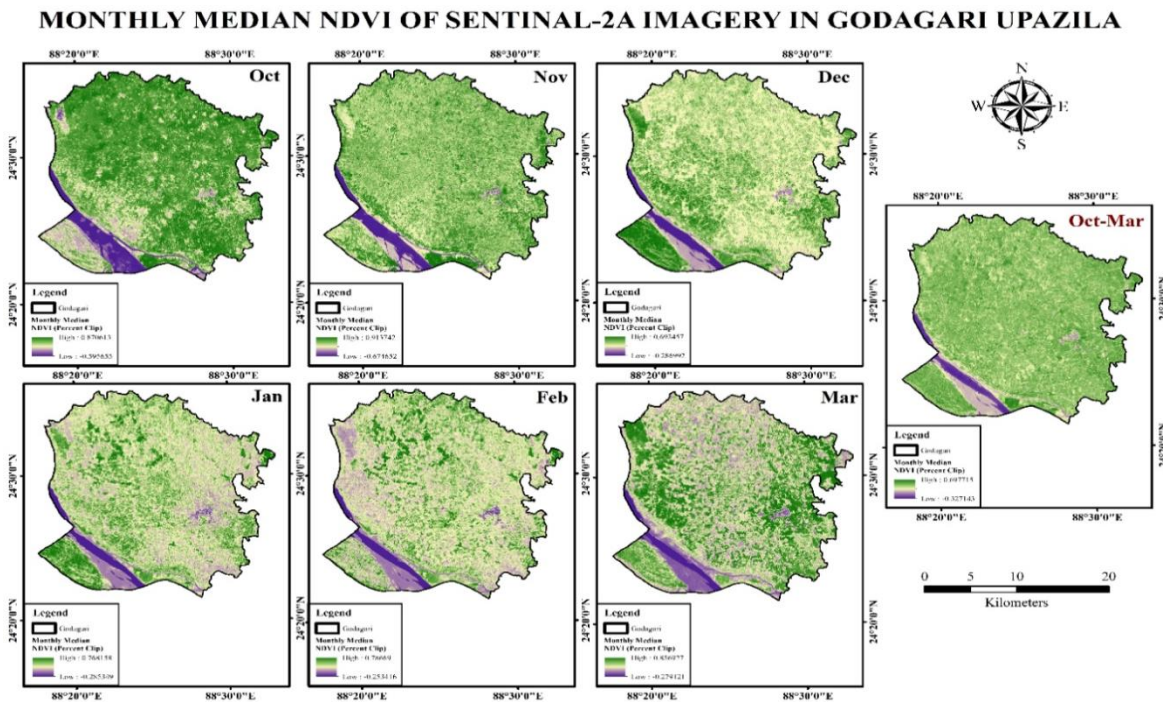


Figure 13. Median monthly and seasonal NDVI of Sentinel-2A images (2020-21).

**MONTHLY MEDIAN NDVI OF SENTINAL-2A IMAGERY (2021-2022)
GODAGARI UPAZILLA**

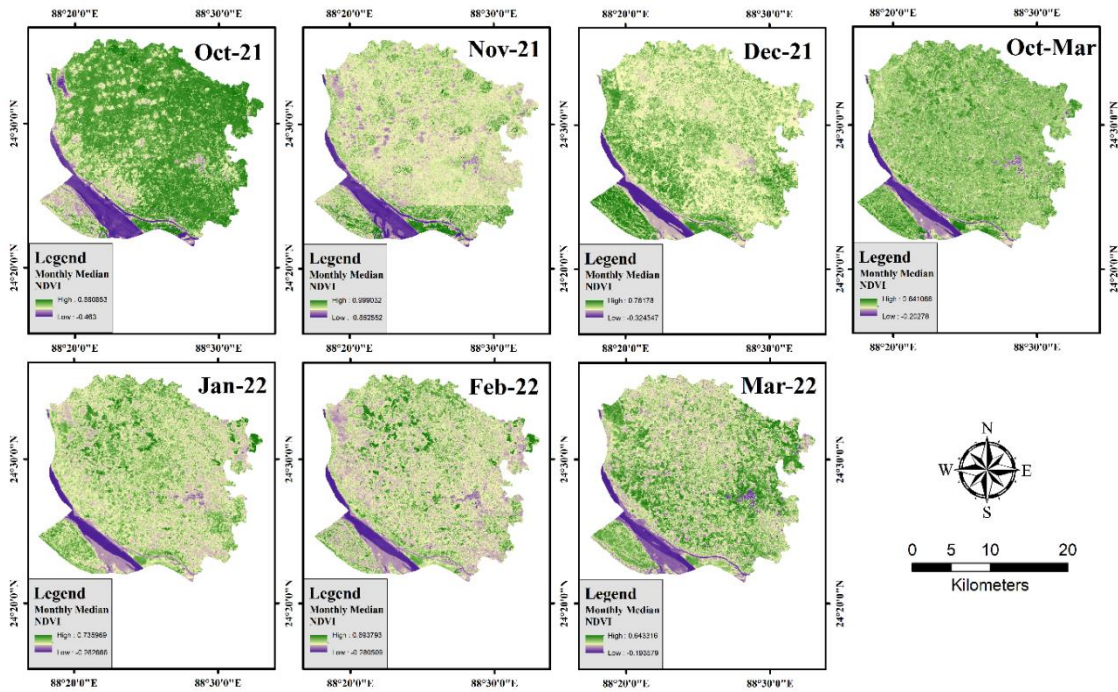


Figure 14. Median monthly and seasonal NDVI of Sentinel-2A images (2021-22)

**MONTHLY MEDIAN NDVI OF SENTINAL-2A IMAGERY (2022-2023)
GODAGARI UPAZILLA**

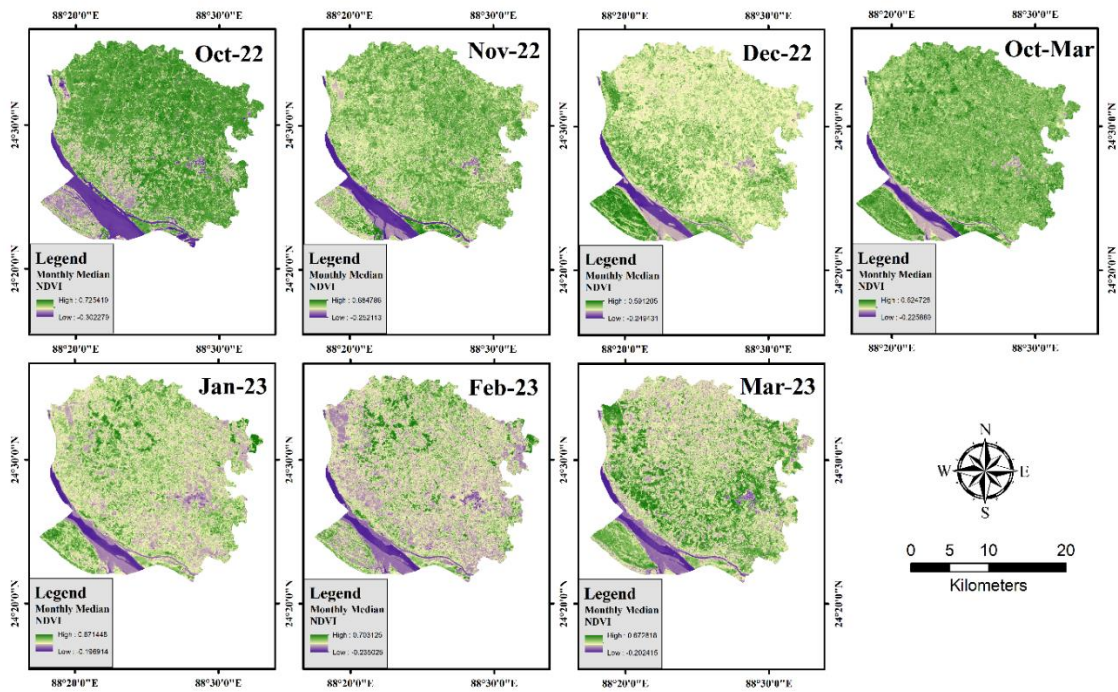


Figure 15. Median monthly and seasonal NDVI of Sentinel-2A images (2022-23)

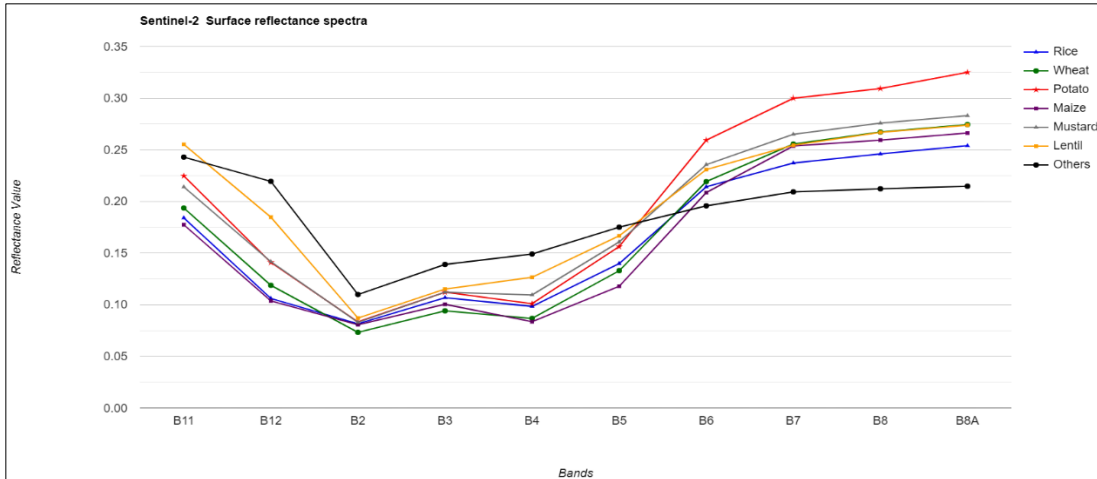


Figure 16. Surface reflectance values of target crop types in Sentinel-2 spectrum

Crop-specific band reflectance and indices values were investigated before the experimental design and classification procedure. In Figures 16 and 17, band reflectance and vegetation indices values against each class are represented. In the visible and red-edge spectrum, the reflectance of each crop was found very close and not properly distinguishable, though Red-Edge 3 and 4 are found relatively better. On the other hand, Red-Edge 4 and NIR were showing almost similar reflectance except 2/3 of crops overlapping each other. In SWIR-1 and SWIR-2, all the crops were seen as better distinguishable except rice and maize. In Figure 16, NDVI and EVI values are represented against each target class type. Wheat, potato, and maize were found within a very close value range in NDVI but these were better distinguishable in the EVI index.

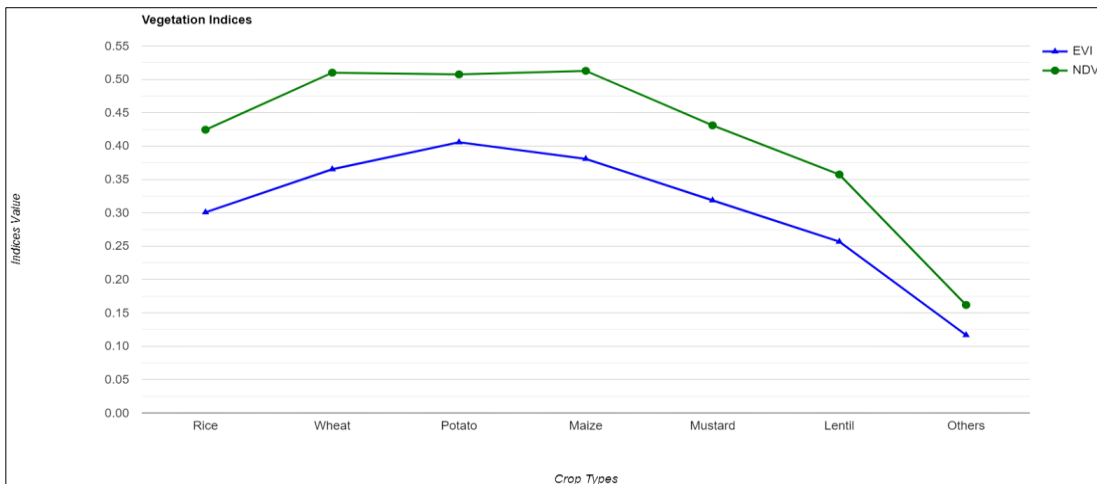
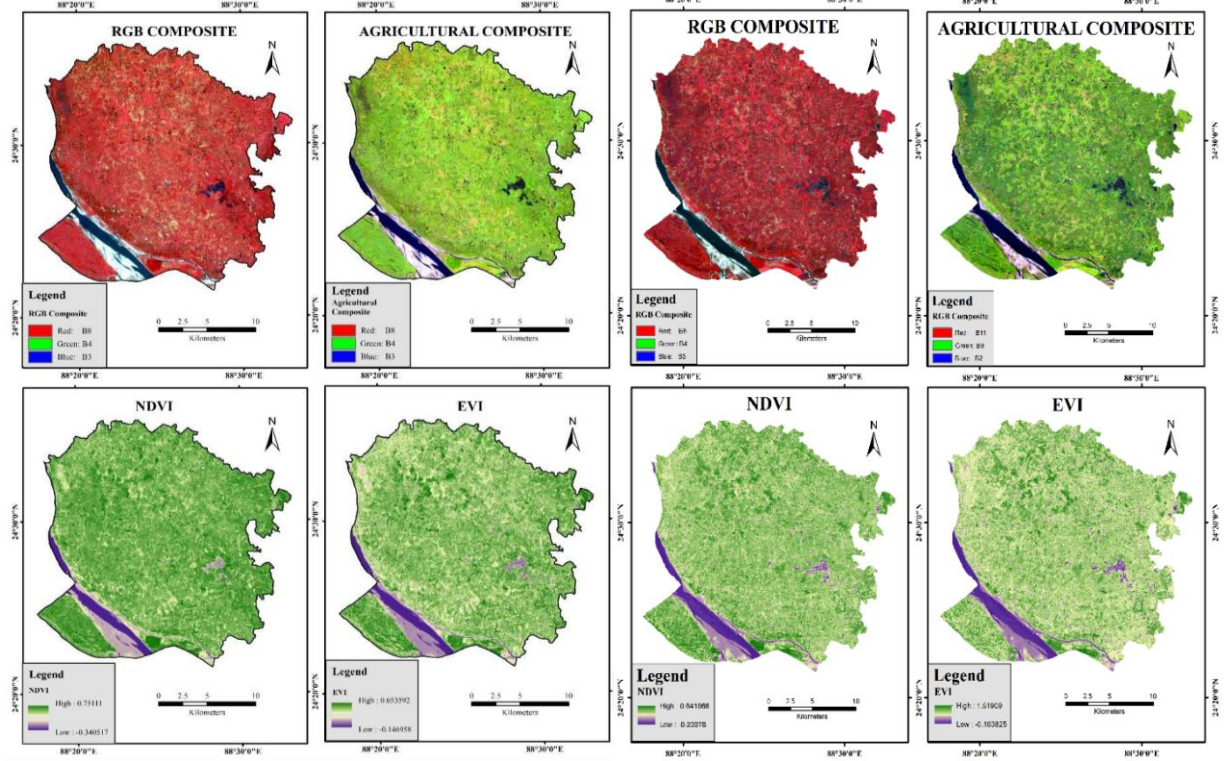


Figure 17. Vegetation indices value of target crop types derived using Sentinel-2 bands

The above season-wise monthly median time-series images (Fig. 10-15) were stacked together to make a seasonal composite (Fig. 18) of the study area. All the bands of this Sentinel-2A median composite were resampled to 10 meters using custom JavaScript code in GEE. NDVI and EVI as vegetation indices were also derived in the GEE platform to include in the classification procedure (Fig. 17).

SENTINAL-2A IMAGERY IN GODAGARI UPAZILA
Dry Season (Oct.20-Mar.21)

SENTINAL-2A IMAGERY IN GODAGARY UPAZILLA
Dry Season (Oct.21-Mar.22)



SENTINAL-2A IMAGERY IN GODAGARY UPAZILLA
Dry Season (Oct.22-Mar.23)

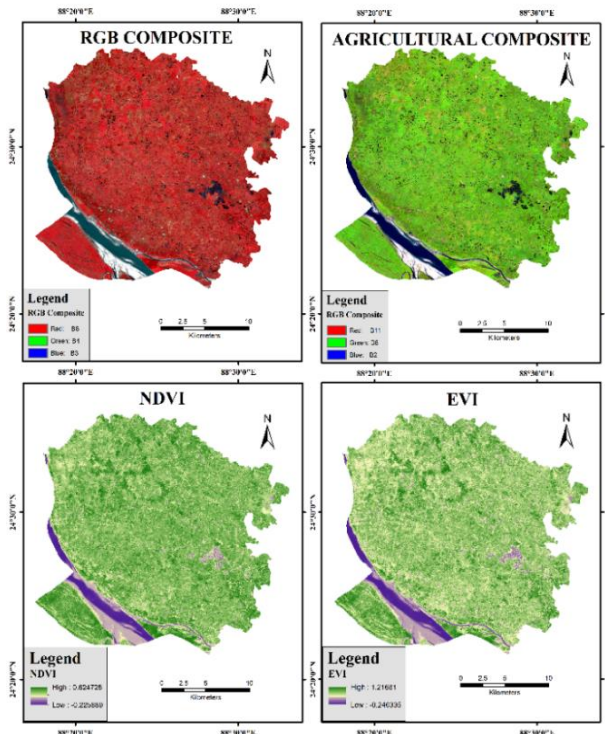


Figure 18. Seasonal median images of Sentinel-2A for 2020-21, 2021-22 and 2022-23

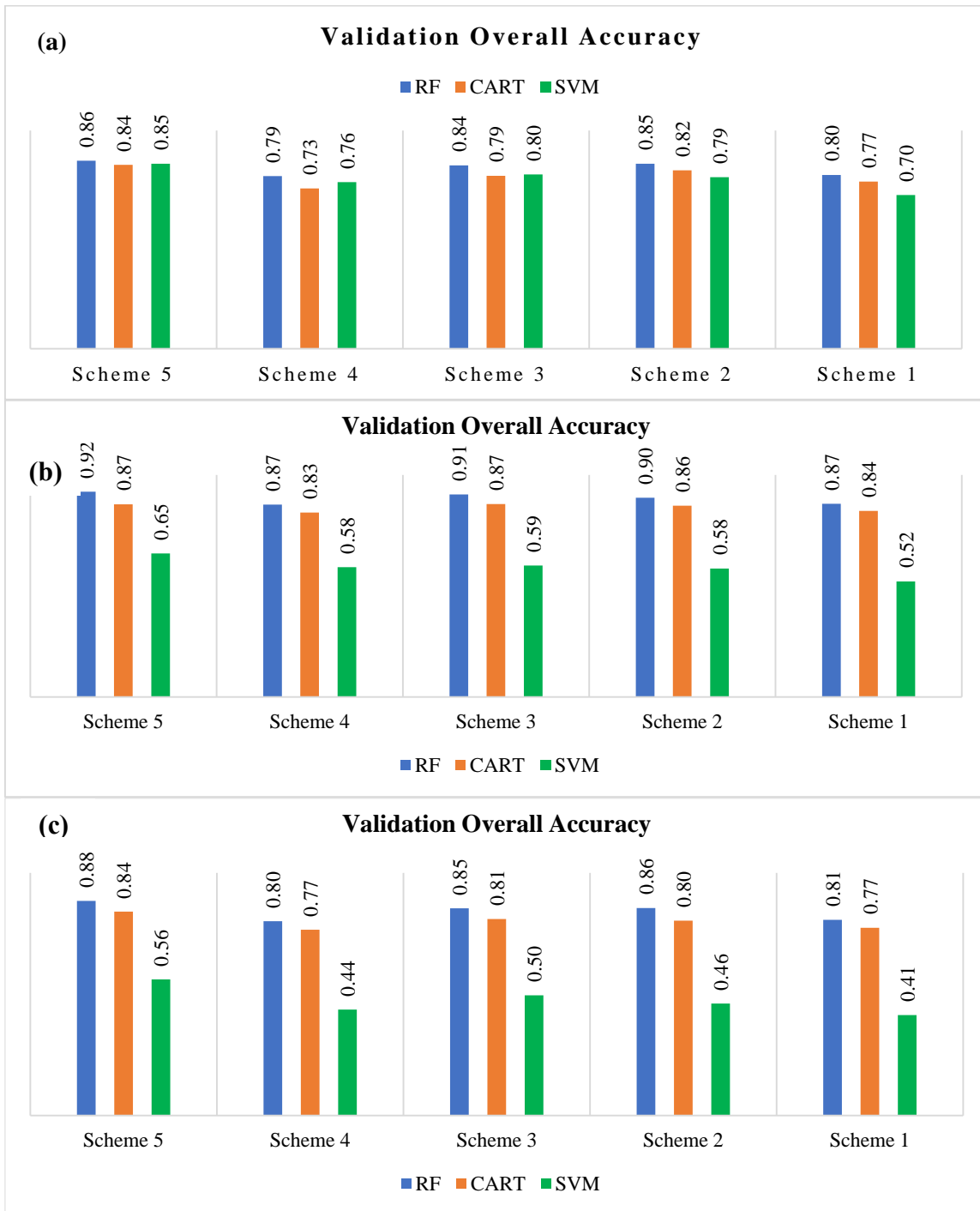


Figure 19. Classification accuracy based on Machine Learning Algorithms using different experimental schemes for season (a) 2020-21 (b) 2021-22 and (c) 2022-23

Furthermore, a few experiments by combining these bands and indices into five distinct schemes was investigated to classify the crop types precisely. The performance of the selected three machine learning algorithms (RF, CART and SVM) using different experimental schemes are represented in Figure 19. Among all the schemes, higher accuracies were found in scheme 5 which includes all ten spectral bands

along with 2 selected vegetation indices. Random Forest (0.86, 0.92 and 0.88) showed the highest accuracy for 2020-21, 2021-22 and 2022-23 cropping season followed by CART (0.84, 0.87 and 0.84), and SVM (0.85, 0.65 and 0.56) accordingly.

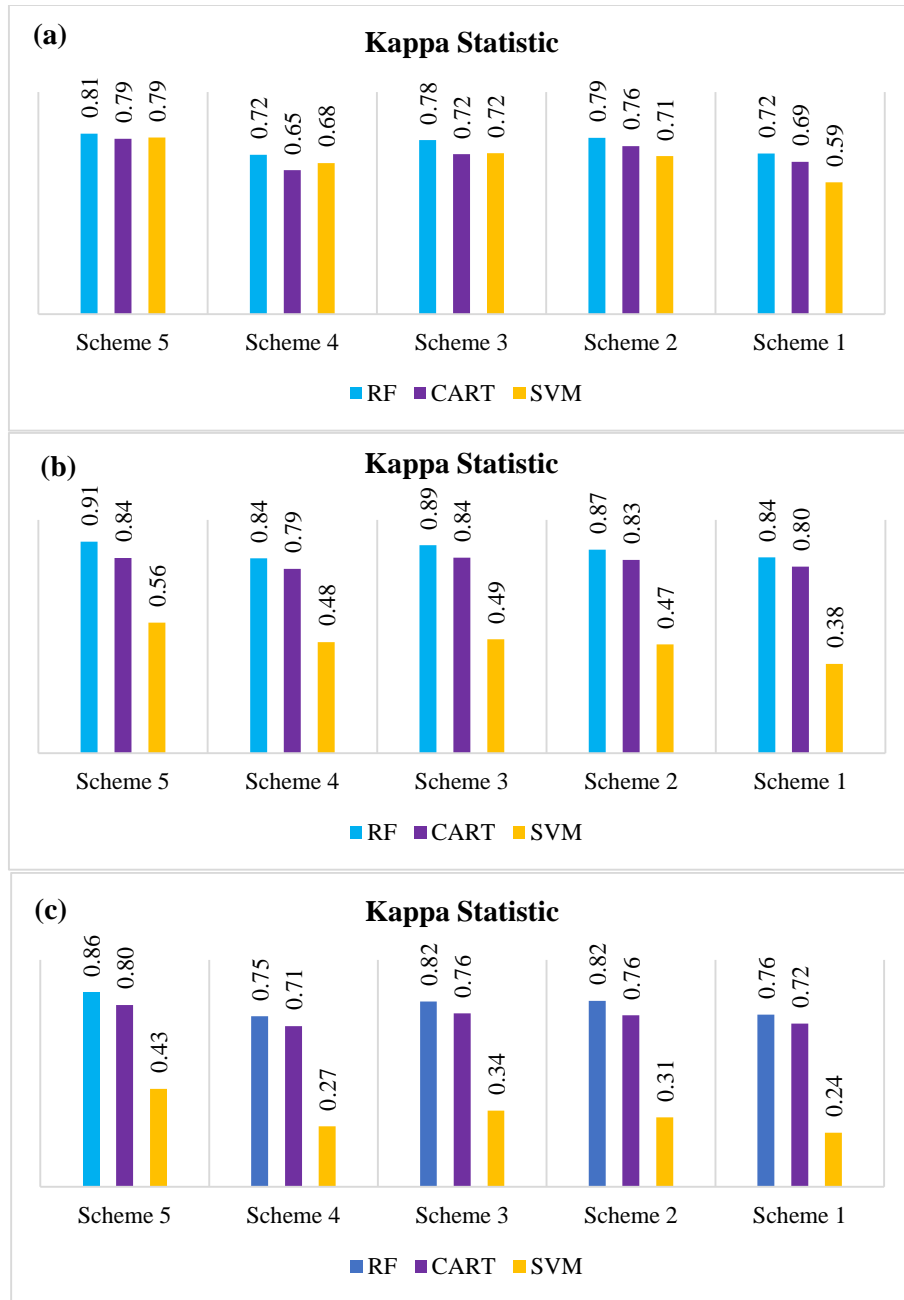


Figure 20. Kappa Statics from classification procedure using different experimental schemes for season (a) 2020-21, (b) 2021-22, and (c) 2022-23

Kappa statistics of the classification trials are represented in Figure 20. All the machine learning algorithms performed better in scheme five and RF was found to be the best (0.81, 0.91, and 0.86) for the 2020-21, 2021-22, and 2022-23 performing among other algorithms. On the other hand, the F1 Score from the experiments is represented in Figure 21. Overall, the highest F1 score (82%) was found in scheme 2 using

SVM while the minimum (50%) was found in scheme 4 using CART. SVM was found to have the highest value of all schemes followed by RF and CART accordingly. On the other hand, for the 2021-22 and 2022-23 cropping seasons, RF showed the highest F1 score around 93% and 87% while SVM present the minimum F1 for both cropping seasons.



Figure 21. F1 Score of different experimental schemes schemes for season (a) 2020-21, (b) 2021-22, and (c) 2022-23

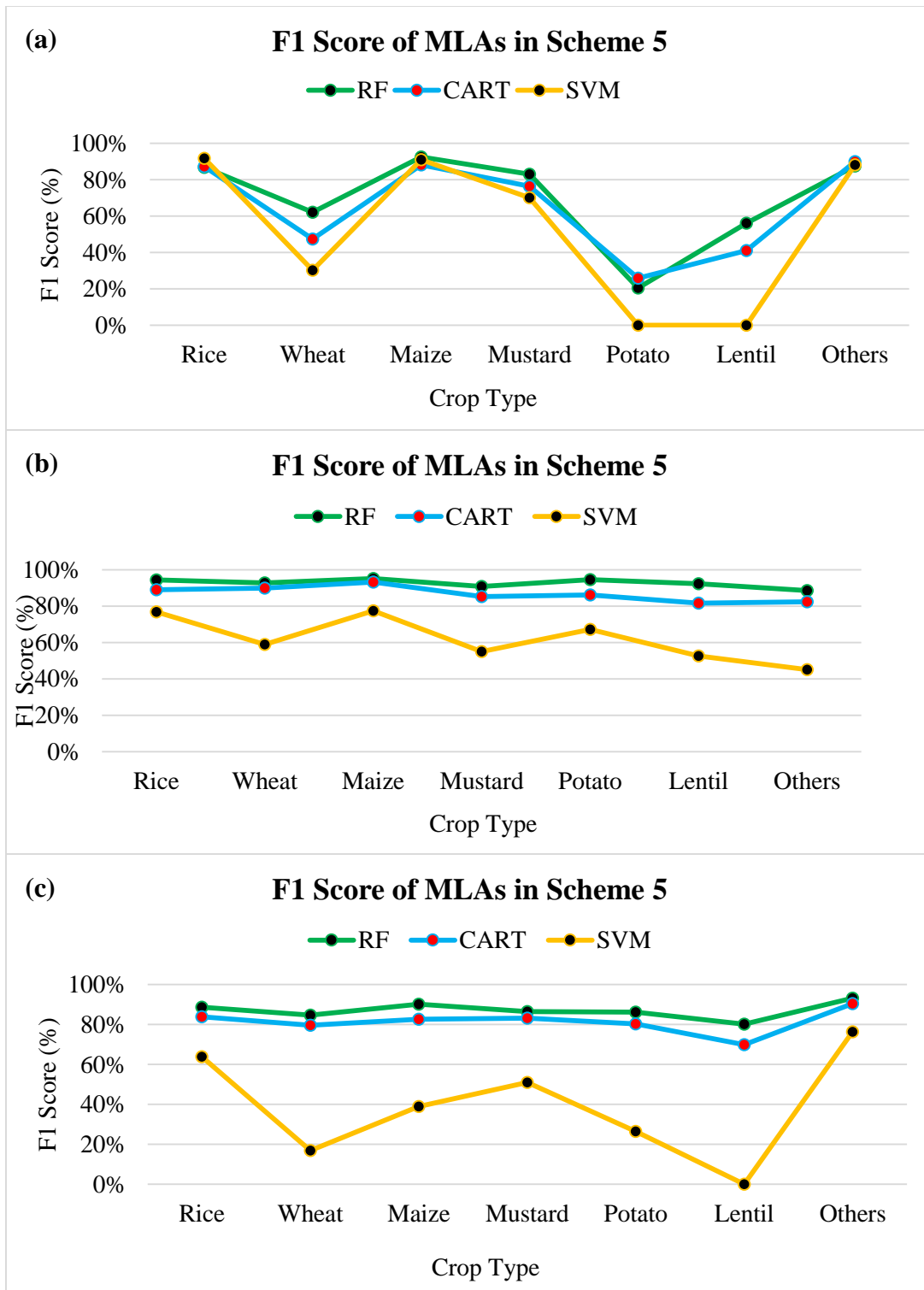


Figure 22. F1 Score of different MLAs in scheme 5 for season (a) 2020-21, (b) 2021-22, and (c) 2022-23

The F1 Score of different MLAs is shown in Figure 22. In scheme 5, all the MLAs were found better for rice, maize, mustard, and others. For wheat and lentil, RF performed better while CART for potato. So,

based on the above evaluation matrices (OA, Kappa coefficient, and F1 Score), Random Forest along with scheme 5 has been considered the most suitable Machine learning algorithm to classify 6 major crop types for the study area. The confusion matrix of the RF classifier using scheme 5 has been represented in Table 9.

Table 9. Accuracy assessment matrix for season (a) 2020-21 (b) 2021-22 and (c) 2022-23.

Confusion Matrix for 2020-21 RF (Scheme 5)										
Crop Type		Classified Data							Total	PA
		Rice	Wheat	Potato	Maize	Mustard	Lentil	Others		
Reference Data	Rice	2440	23	74	7	1	1	11	2557	95%
	Wheat	70	189	10	23	0	0	14	306	62%
	Potato	59	0	1473	0	1	7	7	1547	95%
	Maize	87	22	0	676	0	0	62	847	80%
	Mustard	36	1	23	0	9	4	2	75	12%
	Lentil	0	19	31	0	1	66	29	146	45%
	Others	371	48	25	74	1	11	2308	2838	81%
Total		3063	302	1636	780	13	89	2433	8316	
UA		80%	63%	90%	87%	69%	74%	95%	OA=	86%
Confusion Matrix for 2021-22 RF (Scheme 5)										
Crop Type		Classified Data							Total	PA
		Lentil	Maize	Mustard	Rice	Potato	Wheat	Others		
Reference Data	Lentil	102	3	7	1	0	0	0	113	90%
	Maize	0	119	0	0	0	2	0	121	98%
	Mustard	2	0	152	7	0	2	3	166	92%
	Rice	0	0	0	343	0	0	3	346	99%
	Potato	1	0	2	0	60	0	0	63	95%
	Wheat	0	2	2	2	2	83	0	91	91%
	Others	3	5	6	28	2	1	196	241	81%
Total		108	129	169	381	64	88	202	1141	
UA		94%	92%	90%	90%	94%	94%	97%	OA=	92%
Confusion Matrix for 2022-23 RF (Scheme 5)										
Crop Type		Classified Data							Total	PA
		Lentil	Maize	Mustard	Rice	Potato	Wheat	Others		
Reference Data	Lentil	97	2	15	2	0	3	6	125	78%
	Maize	0	178	10	6	0	2	6	202	88%
	Mustard	7	1	567	19	5	11	7	617	92%
	Rice	8	4	41	473	0	5	12	543	87%
	Potato	0	2	16	0	109	2	4	133	82%
	Wheat	0	4	18	16	6	236	7	287	82%
	Others	5	2	28	8	0	11	650	704	92%
Total		117	193	695	524	120	270	692	2611	
UA		83%	92%	82%	90%	91%	87%	94%	OA=	88%

Note: OA = Overall accuracy, PA = Producer accuracy & UA = User accuracy

The overall accuracy has been achieved at 86%, 92%, and 88% during 2020-21, 2021-22, and 2022-23 accordingly for all the target classes (Table 9). Maximum PA was found for rice (99%) during the 2021-22 season and maize (98%) followed by others, maize, wheat, lentil, and mustard accordingly. On the other hand, maximum UA was found for others (97%) for the season 2021-22 and others (94%) during 2020-22 followed by potato, maize, rice, lentil, mustard, and wheat respectively. So, based on these accuracy matrices it can be said that rice, potato, and maize can be classified quite well rather than mustard, lentil, and wheat. Poor accuracy can appear due to a smaller number of samples or the spectral resolution of the sensors. An increased number of reference data along with high-resolution sensor data like UAVs might mitigate these issues in future tasks.

Crop suitability analysis

The cropland-suitability classes of Rabi crops, namely rice, wheat, maize, mustard, potato, and lentil rice, were estimated using climatic, soil, and topographical parameters, which are consistent with other previous research results. Since GIS provides flexibility and accuracy in the land-use organization, several studies have emphasized the technique of GIS combined with AHP for integrating expert opinion in pairwise comparison among criteria at each hierarchy level, which is comparable to the approach used in this work. While the accuracy of the weights used is subjective, as evaluated by experts, relative weights findings were included in the cropland-suitability evaluation since the consistency ratios were within the stated acceptable ranges (0.1). Consistency ratios of rice, wheat, maize, mustard, lentil, and potato (Table 10-15) were computed as 0.089, 0.073, 0.082, 0.09, 0.09, and 0.1, respectively, and are regarded acceptable.

The results showed that integrating the AHP technique with GIS may help policymakers and planners make better decisions. It is essential to assess the amount and types of farmland suitability in the state for cereal crops to pick the best crop for the target location. During this examination, the crops' particular requirements were compared with the land characteristics, and the area's appropriateness for the crops was assessed based on the degree of matching. The categorization was based on the intrinsic soil qualities, exterior land features, and climatic elements that limited the land's use for various purposes.

In the AHP analysis, the weight of eleven factors was determined crop by crop to establish the importance of the criteria about each other, which affects the final suitability map of each crop. According to the AHP findings, land type was the most significant factor, accounting for 32.8% of the weightage in the case of the wheat crop. Temperature, on the other hand, was the most essential factor for rice, accounting for 23.1% of the weightage. Wheat and rice have the least significant dem, slope, and aspect. Land type, temperature, and rainfall were found to be the most relevant parameters with weights for maize, potato, mustard, and lentil (Tables 10-15). Since the predicted score was determined using a ratio scale, these preferences are mathematically correct and intuitively obvious.

A land-suitability study was conducted to determine the extent and level of the land's capacity to produce different crops (rice, wheat, sorghum, rice, maize, mustard, potato and lentil). To evaluate the appropriateness of the target region for various crops taking into account particular meteorological factors, and topographical and physicochemical land features, the AHP and GIS approach were integrated. This research shows that using identical soil properties in a particular agro-climatic zone under intentional management approaches might result in greater crop output. After running the program, the suitability maps for each crop were produced.

Based on the results (Table 17 and Figure 28), 52.99% of the land is moderately good for growing rice. In contrast, 71.71% of the calculated arable land is made up of land that is only "marginally suitable." The main problems with growing rice in the area being studied are the lack of organic carbon, the fact that the soil drains well to almost too well, and the fact that it doesn't rain much in this area. The results of the AHP analysis of how well the wheat crop fits are shown in Table 17 and Figure 23b. Based on the results, only 10.68% of the farmland is good for growing wheat. Most of the calculated arable area (61.71%) is made up of areas that are only somewhat suitable. On the other hand, 14.97% of the calculated arable land is

"marginally suitable." The result showed that moderately suitable for lentil production includes the most land, with 60.39% of the calculated arable region. Due to good conditions, about 6.53% of the land in almost all districts is highly suitable, while only 20.37% of the arable land is marginally suitable. The results of the maize-suitability assessment showed that 56.62% of the calculated arable region for maize was in the moderately suitable category.

Table 15: Pairwise comparison matrix and parameters' weights in AHP for potato crop

Crops	Criteria	Temperature	Rainfall	DEM	Slope	Aspect	Soil Moisture	Soil Reaction (pH)	Soil Texture	Soil Consistency	Soil Type	Land Type
Rice	Weight	23.1%	8.8%	2.9%	3.0%	3.1%	14.7%	16.6%	8.6%	7.3%	13.5%	20.7%
	λ_{max}	12.350										
	Consistency Index	0.135										
	Consistency Ratio	0.08944										
	Constant	1.51										
Wheat	Weight	30.4%	8.6%	3.0%	2.6%	3.9%	15.9%	20.5%	4.6%	8.2%	15.9%	32.8%
	λ_{max}	12.113										
	Consistency Index	0.111										
	Consistency Ratio	0.07373										
	Constant	1.51										
Maize	Weight	30.4%	7.3%	3.0%	3.2%	3.7%	16.8%	20.5%	5.0%	8.2%	16.8%	32.5%
	λ_{max}	12.239										
	Consistency Index	0.124										
	Consistency Ratio	0.08205										
	Constant	1.51										
Lentil	Weight	32.1%	7.2%	3.2%	2.9%	2.7%	17.9%	20.4%	4.5%	8.4%	18.5%	32.6%
	λ_{max}	12.084										
	Consistency Index	0.108										
	Consistency Ratio	0.07177										
	Constant	1.51										
Mustard	Weight	31.5%	8.8%	2.9%	3.0%	5.3%	15.3%	18.2%	4.8%	7.6%	15.9%	28.4%
	λ_{max}	12.353										
	Consistency Index	0.135										
	Consistency Ratio	0.08962										
	Constant	1.51										
Potato	Weight	29.4%	9.2%	3.9%	2.8%	4.6%	15.2%	16.2%	6.5%	6.7%	14.6%	26.0%
	λ_{max}	12.353										
	Consistency Index	0.135										
	Consistency Ratio	0.08962										
	Constant	1.51										

Outputs/Results

Crop type mapping

Considering RF in Scheme 5 as the most suitable MLA, the classified map for the 2020-21 dry season is represented in Figure 22, and different crop types are represented in the inset maps. The total area covered by each crop type is represented in Table 10. The results showed that rice covered 22253.46 (45.17%) maximum area of the Godagari Upazila. Other's area had the second-highest area coverage which is more than 28% (14107.45 ha) of the study area.

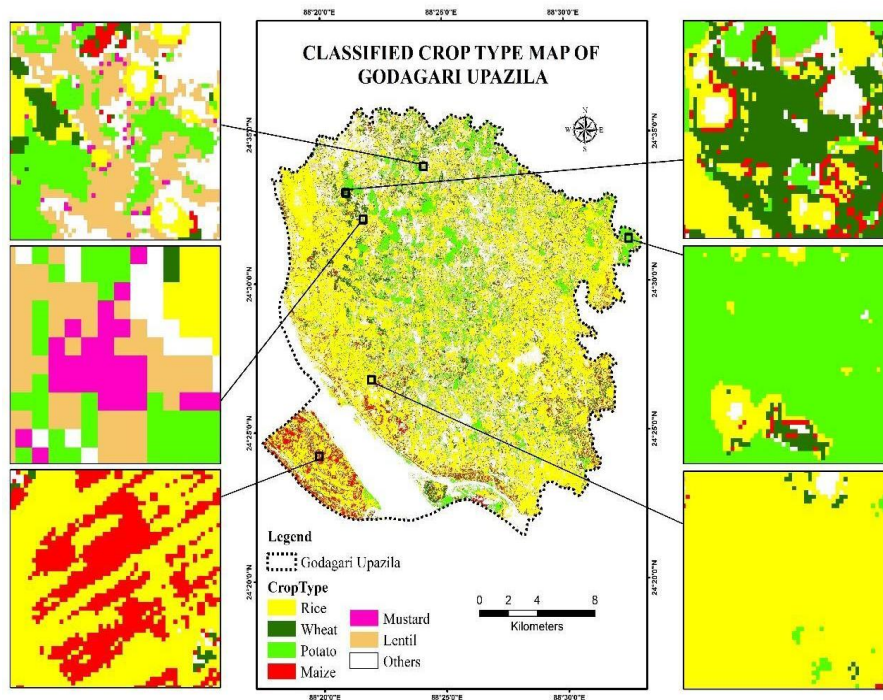


Figure 23. Classified crop type map of Godagari Upazila during 2020-21dry season

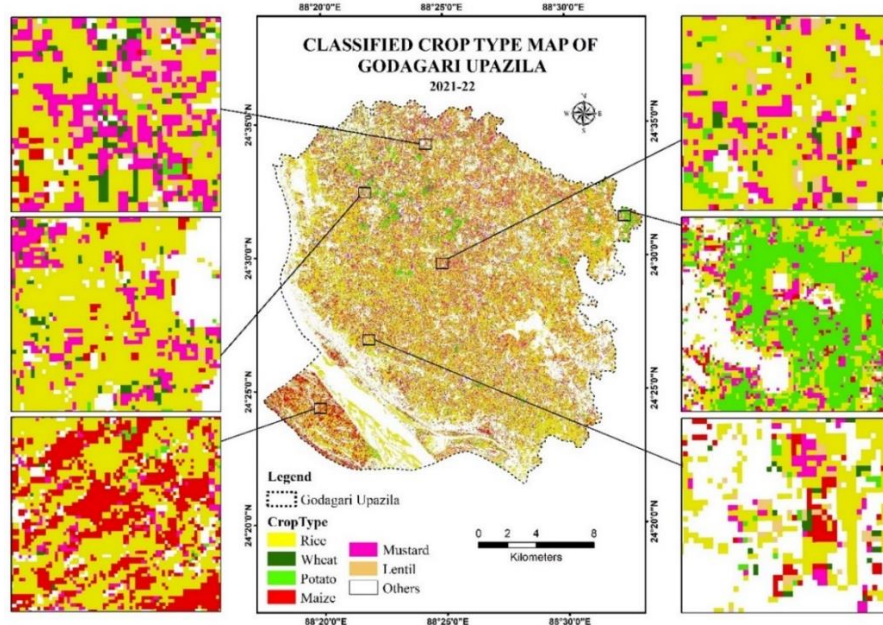


Figure 24. Classified crop type map of Godagari Upazila during 2021-2022 dry season

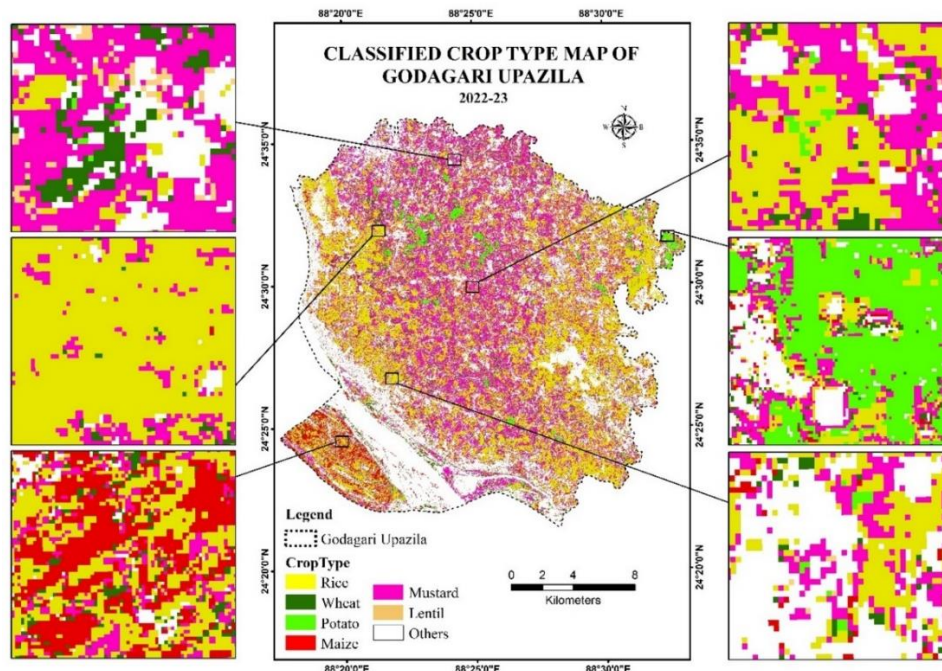


Figure 25. Classified crop type map of Godagari Upazila during 2022-2023 dry season

On the other hand, potato (9.31%), wheat (6.75%), lentil (5.15%), maize (4.66%), and mustard (0.32%) covered 4588.75 ha, 3326.96 ha, 2535.75 ha, 2296.02 ha, and 159.63 ha accordingly. Maize and lentil occupied equally about 5% of the whole study area but mustard covered only 0.32% which was very small compared to other crop types. For Cropping Season 2021-22 and 2022-23, the area occupied for rice (36.72% and 28.86%) has dropped while mustered cultivation was busted (0.32% to 12.38%, and 26.89%) according to analysis.

Table 17. Distribution of area (hector) coverage and percentage of classified crop types

Class Name	Area (ha)	Area (%)
2020-21		
Rice	22253.46	45.17%
Wheat	3326.96	6.75%
Potato	4588.75	9.31%
Maize	2296.02	4.66%
Mustard	159.63	0.32%
Lentil	2535.75	5.15%
Others	14107.45	28.63%
Total	49268	100%
2021-22		
Rice	15875.61	32.22%
Wheat	1947.55	3.95%
Maize	1445.775	2.93%
Mustard	9659.31	19.61%
Potato	1746.707	3.55%
Lentil	4086.375	8.29%
Others	14506.69	29.44%
Total	49268	100%

2022-23		
Rice	10888.6	22.10%
Wheat	2753.165	5.59%
Maize	1878.546	3.81%
Mustard	14367.67	29.16%
Potato	711.9434	1.45%
Lentil	1460.911	2.97%
Others	17207.18	34.93%
Total	49268	100%

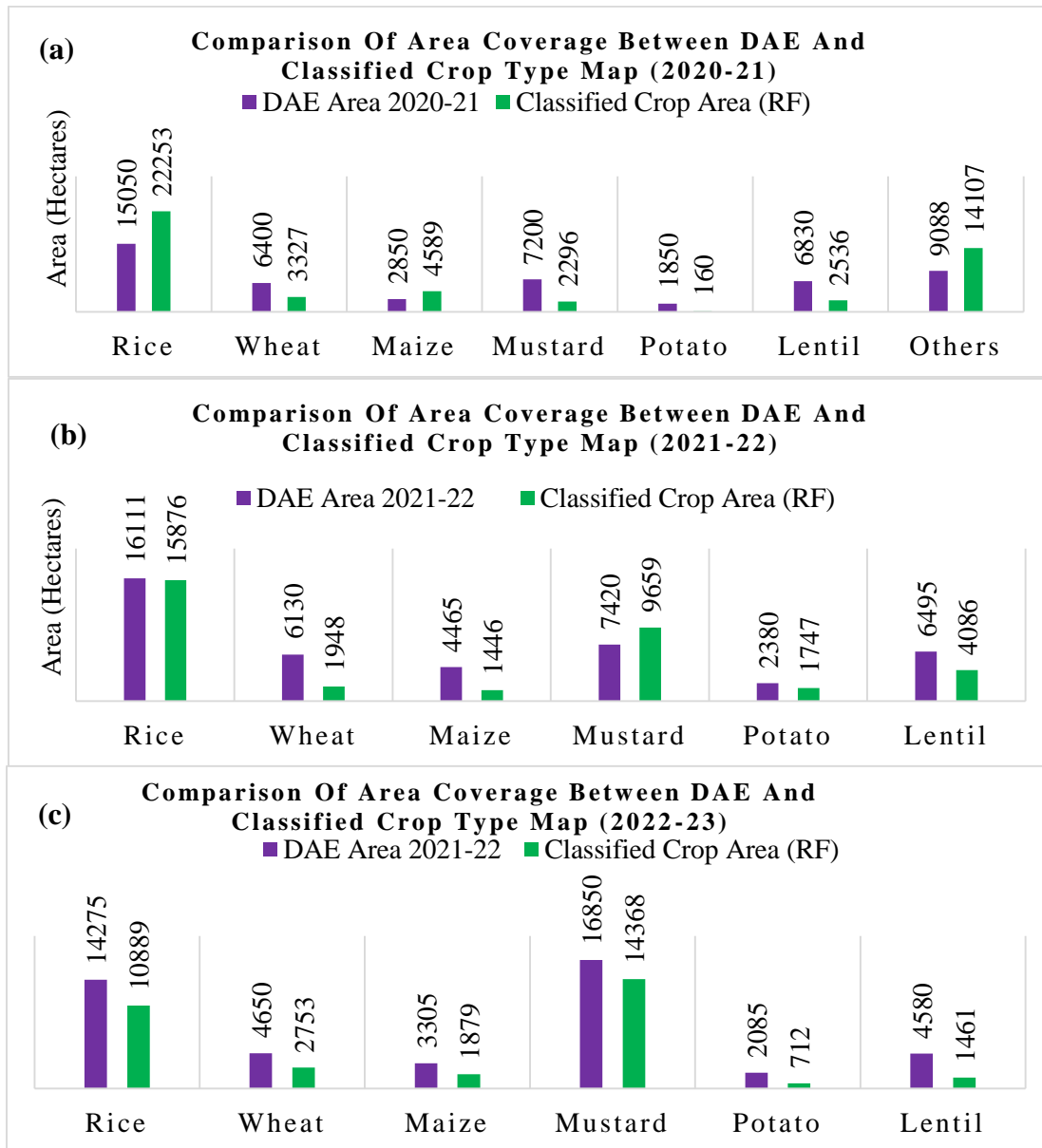


Figure 26. Comparison of area coverage between DAE data and classified crop type map (2020-2021)

Crop Suitability analysis

The area coverage of different crop types was compared to the DAE dataset as shown in Figure 24. The MLA (RF) over-estimated area coverage for rice, maize, and others but under-estimated for wheat, mustard, potato, and lentil for season 2020-21 while for 2021-22 and 2022-23 except rice almost all crops showed under-estimated (Fig. 25). Percent deviation, as well as areal underestimation or overestimation, is shown in Figure 22. The minimum deviation was found for rice (48%, overestimated) and wheat (48%, underestimated) while the maximum (91%, underestimated) was found for potato.

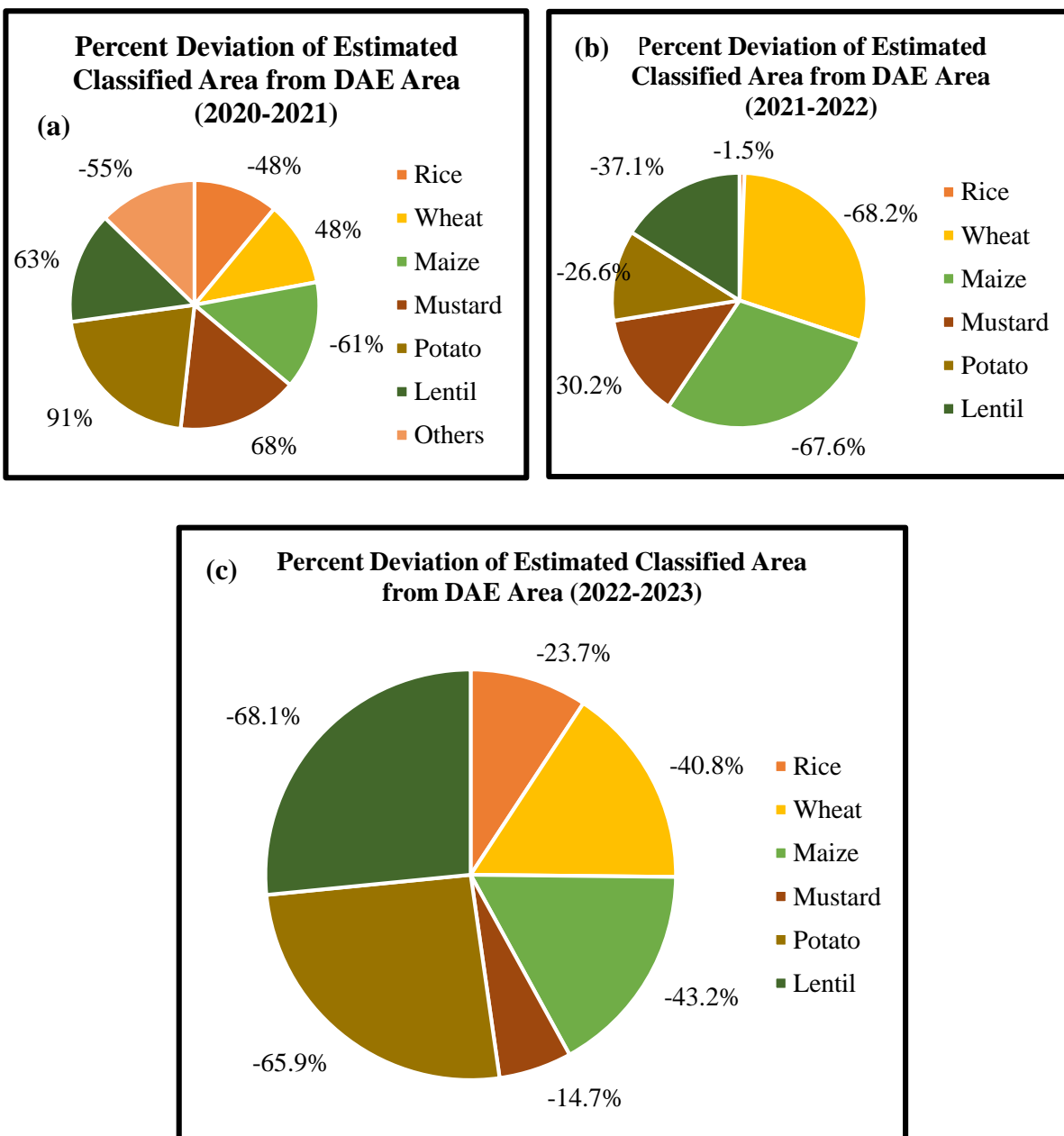


Figure 27. Percent deviation in area coverage by classified crop types to DAE dataset of 2020-2021 cropping season

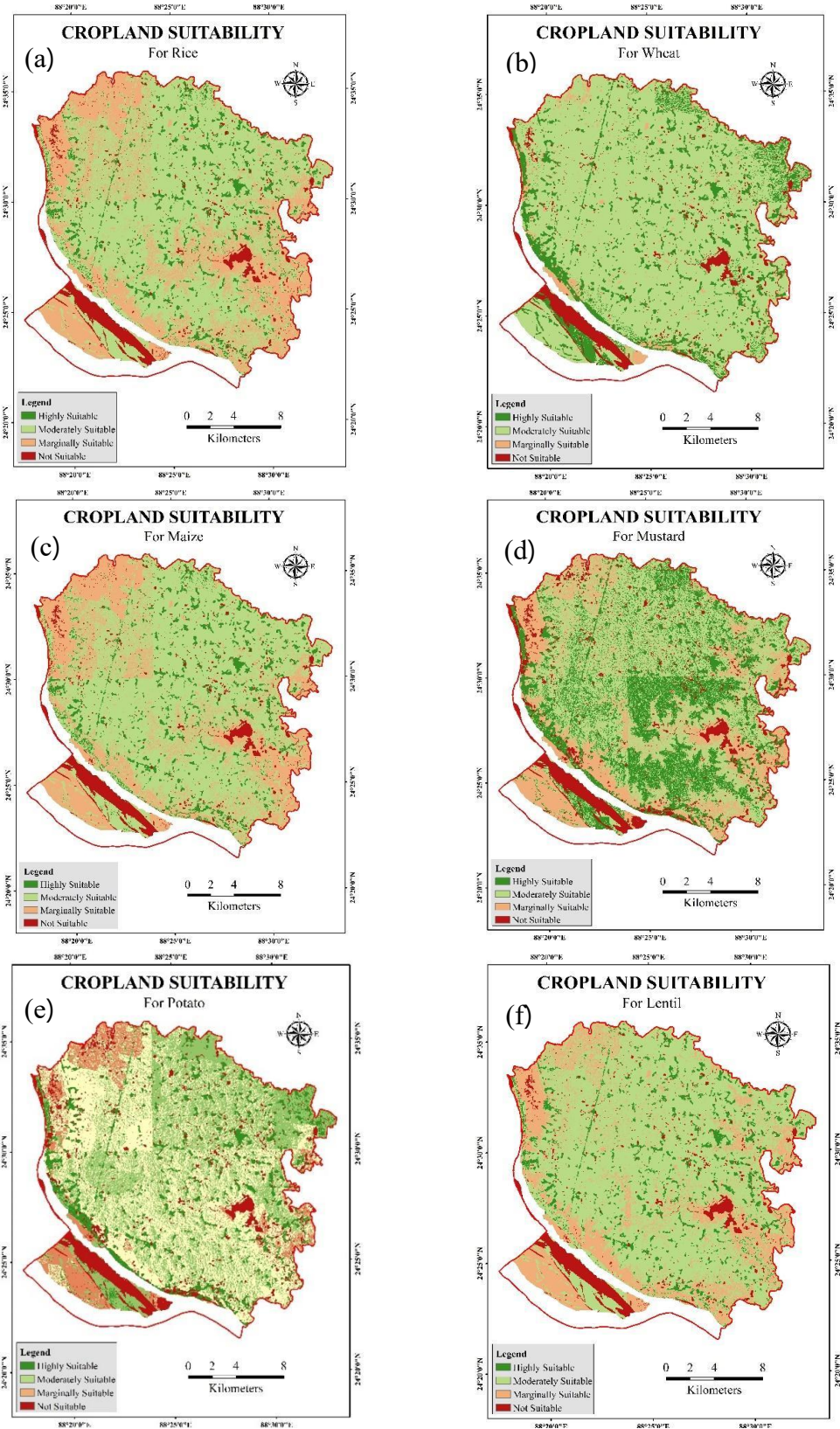


Figure 28: Crop Suitability Map for (a) Rice, (b) Wheat, (c) Maize, (d) Mustard,

Table 18: The distribution of crop suitability classes with crop specific area coverage

Class/Area	Rice		Wheat		Maize		Mustard		Potato		Lentil	
	Hectare	%	Hectare	%	Hectare	%	Hectare	%	Hectare	%	Hectare	%
S1	3024.1	6.2	5234.7	10.7	3246.3	6.6	1957.9	4.0	4381.8	8.9	3202.3	6.5
S2	25930.2	53.0	30252.8	61.7	27756.8	56.6	16834.7	34.3	14252.6	29.1	29604.2	60.4
S3	13756.4	28.1	7340.6	15.0	11755.5	24.0	22114.0	45.1	23863.4	48.7	9987.5	20.4
N	6220.9	12.7	6193.2	12.6	6262.7	12.8	8114.7	16.6	6523.5	13.3	6227.2	12.7
S1+S2	28954.2	59.2	35487.5	72.4	31003.0	63.2	18792.6	38.3	18634.4	38.0	32806.5	66.9
S1+S2+S3	42710.6	87.3	42828.0	87.4	42758.6	87.2	40906.5	83.4	42497.8	86.7	42794.1	87.3

S1= Highly Suitable, S2= Moderately Suitable, S3= Marginally Suitable, and N= Not Suitable

For example, Figure 10 shows the model made for wheat crop suitability, and Table 17 shows how the different crop suitability classes are spread out (by percentage of area covered) for each crop. Figure 26 shows the map for each crop that shows where it will grow best.

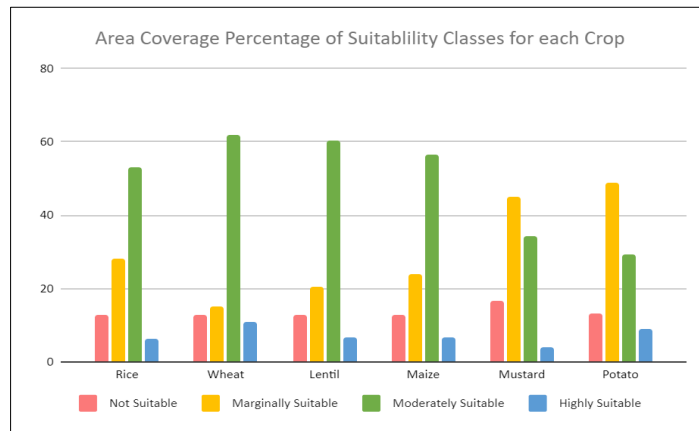


Figure 29: Area coverage percentage of suitability classes for each crop

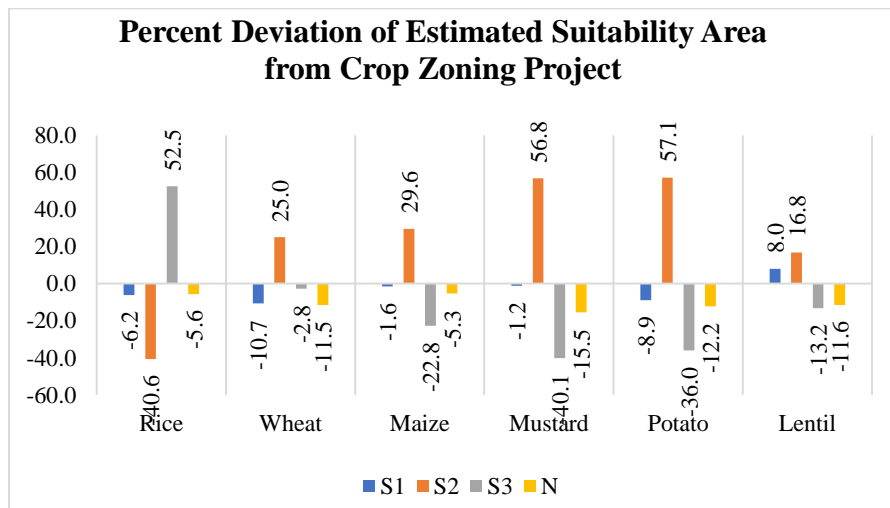


Figure 30: Percent deviation in area coverage by suitability tool to crop zoning project

On the other hand, sandy soil and slightly too much drainage made only 23.98% of the calculated arable land marginally suitable (Tab. 17 and Fig. 23). The analysis of the land's suitability showed that mustard is a crop that does not grow well on most of the state's land. The result showed that 45.11% of the calculated arable region is in the "marginally suitable" category, which is the most important for mustard. Even though 34.34% of the calculated arable land is moderately suitable, some of the target area falls into the highly suitable group because of the way things are now. The results showed that 29.07% of the land is only somewhat good for growing potatoes. In contrast, 71.71% of the arable land is considered to be marginally suitable. Besides wheat (72.4%), lentils (66.9%) and maize (63.2%) are the most dominating crops which may be cultivated based on their combined share of highly suitable and moderate suitability.

Conclusions and Recommendations

The crop type mapping and cropping pattern analysis in our study reveals that the major study area has substantial potential for major less irrigated Rabi crops production among which wheat, lentil, and maize would be the most dominating crops in crop suitability for this region with 72.39%, 66.92%, and 63.24% respectively whereas, high irrigated Boro rice (59.17%) is found to be the less suitable rabi crop than wheat, lentil, and maize. The results of the study can be utilized by policymakers in the study areas and at having similar soil and climatic conditions of any areas to adopt a proper crop production strategy, providing special agricultural incentive policies as a provision for the increased food production of our country.

Accurate crop type mapping and crop suitability assessment by Remote Sensing and Geospatial modeling using Machine Learning Algorithms is a crucial prerequisite for monitoring agricultural productivity. However, this remote sensing-based crop type is quite difficult for Bangladesh conditions even during the Rabi/dry season, particularly due to small plot sizes and high heterogeneity in their spatial and temporal distribution. The study brought out the spatial distribution of selected crops derived from geospatial modeling in conjunction with machine learning and evaluation of climatic, soil, and morphological variables in a GIS context. This study is a scientific evaluation that provides information at a local level that could be used by judicious utilization of valuable natural resources help to develop policies of decision makers ensuring the food security of a country and farmers to select crops for their fields. Additionally, the results of this study could be useful for other investigators who could use these results for diverse studies. For further study, we propose to select a greater and more diverse area to develop algorithms to assess the whole country.

Recommendations

- Policymakers may use the study's findings to develop a crop production plan and provide special agricultural incentive programs to boost our nation's food supply.
- The study findings may be utilized in other projects associated with BARI, BRRI, BINA, and other relevant organizations.
- Similar studies may be carried out in other regions to develop location/case-specific methodologies as cropping pattern varies region to region with different time frames.
- Usages of microwave and lidar sensors may enhance the capabilities to carry out the study in all year round.

Bibliography

- Ahmad, M. ud D. *et al.* (2014). Groundwater use for irrigation and its productivity: status and opportunities for crop intensification for food security in Bangladesh. *Water Resources Management*, 28(5):1415–1429.
- Akpoti, Komlavi, Amos T. Kabo-bah, and Sander J. Zwart. (2019). Agricultural land suitability analysis: state-of-the-art and outlooks for integration of climate change analysis. *Agricultural Systems* 173:172–208. doi: 10.1016/j.agry.2019.02.013.

- Amy McNally NASA/GSFC/HSL (2018). FLDAS Noah Land Surface Model L4 Global Monthly 0.1 x 0.1 degree (MERRA-2 and CHIRPS), Greenbelt, MD, USA, Goddard Earth Sciences Data and Information Services Center (GES DISC), Accessed: 10.5067/5NHC22T9375G
- Bell, A.R. *et al.*, (2015). Rice productivity in Bangladesh: What are the benefits of irrigation? *Land Use Policy*, 48:1–12.
- Bill, O, Bolvin, D. and Huffman, G. (2019). Land/Sea static mask relevant to IMERG precipitation 0.1x0.1 degree V2, Edited by David Silberstein, Greenbelt, MD, Goddard Earth Sciences Data and Information Services Center (GES DISC), Accessed: 10.5067/6P5EM1HPR3VD
- Bishop C. M. (2006). Pattern recognition and machine learning. Springer. pp. 1-758.
- Breiman, L. 2001. Random forests. *Mach. Learn.* 45: 5–32.
- Brown, C.F., Brumby, S.P., Guzder-Williams, B. *et al.* (2022). Dynamic World, Near real-time global 10 m land use land cover mapping. *Sci Data* 9:251. doi:10.1038/s41597-022-01307-4
- Earth Resources Observation and Science (EROS) Center, (2017). Shuttle radar topography mission (SRTM) 1 arc-second global [Tiff].
- FAO (1976). A framework for land evaluation. FAO Soils bulletin 32. Food and Agriculture Organization of the United Nations, Rome, Italy.
- Fujita, F. and Hossain, F. (1995). Role of the groundwater market in agricultural development and income distribution: a case study in northwest Bangladesh village. *The Developing Economies*, 33(4):442–463.
- Garnett, T. *et al.* (2013). Sustainable Intensification in Agriculture: Premises and Policies. *Science*, 341: 33–34.
- Godfray, H.C.J. *et al.* (2010). Food Security: The Challenge of Feeding 9 Billion People. *Science*, 327:812–818.
- Gorelick, N.(2012). Google Earth Engine. *AGU Fall Meeting Abstracts*, 15:11997. Available at: <http://adsabs.harvard.edu/abs/2012AGUFM.U31A..04G>.
- Gumma, M. K., Tummala, K., Dixit, S., Collivignarelli, F., Holecz, F., Kolli, R. N., and Whitbread, A. M. (2020). Crop type identification and spatial mapping using Sentinel-2 satellite data with focus on field-level information. *Geocarto International*, 37(7):1833–1849. <https://doi.org/10.1080/0106049.2020.1805029>
- Halder, J. C. (2013). Land Suitability assessment for crop cultivation by using remote sensing and GIS. *Journal of Geography and Geology* 5(3): 65-74. doi: 10.5539/jgg.v5n3p65.
- Haq, N. (2013). Fresh Water “More Precious Than Gold” in Bangladesh [Inter Press Service News Agency. Available at: <http://www.ipsnews.net/2013/05/fresh-water-more-precious-than-gold-in-bangladesh/> [Accessed November 22, 2016].
- Hastie, T., Tibshirani, R. and Friedman, J. H. (2009). 10. Boosting and Additive Trees. *The Elements of Statistical Learning* (2nd ed.). New York: Springer. pp. 337–384. ISBN 978-0-387-84857-0. Archived from the original on 2009-11-10.
- Inglada, J., Arias, M., Tardy, B., Hagolle, O., Valero, S., Morin, D., Dedieu, G., Sepulcre, G., Bontemps, S., Defourny, P. and Koetz, B. (2015). Assessment of an operational system for crop type map production using high temporal and spatial resolution satellite optical imagery. *Remote Sensing*, 7(9): 12356–12379. <https://doi.org/10.3390/rs70912356>
- Kirby, M. *et al.* (2013). Review of water, crop production and system modelling approaches for food security studies in the Eastern Gangetic Plains, Available at: www.csiro.au.

- Krupnik, T. J. *et al.* (2017). Sustainable crop intensification through surface water irrigation in Bangladesh? A geospatial assessment of landscape-scale production potential. *Land Use Policy*, 60:206–222.
- Kumbhar, V., Das, S., Kumar, R., Road, C., Model Colony Pune, Gokhale Cross Road, and Model Colony. (2014). Assessment of crop suitability analysis for drought prone areas in semi-arid regions of Maharashtra India using geospatial technology. *American International Journal of Research in Science, Technology, Engineering and Mathematics* 7(3):256–61.
- Loh, W. Y. (2011). Classification and regression trees. *Wiley Interdisciplinary Reviews: Data Mining and Knowledge Discovery*, 1(1):14–23. doi:10.1002/widm.8.
- Maddahi, Z., Jalalian, A., Masoud, M., Zarkesh, K. and Honarjo, N. (2014). Land suitability analysis for rice cultivation using multi criteria evaluation approach and GIS. *European Journal of Experimental Biology*, 4(3): 639–648.
- Mainuddin, M. *et al.* (2014). Sustaining water resources for food security in Bangladesh, Available at: <https://publications.csiro.au/rpr/download?pid=csiro:EP147265&dsid=DS1>.
- Mainuddin, M. and Kirby, M. (2015). National food security in Bangladesh to 2050. *Food Security*, 7(3):633–646.
- Moore, R.T. and Hansen, M.C. (2011). Google Earth Engine: a new cloud-computing platform for global-scale earth observation data and analysis. In AGU Fall Meeting Abstracts.
- Neetu, Ray, S.S. (2019). Exploring machine learning classification algorithms for crop classification using sentinel-2 data. *Internet Arch. Photogramm. Remote Sens. Spat Inform. Science*. <https://doi.org/10.5194/isprs-archives-XLII-3-W6-573-2019>.
- Niu, G. Y., Yang, Z. L., Mitchell, K. E., Chen, F., Ek, M. B., Barlage, M., Kumar, A., Manning, K., Niyogi, D., Rosero, E., Tewari, M. and Xia, Y. (2011). The community Noah land surface model with multiparameterization options (Noah-MP): 1. Model description and evaluation with local-scale measurements. *Journal of Geophysical Research Atmospheres*, 116(12):1–19. <https://doi.org/10.1029/2010JD015139>
- Niu, G.-Y., *et al.* (2011). The community Noah land surface model with multiparameterization options (Noah-MP): 1. Model description and evaluation with local-scale measurements. *J. Geophys. Res.*, 116: D12109, doi: 10.1029/2010JD015139.
- NOAH community (2019). Noah LSM (Noah Land Surface Model), Model Item, OpenGMS, <https://geomodeling.njnu.edu.cn/modelItem/9713beed-2d5b-4b8b-b24c-0c612dcf7054>
- Özkan, B., Dengiz, O. and Demirağ Turan, İ. (2019). Site suitability assessment and mapping for rice cultivation using multi-criteria decision analysis based on fuzzy-AHP and TOPSIS approaches under semi-humid ecological condition in delta plain. *Paddy and Water Environment*, 17(4):665–676. <https://doi.org/10.1007/s10333-019-00692-8>
- Perveen, M. F., Nagasawa, R., Uddin, M. I. and Delowar, H. K. M. (2005). Crop-land suitability analysis using a multi-criteria evaluation and GIS approach. United Graduate School of Agricultural Sciences, Tottori University, Tottori, Japan 1–8.
- Piryonesi, S. M., El-Diraby, Tamer, E. (2020). Data analytics in asset management: cost-effective prediction of the pavement condition index. *Journal of Infrastructure Systems*. 26 (1): 04019036. doi:10.1061/(ASCE)IS.1943-555X.0000512. ISSN 1943-555X. S2CID 213782055.
- Pretty, J. and Bharucha, Z. P. (2014). Sustainable intensification in agricultural systems. *Annals of Botany*, 114(8):1571–96.

- Riches, C. R. *et al.* eds. (2008). Improving agricultural productivity in rice-based systems of the high Barind tract of Bangladesh, Los Baños: International Rice Research Institute. Available at: http://books.irri.org/9789712202292_content.pdf.
- Saaty, R. W. (1987). The analytic hierarchy process-what it is and how it is used. *Mathematical Modelling*, 9(3–5): 161–176. [https://doi.org/10.1016/0270-0255\(87\)90473-8](https://doi.org/10.1016/0270-0255(87)90473-8)
- Saaty, T. L. (1994). How to make a decision: the analytic hierarchy process. *Interfaces*, 24(6):19-43.
- Schulthess, U. *et al.* (2015). Technology targeting for sustainable intensification of crop production in the delta region of Bangladesh. The International Archives of the Photogrammetry, *Remote Sensing and Spatial Information Sciences*, 60(7):1475–1481.
- Shahid, S. (2011). Impact of climate change on irrigation water demand of dry season Boro rice in northwest Bangladesh. *Climatic Change*, 105(3–4):433–453.
- Shahid, S. (2010). Spatial assessment of groundwater demand in Northwest Bangladesh. *Int. J. Water*, 5(3):263–283.
- Shaloo, R. P. S., Bisht, H., Jain, R., Suna, T., Bana, R. M., Godara, S., Shivay, Y. S., Singh, N., Bedi, J., Begam, S., Tamta, M. and Gautam, S. (2022). Crop-suitability analysis using the analytic hierarchy process and geospatial techniques for cereal production in North India. *Sustainability* 14(9): 5246. doi: 10.3390/su14095246.
- Shaloo, S., Bisht, R. P., Jain, H., Suna, R., Bana, T., Godara, R. S., Shivay, S., Singh, Y. S., Bedi, N., Begam, J., Tamta, S. and Gautam, S. (2022). Crop-suitability analysis using the analytic hierarchy process and geospatial techniques for cereal production in North India. *Sustainability*, 14(9):5246. <https://doi.org/10.3390/su14095246>
- Singh, P., Upadhyay, R. K., Hireen, P. Bhatt, Markand, P. O. and Vyas, S. P. (2018). Crop suitability analysis for cereal crops of Uttar Pradesh, India. *International Archives of the Photogrammetry, Remote Sensing and Spatial Information Sciences - ISPRS Archives* 42(5):353–60. doi: 10.5194/isprs-archives-XLII-5-353-2018.
- Tatsumi, K., Yamashiki, Y., Morante, A. K. M., Fernández, L. R., Nalvarte, R. A. (2016). Pixel-based crop classification in Peru from landsat 7 ETM+ images using a random forest model. *J. Agric. Meteorol.* 72(1): 1–11.
- Timsina, J. *et al.* (2018). Can Bangladesh produce enough cereals to meet future demand? *Agricultural Systems*, 163:36-44. <https://doi.org/10.1016/j.agry.2016.11.003>
- Wahlqvist, M. L. *et al.* (2012). Rethinking the food security debate in Asia: Some missing ecological and health dimensions and solutions. *Food Security*, 4(4):657–670.
- Xiong, J., Thenkabail, P. S., Tilton, J. C., Gumma, M. K., Teluguntla, P., Oliphant, A., Congalton, R. G., Yadav, K. and Gorelick, N. (2017). Nominal 30-m cropland extent map of continental Africa by integrating pixel-based and object-based algorithms using Sentinel-2 and Landsat-8 data on google earth engine. *Remote Sensing*, 9(10): 1–27. <https://doi.org/10.3390/rs9101065>
- Yang, Z.-L., Niu, G. Y., Mitchell, K. E., Chen, F., Ek, M. B., Barlage, M., Manning, K., Niyogi, D., Tewari, M. and Xia, Y. (2011). The Community Noah Land Surface Model with Multi-Parameterization Options (Noah-MP): 2. Evaluation over Global River Basins. *J. Geophys. Res.*, doi:10.1029/2010JD015140.

GROWTH AND INSTABILITY ANALYSIS IN AREA AND PRODUCTION OF MAJOR PULSES IN BANGLADESH

K. Saidur Rahman, J. K. Prioty and M. A. Monayem Miah

Abstract

Instability is a crucial characteristic of agriculture. Since agriculture is dependent on weather conditions, the area, production, and yield of the crops are subject to significant variations over time. Pulses are not only a vital ingredient of the human diet; they are equally important to the health of humans and agricultural soils as well. This study examined the changes in area, production, and yield of major pulses in Bangladesh through growth rate and instability analysis based on secondary data for the last 40 years (1981-2020). The entire period was divided into three sub-periods: 1981-1990, 1991-2000, and 2001-2010 for analysis through different statistical tools. Growth rates were calculated by fitting an exponential growth function, and instability was analyzed by generating the Cuddy-Della Valle index for the six major pulses of Bangladesh and pulses as a whole. The analysis revealed that the area and production of pulses were not increased satisfactorily. Though the pulses yields were increased significantly, the rate of growth is slow, and it is insufficient to meet our country's demand. The analysis also revealed that the area, production, and yield of pulses were not stable during the study period.

Introduction

Pulses are important food crops in Bangladesh. They are an important source of nutrition for the human diet (Das et al., 2016.), grow quickly, provide feed for the animal, and generate good profits for farmers (Miah et al., 2009). Pulses contribute to agricultural and environmental sustainability through the addition of nitrogen, carbon, and organic matter (Senanayake et al., 1987; Zapata et al., 1987; Sarker and Kumar, 2011). A favourable climatic condition exists in Bangladesh for growing different types of pulses all over the country. Because of the high protein content and low price pulses are called *poor man's meat*. So, most of the low-income populations can use this nutritious crop as their staple food. The per capita consumption of pulse in our country is only 15.7 g/day (HIES, 2016) which is much lower than the desirable intake of 50 g/day (DDP, 2013).

The local production of pulses almost remained static in the last couple of years, causing a rise in imports of pulses to meet the increasing demand (Miah et al., 2022). Bangladesh had to import a huge quantity of pulses to meet the demand. Bangladesh imported 1363.39 thousand tons of pulses valuing 707.172 million USD in 2021 (FAOStat, 2021). According to Bangladesh Bank's statistics, Bangladesh spent Tk. 6,185 crore to import pulses in the last fiscal year of 2021-22, an increase of 11% year-on-year. In recent years, due attention has been given to pulse cultivation in Bangladesh. As a result, pulse acreage in this country has gradually increased. Of course, there is real hope and a bright possibility of solving the crucial national food crisis by cultivating pulses.

Instability is a very important characteristic of agriculture. Since agriculture is dependent on weather conditions, the area, production and yield of crops are subject to significant variations over time. Instability also exist in the area, production and yield of pulse crops. There has been a dearth of studies dealing with the growth and instability of pulse crops in Bangladesh. Hence, the present study was undertaken to analyze the growth and instability in the area, production and yield of pulse crops along with the contributory factors affecting the growth and instability of pulse production. The findings of this study will provide useful guidelines for the relevant researchers, policymakers, and planners of the country.

- (i) To determine the growth rates of area, production, and yield of major pulses in Bangladesh;
- (ii) To measure the change and instability in area, production, and yield of major pulses; and
- (iii) To derive some policy implications from the above objectives.

Materials and Methods

Data and Its Sources

The study was based on secondary data collected from various published sources. Times series data on the area, production, and yield of different pulse crops for 40 years from 1981 to 2020 were collected from different issues of the *Yearbook of Agricultural Statistics of Bangladesh*.

Analytical Procedures

To examine the nature of change, instability, and degree of relationship in area, production, and yield of different pulse crops in Bangladesh, various statistical measures were used to analyze the data.

Trend analysis: Trend analysis aims to find out the extent and causes of instability of area and production of pulse crops over time. This information may lead research managers as well as policymakers to prepare appropriate policy documents for the improvement of pulse crops for the country. A simple line graph and bar diagram were used to show the trends of area, production, and yield of different pulse crops in Bangladesh.

Index number: We can measure the relative changes in area, production and yield of pulse crops that are changed or produced within a stipulated period by using an index number. At first, the entire study period is divided into four sub-periods: 1981 to 1990, 1991-2000, 2001-2010, and 2011-2020. The reason for the division was to know the changes that occurred in the area, production, and yield of pulses after 10 years period. The 10 years (e.g. 1981-1990) average value of area, production, and yield was considered the base year.

Annual growth rates: Growth rates are *the percent change of a variable over time*. It is important because it can help researchers and policymakers predict future growth. For simplicity and widely used even in the recent past (Das and Mishra 2020; Chaudhary et al., 2016) the compound growth rates of area, production, yield, and price of pulses were worked out by fitting an exponential function of the following type (equation 1):

$$Y = ae^{bt} \quad \text{or} \quad \ln Y = \ln a + bt \text{-----} (1)$$

Where, Y is the area/production/yield of pulses, 't' is the time in a year, and 'a' is the constant, $e^b - 1$ be the compound growth rate which is expressed in percentage.

The component analysis model has been used to measure the relative contributions of area and yield toward the overall output change with regard to individual crops. The growth performance of the crops has been studied using this model (Equation 2) by numerous researchers in the literature (Gupta and Saraswat, 1997; Singh and Ranjan, 1998; Siju and Kombairaju, 2001; Kakali and Basu, 2006).

$$\Delta P = A \circ \Delta Y + Y \circ \Delta A + \Delta A \Delta Y \text{-----} (2)$$

Change in production = Yield effect + Area effect + Interaction effect

Thus, the total change in production is attributed due to area and yield that can be decomposed into three effects viz; yield, area and interaction effects.

Instability index: Instability means the quality or state of being unstable or lack of stability. Agricultural instability can be measured by different methods, such as the coefficient of variation (CV), dispersion, Cuddy Della Valle Index (CDI), Coppock Instability index, etc. The present study applied the Cuddy and Valle (1978) Index for examining the nature and degree of instability in the area, production, and yield of pulses in Bangladesh. The use of CV as a measure to show the instability in any time series data has some limitations. It does not explain properly the trend component inherent in the time series data. If the time

series data exhibit any trend, the variation measured by CV can be overestimated, i.e. the region which has growing production at a constant rate will score high in instability of production if the CV is applied for measuring instability. As against that, CDI first attempts to de-trend the CV by using the coefficient of determination (R^2). Thus it is a better measure to capture instability in agricultural production. A low value of this index indicates low instability in farm production and vice-versa. The estimable form of equation (3) is as follows:

$$CV_t = (CV) \times \sqrt{1 - R^2} \text{ ----- (3)}$$

Where CV_t is the coefficient of variation around the trend; CV is the coefficient of variation around the mean in percent; and R^2 is the coefficient of determination from time trend regression adjusted by the number of degrees of freedom.

$$CV = \frac{\text{Standard deviation}}{\text{Mean}} \times 100$$

$$R^2 = 1 - \frac{\text{Unexplained variation}}{\text{Total variation}}$$

Results and Discussion

Lentils

Lentil (*Lens culinaris*) is the most popular pulse crop in Bangladesh. It is grown as a winter crop. It cannot tolerate extreme cold or hot climates. This crop has some level of drought tolerance, but it is highly susceptible to waterlogging. It placed the first position in terms of area coverage (40% of total pulse area) and production (45% of total pulse production). It constitutes one of the main items in the daily diet of a vast majority of the people of Bangladesh. Therefore, it also ranks the highest in consumer preference and total consumption. Lentil seed is a rich source of protein and several essential micronutrients like Fe, Zn, and b-carotene (Bhatty, 1988). Lentil straw is a valuable animal feed. Different studies (Miah et al., 2021; Sarker et al., 2020; Matin et al., 2018; Tithi and Barmon, 2018) revealed that lentil production is profitable to farmers. Hence, it is cultivated in different parts of the country covering 146.03 thousand hectares of land producing 185.50 thousand metric tonnes per year with a productivity of 1.27 t/ha (BBS, 2022). Bangladesh's lentil imports are on the rise due to increased consumption amid inadequate domestic production. In 2021, Bangladesh imported 455.30 thousand tons of lentils valuing 284.95 million USD (FAOStat, 2021).

Trends of Area and Production of Lentil in Bangladesh

The area and production of lentils were found to fluctuate in nature, but the yield registered an increasing trend over the years. Figure 1 shows that the area and production of lentils for the period from 1981/82 to 1985/86 were very low compared to the succeeding years. Despite various positive sides, the crop faced tough competition in the recent past from cereals, particularly wheat and *Boro* rice, due to the expansion of irrigation facilities, and the availability of high-yielding varieties (Sarker et al., 1989). To halt this steady decline trend, BARI and BINA disseminated some improved lentil varieties and popularized them through different projects. The inclusion of these varieties in the cropping patterns replacing local with improved varieties might be the cause of the increase in area, production, and yield of lentils. Therefore, both area and production of lentils were very high for the period of 1986/87-1998/99. Again in the period 1999/00-2008/09, the overall area and production of lentils in the country were found decreasing trend which might be due to susceptible crops and less remunerative in production. After that period the area, production, and yield of lentils further increased steadily from 2009/10 to 2019/20.

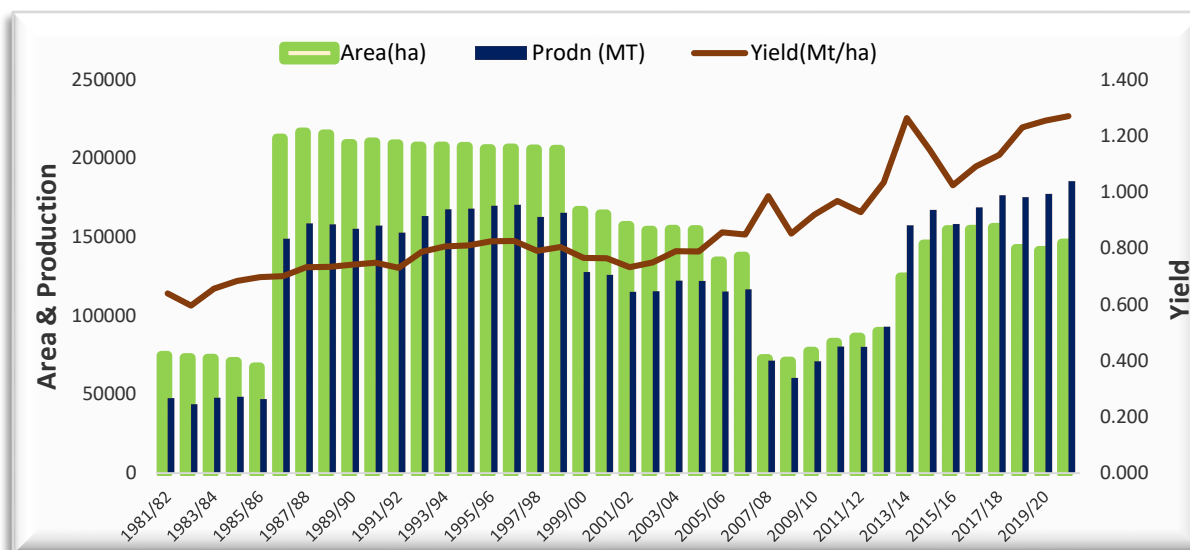


Figure 1. Trend of area, production and yield of lentil, 1981/82-1999/20

Source: Using data from various issues of BBS

The overall indices show that the area and production of lentils increased to a great extent from its base period of 1981-1990 during 1991-2000 (Table 1). But the overall indices of area and production show a decreasing trend over the period 2001-2010. On the other hand, the productivity indices revealed an increasing trend during the period from 1981-1990 to 2011-2020. Despite the decrease in area, the per hectare yield of lentils has gone up in that period which was mainly due to the adoption of improved variety and management technologies.

Table 1: Index of area, production and yield of lentil

Time Period	Area (%)	Production (%)	Yield (%)
1981-1990	100 (142345)	100 (101307)	100 (0.69)
1991-2000	139.6	155.4	114.1
2001-2010	84.1	97.8	122.5
2011-2020	94.3	152.0	164.1

Note: Figures within parentheses indicate 10(ten) year average value in the base year of the indices.

Source: various issues of BBS

Annual Growth of Lentil production

The overall annual growth rates scenario reveal that the production and yield of lentil registered positive and significant growth rates during 40 years period (1981-2020), but the area growth rate was negative and not significant at all (Table 2). The growth rates of different periods show that some growth rates registered in area and production were found positive and significant from 1981 to 1990 and 2011-2020. Both area and production growth rates ((-2.27 & -2.2) and (-10.13 & -7.113)) were significantly negative during 1991-2000 and 2001-2010 due to delayed sowing, yield instability for biotic and abiotic stresses, local cultivars' susceptibility to major diseases, and the low yield potential of local cultivars (Sarker et al., 2004). However, the growth rates of yield were positive and highly significant for all periods except the period 1991-2000. The highly significant growth rates of yield were mainly due to the adoption of improved lentil variety and technology. This indicates that more adoption of the modern varieties of lentils is needed in the farmers' fields.

Table 2: Annual growth rates of area, production and yield of lentil, 1981-2020

Time period	Area	Production	Yield
1981-1990	16.10***	18.34***	2.24***
1991-2000	-2.27***	-2.20*	0.08
2001-2010	-10.13***	-7.11***	3.02***
2011-2020	5.32**	7.77***	2.45**
1981-2020	-0.21	1.36**	1.57***

Note: '***', '**' and '*' represent 1%, 5% and 10% level of significant

Sources of growth of lentil production

Change in the mean area appeared to be the largest source of change in the mean production of lentils in all the periods. At the national level, changes in the mean area and yield were the main two sources of changes in lentil production in Bangladesh. The change in area and yield contributed respectively 41.7% and 55.5% to the changes in the mean production of lentils at the national level. This means that the positive change in production has been attributed to the positive change in area and yield (Table 3).

Table 3: Growth decomposition in the production of lentil during 1981-2020

Time period	Effect (%)				
	Area (A)	Yield (Y)	Interaction	Residual	Total
	$\Delta A * Y$	$A * \Delta Y$	$\Delta A * \Delta Y$	$\Delta COV(A, Y)$	ΔQ
1981-1990	86.76	13.62	0.38	-0.76	100
1991-2000	111.60	-16.09	-4.50	8.99	100
2001-2010	167.15	-47.13	20.03	-40.05	100
2011-2020	69.90	33.38	3.28	-6.56	100
1981-2020	41.70	55.50	-2.78	5.58	100

Source: Author's calculation using BBS data of different years

Instability of Lentil Cultivation

The estimates of instability in the area, production, and yield of lentils are presented in Table 4. The instabilities of the mung bean area (3.43%) and production (3.62%) at the national level were not so high, but the instability of production was a little bit higher than the area instability. On the other side, the instability related to productivity was about -48.68% during 1981-2020 meaning that lentil productivity was almost stable over the stipulated period.

Table 4: Instability indices for area, production and yield of lentil, 1981-2020

Time period	Instability (%)		
	Area (ha)	Production (t)	Yield (t/ha)
1981-1990	2.59	2.67	-7.79
1991-2000	0.52	0.79	-16.31
2001-2010	1.52	1.47	-26.82
2011-2020	1.25	1.48	61.44
1981-2020	3.43	3.62	-48.68

Source: Author's calculation using BBS data

Mungbean

Mung bean (*Vigna radiata* L.) popularly known as green gram is an ancient and well-known pulse crop that belongs to the *Papilionoideae* family and originated from South East Asia. It is widely cultivated throughout Asia, including India, Pakistan, Bangladesh, Sri Lanka, Thailand, Laos, Cambodia, Vietnam, Indonesia, Malaysia, South China, and the Republic of Formosa (Mogotsi, 2006). It is a source of high-quality protein

which can be consumed as whole grains, dhal, or sprouted form and is an excellent complement to rice concerning balanced human nutrition. Dry beans are sometimes used for animal food, mainly poultry, and their biomass is used as fodder (Winch, 2006). Thus, it has great value as food and fodder. Mungbean supplies a substantial amount of nitrogen to the succeeding non-legume crops (i.e. rice) grown in rotation (Sharma and Prasad 1999).

Mung bean is grown round the year (three times) in Bangladesh. At present, this crop is being cultivated after harvesting *Rabi* crops (i.e. wheat, mustard, lentil, etc.). As a short-duration crop, it can be fitted in as a cash crop between major cropping seasons. The present area under mungbean cultivation is 44.25 thousand ha with a total production of 41.19 thousand tons and an average yield of 93.08 t/ha (BBS, 2021).

Trends of Area and Production of Mungbean

Figure 2 shows that the area and production of mung bean for the period from 1981/82 to 1985/86 were very low compared to the succeeding years. Besides various positive sides, most of the mungbean areas in the aforesaid period were replaced by cereals (Abedin and Anwarul 1991). After that mungbean cultivation is gaining popularity among farmers day by day. The reasons for its higher adoption were: i) short duration crop; ii) many HYVs were available to the farmers; iii) highly responsive to irrigation and fertilizer use; iv) possible to cultivate three seasons due to its photo-insensitive nature; and iv) profitable replacement of *Aus* rice and upland jute by mungbean (Miah et al. 2004). It revealed that the Pulse Research Centre of BARI developed four improved mungbean varieties namely BARI Mung-2, BARI Mung-3, BARI Mung-4, and BARI Mung-5 during 1987-1997 (Razzaque et al., 2000). Besides, several HYV of mung bean varieties were also developed by BINA and Bangladesh Sheikh Muzibur Rahman Agricultural University (BSMRAU). Therefore, both area and production of mungbean were very high for the period of 1987/88-1999/00 due to the higher adoption of improved varieties and technologies of mungbean at the farm level. In the period 2001/02 to 2009/10, the overall area and production of mung beans in the country decreased due to insect infestation, insecticides not working properly, a lack of training about improved mung bean cultivation, and the high price of insecticides (Islam et al., 2013). After that period it again shows an increasing trend.

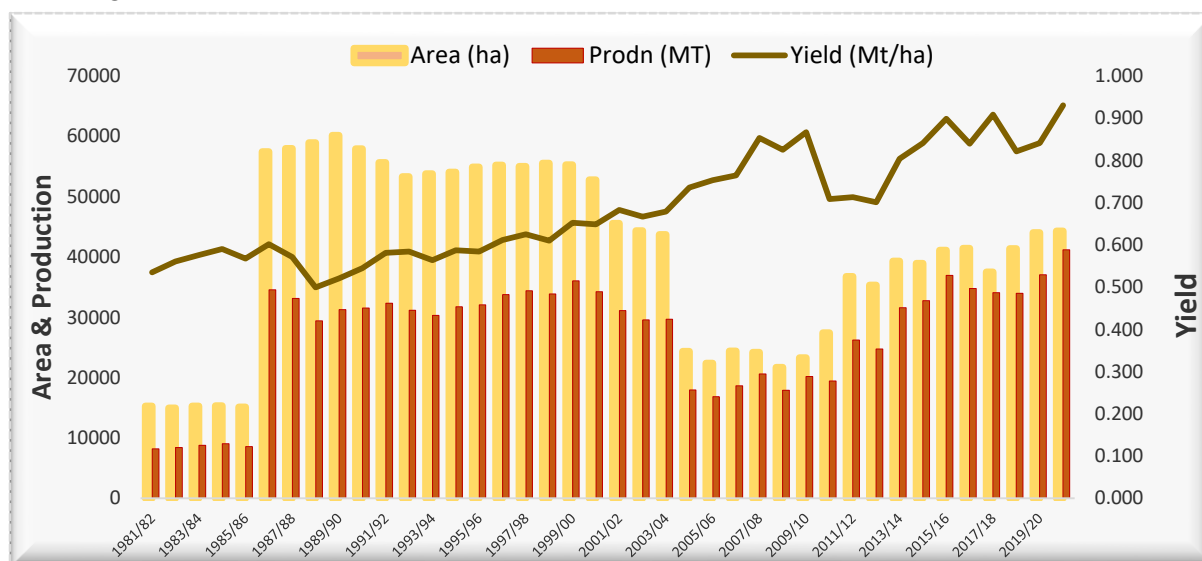


Figure 2. Trend of area, production and yield of mungbean, 1981/82-1999/20

Source: Using data from various issues of BBS in different years

The overall indices show that the area of mungbean increased to some extent from its base period during 1991-2000. But the overall indices of the area show a decreasing trend over the period from 2001-2010 to

2011-2020. On the other hand, the productivity indices revealed an increasing trend during the period from 1981-1990 to 2011-2020 with little fluctuating nature (Table 5). Despite the decrease in area, the yield of mung bean has gone up in those periods which was mainly due to the adoption of improved varieties along with management technologies of mung bean.

Table 5: Index of area, production and yield of mungbean

Time period	Area (%)	Production (%)	Yield (%)
1981-1990	100 (36846)	100 (20297)	100 (0.556)
1991-2000	148	163	109
2001-2010	82	109	135
2011-2020	109	164	149

Note: Figures within parentheses indicate 10 year average value in the base year of the indices.

Source: Various issues of BBS

Annual Growth of Mungbean Production

The overall annual growth rates scenario reveals that the area, production, and yield of mug beans registered positive growth rates during 40 years period (1981-2020) although the area growth rate was not significant at all (Table 6). The growth rates of different periods show that some growth rates registered in the area were found positive and significant from 1981 to 1990 and 2011-2020. Similarly, highly significant positive growth rates of production were observed from 1981 to 1990, 1991-2000, and 2011-2020. Both area and production growth rates (-7.58 & -5.41) were found significantly negative during 2001-2010 due to insect infestation, insecticides not working properly, a lack of training about improved mung bean cultivation, and the high price of insecticides (Islam et al., 2013). However, the growth rates of yield were positive and highly significant for all periods except the period 1981-1990 (-0.67). The highly significant growth rates of yield were mainly due to the adoption of improved mungbean variety and technology. This indicates that more adoption of the modern varieties of mungbean is needed in the farmers' fields

Table 6: Annual growth rates of area, production and yield of mungbean, 1981-2020

Time period	Area	Production	Yield
1981- 1990	20.47***	19.80***	-0.67
1991- 2000	-0.002	1.44***	1.45***
2001- 2010	-7.58**	-5.41**	2.18**
2011- 2020	2.04***	4.42***	2.38***
1981- 2020	0.45	1.85***	1.40***

Note: '***' & '**' represent 1% and 5% level of significant

Sources of growth of mungbean production

Change in the mean area appeared to be the largest source of change in the mean production of mung bean in all the periods except 1991-2000. At the national level, changes in the mean area and yield were the main two sources of changes in mung bean production in Bangladesh. The change in area and yield contributed respectively 51.3% and 46.8% to the changes in mean production of mung bean at the national level. This means that the positive change in production has been attributed to the positive change in area (Table 7).

Table 7. Growth decomposition in the production of mungbean during 1981-2020

Time period	Effect (%)				
	Area (A)	Yield (Y)	Interaction	Residual	Total
	$\Delta A * Y$	$A * \Delta Y$	$\Delta A * \Delta Y$	$\Delta COV(A, Y)$	ΔQ
1981-1990	109.4	-3.7	5.7	-11.4	100
1991-2000	-119.3	215.4	-3.8	7.7	100
2001-2010	123.6	-10.7	12.8	-25.7	100

2011-2020	58.9	41.2	0.2	-0.3	100
1981-2020	51.3	46.8	-1.9	3.8	100

Source: Author's calculation using BBS data of different years

Instability of Mungbean Cultivation

The estimates of instability in area, production, and yield of mung bean are presented in Table 8. The instabilities of the mung bean area (4.3%) and production (4.08%) at the national level were not so high, but the instability of the area was a little bit higher than the production instability. On the other side, the instability related to productivity was about -17.75% during 1981-2020 meaning that mungbean productivity was almost stable over the stipulated period.

Table 8. Instability indices for area, production and yield of mungbean, 1981-2020

Time period	Instability (%)		
	Area (ha)	Production (t)	Yield (t/ha)
1981-1990	3.36	3.58	-9.22
1991-2000	0.17	0.29	-4.43
2001-2010	1.98	1.71	-24.31
2011-2020	0.4	0.75	-32.05
1981-2020	4.3	4.08	-17.75

Source: Author's calculation using BBS data of different years

Black gram

Black gram (locally called *Mashhkalai*) is a leguminous plant under the *Vigna mungo* species. It is a drought-resistant crop grown both as a summer and winter crop; often in rotation with rice but sometimes in mixed cultivation. Black gram is one of the highly prized pulses in Bangladesh. It is boiled and eaten whole or after splitting into the *Dal*. It contains approximately 9.7% water, 23.4% protein, 1% fat, 57.3% carbohydrate, 3.8% fibre, and 4.8% ash (https://en.banglapedia.org/index.php/Black_Gram). Black gram is also used as a green manure and cover crop or fodder crop, and as a short-lived forage. In 2020/21, it is cultivated in about 40.64 thousand hectares of land producing 37.35 thousand MT with an average yield of 0.919 t/ha (BBS, 2021).

Trends of Area and Production of Black Gram

The area and production of black gram for the period from 1981/82 to 1985/86 were very low compared to its subsequent years (Fig 3). After that, its cultivation is gaining popularity among farmers day by day. The reasons for its popularity were more tolerant to waterlogging, had fewer disease and insect problems compared to other pulses, had more stable yields, and can be grown with minimum care (Rahman, 1989). Therefore, both area and production of black gram were very high for the period of 1987/88-1997/98. In the period 1998/99 to 2004/05, the overall area and production of black gram in the country showed a decreasing trend due to traditional methods of farming, low yields, shortages of key inputs, and a shortage of irrigation water (Rahman and Baten, 2013). After that period it again shows an increasing trend.

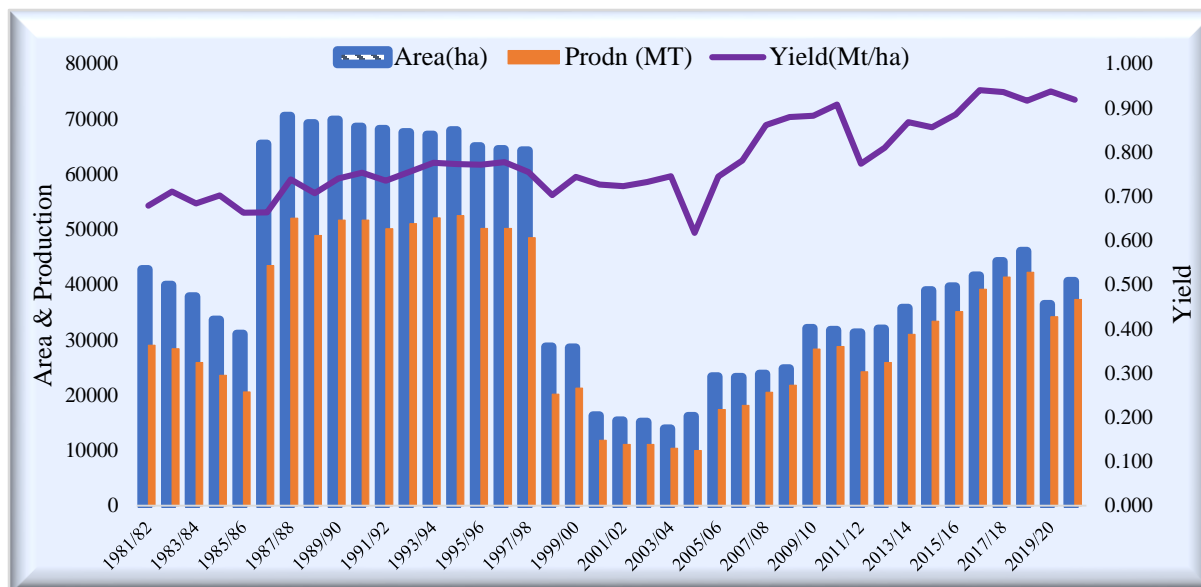


Figure 3. Trends of area, production and yield of black gram, 1981/82-2019/20

Source: Using data from various issues of BBS in different years

The overall indices show that the area and production of black gram increased to some extent from its base period of 1981-1990 during 1991-2000. But the overall indices of area and production show a decreasing trend over the period from 2001-2010 to 2011-2020. On the other hand, the productivity indices revealed an increasing trend during the period from 1981-1990 to 2011-2020 (Table 9). Despite the decrease in area, the yield of black gram has gone up in those periods which was mainly due to the adoption of improved varieties (BARI Mash-1, -2, -3, -4 & -5) along with management technologies of black gram.

Table 9: Index of area, production and yield of black gram

Time period	Area (%)	Production (%)	Yield (%)
1981-1990	100 (52914)	100 (37565)	100 (0.704)
1991-2000	101.8	108.7	106.8
2001-2010	41.6	47.3	111.8
2011-2020	73.1	91.6	125.6

Note: Figures within parentheses indicate 10 year average value in the base year of the indices.

Source: Various issues of BBS

Annual Growth of Black Gram Production

The overall annual growth rates scenario reveals that the area and production of black gram registered a negative growth rate during 40 years period (1981-2020) although the production growth rate was not significant at all (Table 10). On the other hand, black gram yield had a significant positive growth rate during 40 years period. The growth rates of different periods show that some growth rates registered both in area and production were found positive and significant from 1981 to 1990, 2001-2010, and 2011-2020. Both area and production growth rates were found negative during 1991-2000 due to the limited adoption of HYV black gram technology (BARI released 3 black gram varieties during 1990-1996). However, the growth rates of yield were positive and highly significant for all periods except the period 1991-2000. The highly significant growth rates of yield were mainly due to the adoption of improved black gram varieties and technologies. This indicates that more adoption of the modern varieties of black gram is needed in the farmers' fields.

Table 10: Annual growth rates of area, production and yield of black gram, 1981-2020

Time period	Area (ha)	Production (mt)	Yield (t/ha)
1981-1990	8.57***	9.50***	0.93*
1991-2000	-14.13***	-14.60	-0.47
2001-2010	9.60***	12.77***	3.17***
2011-2020	3.01**	4.92***	1.92***
1981-2020	-1.43**	-0.68	0.76***

Note: '***', '**' & '*' represent 1%, 5% and 10% level of significant

Sources of Growth of Black Gram Production

Change in the mean area appeared to be the largest source of change in the mean production of black gram in all the periods. At the national level, changes in the mean yield were the main source of changes in black gram production in Bangladesh. The change in yield contributed 142.25% of the changes in the mean production of a black gram at the national level. The overall scenario indicates that the positive change in production has been attributed to the positive change in the area (Table 11).

Table 11: Growth decomposition in the production of blackgram during 1981-2020

Time period	Effect (%)				
	Area (A)	Yield (Y)	Interaction	Residual	Total
	$\Delta A * Y$	$A * \Delta Y$	$\Delta A * \Delta Y$	$\Delta COV(A, Y)$	ΔQ
1981-1990	75.26	26.62	1.89	-3.77	100
1991-2000	93.71	1.14	-5.15	10.30	100
2001-2010	72.99	31.04	4.03	-8.06	100
2011-2020	89.73	11.20	0.93	-1.86	100
1981-2020	-3.29	142.25	38.97	-77.93	100

Source: Author's calculation using BBS data of different years

Instability of Black Gram Cultivation

The estimates of instability in area, production, and yield of black gram are presented in Table 12. The instabilities of the black gram area (4.37%) and production (4.89%) at the national level were not so high, but the instability of production was a little bit higher than the area instability. On the other side, the instability related to productivity was about -25.7% during 1981-2020 meaning that black gram productivity was almost stable and increasing over the stipulated period.

Table 12: Instability indices for area, production and yield of black gram, 1981-2020

Time period	Instability (%)		
	Area (ha)	Production (t)	Yield (t/ha)
1981-1990	2.03	2.20	-10.21
1991-2000	2.72	3.01	-10.52
2001-2010	1.03	1.45	-29.96
2011-2020	0.86	1.08	-26.21
1981-2020	4.37	4.89	-25.70

Source: Author's calculation using BBS data of different years

Chickpea

Chickpea (*Cicer arietinum* L.) is one of the most important pulse crops in Bangladesh considering consumers' choice and consumption. It has been traditionally cultivated under rainfed conditions. The major chickpea-growing areas of Bangladesh are Jessore, Faridpur, Rajshahi, Kushtia, Pabna, Chapainawabganj, and Dinajpur districts. Currently, chickpea is cultivated on about 4.584 thousand hectares of land producing

5.01 thousand tons with an average yield of 1.093 t/ha. The production of chickpea lessened from 59,900 tons (1997/98) to 5009 tons (2020/21) in the last two decades even though yield soared from 0.712 to 1.093 t/ha over the period (BBS, 2021). To meet the country's demand, Bangladesh imported 354.14 thousand tons of dry chickpeas valuing 210.94 million USD in 2021 (FAOStat, 2021).

Trends of Area and Production of Chickpea

Figure 4 shows that the area and production of chickpeas for the period from 1981/82 to 1985/86 were very low compared to the succeeding years. After that chickpea cultivation is gaining popularity among farmers. Therefore, both area and production of chickpeas were very high for the period of 1986/87-1997/98 due to the higher adoption of improved varieties (BARI Chola-2, -3, -4, -5 & -6) and technologies of chickpeas at the farm level (Kabir et al. 2009). Again, the overall area and production of chickpeas in the country were found to decrease for the period from 1998/99 to 2019/20. The reason for decreasing trend was to put high emphasis on increasing the area and production of cereals like rice, wheat, maize, and other short-duration oilseed crops throughout the country (Rashid et al., 2014).

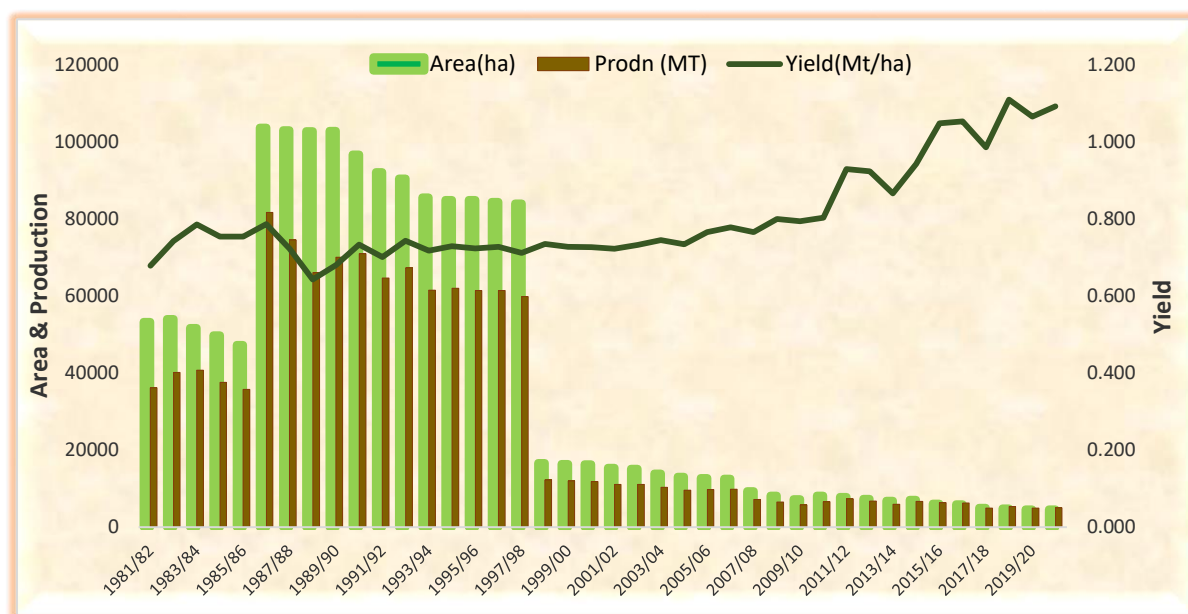


Figure 4. Trend of area, production and yield of chickpea, 1981/82-1999/20

Source: Using data from various issues of BBS in different years

The overall indices show that the area and production of chickpea shows a decreasing trend from its base period during 2011-2020. On the other hand, the productivity indices revealed an increasing trend during the period from 1981-1990 to 2011-2020 (Table 13). Despite the decrease in area, the yield of chickpeas has gone up in those periods which was mainly due to the adoption of improved varieties along with management technologies of chickpeas.

Table 13: Index of area, production and yield of chickpea

Time period	Area (%)	Production (%)	Yield (%)
1981-1990	100 (76582)	100 (55401)	100 (0.73)
1991-2000	85.7	85.7	99.5
2001-2010	15.1	15.9	104.9
2011-2020	7.9	10.8	137.5

Note: Figures within parentheses indicate 10 year average value in the base year of the indices.

Source: Various issues of BBS

Annual Growth of Chickpea Production

The overall annual growth rates scenario reveals that the area and production of chickpea registered highly significant negative growth rates during 40 years period (1981-2020). The growth rates registered in area and production from 1981 to 1990 were found positive and significant (Table 14). Both area and production growth rates were found significantly negative during 1991-2020 due to putting a high emphasis on increasing the area and production of cereals like rice, wheat, maize, and other short-duration oilseed crops (Rashid et al., 2014). However, the growth rates of yield were positive and highly significant for all periods except the period 1981-1990 and 1991-2000 (-0.607 & 0.134). The highly significant growth rates of yield were mainly due to the adoption of improved chickpea variety and technology. This indicates that more adoption of the modern varieties of chickpea is needed for the expansion of this crop throughout the country.

Table 14: Annual growth rates of area, production and yield of chickpea, 1981-2020

Time period	Area	Production	Yield
1981-1990	9.86***	9.25***	-0.61
1991-2000	-21.67***	-21.53***	0.14
2001-2010	-8.78***	-7.56***	1.21***
2011-2020	-6.60***	-4.28***	2.32***
1981-2020	-8.91***	-7.92***	0.99***

Note: '***', '**' & '*' represent 1%, 5% and 10% level of significant

Sources of Growth of Chickpea Production

Change in the mean area appeared to be the largest source of change in the mean production of chickpeas in all the periods. At the national level, changes in the mean area were the main source of changes in chickpea production in Bangladesh. The change in area contributed 108.82% to the changes in the mean production of chickpeas at the national level. This means that the positive change in production has been attributed to the positive change in the area (Table 15).

Table 15: Growth decomposition in the production of chickpea during 1981-2020

Time period	Effect (%)				
	Area (A)	Yield (Y)	Interaction	Residual	Total
	$\Delta A * Y$	$A * \Delta Y$	$\Delta A * \Delta Y$	$\Delta COV(A, Y)$	ΔQ
1981-1990	99.79	4.76	4.54	-9.09	100
1991-2000	99.64	2.63	2.27	-4.54	100
2001-2010	116.70	-16.63	0.07	-0.14	100
2011-2020	226.20	-121.94	4.25	-8.51	100
1981-2020	108.82	-9.36	-0.55	1.09	100

Source: Author's calculation using BBS data of different years

Instability of Chickpea Cultivation

The estimates of instability in area, production, and yield of chickpeas are presented in Table 16. The instabilities of the chickpea area (4.87%) and production (4.94%) at the national level were not so high, but the instability of production was a little bit higher than the area instability. On the other side, the instability related to productivity was about -38.37% during 1981-2020 meaning that chickpea productivity was almost stable over the stipulated period.

Table 16: Instability indices for area, production and yield of chickpea, 1981-2020

Time period	Instability (%)		
	Area (ha)	Production (t)	Yield (t/ha)
1981-1990	1.87	1.89	-20.06
1991-2000	4.25	4.34	-4.98
2001-2010	1.00	1.04	-4.36
2011-2020	0.48	0.72	-48.25
1981-2020	4.87	4.94	-38.37

Field Pea

Field pea (*Pisum sativum L.*) is a cool-season legume crop (popularly known as *Field pea*) grown as a green manure cover crop and pasture forage for its smooth dried seeds used as food or feed crops in many countries all over the world. It is a good source of protein (21-25%) and plays an important role in human nutrition since they are also rich in calories, vitamins, and minerals (Bhat et al., 2013). Field pea is grown by smallholder farmers in most African countries as a source of food, fodder, income, and soil fertility (Gufi et al., 2022). However, its production is scattered almost throughout the country. A big amount of the total area of field pea production belongs to three districts: Dhaka, Faridpur, and Cumilla. Other major field pea-growing districts are Noakhali, Jashore, Kushtia, Kishoregonj, Khulna, Pabna, and Rajshahi. In 2020/21, field pea was cultivated on about 7.493 thousand hectares of land producing 8.052 thousand tons with an average yield of 1.075 t/ha (BBS, 2021).

Trends of Area and Production of Field Pea

The area and production of field peas for the period from 1981/82 to 1985/86 were very low compared to the succeeding years. After that field pea cultivation is gaining popularity among farmers (Fig 5). Therefore, both area and production of field peas were very high for the period of 1986/87-2003/04 due to the higher adoption of improved varieties and technologies of field peas at the farm level. The overall area and production of field peas in the country decreased from 2004-2005 to 2012-2013; this trend could be attributed to a lack of knowledge among farmers because sowing date, variety, and their interaction had a significant effect on growth, yield, and yield attributes of field peas (Ahmed et al., 2020.). After that period it remains almost stable.

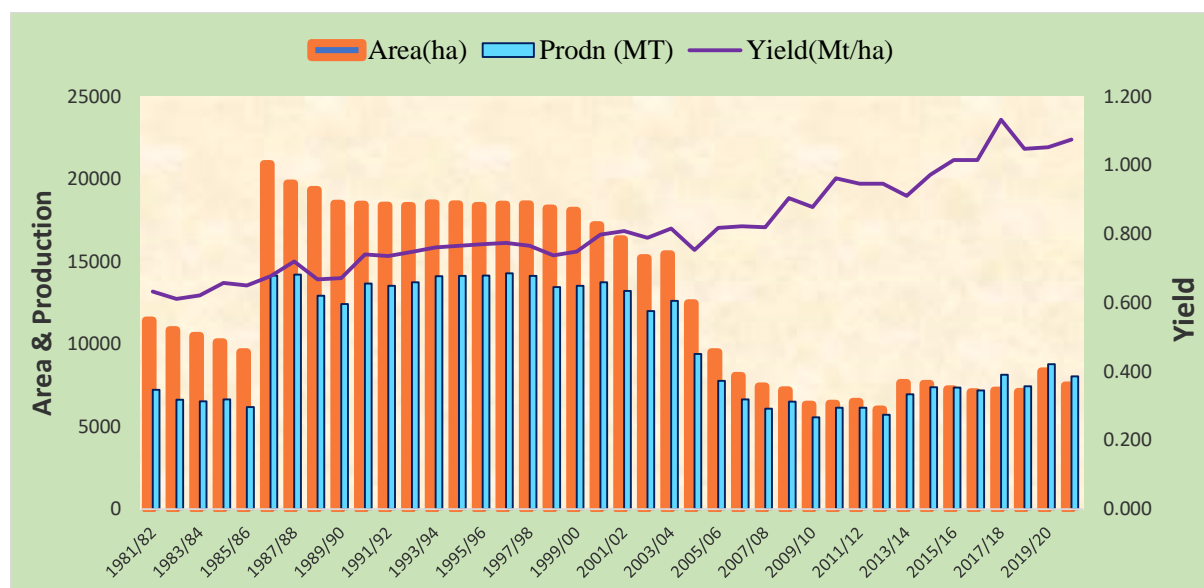


Figure 5. Trend of area, production and yield of field pea, 1981/82-1999/20

Source: Using data from various issues of BBS in different years

The overall indices show that the area and production of field peas increased to some extent from its base period during 1991-2000. But the overall indices of area and production show a decreasing trend over the period from 2001-2010 to 2011-2020. On the other hand, the productivity indices revealed an increasing trend during the period from 1981-1990 to 2011-2020 (Table 17). Despite the decrease in area, the yield of field peas has gone up in those periods which was mainly due to the adoption of improved varieties along with management technologies of field peas.

Table 17: Index of area, production and yield of field pea

Time period	Area (%)	Production (%)	Yield (%)
1981-1990	100 (14929)	100 (10059)	100 (0.665)
1991-2000	122.2	138.0	114.3
2001-2010	70.0	85.5	125.9
2011-2020	48.4	72.8	152.0

Note: Figures within parentheses indicate 10 year average value in the base year of the indices.

Source: Various issues of BBS

Annual Growth of Field Pea Production

Table 18 shows that the overall annual growth rates of area and production of field peas are highly significant and negative; on the other hand, the field of field peas is highly significant and positive during 40 years period (1981-2020). The growth rates of different periods show that some growth rates registered in the area were found positive and significant from 1981 to 1990 and 2011-2020. Similarly, highly significant positive growth rates of production were observed during the period from 1981 to 1990 and 2011-2020. Both area and production growth rates (-12.19 & -10.32) were found to be significantly negative during 2001-2010, which could be attributed to a lack of knowledge among farmers because sowing date, variety, and their interaction had a significant effect on growth, yield, and yield attributes of field peas (Ahmed et al., 2020.). However, the growth rates of yield were positive and highly significant for all periods except the period 1991-2000 (0.362). The highly significant growth rates of yield were mainly due to the adoption of improved field pea variety and technology. This indicates that more adoption of the modern varieties of field peas is needed in the farmers' fields.

Table 18: Annual growth rates of area, production and yield of field pea, 1981-2020

Time period	Area	Production	Yield
1981-1990	8.42***	10.09***	1.67***
1991-2000	-0.48	0.12	0.36
2001-2010	-12.19***	-10.32***	1.86***
2011-2020	1.80*	3.64***	1.84***
1981-2020	-2.54***	-1.12**	1.35***

Note: '***', '**' & '*' represent 1%, 5% and 10% level of significant

Sources of growth of field pea production

Change in the mean area appeared to be the largest source of change in the mean production of field peas in all the periods except 1991-2000. At the national level, changes in yield were the main sources of changes in field peas production in Bangladesh. The change in yield contributed 591% to the changes in the mean production of field peas at the national level. This means that the positive change in production has been attributed to the positive change in yield (Table 19).

Table 19: Growth decomposition in the production of field pea during 1981-2020

Time period	Effect (%)				
	Area (A)	Yield (Y)	Interaction	Residual	Total
	$\Delta A * Y$	$A * \Delta Y$	$\Delta A * \Delta Y$	$\Delta COV(A, Y)$	ΔQ
1981-1990	74.34	29.73	4.11	-8.18	100
1991-2000	-1632.04	1671.32	-60.73	121.45	100
2001-2010	114.50	-14.72	-0.22	0.44	100
2011-2020	51.68	44.71	-3.61	7.22	100
1981-2020	-470.00	591.18	21.19	-42.37	100

Source: Author's calculation using BBS data of different years

Instability of Field Pea Cultivation

The estimates of instability in area, production, and yield of field peas are presented in Table 20. The instabilities of field pea (3.42%) and production (3.53%) at the national level were not so high, but the instability of production was a little bit higher than the area instability. On the other side, the instability related to productivity was about -20.21% during 1981-2020 meaning that field pea productivity was almost stable over the stipulated period.

Table 20: Instability indices for area, production and yield of field pea, 1981-2020

Time period	Instability (%)		
	Area (ha)	Production (t)	Yield (t/ha)
1981-1990	2.19	2.40	-8.23
1991-2000	0.17	0.23	-8.05
2001-2010	1.01	1.28	-23.73
2011-2020	0.79	0.73	406.50
1981-2020	3.42	3.53	-20.21

Source: Author's calculation using BBS data of different years

Grass Pea

Grass pea (*Lathyrus sativus* L.) is a legume crop popularly known as Indian vetch or *Khesari*, popularly known as Indian vetch or *khesari*, which has vast economic importance, especially in developing countries including Bangladesh, India, Pakistan, Nepal, and Ethiopia (Kumar et al., 2011). Its seeds are often broadcasted into standing rice crops one or two weeks before the rice harvest. Grass pea serves various purposes including food, feed, and fodder, owing in part to their nutritive qualities (Biswas, 2007; Malek, 1998). The protein concentration in this legume is 17.7-49.3% (Rizvi et al., 2016). In South Asian countries, grass peas is commonly grown for both grain and fodder purposes. Human diets include grass peas as grains that are boiled and then either consumed whole or processed for split dal (Kaul, 1986). In 2020/21, grass pea is cultivated on 115.97 ha with a total production of 130.63 tons and the average yield of 1.126 kg/ha both in dry areas and in flooded rice fields.

Trends of Area and Production of Grass Pea

Figure 6 shows that the area and production of grass peas for the period from 1981/82 to 1985/86 were very low compared to the succeeding years. After that field pea cultivation is gaining popularity among farmers (Fig 6). Therefore, both area and production of grass peas were very high for the period of 1986/87-1997/98 due to the higher adoption of improved varieties and technologies of grass pea at the farm level. Mention that, BARI Khesari-1 and BARI khesari-2 had been released in 1995 with higher seed and biomass yields having low ODAP content (Malek, et al., 1996). In the period 1998/1999 to 2007/08, the overall area and production of grass peas in the country showed decreasing trend might be due to their unpopularity to the governments and donors because grass pea contains small amounts of toxin, b-N-oxalyl-L-a-diamino propanoic acid. Besides, this toxin can cause irreversible paralysis known as *lathyrism*, in the case of consuming in large quantities unaccompanied by other foodstuffs (Lambein et al., 2009). After that period it again shows an increasing trend by creating awareness among people and farmers.

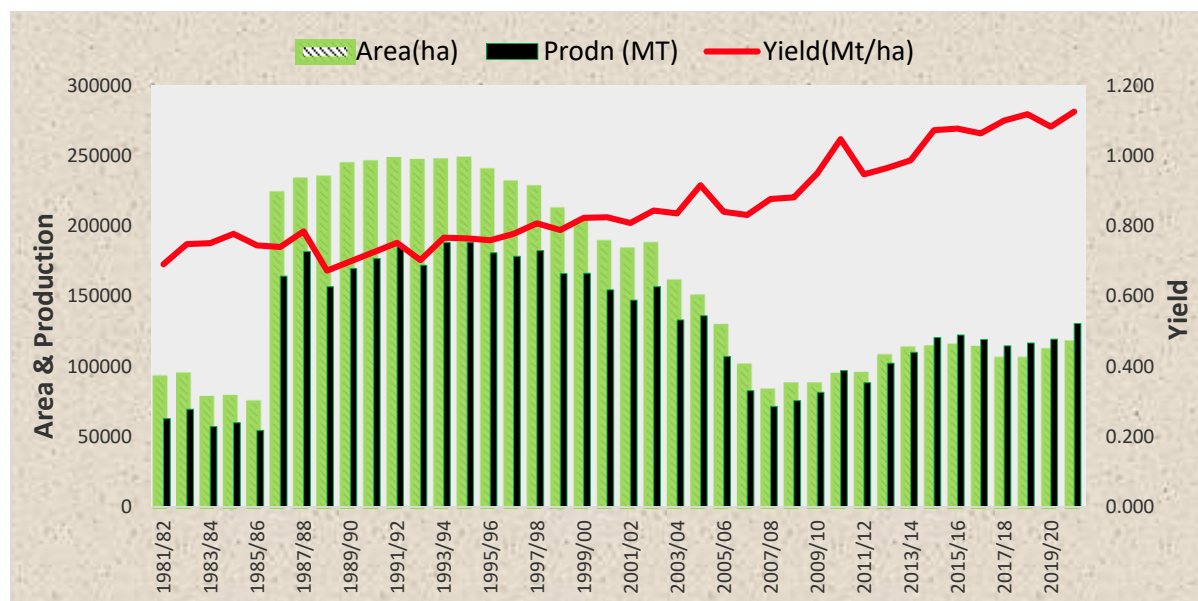


Figure 6. Trend of area, production and yield of grass pea, 1981/82-1999/20

Source: Using data from various issues of BBS in different years

The overall indices show that the area and production of grass peas increased to some extent from its base period of 1981-1990 during 1991-2000. But the overall indices of area and production show a decreasing trend over the period from 2001-2010 to 2011-2020. On the other hand, the productivity indices revealed an increasing trend during the period from 1981-1990 to 2011-2020. Despite the decrease in area, the yield of grass peas has gone up in those periods which was mainly due to the adoption of improved varieties along with management technologies of grass peas (Table 21).

Table 21: Index of area, production and yield of grass pea

Time period	Area (%)	Production (%)	Yield (%)
1981-1990	100.0	100.0	100.0
1991-2000	143.7	152.7	105.9
2001-2010	78.8	94.4	120.4
2011-2020	68.4	99.2	143.7

Note: Figures within parentheses indicate 10 year average value in the base year of the indices.

Source: Various issues of BBS

Annual Growth of Grass Pea Production

The overall annual growth rates scenario reveals that the area of grass peas registered a significant negative growth rate and production registered a non-significant negative growth rate during the period from 1981 to 2020 (Table 22). The growth rates of different periods show that some growth rates registered in the area were found positive and significant for the period from 1981 to 1990. Similarly, highly significant positive growth rates of production were observed during the period from 1981 to 1990 and 2011-2020. Both area and production growth rates were found significantly negative during 1991-2000 and 2001-2010 due to the aforesaid causes (see page **). However, the growth rates of yield were positive and highly significant for all periods except the period 1981-1990 (-0.34). The highly significant growth rates of yield were mainly due to the adoption of improved grass pea variety and technology.

Table 22: Annual growth rates of area, production and yield of grass pea, 1981-2020

Time period	Area	Production	Yield
1981-1990	15.50***	15.15***	-0.34
1991-2000	-2.95***	-1.57**	1.37***
2001-2010	-10.05***	-8.06***	1.98***
2011-2020	0.99	2.83***	1.84***
1981-2020	-1.24**	-0.03	1.21***

Note: '***' & '**' represent 1% and 5% level of significant

Sources of Growth of Grass Pea Production

Change in the mean area appeared to be the largest source of change in the mean production of grass peas in all the periods. At the national level, changes in the mean area and yield were the main two sources of changes in grass pea production in Bangladesh. The change of area and yield contributed respectively 18% and 84.2% to the changes in the mean production of grass peas at the national level. This means that the positive change in production has been attributed to the positive change in the area (Table 23).

Table 23: Growth decomposition in the production of grass pea during 1981-2020

Time period	Effect (%)				
	Area (A)	Yield (Y)	Interaction	Residual	Total
	$\Delta A * Y$	$A * \Delta Y$	$\Delta A * \Delta Y$	$\Delta COV(A, Y)$	ΔQ
1981-1990	99.10	0.98	0.09	-0.17	100
1991-2000	201.40	-101.04	0.36	-0.73	100
2001-2010	137.50	-39.73	-2.26	4.53	100
2011-2020	69.35	31.04	0.39	-0.78	100
1981-2020	17.94	84.19	2.13	-4.26	100

Source: Author's calculation using BBS data of different years

Instability of Grass Pea Cultivation

The estimates of instability in area, production, and yield of grass peas are presented in Table 24. The instabilities of the grass pea area (3.41%) and production (3.23%) at the national level were not so high, but the instability of the area was a little bit higher than the production instability. On the other side, the instability related to productivity was about -34.84% during 1981-2020 meaning that grass pea productivity was almost stable over the stipulated period.

Table 24: Instability indices for area, production and yield of grass pea, 1981-2020

Time period	Instability (%)		
	Area (ha)	Production (t)	Yield (t/ha)
1981-1990	2.60	2.59	-15.78
1991-2000	0.29	0.37	-9.51
2001-2010	1.04	1.41	-39.24
2011-2020	0.48	0.58	-53.79
1981-2020	3.41	3.23	-34.84

Source: Author's calculation using BBS data of different years

Other Pulses

Other pulse includes three minor pulses namely *Arhar*, *Fallon* and *Garikalai*. The major growing areas of *Arhar* are Chottogram Hill Tracts (22.24% of the total area), Kushtia (8.23%), and Rangpur (7.51%) districts. In 2020/21, the total area of *Arhar* in the country is 447.77 ha producing a total of 474.34 MT with an average yield of 1.06 t/ha (BBS, 2022). Again, Fallon cultivation is concentrated in Chottogram and Barisal divisions. National statistics show that about 70% of the total Fallon area is under the Chottogram division (mainly Chottogram, Noakhali, and Feni districts) and only 30% area is under the Barisal division

(mainly Bhola district). In 2020/21, the total area of *Fallon* in Bangladesh is 12,239.68 ha producing a total of 16,083 MT with a mean yield of 1.314 t/ha (BBS, 2022). Finally, the major growing areas of *Garikalai* are the Jhenaidah (92.89% of the total area), Rajbari (4.43%) and Satkhira (1.27%) districts. The total area of *Garikalai* in the country is 575.34 ha producing a total of 433.2 MT with an average yield of 753 kg/ha (BBS, 2022).

Trends of Area and Production of Other pulses

Figure 7 shows that the area and production of other pulses for the period from 1981/82 to 1985/86 were very low compared to the succeeding years. Afterward, both area and production of other pulses were very high for the period from 1986/87 to 1997/98 due to the higher adoption of improved varieties and technologies of other pulses at the farm level. After that period 1998/99 to 2021/22, the overall area and production of other pulses in the country were found decreasing trend with little fluctuating nature.

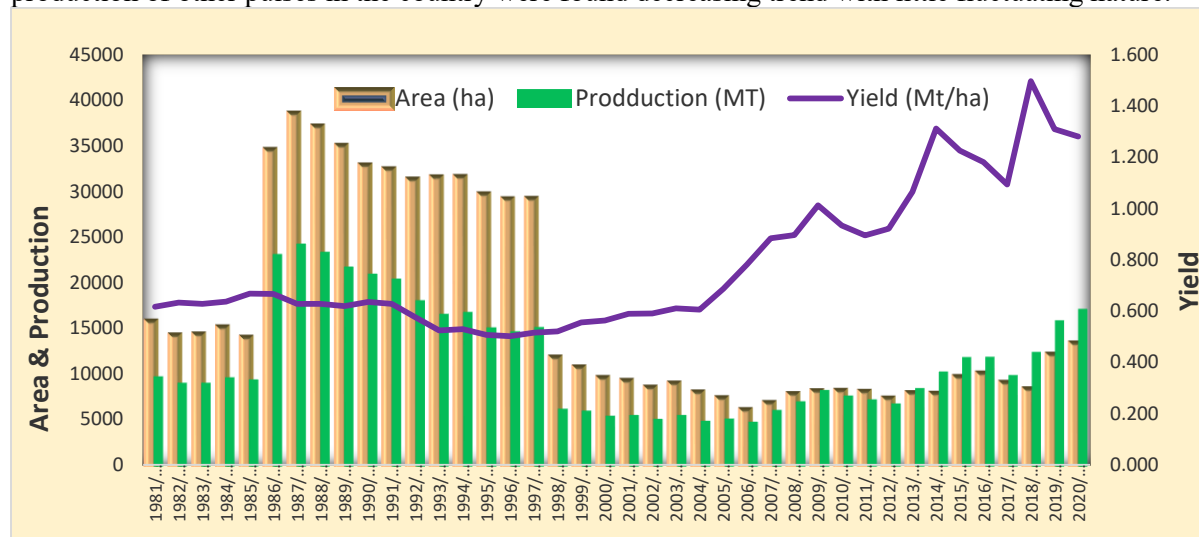


Figure 7. Trend of area, production and yield of other pulses, 1981/82-1999/20

Source: Using data from various issues of BBS in different years

The overall indices of area and production of other pulses show a decreasing trend from its base period during 1981-1990. On the other hand, the productivity indices revealed an increasing trend during the period from 1981-1990 to 2011-2020 except for the period 1991-2000 (Table 25). Despite the decrease in area and production, the yield of other pulses has gone up in those periods which was mainly due to the adoption of improved varieties along with management technologies of other pulses.

Table 25: Index of area, production and yield of other pulses

Time period	Area (%)	Production (%)	Yield (%)
1981-1990	100 (25014)	100 (15895.8)	100 (0.64)
1991-2000	98.3	83.8	85.2
2001-2010	31.2	36.9	119.4
2011-2020	37.1	69.6	185.2

Note: Figures within parentheses indicate 10 years average value in the base year of the indices.

Source: Various issues of BBS

Annual Growth of other pulses Production

The overall annual growth rates scenario reveals that the area, and production of other pulses registered a negative growth rates during 40 years period (1981-2020) although the production growth rate was not highly significant at all (Table 26). The growth rates of different periods show that some growth rates registered in the area were found positive and significant for the period from 1981 to 1990 and 2011-2020. Similarly, highly significant positive growth rates of production were observed during 1981-1990, 2001-2010, and 2011-2020. Both area and production growth rates (-14.4 & -15.23) were found significantly

negative during 1991-2000 might be due to the lack of improved varieties, susceptibility to the environment, less profitable, and higher competition with other crops. However, the growth rates of yield were positive and highly significant for all periods except the period 1981-1990 and 1991-2000 (0.0488 and -0.822). The highly significant growth rates of yield were mainly due to the adoption of improved other pulses variety and technology. This indicates that more adoption of the modern varieties of other pulses is needed in the farmers' fields.

Table 26: Annual growth rates of area, production and yield of other pulses, 1981-2020

Time period	Area	Production	Yield
1981-1990	13***	13.05***	0.0488
1991-2000	-14.41***	-15.23***	-0.822
2001-2010	-1.7	5.02***	6.72***
2011-2020	5.4***	9.52***	4.123***
1981-2020	-3.52***	-1.36*	2.16***

Note: '***', '**' & '*' represent 1%, 5% and 10% level of significant

Sources of growth of other pulses production

Change in the mean area appeared to be the largest source of change in the mean production of other pulses in all the periods except 2001-2010. At the national level, changes in the mean area were the main source of changes in other pulses production in Bangladesh. The change in area and yield contributed respectively 76.06% and 4.79% to the changes in the mean production of other pulses at the national level. This means that the positive change in production has been attributed to the positive change in area (Table 27).

Table 27: Growth decomposition in the production of other pulses during 1981-2020

Time period	Effect (%)				
	Area (A)	Yield (Y)	Interaction	Residual	Total
	$\Delta A * Y$	$A * \Delta Y$	$\Delta A * \Delta Y$	$\Delta COV(A, Y)$	ΔQ
1981-1990	102.77	-4.98	-2.21	4.41	100
1991-2000	79.2	21.03	0.22	-0.44	100
2001-2010	-20.56	118.7	-1.86	3.71	100
2011-2020	72.39	16.38	-11.23	22.46	100
1981-2020	76.06	4.79	-18.62	37.77	100

Source: Author's calculation using BBS data of different years

Instability of other pulses cultivation

The estimates of instability in area, production, and yield of other pulses are presented in Table 28. The instabilities of other pulses area (4.78%) and production (5.32%) at the national level was not so high, but the instability of production was a little bit higher than the area instability. On the other side, the instability related to productivity was about -64.45% during 1981-2020 meaning that other pulses' productivity was almost stable over the stipulated period.

Table 28: Instability indices for area, production and yield of other pulses, 1981-2020

Time period	Instability (%)		
	Area (ha)	Production (t)	Yield (t/ha)
1981-1990	2.58	2.68	-6.06
1991-2000	2.78	2.48	-10.56
2001-2010	1.32	1.49	-21.61
2011-2020	1.28	1.24	68.81
1981-2020	4.78	5.32	-64.45

Source: Author's calculation using BBS data of different years

Comparative Scenario of Growth and Instability of Different Pulses

The overall annual area growth rates scenario revealed that the cultivated area of different pulses demonstrated a significant negative growth rate except for lentil and mung bean during 1981-2020. Again,

the productions of lentil and mung bean have shown significant positive growth rates while other pulses have shown negative growth rates. However, the variations in area and production growth rates occurred might be due to change in agricultural practices, climate variability, and market demand. On the other hand, the growth rates of yield have been relatively more consistent across pulses and time periods. All pulses have shown significantly a positive growth rate in yield, indicating productivity improvements (Table 29). This suggests that efforts to enhance yield have succeeded even when the area under cultivation or total production may have faced challenges. This is due to the widespread adoption of improved varieties and management technologies.

Among pulses, mung bean recorded the highest growth in area and production, while chickpea had the least. The overall scenario also revealed that the contribution of yield (55.5% to 591.18%) in the production growth performance was higher than the contribution of area expansion for all pulses at the national level except for mung bean and chickpea. Again, over four distinct periods: 1981-1990, 1991-2000, 2001-2010, and 2011-2020, we see that 2011-2020-time period showed relatively a positive growth across all pulses in terms of area, production, and yield except for the slide difference in chickpea (Table 30).

Table 29: Comparative scenario of the annual growth rates of different pulses

Time period		Lentil	Mungbean	Blackgram	Chickpea	Field pea	Grass pea
1981-1990	Area	16.10***	20.47***	8.57***	9.86***	8.42***	15.50***
	Production	18.34***	19.80***	9.50***	9.25***	10.09***	15.15***
	Yield	2.24***	-0.67	0.93*	-0.61	1.67***	-0.34
1991-2000	Area	-2.27***	-0.002	-14.13***	-	-0.48	-2.95***
	Production	-2.20*	1.44***	-14.60	-	0.12	-1.57**
	Yield	0.08	1.45***	-0.47	0.14	0.36	1.37***
2001-2010	Area	-	-7.58**	9.60***	-8.78***	-	-
	Production	10.13***	-5.41**	12.77***	-7.56***	12.19***	10.05***
	Yield	3.02***	2.18**	3.17***	1.21***	1.86***	1.98***
2011-2020	Area	5.32**	2.04***	3.01**	-6.60***	1.80*	0.99
	Production	7.77***	4.42***	4.92***	-4.28***	3.64***	2.83***
	Yield	2.45**	2.38***	1.92***	2.32***	1.84***	1.84***
1981-2020	Area	-0.21	0.45	-1.43**	-8.91***	-2.54***	-1.24**
	Production	1.36**	1.85***	-0.68	-7.92***	-1.12**	-0.03
	Yield	1.57***	1.40***	0.76***	0.99***	1.35***	1.21***

Table 30: Comparative scenario of the growth decompositions for different pulses production

Time period		Lentil	Mungbean	Blackgram	Chickpea	Field pea	Grass pea
1981-1990	Area	86.76	109.40	75.26	99.79	74.34	99.10
	Yield	13.62	-3.70	26.62	4.76	29.73	0.98
	Interaction	0.38	5.70	1.89	4.54	4.11	0.09
1991-2000	Area	111.60	-119.30	93.71	99.64	-1632.04	201.40
	Yield	-16.09	215.40	1.14	2.63	1671.32	-101.04
	Interaction	-4.50	-3.80	-5.15	2.27	-60.73	0.36
2001-2010	Area	167.15	123.60	72.99	116.70	114.50	137.50
	Yield	-47.13	-10.70	31.04	-16.63	-14.72	-39.73
	Interaction	20.03	12.80	4.03	0.07	-0.22	-2.26
2011-2020	Area	69.90	58.90	89.73	226.20	51.68	69.35
	Yield	33.38	41.20	11.20	-121.94	44.71	31.04
	Interaction	3.28	0.20	0.93	4.25	-3.61	0.39

1981-2020	Area	41.70	51.30	-3.29	108.82	-470.00	17.94
	Yield	55.50	46.80	142.25	-9.36	591.18	84.19
	Interaction	-2.78	-1.90	38.97	-0.55	21.19	2.13

The overall instability of the production of all pulses was a little bit higher than the area instability except for the grass pea, but this difference is too low. On the other side, the instability related to productivity for all pulses was negative during 1981-2020 meaning that all pulses productivity was almost stable over the stipulated period (Table 31).

Table 31: Comparative scenario of instabilities for different pulses

Time period		Lentil	Mungbean	Blackgram	Chickpea	Field pea	Grass pea
1981-1990	Area	2.59	3.36	2.03	1.87	2.19	2.60
	Production	2.67	3.58	2.20	1.89	2.40	2.59
	Yield	-7.79	-9.22	-10.21	-20.06	-8.23	-15.78
1991-2000	Area	0.52	0.17	2.72	4.25	0.17	0.29
	Production	0.79	0.29	3.01	4.34	0.23	0.37
	Yield	-	-4.43	-10.52	-4.98	-8.05	-9.51
2001-2010	Area	0.52	1.98	1.03	1.00	1.01	1.04
	Production	1.47	1.71	1.45	1.04	1.28	1.41
	Yield	-	-24.31	-29.96	-4.36	-23.73	-39.24
2011-2020	Area	1.25	0.4	0.86	0.48	0.79	0.48
	Production	1.48	0.75	1.08	0.72	0.73	0.58
	Yield	61.44	-32.05	-26.21	-48.25	406.50	-53.79
1981-2020	Area	3.43	4.3	4.37	4.87	3.42	3.41
	Production	3.62	4.08	4.89	4.94	3.53	3.23
	Yield	-	-17.75	-25.70	-38.37	-20.21	-34.84

Conclusions

During the study period (1981–2020), the trend analysis of major pulses revealed that all the pulses have fluctuated in nature in terms of area and production. Among pulses, black gram has recorded the highest fluctuations in area and production, while lentil has the least. But the yield of all the pulses has shown an increasing trend that may be due to the adoption of improved varieties along with management technologies. Now, if we focus on only the last decade, our study shows that area and production have an increasing trend for mung bean, lentil, and black gram, while other pulses have a decreasing trend.

A high growth rate and low instability in production are prerequisites for sustainable agricultural performance and have serious implications for policymakers. This study has examined the growth of pulses production in Bangladesh and found positive and significant growth rates in yield for all the major pulses, but this growth is very low, while negative growth rates are observed in the area for all the major pulses except the mung bean (which indicates that either we are losing cultivable land or farmers are not having an interest in cultivating the crop pulses) and negative growth rates in production for all the major pulses except mung bean and lentil. Among pulses, mung bean has recorded the highest growth in area and production, while chickpea has the least. Due to natural calamities, instability always exists in agricultural production in Bangladesh. Our analyses also support this claim. But the instability in the area, production, and yield of pulses is low at the national level.

Recommendations

Based on the findings of this study, a number of recommendations can be made to promote sustainable growth in the pulse production in Bangladesh. Firstly, agricultural scientists should develop more climate-friendly and high-yielding varieties of pulses to meet the increasing demand. Secondly, existing BARI-

developed improved pulses varieties and technologies should be disseminated among farmers through pilot projects. Thirdly, research and policy support are needed to increase the acreage and yield of pulses that will help increase the per capita availability of pulses, reduce import dependence, and to some extent stabilize pulse prices. Finally, collaboration between government agencies, NGOs, and private sector stakeholders should be given priority for increasing the growth and stability of major pulses in Bangladesh.

References

- Abedin, M. Z. and M. Anwarul. 1991. Prospects of increasing pulse production through improved cropping systems. In: Proceedings of the 2nd National Workshop on Pulses, BARI, Joydebpur, Gazipur, 65-73.
- Ahmed, B.; A. Hasan; B. Karmakar; M. S. Hasan; F. Akter; P. Saha and M. E. Haq, 2000. Influence of date of sowing on growth and yield performance of field pea (*Pisum Sativum* L.) genotypes. *Asian Research Journal of Agriculture*, 13(2):26-34 Doi:[10.9734/arja/2020/v13i230099](https://doi.org/10.9734/arja/2020/v13i230099)
- BBS, 2022. Bangladesh Bureau of Statistics, *Yearbook of Agricultural Statistics of Bangladesh-2021*, Statistics Division, Ministry of Planning, Government of the People's Republic of Bangladesh, Dhaka.
- Bhatty, R. S. 1988. Composition and quality of lentil (*Lens culinaris* M.): A review. *Canadian Institute of Food Science and Technology*, 11(2): 144-160.
- Bhat, T.A. M.; M. Gupta; M. A. Ganai; R. A. Ahanger and H. A. Bhat. 2013. Yield, soil health and nutrient utilization of field pea (*Pisum sativum* L.) as affected by phosphorus and Biofertilizers under subtropical conditions of Jammu. *Int. J. Modern Plant Animal Sci.* 1(1):1-8.
- Biswas, A. K. 2007. Induced mutation in grass pea (*Lathyrus sativus* L.). S. J. Ochatt, S. M. Jain (Eds.): Underutilized and Neglected Crops, Herbs and Spices, Science Press, Enfield, USA, pp. 29-39.
- Chaudhari, D. D.; Prajapati, M. R.; Thakar, K. P. and Chaudhary, K. L. 2016. Estimate the compound growth rates of area, production and productivity of summer bajra in Banaskantha district of Gujrat. *International Journal of Current Research*, 8(1): 24930-24932.
- Cuddy, J. D. A. and D. Valle. 1978. Measuring the instability of time series data. *Oxford Bulletin of Economics and Statistics*. Available at: <https://onlinelibrary.wiley.com/doi/10.1111/j.1468-0084.1978.mp40001006.x>
- Das, K. R.; J. R. Sarker and S. Akhter. 2016. Measurement of inconsistency between area and production of pulse in Bangladesh. *International Journal of Statistics and Applications*, 6(3): 89-95.
- Das, A. and Mishra, R.R. (2020). Compound annual growth (CAGR) rate of fresh tea leaf (*Camellia sinensis*) production in Assam: a statistical approach. *SSRN Electronic Journal*. Available at: <https://ssrn.com/abstract=3728002>
- DDP, 2013. Desirable Dietary Pattern. Dietary Guidelines for Bangladesh. Bangladesh Institute of Research and Rehabilitation in Diabetes, Endocrine and Metabolic Disorders (BIRDEM), Dhaka.
- FAOstat, 2021. Food and Agriculture Data. Food and Agriculture Organization (FAO), Rome, Italy.
1. **Gufi, Y.; A. Tsegay; Morgan; L. Ruelle; K. Teka; S. T. Berhan and G. A. Power. 2022.** Field pea diversity and its contribution to farmers' livelihoods in northern Ethiopia. *Legume Science*, Available at: <https://doi.org/10.1002/leg3.141>
- Gupta, B. S. and P. K. Saraswat. 1997. Growth of Rapeseed and Mustard in Western Rajasthan. *Agric. Situation in India*. **54(5)**: 449-466.
- HIES, 2016. Household Income and Expenditure Survey 2016. Bangladesh Bureau of Statistics, Statistics and Informatics Division, Ministry of Planning, Govt. of the Peoples' Republic of Bangladesh, Dhaka.
- Islam, Q. M. S.; M. A. M. Miah; M.S. Rahman and M. S. Hossain. 2013. Adoption of BARI mung varieties and its constraints to higher production in southern region of Bangladesh. *Bangladesh J. Agril. Res.* 38(1): 85-96, Doi: <http://dx.doi.org/10.3329/bjar.v38i1.15193>
- Kabir, A. H. M. F. and M. N. Bari et al., 2009. Effect of sowing time and cultivars on the growth and yield of chickpea under rainfed condition. *Bangladesh J. Agril. Res.* 34(2): 335-342.
- Kakali, M. and P. Basu. 2006. Measurement of growth trend: An econometric study of food grains production in west. *Bangladesh.J. Agric. Econ.* 3(3):44-55.
- Kaul, A.K.; M. Q. Islam and A. Hamid. 1986. Screening of *Lathyrus* germplasm of Bangladesh for BOAA content and some agronomic characters. A. K. Kaul, D. Combes (Eds.), *Lathyrus and Lathyrism*, Third World Medical Research Foundation, New York, pp. 130-141
- Kumar, S.; G. Bejiga; S. Ahmed; H. Nakkoul and A. Sarker. 2011. Genetic improvement of grass pea for low neurotoxin (ODAP), *Food Chem. Toxicol.*, 49: 589-600

- Lambein, F.; D. D. Ngudi and Y. H. Kuo. 2009. Progress in prevention of toxico-nutritional neurodegenerations. Institute of Plant Biotechnology for Developing Countries (IPBO), Ghent University, K. L. Ledeganckstraat 35, 9000 Gent, Belgium. <http://www.atdforum.org/journal/html/2009-34/8/>.
- Malek, M. A. 1998. Genetic Resources of Grass Pea (*Lathyrus sativus* L.) in Bangladesh. P.N. Mathur, V.R. Rao, R.K. Arora (Eds.), *Lathyrus* Genetic Resources Network: Proceedings of a IPGRI-ICARDA-ICAR Regional Working Group Meeting, December 8–10, 1997, National Bureau of Plant Genetic Resources, New Delhi, pp. 1-6
- Malek, M.A.; C.D.M. Sarwar; A. Sarker and M.S. Hassan. 1996. Status of grass pea research and future strategy in Bangladesh. In: Arora RK, Mathur PN, Riley KW, Adham Y (eds) *Lathyrus* genetic resources in Asia. International Plant Genetic Resources Institute, Rome, pp 7–12.
- Matin, M.A.; S.M.Q. Islam and S. Huque. 2018. Profitability of lentil cultivation in some selected sites of Bangladesh. *Bangladesh Journal of Agricultural Research*, 43(1):135-147.
- Meena N. S. 2016. Trends in production productivity of principal crops in Haryana. *International Journal of Advanced Research in Management and Social Sciences*, 5(6):740-752.
- Miah, M.A.M; M.S. Akter and M.A. Bakr. 2004. Status of pulses varieties adoption in Bangladesh: a farm level study. *Bangladesh J. Agril. Econ.*, 27 (2): 107-122.
- Miah, M.A.M.; Q.M. Alam; A. Sarker and M.S. Aktar. 2009. Socio-economic impact of pulse research in some selected areas of Bangladesh. *Asia Pacific Journal of Rural Development*, 19(2):115-141.
- Miah, M.A.M.; M. A Rashid and M. S. Rahman. 2021. Profitability analysis and comparative advantage of lentil production in Bangladesh. *The Bangladesh Journal of Agricultural Economics*, 42(2): 49-64.
- Miah, M.A.M.; M. A. Rashid and M.S. Rahman. 2022. Factors of adoption and farmers' perceptions on improved lentil variety cultivation in Bangladesh. *Farm Economy* 17: 75-89.
- Mogotsi, K. 2006. Mung bean (*Vigna radiata* L.). In: M. Brink, M. and Belay, G. (Editors). *Plant Resources of Tropical Africa (Vol-1). Cereals and Pulses* (pp. 23–29), Foundation Prota, Wageningen, Netherlands.
- Rahman, N. M. F. and M. A. Baten. 2016. Forecasting area and production of black gram pulses in Bangladesh using ARIMA models. *Pak. J. Agri. Sci.*, 53 (4): 759-765, Doi:10. 21162/PAKJAS/16.1892
- Rahman, M. M. 1989. Progress and prospect of minor pulses of Bangladesh: Second national workshop on pulses, BARI, Joydebpur, Gazipur.
- Rashid, M.A., S. Hossain, U. Deb, D. K. Charyulu, D. M. Shyam and Cynthia. 2014. Targeting and introduction of chickpea improved cultivars in Barind region of Bangladesh. Paper presented in the 8th International Conference on *Viability of Small Farmers in Asia*, 15-17th October 2014, Savar, Bangladesh.
- Razzaque, M. A., M. A. Satter, et al., 2000. *Agriculture Technology Handbook*. Bangladesh Agricultural Research Institute (BARI), Joydebpur, Gazipur.
- Rizvi, A. H.; A. Sarker and A. Dogra. 2016. Enhancing grass pea (*Lathyrus sativus* L.) production in problematic soils of South Asia for nutritional security. *Indian J. Genet. Plant Breed.* 76: 583-592. Doi: 10.5958/0975-6906.2016.00074.2
- Sarker, A.; M. M. Rahman; W. Zaman; M. O. Islam, et al. 1989. Status of lentil breeding and future strategy. Bangladesh Agricultural Research Institute (BARI), Joydebpur, Gazipur.
- Sarker, A. and S. Kumar. 2011. Lentils in production and food systems in West Asia and Africa. International Center for Agricultural Research in the Dry Areas (ICARDA), Aleppo, Syria. *Grain Legumes*, 57: 46-48.
- Sarkar, M. M. A.; M. H. Rahman; M. R Haque; S. Islam and R. Sultana. 2020. Socio-economic determinants and profitability analysis of Binamasur-8 production in some selected areas of Bangladesh. *IOSR Journal of Economics and Finance*, 11(6): 20-27.
- Sarker, A.; M. A. Bakr; M. A. Afzal; W. Erskine; M. Rahman and M. C. Saxena. 2004. Lentil Improvement in Bangladesh. Bangkok, Thailand: The Asia-Pacific Association of Agricultural Research Institutions (APAARI).
- Senanayake, L.; D. P. Kniewel and S. E. Stevena. 1987. Nodulation and symbiotic nitrogen fixation of cowpea. *Plant Soil*, 99:435-439.
- Sharma, S. N. and R. Prasad. 1999. Effects of sesbania green manuring and mungbean residue incorporation of productivity and nitrogen uptake of a rice- wheat cropping system. *Bioresource Technology* 67(2): 171-175.
- Siju, T. and S. Kombairaju. 2001. Rice production in Tamil Nadu: A trend & decomposition analysis. *Agric. Situation in India*. 58(4): 143-145.
- Singh, R.K.P. and K. P. Ranjan. 1998. Growth and Instability in production of principle food grains crops: A case of background economy. *Bangladesh J. Agric. Econ.* 21(1-2): 1-20.
- Tithi, S. M. and B. K. Barmon. 2018. Comparative advantages of lentil and mustard production and their profitability in a selected district of Bangladesh. *The Agriculturists*, 16(1): 21-33.
- Zapata, F.; S. K. A. Danso; G. Hardarson and M. Fried. 1987. Nitrogen fixation and translocation in field-grown fababeans. *Agronomy Journal*, 79:505-509.
- Winch, T. 2006. *Growing Food, A Guide to Food Production*. Springer Dordrecht. ISBN 978-1-4020-4827-2, Published in 12 October 2006.

FORECASTING ONION YIELD BY USING SATELLITE-BASED REMOTE SENSING TECHNIQUE IN BANGLADESH

NUR MOHAMMAD¹, MOHAMMAD MUKHLESUR RAHMAN¹, ISTIAK AHMED¹, MOHAMMAD RASEL¹, AND MD. ABDUL MONAYEM MIAH²

Abstract

Onion is one of the major vegetables as well as spices crops with the largest production worldwide. Onion plays as a major contribution as spices crop which is used in daily meal in Bangladesh. Therefore, it is imperative to do research aimed at forecasting the yield of onion crops. Pre-harvest prediction of a crop yield may prevent a disastrous situation and help decision-makers to apply more reliable and accurate strategies regarding food security. Remote sensing can be used for yield estimation prior to harvest at the field level to provide helpful information for agricultural decision making. Remote sensing images are capable of identifying crop health, as well as predicting its yield. Vegetation indices (VIs), such as the normalized difference vegetation index (NDVI) calculated from remotely sensed data have been widely used to predict crop yield. Yield prediction models based on a time series of satellite images and high-density yield data, and to indicate the best phenological stage of onion crop to obtain satellite images for this purpose. The study used 16-day (~ 30 m) Landsat 8 OLI (Operational Land Imager) high resolution reflectance data for the first year 2022-2023 at three different locations viz. Sujanagar, Pabna; Baliakandi, Rajbari and Durgapur, Rajshahi in Bangladesh. The single date of cloud free image acquisition based on maximum NDVI for Landsat 8 OLI satellite image was used for 2022-2023 onion growing period to develop the yield prediction model. Regression model was performed between NDVI values and 35 farmers filed level onion yields for all locations. The yield vs. NDVI relationship for Landsat 8 image exposed that the multiple determination of coefficient (R^2) which is highest (84.1%) for Baliakandi, Rajbari followed by $R^2=83.8\%$ for Sujanagar, Pabna and $R^2=72.3\%$ for Durgapur, Rajshahi for first year onion growing season i.e., 2022-2023.

Key words: NDVI, Landsat 8, Onion, Prediction, Yield and Satellite image

Introduction

Onions (*Allium cepa L.*) of various cultivars and forms are used for consumption all over the world, and their growth depends on numerous environmental factors, such as the climate and the soil's nutrient and moisture content (Newton et al., 2011). Over 140 countries grow onion owing to its nutritional and medicinal properties. Onions can be consumed as raw, fresh, or processed and contain antioxidants and anti-inflammatory compounds that reduce cholesterol levels, diabetes, high blood pressure, and the risk of cardiovascular diseases (Lee et al., 2012; Akash et al., 2014 and Yoshinari et al., 2012). The global production of 98 Mt of onion makes it the second most important vegetable crop after tomato (Recciardi et al., 2020; Venâncio et al., 2014 and FAO, 2021). Bangladesh is basically an agricultural country. Onion is one of the most significant profitable vegetable crops, which is used as spices in our daily meal in Bangladesh. Besides Bangladesh, it has also huge demand all over the world. It can be used in both mature and immature level as vegetable and spices, and increases the taste of food by its flavor that contains protein, calcium, carbohydrates and vitamin C. It is also used as medicine to recover from insect injury and raw throat (Bose and Som, 1990). Onion is cultivated all over the country extensively in winter season. In Bangladesh, onion ranks top among all the spice crops in production and almost 47% area covered in all spices crops (BBS, 2022). Although production of onion is increasing day by day, but in a land hungry country like Bangladesh it may not be possible to meet the domestic demand due to increase in population. There is an acute shortage of onion in relation to its requirement. Every year, Bangladesh has to import a

big amount of onion from neighboring and other countries to meet up its demand (Haque et al., 2011). For these reasons, the accurate forecasting of onion yield is hugely important in ensuring the accurate determination of their product.

The precise and timely monitoring of potential yields is crucial for decision making as it influences markets, export–import decisions and farm income budgeting (Zhao et al., 2020). Currently crop statistics in Bangladesh are mostly gathered by accumulation of representative field sampling data which is time consuming and missing with information from spatial distribution of field variability. On the other hand, the prediction of crop yield before the harvest is one of the most significant concerns in agriculture since variations in crop yield from year to-year impact international trade, food supply, and market prices. However, both crop statistics and yield estimation are estimated usually through conventional means (field experiments or surveys). Currently, remote sensing (RS) techniques are using to measure these statistics at high spatial and temporal resolutions. The crop-yield prediction model can be extended with the remote sensing technology, based on an image sensor and a ground positioning system (Ryu et al., 2011). The RS technology makes it possible to improve the performance of the prediction models and monitor the crop's growth status in a non-destructive and timely manner at a specific regional scale (Cai et al., 2019). Satellite based remote sensing is one of the best tools to provide vital information about the distribution of crops and its growing conditions over large areas, it can be applied for onion growth monitoring and yield forecast.

Pre-harvest crop yield prediction is essential for planning and making various policy decisions. Traditional methods are time consuming, subjective, and costly. Developing empirical models that are using weather data is also determined by several problems. Enormous types of sensors such as aerial photogrammetry, multi-spectral scanners airborne, satellite imagery, high and low spectral and spatial resolution and field-based spectrometer analysis were used to collect electromagnetic radiation information (Zhou et al., 2017). During the last few years, many empirical models have been developed to predict crop yield before the harvesting, but many of them have become unpractical, especially those are depending on filed data collection. As the satellite based remote sensing is one of the best tools to provide vital information about the distribution of crops and its growing conditions over large areas, it can be applied for onion growth monitoring and yield forecast. Nogueira et al. (2018) reported the use of vegetation indices obtained with images from the Landsat-8 satellite's OLI sensor to estimate yield. Evaluating two seasons considered low- and high-yielding, they found that NDVI had the strongest yield correlation during the dormancy and flowering stages. Zhang et al. (2019) predicted rice paddy productivity from a vegetation index extracted from Landsat 8 satellite imagery and Sari et al. (2013) utilized Landsat 8 satellite imagery to estimate rice paddy yield. The combination of data acquired by Landsat 8 and Sentinel 2 remote sensing satellites can provide a high temporal resolution (3–5 days) which is crucial for several applications requiring dense satellite data time series (Li et al., 2017). Several studies have been carried out by the correlation of normalized difference vegetation index (NDVI) with yield (Liu W.T et al., 2002). Recent studies took benefit of Landsat 8 and Sentinel 2 data to approach crop yield forecasting at a moderate spatial resolution. For example, Lai et al. (2018) applied time-integrated Landsat NDVI for wheat yield estimation in Australia. They applied an asymmetric bell-shaped growth model to fit NDVI against time. Skakun et al. (2019) applied the combination of Landsat 8 and Sentinel 2 high frequency of observations (3–5 days) at moderate spatial resolution (10–30 m), which is important for crop yield studies which were executed for the model with near infrared (NIR) and red spectral bands and derived AUC, constant, quadratic and linear coefficients of the quadratic model.

In Bangladesh, Bala & Islam (2009) expanded potato yield estimations models by using NDVI, LAI (leaf area index), and fraction of photosynthetically active radiation (fPAR) vegetation indices for Munshiganj District of Bangladesh by applying Moderate Resolution Imaging Spectroradiometer (MODIS) (with lowest resolution greater than 250m) 8-day composite surface reflectance data and noticed that an average error of estimation is about 15% for the study location. Newton et al. (2018) improved a potato yield prediction model by applying 16-day high resolution (~ 30 m) Landsat surface reflectance data to identify

the maximum normalized difference vegetation index (NDVI) value of a potato growing season in Munshiganj District of Bangladesh. The maximum coefficient of determination (R^2) of yield forecasting equation was found to be 0.81 between the mean NDVI and potato yield and the result revealed that the difference between predicted and actual filed yield is about 10.4%. However, very few studies have been conducted on the relationship between high resolution (~ 30 m) Landsat 8 satellite data and crop yield in Bangladesh. Even though, this study made an attempt to construct a onion yield prediction model based on NDVI at Sujanagar Upazila, Pabna; Baliakandi Upazila, Rajbari and Durgapur Upazila, Rajshahi districts of Bangladesh respectively using high-resolution Landsat 8 Operational Land Imager (OLI) surface reflectance data. The use of high resolution Landsat 8 image has been applied in this study to improve yield assessment model for the onion crop for all selected locations in Bangladesh.

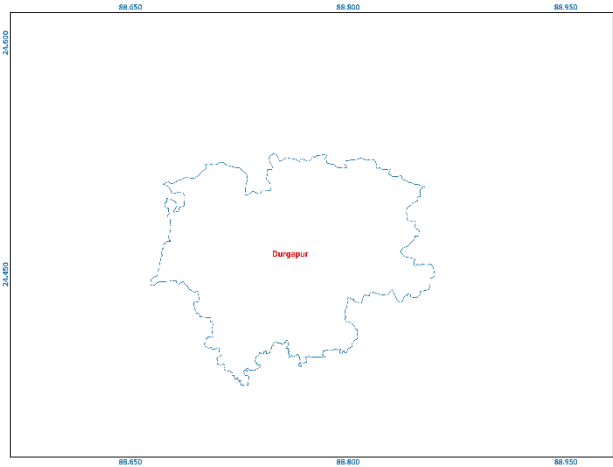
Objectives

1. To develop yield prediction model of onion crop using remote sensing technique
2. To forecast onion yield by satellite based remote sensing technique

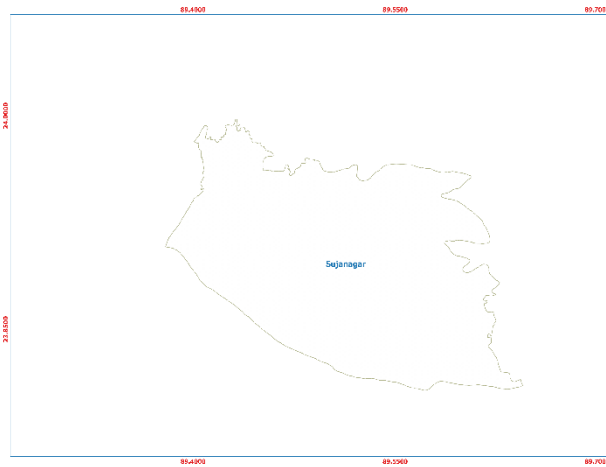
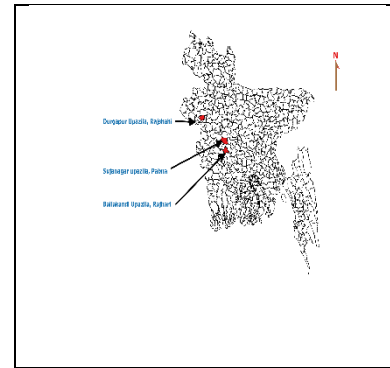
Materials and Methods

Study Area

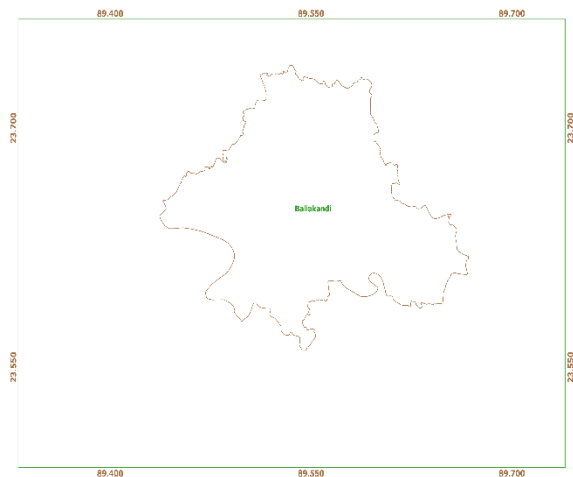
The study was conducted at Sujanagar, Baliakandi and Durgapur upazila in Pabna, Rajbari and Rajshahi district respectively which are the major and promising onion growing areas of Bangladesh. Three districts viz. Pabna, Rajbari and Rajshahi were covered almost 43 % area coverage as well as ranked first, third and fifth position for cultivation onion in Bangladesh. These three districts covered 20.86%, 13.94% and 7.60% onion cultivated area all over Bangladesh respectively (BBS, 2022). The three upazilas Sujanagar, Baliakandi and Durgapur lie between 23° 85' to 24° 0' N latitude and 89° 40' to 89° 70' E longitude, 23° 55' to 23° 70' N latitude and 89° 40' to 89° 70' E longitude and 24° 30' to 24° 60' N latitude and 89° 45' to 89° 95' E longitude, respectively (Figure 1). All upazilas like Sujanagar, Baliakandi and Durgapur cover 334.34 km² and 225.0 km² and 195.03 km² areas where 75%, 70% and 80% areas are cultivable land respectively. The climate condition of those areas are hot and humid from April to October (summer) and cool and dry from November to March (winter). The agricultural pattern of those areas are categorized by two growing seasons, one is Rabi and the rest is Kharif. Rabi is the main growing season, which is dominated by onion, oilseeds and vegetables that starts in late October or the beginning of early November and ends in April for those upazilas. On the other hand, Kharif is dominated by rice and jute, which starts in May and ends until September. Other foods which include potato, pepper, pulses, sugarcane, and wheat are also cultivated in those areas.



Durgapur, Rajshahi



Sujanagar, Pabna



Baliakandi, Rajbari

Figure 1: Study area map of selected locations

Yield data collection from farmer's fields

35 farmer's onion fields were selected for the three onion growing seasons 2022-2023, 2023-2024 and 2024-2025 respectively with agreement of the farmers at three selected upazilas (Figure 2, 3 and 4). A total of 35 farmer's different onion field data were collected from those selected locations for each season. Crop information data such as field GPS locations, planting and harvesting time and yield were collected from those selected upazilas farmers' fields.

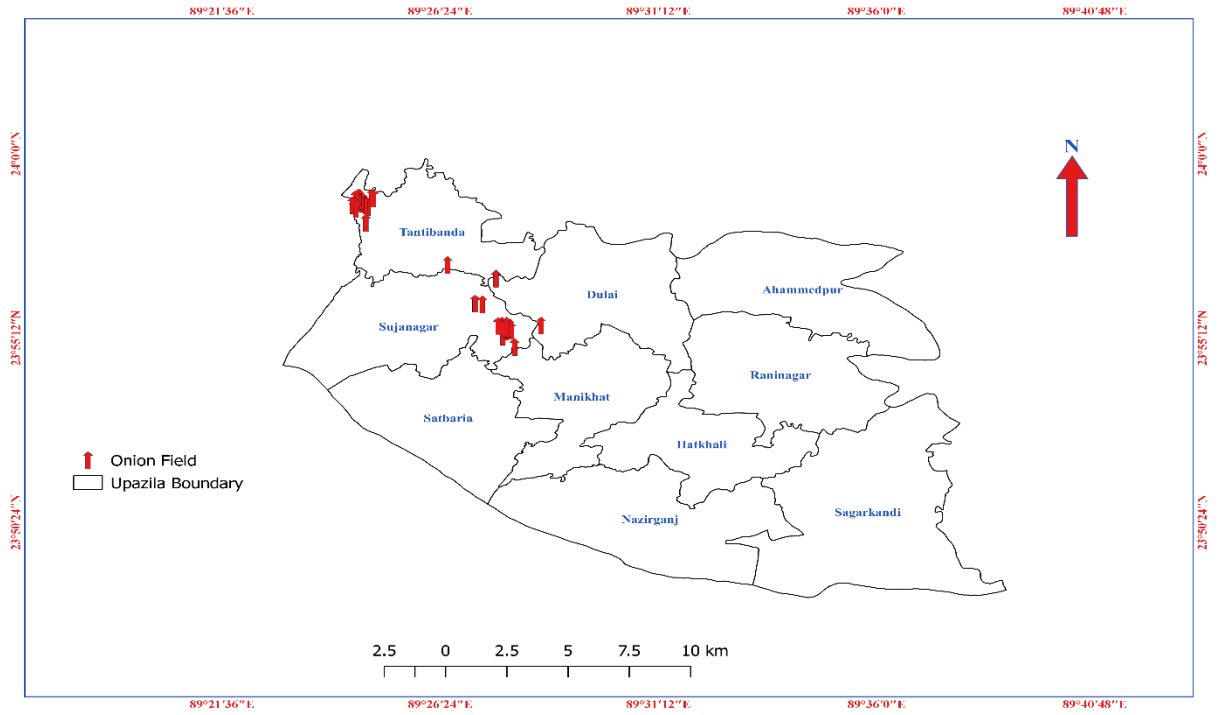


Figure 2: Location of selected 35 onion fields (red arrows) over Sujanagar, Pabna.

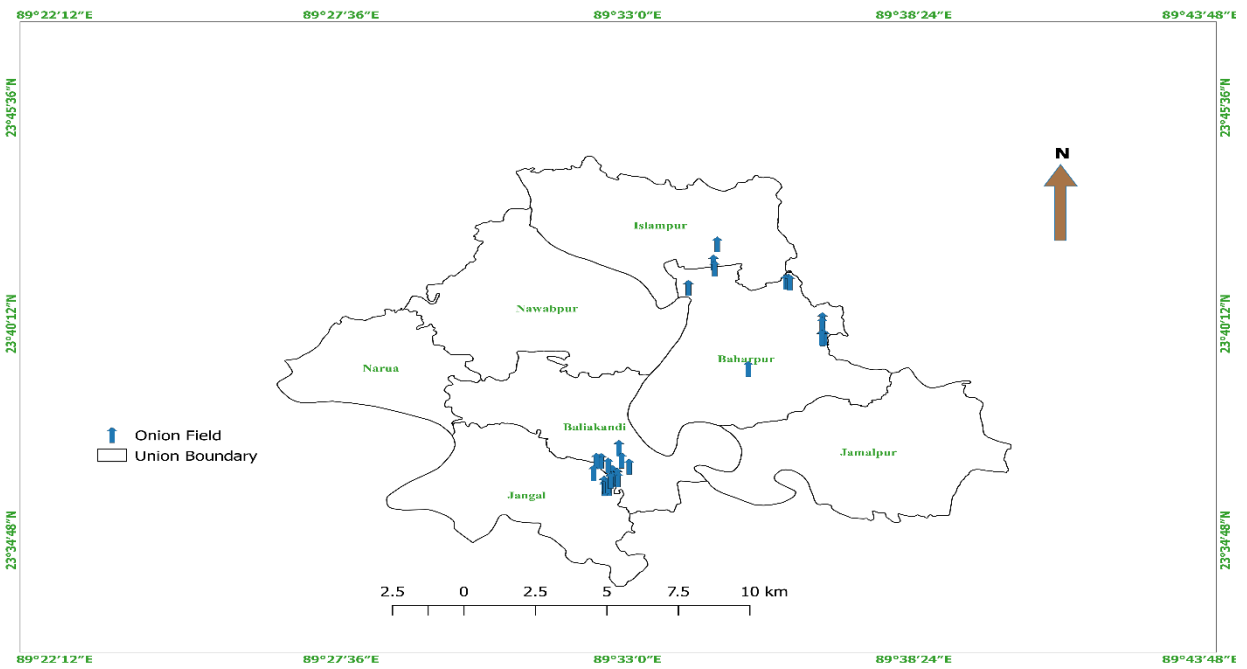


Figure 3: Location of selected 35 onion fields (blue arrows) over Baliakandi, Rajbari.

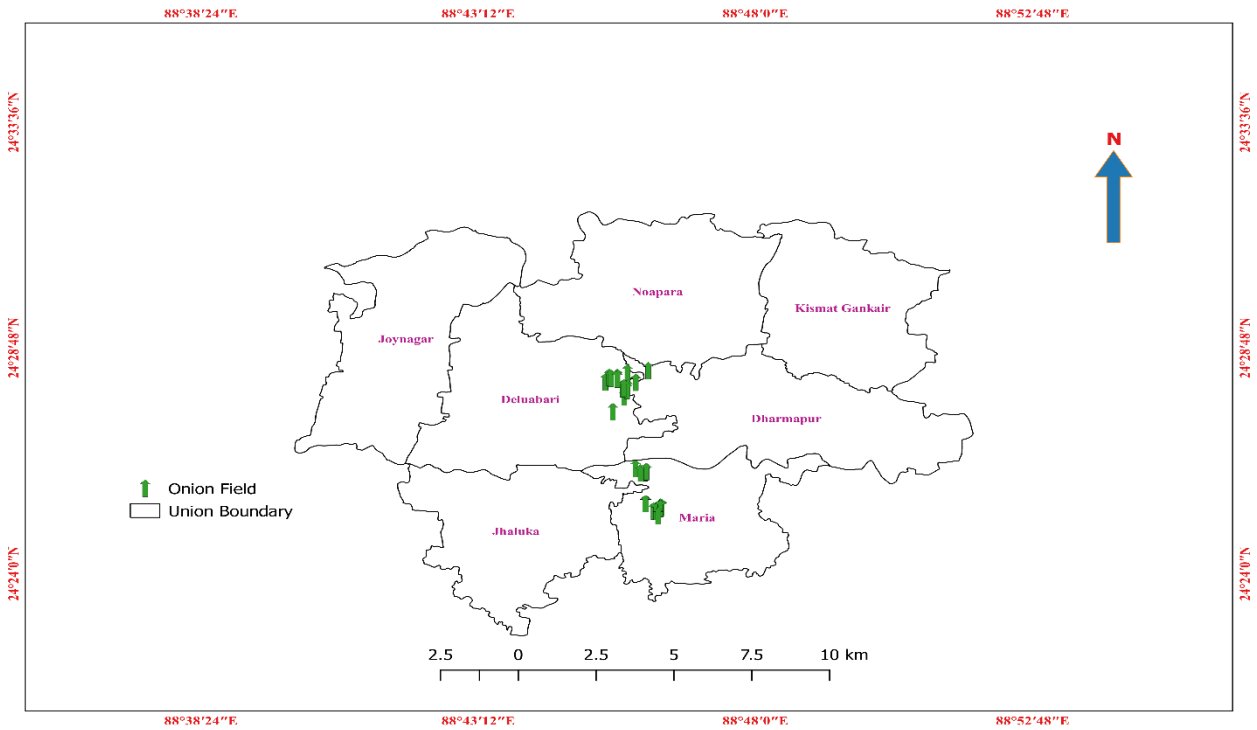


Figure 4: Location of selected 35 onion fields (green arrows) over Durgapur, Rajshahi.

Satellite Data

Landsat 8 Satellite Image

Satellite image Landsat 8 (OLI) was used for the yield estimation analysis, which is available on the USGS Earth Explorer website ([https:// earthexplorer.usgs.gov/](https://earthexplorer.usgs.gov/)). Landsat 8 (OLI) is a sun-synchronous satellite staying at an altitude of 705 km above the earth with a 16-day repeat cycle. Landsat 8 has two types of sensors, especially the Operational Land Imager (OLI) and Thermal Infrared Sensor (TIRS). The OLI sensor equips nine spectral bands, including a pan band, and TIRS produces two spectral bands.

We downloaded total 3 images which was maximum cloud free were collected from Landsat 8 OLI satellite data for Sujanagar, Baliakandi and Durgapur upazila in Pabna, Rajbari and Rajshahi district respectively in the first year 2022-2023. The single date of image acquisition based on maximum greenness was used for each growing period i.e. 2022-2023 for onion cultivation. The onion sowing date was considered to be second week of December and third week of January for those upazilas for a growing season 2022-2023 for the entire study site based on the information taken from the location visits. Every single image was calculated from the starting day of the plantation. The dates of image acquisition of Landsat 8 OLI for the onion growing season 2022-2023, for those locations used for this study are presented in Table 1.

Table 1: Model development of onion using Landsat 8 for selected locations

Satellite Image	Landsat 8 OLI		
	Sujanagar, Pabna	Baliakandi, Rajbari	Durgapur, Rajshahi
Location			
Growing Season	2022-2023	2022-2023	2022-2023
IAD	10/02/2023	26/02/2023	14/03/2023
DAP	72	73	77

IAD=Image acquisition date; DAP= Days after plantation

Satellite Image Pre-Processing

For Landsat data, raw digital numbers (DN) were adjusted to top-of-atmosphere (TOA) reflectance values following reference (Simonetti et al., 2015). Two techniques were used to preprocess the satellite images: (1) radiometric calibration and (2) atmospheric correction. Remote sensing data adopted from satellite sensors are influenced by several factors, such as atmospheric scattering and absorption, sensor-target-illumination geometry, sensor calibration, and also by the data processing procedures (Teillet, 1986). For that, radiometric calibration is needed. Radiometric calibration means a set of correction techniques that are associated to correction for the sensitivity of satellite sensor, topography and sun angle, atmospheric scattering, and absorption (Kim et al., 1990). The radiometric calibration was done by transforming the digital numbers (DNs) to surface reflectance by radiance conversion. Open source-based Quantum Geographic Information System (QGIS) software 2.18.13 version allows a plugin, and the plugin gives a tool for atmospheric correction, which is known as dark object subtraction (DOS-1) level 1. In this study, this tool was used in the radiometrically calibrated images to minimize atmospheric scattering effect. DOS-1 searches each pixel of a band to find the darkest value. The scattering is eliminated by subtracting this value from every pixel in the band.

Normalized Difference Vegetation Index (NDVI)

The NDVI is generally applied extensively around the world to monitor the vegetation quality, growth, and distribution over a large area. Differences in the phenological growth stages of different plants are reflected in the temporal NDVI profiles, since NDVI can measure growth conditions (greenness of vegetation) (Belgiu & Csillik, 2018; Croitoru et al., 2012). It is a dimensionless index, which is performed from the ratio between the surface reflectance of the NIR and RED bands of the spectrum as follows (Equation 1) (Rouse et al., 1974).

$$NDVI = \frac{NIR - RED}{NIR + RED} \quad (1)$$

Where RED (Visible red) and NIR (Near infrared) are reflectance measurements for RED and NIR bands, respectively. The factors like strong reflectance in NIR and strong absorption in Visible Red of specific vegetation distinguish the vegetation from bare soil. NDVI for a given pixel can always output a number that ranges from -1 to +1; however, for natural surfaces NDVI values are within the 0 to +1 range. Negative values of NDVI i.e. values approaching -1 correspond to water. An NDVI close to 0 corresponds to no vegetation, while Values lies between -0.1 to 0.1 generally corresponded to barren areas of rock, sand or snow.

Yield prediction model

The final step is to determine the relationship between NDVI and onion yield from farmers' field with the equation below:

$$y = f(x) \quad (2)$$

Where y and x are onion yield data collected from farmers' field and NDVI, respectively. The relationship between NDVI and crop like onion yield have been observed through the linear regression model, where the response variable denoted by onion yields and the explanatory variables by NDVIs. To develop the onion yield estimation model for those fields, the data of onion yield and Landsat 8 (OLI) image was used for first year 2022-2023.

Performance evaluation of yield prediction model

The coefficient of multiple determinations (R^2), the root mean square error (RMSE), mean absolute percentage error (MAPE) and the normalized RMSE (nRMSE) were selected as performance evaluation metrics. These metrics are mathematically defined as:

$$R^2 = \frac{\sum_{i=1}^n E_i \times O_i - \sum_{i=1}^n E_i \times \sum_{i=1}^n O_i}{\sqrt{\sum_{i=1}^n E_i^2 - (\sum_{i=1}^n E_i)^2} \times \sqrt{\sum_{i=1}^n O_i^2 - (\sum_{i=1}^n O_i)^2}} \quad (3)$$

$$RMSE = \sqrt{\frac{\sum_{i=1}^n (E_i - O_i)^2}{n}} \quad (4)$$

$$MAPE = \frac{\frac{1}{n} \sum_{i=1}^n |E_i - O_i|}{O_i} \times 100 \quad (5)$$

$$nRMSE = \sqrt{\frac{\sum_{i=1}^n (E_i - O_i)^2}{n}} \times \frac{100}{\bar{O}} \quad (6)$$

Where, E_i is the estimated values, O_i is the corresponding observed values, \bar{O} is the mean value of O_i and n is the number of samples.

Generally, the larger R^2 is, the smaller the RMSE and MAPE is, and the better the model fit is. The range of the nRMSE metric generally defines the model accuracy. A value of $nRMSE < 10\%$ indicates that the estimated and measured values are highly consistent, the range $10\% < nRMSE < 20\%$ indicates good consistency, while the range $20\% \leq nRMSE < 30\%$ indicates medium consistency, and finally the range $nRMSE \geq 30\%$ indicates poor consistency.

Results and Discussion

Onion yield from farmers' field and corresponding NDVI values for different locations

Onion yield data and NDVI values from Landsat 8 data for corresponding farmers' fields have been collected from different locations viz. Sujanagar, Pabna; Baliakandi, Rajbari and Durgapur, Rajshahi during the first onion growing season 2022-2023. 35 farmers' field yield data collected from those upazilas and their corresponding NDVI values for Landsat 8 satellite image have been presented in a Table 3 for onion growing seasons 2022-2023.

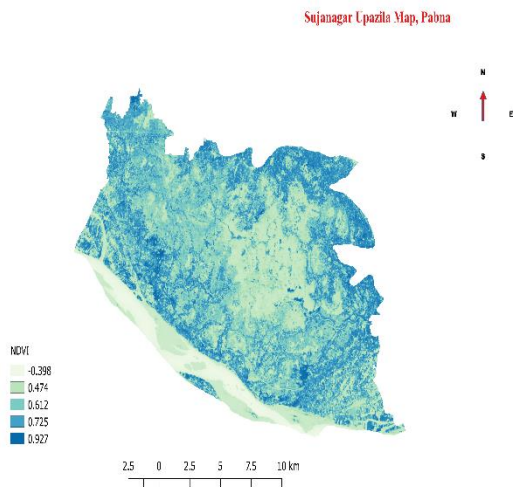
Table 3: NDVI values of Landsat 8 satellite image and yields of corresponding Farmer's fields at Selected locations during the season of 2022-2023.

Farmer's Field	Sujanagar, Pabna		Baliakandi, Rajbari		Durgapur, Rajshahi	
	NDVI	Yield (t/ha)	NDVI	Yield (t/ha)	NDVI	Yield (t/ha)
1	0.63	15.2	0.67	16.5	0.46	14.8
2	0.70	17.5	0.77	19.3	0.55	15.5
3	0.70	17.6	0.35	10.2	0.32	11.2
4	0.79	19.8	0.31	8.90	0.55	16.7
5	0.71	18.2	0.67	16.8	0.47	14.5
6	0.73	18.8	0.60	15.4	0.48	15.2
7	0.73	18.5	0.53	11.4	0.37	12.8
8	0.74	18.8	0.54	12.5	0.39	13.5
9	0.70	17.3	0.58	14.5	0.61	17.2
10	0.76	19.3	0.61	14.8	0.33	13.1
11	0.74	18.5	0.72	17.6	0.41	13.8
12	0.72	18.8	0.51	10.5	0.45	14.5
13	0.68	14.0	0.54	11.8	0.62	17.5
14	0.68	14.5	0.72	17.8	0.49	15.1
15	0.70	16.4	0.55	9.88	0.67	21.5
16	0.47	12.5	0.56	13.5	0.65	20.2
17	0.50	11.0	0.74	18.5	0.43	14.3
18	0.65	15.7	0.51	12.8	0.33	11.7
19	0.51	13.1	0.56	14.8	0.48	15.5
20	0.45	12.2	0.60	15.6	0.30	8.46
21	0.41	9.15	0.74	17.8	0.33	12.5
22	0.64	15.2	0.52	12.5	0.47	14.1
23	0.65	15.6	0.55	13.5	0.46	10.5
24	0.63	15.5	0.74	18.2	0.47	11.5
25	0.72	15.0	0.54	13.8	0.45	10.3
26	0.61	13.5	0.60	14.7	0.52	15.2
27	0.60	14.5	0.55	13.7	0.58	17.2
28	0.63	15.0	0.57	14.1	0.46	12.8
29	0.61	13.0	0.54	14.2	0.45	12.1
30	0.55	12.5	0.54	13.8	0.63	18.4
31	0.64	15.5	0.53	12.8	0.48	14.5
32	0.64	15.3	0.67	15.3	0.39	14.8
33	0.70	17.2	0.62	15.8	0.59	18.2
34	0.62	14.5	0.65	14.8	0.53	17.5
35	0.59	14.2	0.54	11.5	0.54	18.3

Table 3 shows that the highest NDVI value was 0.79 and the lowest was 0.41 and the maximum yield was 19.80 t/ha and the minimum was 9.15 t/ha for farmer's field 4 and 21 respectively for Sujanagar upazila, Pabna. On the other hand, the maximum and the minimum NDVI value and yield for Baliakandi upazila, Rajbari were 0.77 and 0.31 and 19.30 t/ha and 8.90 t/ha for the farmer's field 2 and 4 respectively; the highest and the lowest NDVI value and yield for Durgapur upazila, Rajshahi were 0.67 and 0.30 and 21.50 t/ha and 8.46 t/ha for the farmer's field 15 and 20 respectively for the onion growing season 2022-2023.

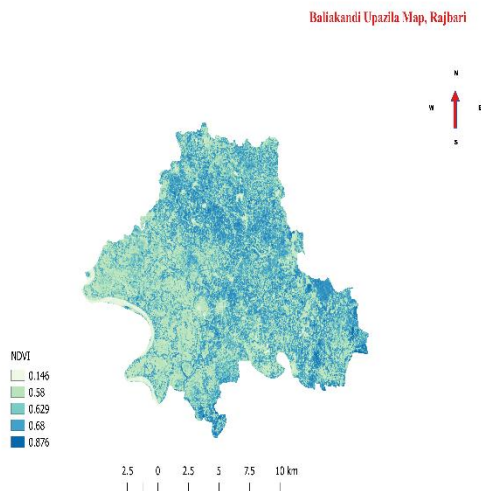
Regression analysis of the NDVI values over the field locations

A total of three Landsat 8 satellite images during the onion growing season 2022-2023 were selected from different locations. Based on available images, the maximum NDVI were found 72th, 73th and 77th days after plantation for Sujanagar, Pabna; Baliakandi, Rajbari and Durgapur, Rajshahi respectively during the onion growing season 2022-2023. The spatial distribution of the NDVI varies from year to year. Spatial distribution of the NDVI over the selected location for selected distinct satellite images against growing season 2022-2023 were presented in Figure 5.

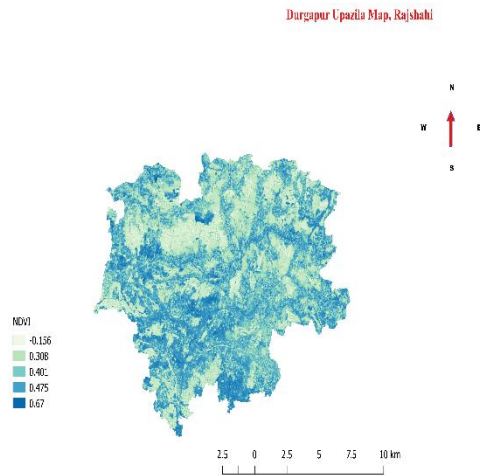


NDVI Map Sujanager, Pabna

a.



NDVI Map Baliakandi, Rajbari



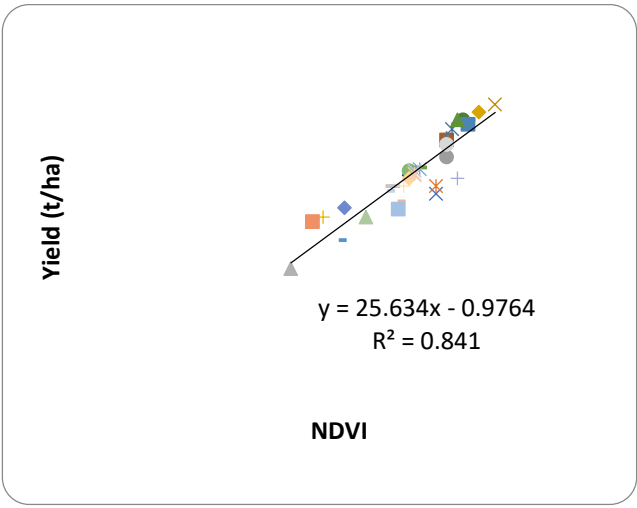
c. NDVI Map Durgapur, Rajshahi

Figure 5: Spatial distribution of the NDVI for Landsat 8 images during growing season 2022-2023. a. 72th days after plantation at Sujanager, Pabna; b. 73th days after plantation at Baliakandi, Rajbari; c. 77th days of plantation at Durgapur, Rajshahi.

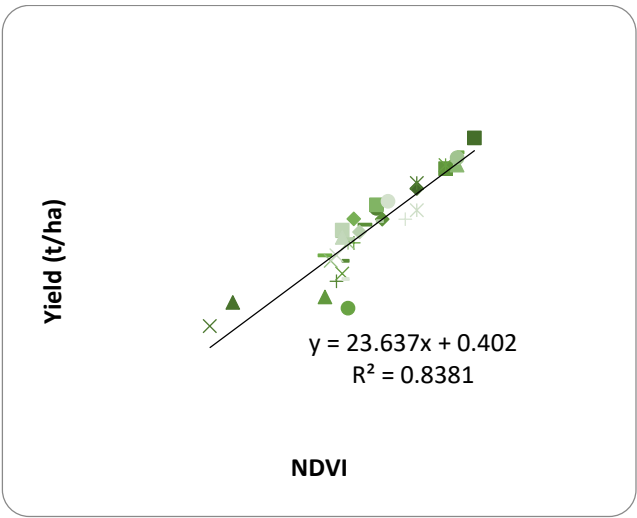
Maximum NDVI distribution from Landsat 8 satellite data was found for Sujanager, Pabna and followed by Baliakand Rajbari and Durgapur, Rajshahi respectively during the onion growing season 2022-2023 (Figure 5).

Onion yield and NDVI relationship using regression model

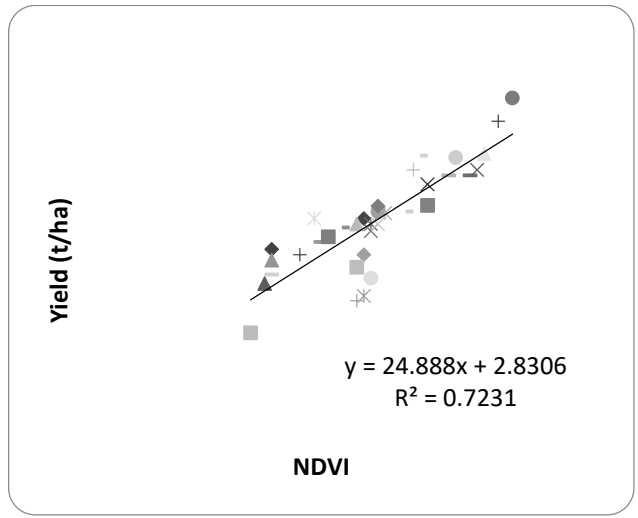
Regression analysis of onion yield against the single season basis (2022-2023) NDVI for different selected locations like Sujanager, Pabna; Baliakandi, Rajbari and Durgapur, Rajshahi was performed for Landsat 8 satellite image was graphically presented in Figure 6.



a. Suganagar, Pabna



b. Baliakandi, Rajbari



c. Durgapur, Rajshahi

Figure 6: Yield prediction model established from regression analysis between yield data collected from 35 farmers' onion field for different images for Landsat 8 during the onion growing season 2022-2023; [a. yield vs NDVI, Suganagar, Pabna; b. yield vs NDVI, Baliakandi, Rajbari; and c. yield vs NDVI Durgapur, Rajshahi.

The relationship between onion yield and NDVI are showed positive correlation among all selected locations for the first year growing season 2022-2023. Here, the regression coefficients of all the fitted model of Landsat 8 image are showing highly significant effect for selected locations. The yield vs. NDVI relationship for Landsat 8 image for all locations like Sujanagar, Pabna; Baliakandi, Rajbari and Durgapur, Rajshahi revealed that the multiple determination of coefficient (R^2) which is highest (84.1%) for Baliakandi, Rajbari followed by Sujanagar, Pabna ($R^2=83.8\%$) and Durgapur, Rajshahi ($R^2=72.3\%$) onion growing season 2022-2023.

Conclusions

The study has investigated the prediction capacity of remote sensing NDVI data for onion yield in selected three locations viz. Sujanagar, Pabna; Baliakandi, Rajbari and Durgapur, Rajshahi of Bangladesh which is known for onion dominating district. In the farmers' fields of the selected locations, the developed system investigates the combined use of satellite remote sensing (RS) and Geographic Information System (GIS) technology. The study has also investigated the relationship between NDVI and yield for the study region. Here the high spatial resolution satellite image Landsat 8 (OLI) was used in this study. The single date of cloud free image acquisition based on maximum NDVI was used for 2022-2023 cropping period for onion cultivation to develop the yield prediction model. The first year's results revealed that in most cases the yield was maximum for the field where the NDVI values were not maximum and vice-versa. Nevertheless, the relationships of the extracted NDVI and yields of onion crop will be established using the classical linear regression model where the model will be developed using the first two years' data and will be validated using the data of the last study period for all selected locations.

References

- Akash MSH, Rehman K, Chen S (2014) Spice plant *Allium cepa*: Dietary supplement for treatment of type 2 diabetes mellitus. *Nutrition* 30:1128–1137. <https://doi.org/10.1016/j.nut.2014.02.011>
- Bala, S. K., Islam, A. S. (2009). Correlation between potato yield and MODIS-derived vegetation indices. *Int J Remote Sens* 30(10): 2491–2507
- BBS, (2022). Bangladesh Bureau of Statistics, Statistical Yearbook of Bangladesh, Statistics Division, Ministry of Planning, Government of the People's Republic of Bangladesh, Dhaka.
- Belgiu, M., and Csillik, O. (2018). Sentinel-2 cropland mapping using pixel-based and object-based time-weighted dynamic time warping analysis. *Remote sensing of environment*, 204, 509–523.
- Bose, T. K. and Som, M. G. (1990). Vegetable crops in India. *Naya Prokash*, Calcutta, 6:545-582.
- Cai, Y., Guan, K., Lobell, D., Potgieter, A.B., Wang, S., Peng, J., Peng, B. (2019). Integrating satellite and climate data to predict wheat yield in Australia using machine learning approaches. *Agric. For. Meteorol.* 274, 144–159.
- Croitoru, A.-E., Holobaca, I.-H., Lazar, C., Moldovan, F., & Imbroane, A. (2012). Air temperature trend and the impact on winter wheat phenology in Romania. *Climatic Change*, 111, 393–410.
- FAO (2021) Crop Statistics, FAOSTAT. In: Food Agric. Organ. United Nations. <http://faostat.fao.org>. Accessed 15 Jul 2022
- Haque, M. A., Miah, M. A. M., Hossain, S., Rahman, M. S. and Moniruzzaman, (2011). Profitability of Onion Cultivation in Some Selected Areas of Bangladesh, *Bangladesh Journal of Agricultural Research*, 36(3):427-435.
- Kim, H. H. and Elman, G. C. (1990). Normalization of satellite imagery. *Int J Remote Sens* 11(8):1331–1347.
- Lai, Y. R.; Pringle, M. J.; Kopittke, P. M.; Menzies, N. W.; Orton, T. G. and Dang, Y. P. (2018). An empirical model for prediction of wheat yield, using time-integrated Landsat NDVI. *Int. J. Appl. Earth Obs. Geoinf.* 2018, 72, 99–108.
- Lee B, Jung J-H, Kim H-S (2012) Assessment of red onion on antioxidant activity in rat. *Food Chem Toxicol* 50:3912–3919. <https://doi.org/10.1016/j.fct.2012.08.004>

- Li, J.; Roy, D.P. (2017). A Global Analysis of Sentinel-2A, Sentinel-2B and Landsat-8 Data Revisit Intervals and Implications for Terrestrial Monitoring. *Remote Sens.* 2017, 9, 902.
- Liu, W. T. and Kogan, F. (2002). Monitoring Brazilian soybean production using NOAA/AVHRR based vegetation condition indices. *Int J Remote Sens* 23(6):1161–1179
- Newton, A.C., Johnson, S.N., Gregory, P.J. (2011). Implications of climate change for diseases, crop yields and food security. *Euphytica* 179 (1), 3–18.
- Newton, I. H, Islam, A. F. M T., Islam, A. K. M. S., Tarekul, G. M., Anika, T. and Razzaque, S. (2018). Yield Prediction Model for Potato Using Landsat Time Series Images Driven Vegetation Indices. *Remote Sensing in Earth Systems Sciences* (2018) 1:29–38.
- Nogueira, S. M. C., Moreira, M. A., Volpato, M. M. L. (2018). Relationship between Coffee Crop Yield and Vegetation Indexes Derived from Oli/Landsat-8 Sensor Data with and without Topographic Correction. *Eng. Agric.* 2018, 38, 387–394.
- Ricciardi L, Mazzeo R, Marcotrigiano AR, et al (2020) Assessment of Genetic Diversity of the “Acquaviva Red Onion” (*Allium cepa* L.) Apulian Landrace. *Plants* 9:260. <https://doi.org/10.3390/plants9020260>
- Ryu, C., Suguri, M., Umeda, M. (2011). Multivariate analysis of nitrogen content for rice at the heading stage using reflectance of airborne hyperspectral remote sensing. *Field Crops Res.* 122 (3), 214–224.
- Sari, D.K., Ismullah, I. H., Sulasdi, W. N. et al. (2013). Estimation of water consumption of lowland rice in tropical area based on heterogeneous cropping calendar using remote sensing technology. *Procedia Environ. Sci.* 2013; 17: 298–307.
- Simonetti, D.; Marelli, A.; Eva, H. (2015). IMPACTool Box: Portable GIS Toolbox for Image Processing and Land Cover Mapping; Publications Oce of the European Union: Luxembourg, 2015; ISBN 978-92-79-50115-9.
- Skakun, S., Vermote, E., Franch, B., Roger, J. C., Kussul, N., Ju, J. and Masek, J. (2019). Winter Wheat Yield Assessment from Landsat 8 and Sentinel-2 Data: Incorporating Surface Reflectance, Through Phenological Fitting, into Regression Yield Models. *Remote Sens.* 2019, 11, 1768:1-19; doi:10.3390/rs11151768. www.mdpi.com/journal/remotesensing.
- Teillet, P. M. (1986). Image correction for radiometric effects in remote sensing. *Int J Remote Sens* 7(12):1637–1651.
- Tucker, C.J. (1979). Red and photographic infrared linear combinations for monitoring vegetation. *Remote Sens. Environ.* 1979, 8, 127–150.
- Venâncio JB, Dias N da S, de Medeiros JF, et al (2022) Yield and Morphophysiology of Onion Grown under Salinity and Fertilization with Silicon. *Sci Hortic (Amsterdam)* 301:111095. <https://doi.org/10.1016/j.scienta.2022.111095>
- Yoshinari O, Shiojima Y, Igarashi K (2012) Anti-Obesity Effects of Onion Extract in Zucker Diabetic Fatty Rats. *Nutrients* 4:1518–1526. <https://doi.org/10.3390/nu4101518>
- Zhang, K., Ge, X., Shen, P. et al. (2019). Predicting rice grain yield based on dynamic changes in vegetation indexes during early to mid-growth stages. *Remote Sens.* 2019; 11(4): 1–24.

- Zhao, Y., Potgieter, A. B., Zhang, M., Wu, B., & Hammer, G. L. (2020). Predicting wheat yield at the field scale by combining high-resolution sentinel-2 satellite imagery and crop modelling. *Remote Sensing*. <https://doi.org/10.3390/rs12061024>
- Zhou, X., Zheng, H.B., Xu, X.Q., He, J.Y., Ge, X.K., Yao, X., Cheng, T., Zhu, Y., Cao, W.X., Tian, Y.C. (2017). Predicting grain yield in rice using multi-temporal vegetation indices from UAV-based multispectral and digital imagery. *ISPRS Journal of Photogrammetry and Remote Sensing* 130, 246–255.

YIELD PREDICTION OF MUSTARD CROP BY USING SATELLITE BASED REMOTE SENSING TECHNIQUE IN BANGLADESH

M. MUKHLESUR RAHMAN¹, NUR MOHAMMAD¹, ISTIAK AHMED¹,
M. A. MONAYEM MIAH¹ AND SUMAN BISWAS²

¹ASICT DIVISION, BARI, GAZIPUR AND ²ISLAMIC UNIVERSITY, KUSHTIA

Abstract

Mustard (*Brassica spp.*) is one of the important oilseed crops which has potential demand as the preferred edible oil for the majority of people of Bangladesh. The accurate estimation of both harvested area and yield of mustard are equally important in ensuring the accurate determination of their product. The traditional measurement of these statistics is time-consuming, tedious, and costly. Whereas remote sensing techniques are being used to easily measure these statistics at high spatial and temporal resolutions. Therefore, an attempt was made to predict the mustard yield through satellite-based remote sensing techniques before its harvesting. To get this done, the high spatial-temporal resolution Satellite imageries of Sentinel 2A (~10m) and Landsat 8 (~30m) were acquired for the three study locations after setting the experiment in a farmer's field for three consecutive mustard growing seasons of 2022-23, 2023-24 and 2024-25. The mean Normalized Difference Vegetation Index (NDVI) was extracted from the maximum NDVI-produced temporal satellite imageries within the growing season from 20 farmer's mustard fields of each study location. The first year's results revealed that in most cases the yield was maximum for the field where the NDVI values were not maximum and vice-versa. However, the relationships of the extracted mean NDVI and yields will be established using the classical linear regression model where the model will be developed using the first two years' data and will be validated using the data of the last study period.

Introduction

Mustard is the most dominant oilseed crop in Bangladesh and has experienced an expansion in area, production, and yield over time while facing the fierce competition for land for the production of cereals, e.g., rice, wheat, and maize. Mustard is a cold-loving *Rabi* crop that grows during October-February usually under rain-fed and low-input conditions in Bangladesh. Crop production estimates are generally portrayed as the product of two components: area (to be) harvested and (expected) yield per unit area. The accurate forecasting/estimation of both harvested area and yield are equally important in ensuring the accurate determination of their product.

Remote sensing images endow with entrance to spatial information at a global scale; of features and phenomena on Earth on an almost concurrent basis (El-Telbany *et al.*, 2019). It has the capability of the recognition of crop classification, crop growth monitoring, and crop yield estimation (Mohd *et al.*, 1994). In terms of how well it works for field research, it can find and give data on spatial variation and approval (Schuler, 2002). Remote sensing technology can play a significant role in the agricultural sector to provide timely and accurate information (Atzberger, 2013).

The agricultural application of satellite RS technology requires quantitative processing of satellite RS data with high accuracy and reliability. For yield prediction and estimation of crops, it is necessary to achieve a very high accuracy and reliability. This is the reason why even after a relatively long time (more than 20 years) no routine yield estimation method for a wide range of operational applications has been developed. However, a large amount of work produced important steps forward in this field. Naturally, most of the experiments and research concentrated on obtaining quantitative relation between satellite (or airborne) RS data and crop yields and used two main types of possible general strategies (Hamar *et al.*, 1988a,b).

These indices are commonly used for drought detection, monitoring excessive soil wetness, assessment of weather impacts on vegetation, and evaluation of vegetation health and productivity (Unganai and Kogan, 1998; Kogan, 2001; Kogan, 2002; Kogan *et al.*, 2003; Singh *et al.*, 2003). The NDVI data were used extensively in vegetation monitoring, crop yield assessment, and *forecasting* (Hayes *et al.*, 1982; Benedetti and Rossinni, 1993; Quarmby *et al.*, 1993).

In Bangladesh researchers and extension personnel collect most of its crop statistics through the compilation of representative field sample data, which takes a lot of time and leaves out information about the spatial distribution of field variability. Nevertheless, this traditional technique is time-consuming, tedious, and costly. Currently, remote sensing techniques are being used to measure these statistics at high spatial and temporal resolutions. The application of remote sensing in estimating agricultural performance indicators is increasing as it offers a time and cost-effective reproducible method for measurement that can cover larger physical areas as compared to in-situ methods (Sadras *et al.*, 2015). Therefore, an attempt was made to predict the mustard yield through satellite-based remote sensing techniques before its harvesting. The specific objectives of this study are given below.

Objectives

1. To create a map of selected mustard fields using satellite images; and
2. To estimate mustard yield by satellite based remote sensing technique.

Materials and Methods

Study area selection: Three promising mustard growing areas namely Sirajganj, Tangail, and Manikganj districts were purposively selected for this study. These three districts covered 15.40%, 8.17%, and 5.97% of the mustard area and shared 15.28%, 7.03%, and 5.53% of the total mustard production in Bangladesh, respectively (BBS, 2022). The Ullabara Upazila of Sirajganj district lies between 24°19' N latitude and 89°34' E longitude, Kalihati Upazila of Tangail district lies between 24°22' N latitude and 89°00' E longitude, and Daulatpur Upazila of Manikganj district lies between 23°57' N latitude and 89°50' E longitude (Figure 1).

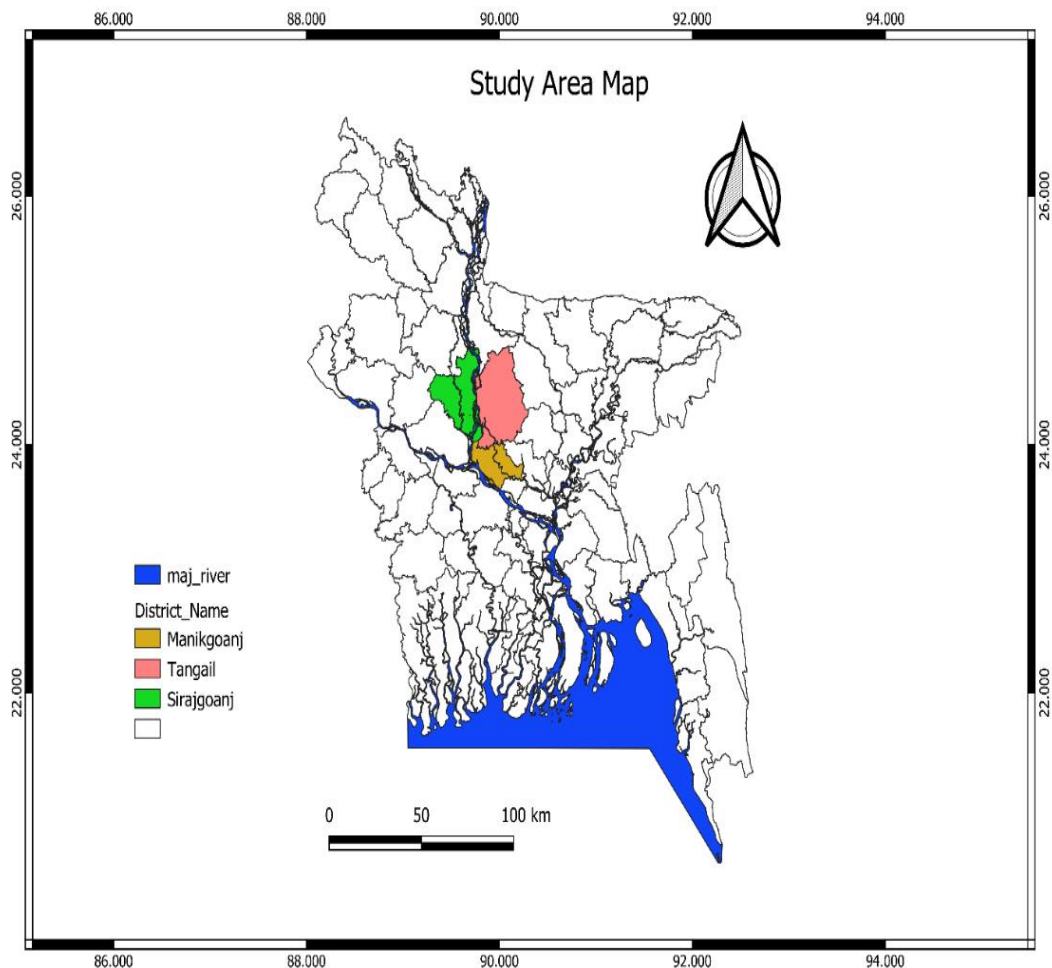


Figure 1: Study area map of Bangladesh

Data collection procedure: In this study, a total of 60 farmers' mustard fields taking 20 fields from each selected location were identified for the three mustard growing seasons 2022-2023, 2023-2029, and 2024-2025 by interviewing the sampled farmers. The identified mustard fields of Ullapara, Kalihati, and Daulatpur Upazila have been indicated in Figure 2, Figure 3, and Figure 4 respectively. It is important to mention here that each of the sampled farmers is committed to growing the same variety of mustard on the same identified plots for the next two succeeding years for the sack of this research. First year's (2022-23) yield data were acquired through direct interviewing sampled farmers from the selected mustard fields of the aforesaid locations.

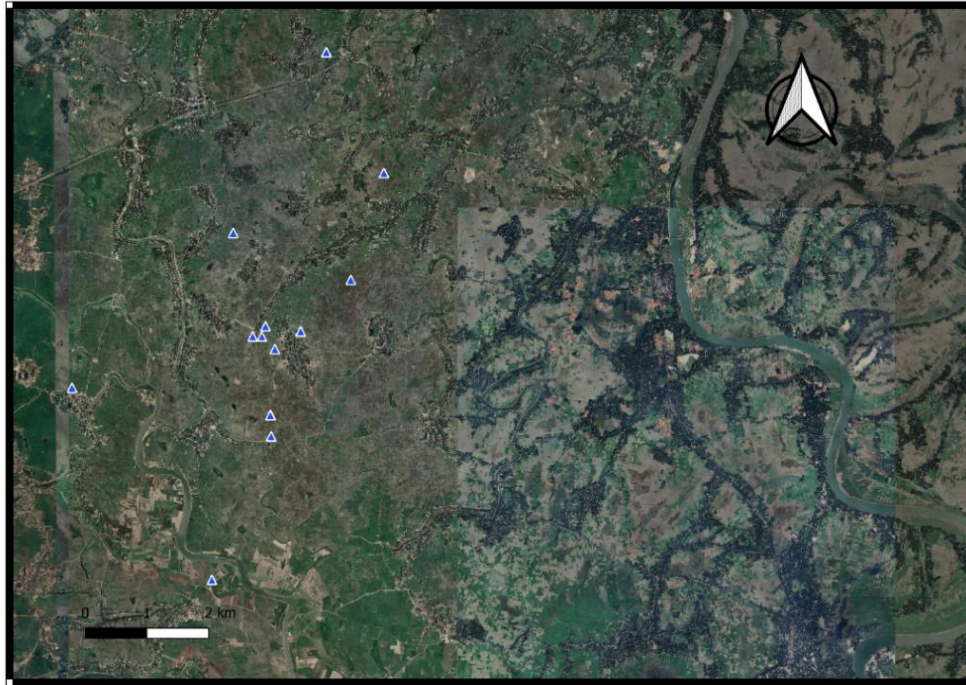


Figure 2: Locations of the selected mustard fields (blue triangles) over Ullapara Upazila, Sirajganj district

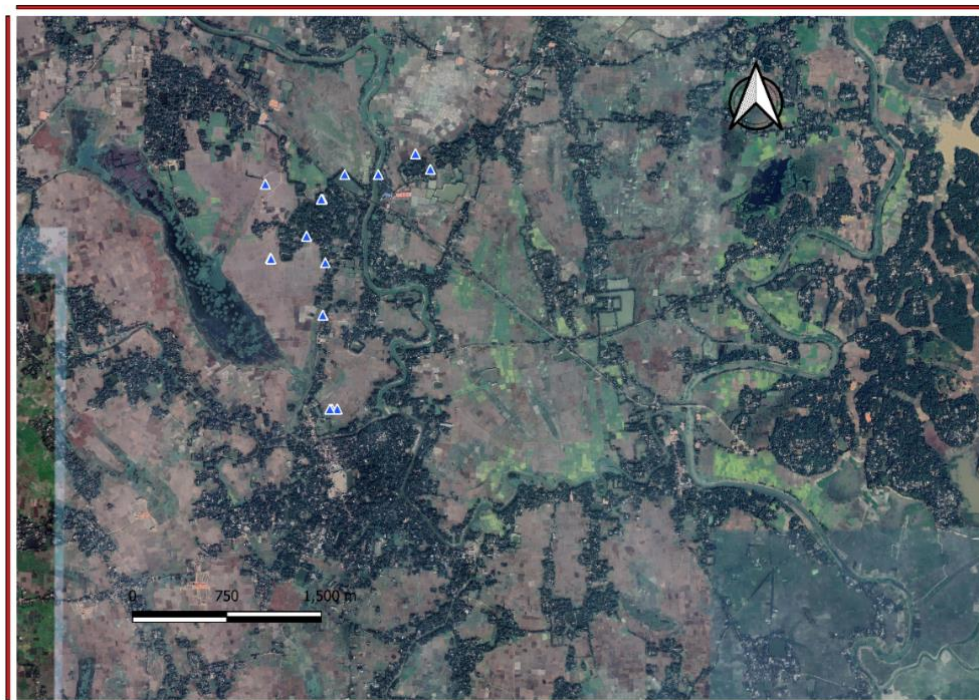


Figure 3: Locations of the selected mustard fields (blue triangles) over Kalihati Upazila, Tangail district



Figure 4: Locations of the selected mustard fields (ping triangles) over Daulatpur Upazila, Manikganj district

Use of satellite images: In this study, the satellite images of Sentinel 2A and Landsat 8 (OLI) were used, and those were compiled from ESA (European Space Agency) and the USGS Earth Explorer website. At Sentinel 2A, the span of 13 spectral bands, from the visible and the near-infrared to the shortwave infrared at different spatial resolutions ranging from 10 to 60 meters on the ground, takes global land monitoring to an unprecedented level (Melillos et al., 2019). MSI (Multispectral Imager) covers 13 spectral bands (443–2190 nm), with a swath width of 290 km and a spatial resolution of 10 m (four visible and near-infrared bands), 20 m (six red edge and shortwave infrared bands) and 60 m (three atmospheric correction bands). Whereas, Landsat 8 (OLI) are Sun-synchronous satellites staying at an altitude of 705 km above the earth with a 16-day repeat cycle (Claverie et al., 2018). Landsat 8 has two types of sensors, namely the Operational Land Imager (OLI) and Thermal Infrared Sensor (TIRS). The OLI sensor provides nine spectral bands, including a pan band, and TIRS provides two spectral bands. However, only Red and NIR spectral bands were used for the study purposes.

Image preprocessing technique: For Landsat data, the Raw Digital Numbers (DN) were changed to Top-of-Atmosphere (TOA) reflection values after reference (Simonetti et al., 2015). Generally, remote sensing data adopted from satellite sensors is greatly influenced by several factors, such as atmospheric scattering and absorption, sensor calibration, and also by data processing procedures (Teillet, 1986). For that, two techniques were used to preprocess the satellite images: (1) radiometric calibration and (2) atmospheric correction (Wang et al., 2019). Radiometric calibration means a set of correction techniques that are associated with correction for the sensitivity of satellite sensors, topography and sun angle, atmospheric scattering, and absorption (Kim and Elman, 1990). The open source-based Quantum Geographic Information System (QGIS) software 3.22.10 version allows a plugin, and the plugin gives a tool for atmospheric correction, which is known as dark object subtraction (DOS-1) level 1. In this study, this tool was employed on the radiometrically calibrated images to minimize its atmospheric scattering effect. DOS-1 searches for every pixel in a band and finds the dark value. Scattering is done by subtracting this value

from each pixel in the band. In this study, two techniques were followed to download and process the Sentinel-2A images. The satellite images of Sentinel 2A and Landsat 8 (OLI) were compiled by the ESA European Space Agency and the USGS Earth Explorer website. Then, the free and open-source QGIS 2.18.10 version software together with the Semi-automatic Classification Plugin (SCP) was used to preprocess the imagery (Congedo, 2016). The benefit of using the SCP is that the user may preview, download, and correct Sentinel-2 images using the same interface for each date and each tile. The vegetation indices can then be calculated, saved, and compared to other dates, all in the same QGIS environment.

Table 1: Model development using Landsat 8 (OLI) single image of the growing season

Location	Ullapara	Kalihati	Daulatpur
Growing Season	2022-23	2022-23	2022-23
IAD	03/01/2023	03/01/2023	01/03/2023
DAP	67	60	63

Note: IAD= Image acquisition date; DAP= Days after plantation

Table 2: Model development using Sentinel 2A single image of the growing season

Location	Ullapara	Kalihati	Daulatpur
Growing Season	2022-23	2022-23	2022-23
IAD	30/12/2022		
DAP	63		

Note: IAD= Image acquisition date; DAP= Days after plantation

Calculation of Normalized Difference Vegetation Index (NDVI)

The NDVI is a dimensionless ratio between surface reflectance from the near-infrared and red bands of the spectrum which can be calculated as the following equations of Table 3.

Table 3: Vegetation index using Sentinel-2 and Landsat-8 satellite images

Index	Sentinel 2A	Landsat 8
NDVI	$\frac{B_8 - B_4}{B_8 + B_4}$	$\frac{B_5 - B_4}{B_5 + B_4}$
	For Sentinel 2A, B ₈ =NIR Band, B ₄ =RED Band	For Landsat 8, B ₅ =NIR Band, B ₄ =RED Band

2. Results and Discussion

3. Mustard Yield of Farmers' Fields and Its Corresponding NDVI

Mustard yield data and NDVI values from Sentinel 2A and Landsat 8 satellite images (Figure 5) were collected from selected 20 farmers' fields of three different locations, i.e. Ullapara, Kalihati, and Daulatpur Upazila for the mustard growing season 2022-23. Yield data of the farmers' fields were collected through direct inspection of the fields. The results have been presented in Table 4 to Table 6 along with their corresponding NDVI values of satellite images for the mustard growing season of 2022-23.

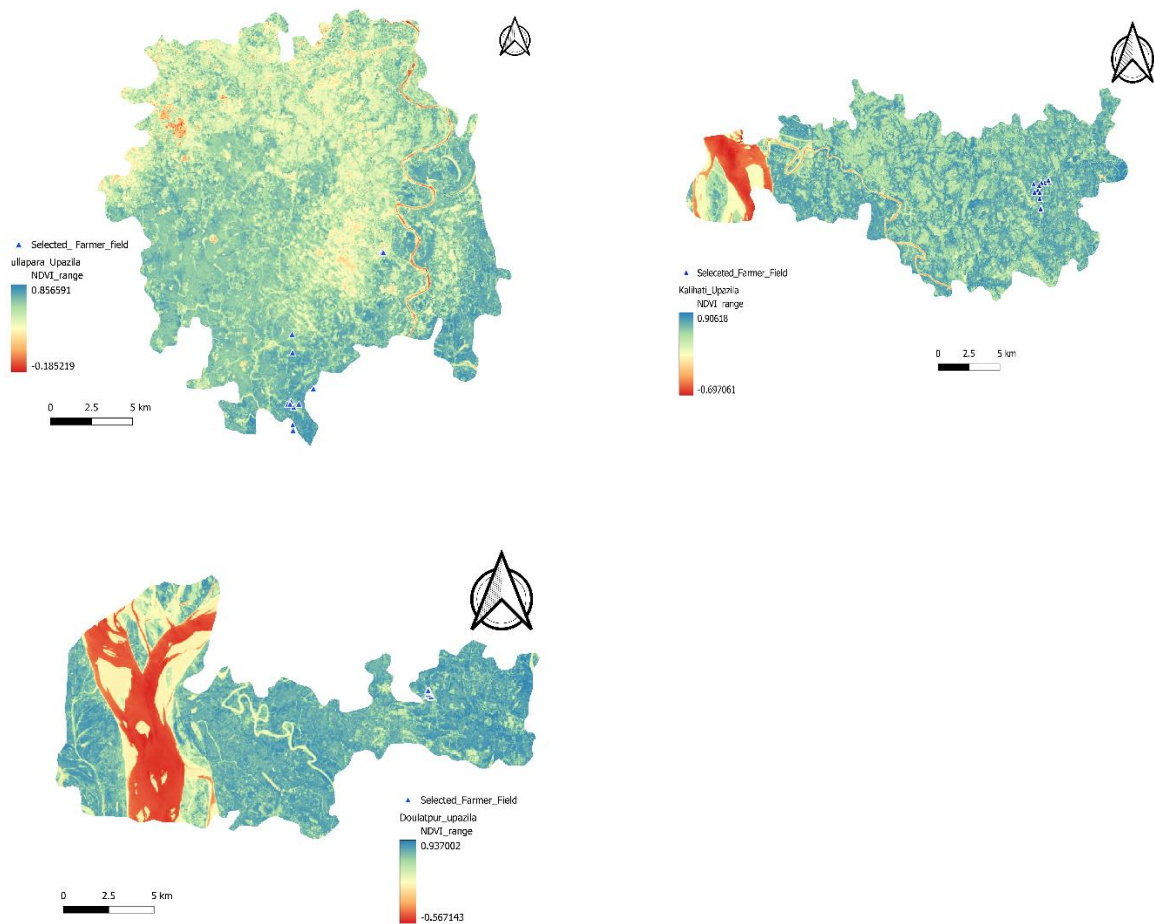


Figure 5: Spatial distribution of the NDVI from satellite images of Ullapara, Kalihati, and Daulatpur Upazilas for 2022-23 mustard growing seasons respectively

Table 4 shows that the NDVI values were a maximum of 0.789 for the 17th field and a minimum of 0.532 for the 19th field at Ullapara Upazila of Sirajganj district. On the contrary, the yield was maximum at 2.29 t/ha for the 19th field, and minimum at 1.07 t/ha for the 12th field. That means the yield was maximum for the field where the NDVI values were maximum. But the minimum yield was not found for the field where the NDVI values were the lowest.

Table 4: NDVI values of satellite images and yields of corresponding Farmer’s fields at Ullapara, Sirajganj during the season of 2022-23

Farmer’s Field No.	Longitude	Latitude	NDVI	Observed Yield (t/ha)
1	89.5671900	24.31072	0.697	1.98
2	89.5024165	24.19310	0.751	2.14
3	89.5679702	24.31071	0.672	1.73
4	89.5117804	24.21701	0.658	1.77
5	89.5117383	24.21701	0.711	1.98

6	89.5118608	24.21394	0.697	1.98
7	89.5024165	24.19320	0.651	1.81
8	89.5089597	24.22843	0.710	1.85
9	89.5024265	24.19320	0.562	1.48
10	89.5089097	24.22842	0.710	2.17
11	89.5109755	24.22991	0.751	1.74
12	89.5124510	24.22657	0.778	1.07
13	89.5103853	24.22842	0.718	1.80
14	89.4135483	24.26348	0.698	1.88
15	89.5679720	24.31071	0.694	1.98
16	89.5679720	24.31072	0.754	2.14
17	89.5124347	24.25667	0.789	2.29
18	89.5123454	24.26657	0.640	1.85
19	89.5156795	24.22833	0.532	1.50
20	89.5245481	24.23664	0.678	1.80

In the Tangail district, the NDVI values were a maximum of 0.775 for the first field and a minimum of 0.532 for the 6th field. On the other hand, the yield was maximum at 2.01 t/ha for the 4th field, and the yield was minimum at 0.33 t/ha for the 16th field (Table 5). That means the yield was maximum for the field where the NDVI values were not maximum. But the minimum yield was not found for the field where the NDVI values were the lowest.

Table 5: NDVI values of satellite images and yields of corresponding Farmer's fields at Kalihati, Tangail during the season of 2022-23

Farmer's Field No.	Longitude	Latitude	NDVI	Observed Yield (t/ha)
1	24.3489000	90.0266000	0.775	1.98
2	24.3488700	90.0266000	0.697	0.99
3	24.3488828	90.0266054	0.728	1.51
4	24.3365546	90.0290074	0.792	2.01
5	24.3469805	90.0280701	0.632	1.24
6	24.3432559	90.0278810	0.593	1.78
7	24.3432573	90.0278850	0.653	1.24
8	24.3432391	90.0278713	0.623	1.48
9	24.3365547	90.0285911	0.717	0.89
10	34.3473045	90.0237759	0.742	1.15
11	24.3472667	90.0238250	0.759	1.56
12	24.3365546	90.0290071	0.691	0.99
13	24.3365547	90.0284241	0.695	1.48
14	24.3365547	90.0284342	0.682	1.46
15	24.3525869	90.0233823	0.753	0.78
16	24.3532672	90.0322156	0.605	0.33
17	24.3536377	90.0362991	0.721	0.44
18	24.3536377	90.0363994	0.581	1.28
19	24.3532678	90.0295907	0.607	0.60
20	24.3547522	90.0351324	0.738	1.20

Table 6 shows that the NDVI values were a maximum of 0.855 for the 10th field and a minimum of 0.738 for the 15th field in the Manikganj district. In contrast to that, the yield was maximum at 2.24 t/ha for the 4th field, and the yield was minimum at 0.88 t/ha for the 18th field. That means the yield was maximum for the field where the NDVI values were not maximum. But the minimum yield was not found for the field where the NDVI values were the minimum.

Table 6: NDVI values of satellite images and yields of corresponding Farmer’s fields at Daulatpur, Manikganj during the season of 2022-23

Farmer’s Field	Longitude	Latitude	NDVI	Yields (t/ha)
1	89.89617	23.96939	0.748	1.73
2	89.89623	23.96851	0.768	1.84
3	89.89586	23.96874	0.853	1.37
4	89.89582	23.96914	0.839	2.24
5	89.89614	23.96795	0.793	1.98
6	89.89599	23.96781	0.799	1.74
7	89.89561	23.96835	0.833	1.83
8	89.89476	23.96858	0.846	1.85
9	89.89457	23.96891	0.827	1.98
10	89.89493	23.96909	0.855	1.73
11	89.89591	23.96835	0.833	1.80
12	89.89551	23.96846	0.829	1.98
13	89.89641	23.9681	0.741	1.76
14	89.89619	23.96942	0.748	1.65
15	89.89603	23.96978	0.738	1.78
16	89.89474	23.96957	0.828	1.59
17	89.89518	23.97038	0.775	1.76
18	89.89464	23.97102	0.845	0.88
19	89.89537	23.97092	0.764	1.76
20	89.89479	23.97112	0.848	1.98

Conclusions

This research aims to provide an operational technique with adequate technological components for monitoring and forecasting mustard yield in Bangladesh. In the farmers' fields of the selected locations, the developed system investigates the combined use of satellite remote sensing (RS) and Geographic Information System (GIS) technology. The objective of the study is to construct a remotely sensed yield prediction model that used the high spatial resolution of Sentinel 2A and Landsat 8 satellite images to forecast mustard yield one month ahead of harvest. The first year’s results revealed that in most cases the yield was maximum for the field where the NDVI values were not maximum and vice-versa. However, the relationships of the extracted mean NDVI and yields will be established using the classical linear regression model where the model will be developed using the first two years’ data and will be validated using the data of the last study period.

References

- Hamar, D., Ferencz, C.S., Lichtenberger, J., Tarcsai, G.Y. and Ferencz A.R.I. (1988a) The use of remotely sensed data in yield forecasting I. Ground based experiments. *No`ve nytermele`s*, 37:165–179 (in Hungarian).
- Hamar, D., FERENCZ, C.S., Lichtenberger, J., Tarcsai, G.Y. and Ferencz A.R. I. (1988b) The use of remotely sensed data in yield forecasting II. Satellite experiments. *No`ve nytermele`s*, 37: 357–367 (in Hungarian)
- National Research Council (1989). *Diet and Health: Implications for Reducing Chronic Disease Risk*. Washington, DC: The National Academies Press, 1989. doi:10.17226/1222
- Kogan, F.N. (2001). Operational space technology for global vegetation assessment. *Bull. Am. Meteorol. Soc.* 82 (9):1949–1964.
- Kogan, F. N. (2002). World Droughts in the new millennium from AVHRR-based vegetation health indices. *Eos Trans. Am. Geophys. Union* 48 (557): 562–563.
- Kogan, F.N., Gitelson, A., Zakarin, E., Spivak, L. and Lebed, L. (2003). AVHRR-based spectral vegetation index for quantitative assessment of vegetation state and productivity: calibration and validation. *Photogrammetric Eng. Remote Sens.* 69 (8): 899–906.
- Singh, R.P., Roy, S. and Kogan, F. (2003). Vegetation and temperature condition indices from NOAA AVHRR data for drought monitoring over India. *Int. J. Remote Sens.* 24: 4393–4402.
- Unganai, L.S. and Kogan, F.N. (1998). Drought monitoring and Corn yield estimation in Southern Africa from AVHRR data. *Remote Sens. Environ.* 63: 219–232.
- Hayes, J.T., O'Rourke, P.A., Terjung, W.E., and Todhunter, P.E. (1982). YIELD: A numerical crop yield model of irrigated and rainfed agriculture. *Publications in Climatology*, p. 35
- Quarmby, N.A., Milnes, M., Hindle, T.L. and Silicos, N. (1993). The use of multitemporal NDVI measurements from AVHRR data for crop yield estimation and prediction. *Int. J. Remote Sens.* 14: 199–210
- Benedetti, R. and Rossinni, P. (1993). On the use of NDVI profiles as a tool for agricultural statistics: the case study of wheat yield estimate and forecast in Emilia Romagna. *Remote Sens. Environ.* 45: 311–326.
- Mohd, D.M., Ahmad, S. and Abdullah, A. (1994). Agriculture application of remote sensing: paddy yield estimation form Landsta-5 thematic mapper data.
- El-Telbany, M.E. and Maged, M.A. (2019). Wireless sensor networks for extreme environments: remote sensing and space industry. *International Journal of Hybrid Intelligence* 12(1): 41-54.
- Atzberger, C. (2013). Advances in remote sensing of agriculture: Context description, existing operational monitoring systems and major information needs. *Remote Sensing* 5(2): 949-881.
- Sadras, V. O., Cassman, K., Grassini, P., Bastiaanssen, W. G. M., Laborte, A. G., Milne, A. E., ... & Steduto, P. (2015). *Yield gap analysis of field crops: Methods and case studies*.
- Melillos, G., Agapiou, A., Themistocleous, K., Michaelides, S., Papadavid, G. and Hadjimitsis, D.G. (2019). Field spectroscopy for the detection of underground military structures. *European Journal of Remote Sensing* 52(1): 385-399.
- Claverie, M., Ju, J., Masek, J. G., Dungan, J.L., Vermote, E.F., Roger, J. C., Skakun, S.V. and Justice, C. (2018). The Harmonized Landsat and Sentinel-2 surface reflectance data set. *Remote Sensing of Environment* 219: 145-161.

- Simonetti, D., Marelli, A. and Eva, H.D. (2015). IMPACT: Portable GIS Toolbox for image processing and land cover mapping. Publication Office of the European Union 10: 143497.
- Teillet, P.M. (1986). Image correction for radiometric effects in remote sensing. *International Journal of Remote Sensing* 7(12): 1637-1651.
- Wang, R. F., Zhang, Y., Li, J. G., Zhao, W., Wang, F.Z., Cao, H. J. and Duan, Y. P. (2019). Development of green tide monitoring with satellite images. *Journal of Coastal Research* 90(SI): 104-111.
- Congedo, L. (2016). Semi-automatic classification plugin documentation. Release 4(0.1): 29.

End Note:

Characteristics of Landsat 8 Sensors

Landsat 8, also known as the Landsat Data Continuity Mission (LDCM), was sent into space on an Atlas-V rocket on February 11, 2013, from Vandenberg Air Force Base in California (<https://www.usgs.gov/tools/landsat-8-overview>). With the launch of Landsat 8, NASA has launched the most recent Landsat satellite, which is equipped with the Operational Land Imager (OLI) and the Thermal Infrared Sensor (TIRS) sensors (https://www.usgs.gov/landsat_missions/landsat-8).

Table 1: Characteristics of Landsat 8 sensors

Satellite	Sensors	Band types	Wavelength (µm)	Resolution (m)
Landsat 8	Operational Land Imager (OLI)	Band 1 – Coastal aerosol (deep blue)	0.43-0.45	30
		Band 1 - Blue	0.45-0.51	30
		Band 3 – Green	0.53-0.59	30
		Band 4 – Red	0.64-0.67	30
		Band 5 – NIR	0.85-0.88	30
		Band 6 – Shortwave infrared (SWIR) 1	1.57-1.65	30
		Band 7 – Shortwave infrared (SWIR) 2	2.11-2.29	30
		Band 8 –Panchromatic	0.50-0.68	15
		Band 9 – Cirrus	1.36-1.38	30
	Thermal infrared sensor (TIRS)	Band 10 – TIRS1	10.60-11.19	100
		Band 11 – TIRS2	11.50-12.51	100

Characteristics of Sentinel-2 sensors

Copernicus Sentinel-2 consists of two sun-synchronous polar-orbiting satellites phased 180° apart. Its huge sweep width (290 km) and high revisit duration (10 days at the equator with one satellite and 5 days with two satellites in cloud-free circumstances, resulting in 2-3 days at mid-latitudes) will aid in monitoring of Earth’s surface changes. (<https://sentinel.esa.int/web/sentinel/missions/sentinel-2>). Detailed descriptions of the mission goals, satellite description, and ground section are provided in this Sentinel-2 Mission Guide at a high level. Also included are discussions on relevant legacy missions, thematic areas, and Copernicus services, as well as orbital parameters and coverage, instrument payload, and data outputs. This document describes the data products available to users at the Level-1B, Level-1C, and Level-2A levels, as well as the Level-1C tiling grid.

Table 2: Spectral bands for the Sentinel-2 sensors

Sentinel-2 bands	Sentinel-2A		Sentinel-2B		Spatial resolution (m)
	Central wavelength (nm)	Bandwidth (nm)	Central wavelength (nm)	Bandwidth (nm)	
Band 1 – Coastal aerosol	442.7	21	442.2	21	60
Band 2 – Blue	492.4	66	492.1	66	10
Band 3 – Green	559.8	36	559.0	36	10
Band 4 – Red	664.6	31	664.9	31	10
Band 5 – Vegetation red edge	704.1	15	703.8	16	20
Band 6 – Vegetation red edge	740.5	15	739.1	15	20
Band 7 – Vegetation red edge	782.8	20	779.7	20	20
Band 8 – NIR	832.8	106	832.9	106	10
Band 8A – Narrow NIR	864.7	21	864.0	22	20
Band 9 – Water vapour	945.1	20	943.2	21	60
Band 10 – SWIR – Cirrus	1373.5	31	1376.9	30	60
Band 11 – SWIR	1613.7	91	1610.4	94	20
Band 12 – SWIR	2202.4	175	2185.7	185	20

POTATO YIELD FORECASTING USING SATELLITE IMAGES AND CROP SIMULATION MODEL UNDER CHANGING CLIMATE

ISTIYAK AHMED, S. BISWAS, AFM TARIQUL ISLAM, M. G. MAHBOOB, A. K. CHOUDHURY AND M. A. MONAYEM MIAH

Abstract

Traditional methods of yield estimation often rely on laborious field surveys and manual data collection, which can be time-consuming and resource-intensive. This study presents a comprehensive investigation into forecasting potato yield using satellite imagery and the AquaCrop model, with a specific focus on the utilization of the Normalized Difference Vegetation Index (NDVI) as a vital indicator of vegetation health and productivity. The research aims to address the challenges posed by climate variability in agriculture and offers valuable insights into crop dynamics, yield estimation, and the potential benefits of remote sensing and machine learning techniques. To achieve these objectives, nine Sentinel-2 satellite images were analyzed during the ingestion period between December 2022 and February 2023. Five images with less than 40% cloud cover were selected for further analysis. The research demonstrated the effectiveness of machine learning approaches, specifically Support Vector Machine (SVM) and Random Forest (RF) models, for yield prediction. The exploratory data analysis (EDA) revealed a significant correlation between potato yield and the NDVI, particularly during the full vegetative stage observed in February. The AquaCrop simulated yield of potato showed an increasing trend over time, aligning with the mean yield during the harvesting period. Notably, as the crop approached maturity, AquaCrop outperformed machine learning models in yield estimation. The study serves as a stepping stone towards enhancing crop productivity and resilience, empowering farmers, agronomists, and policymakers to make informed decisions for a sustainable agricultural future.

Keywords: Potato yield, Satellite image, Remote sensing, Machine Learning, NDVI, AquaCrop

Introduction

Agricultural productivity, particularly of vital staple crops like potatoes, plays a significant role in ensuring food security and sustaining global economics. However, the agriculture sector is inherently susceptible to the adverse impacts of climate change, which presents numerous challenges to farmers and policymakers alike. As the world faces a changing climate with escalating temperatures, altered precipitation patterns, and more frequent extreme weather events, the need for precise and reliable agricultural forecasting methods becomes increasingly evident. Crop type discrimination and mapping using remotely sensed satellite data are very crucial in the context of acreage estimation, yield prediction, food security measures, and for developing agro-economic policies. The accurate and reliable crop type map at various spatial scales offers an essential way for precise acreage and yield estimation, and thereby indispensable for decision-makers to establish regional to global food security measures. On the other hand, the prediction of crop yield before the harvest is one of the most significant concerns in agriculture since variations in crop yield from year-to-year impact international trade, food supply, and market prices. However, both crop statistics and yield estimation are estimated usually through conventional means (field experiments or surveys). Remote sensing technology plays an important role in the agriculture sector by providing timely and accurate information (Atzberger, 2013). Currently, remote sensing techniques are using to measure these statistics at high spatial and temporal resolutions. It has the ability to identify crop classes, crop growth monitoring, and crop yield estimation (Mohammad et al., 1994). The application of remote sensing in estimating agricultural performance indicators is increasing as it offers a time and cost-effective reproducible method for measurement that can cover larger physical areas as compared to in-situ methods (Mohammad et al., 1994). On the other hand, climate parameters are the primary determinant of crop yield. Any change in these climate parameters will affect the crop yield, which is highly vulnerable to climate change. In this context, crop simulation models are used in predicting crop productivity under various crop management options and changing climatic parameters. AquaCrop requires a relatively smaller number of parameters, and recently its parameterization was performed for table grapes for the

growing season from 2005 to 2006 (Er-Raki et al., 2020).

Potato (*Solanum tuberosum* L.) is one of the major vegetable crops in Bangladesh after rice and wheat, which contributes a significant part to the total food supply (Zhang et al., 2010), as the climate and soil conditions are very favorable for potato cultivation. During the last few years, potato cultivation in Bangladesh showed an increasing trend. During 2020–2021, total potato cultivation area and production were 468.626 ha (0.46 million) and 9,887,000 (9.8 million) metric tons, respectively, while in 2021–2022, the area decreased to 464.174 ha and production increased to 10,144,000 (10.1 million) metric tons, respectively (BBS, 2022). With proper planning, potato has the potential to generate revenue by exporting. Henceforth, potato growth monitoring and its yield prediction have become an important fact of consideration.

Traditional field-based crop data collection becomes clumsy, costly, time-consuming, and has the possibility of error (Reynolds et al., 2000). In addition, yield estimation with conventional methods is no longer beneficial for the decision-makers as it takes too much time. During the last couple of years, many empirical models have been developed to estimate potato yield before harvesting, but many of them have become unpractical, especially those depending on field data collection. As a satellite, remote sensing is one of the best tools to derive essential information about the distribution of crops and their growing conditions over large areas; it can be used for potato growth monitoring and yield estimation. Remote sensing (You J. et al., 2017, Kuwata K. et al., 2015), crop simulation models (CSM) (Hammer R.G. et al., 2020, Yadav S. et al., 2018), and other statistical methods (Kern A. et al., 2018, Lobell D.B. et al., 2010) are the most popular methods to estimate crop yields. These techniques are also used to find the climate impact on the yield of different types of crops. During the last few years, many studies were conducted to develop a correlation between crop yield and remote sensing-derived vegetation indices (VIs) for early yield prediction (Akhand et al., 2016; Al-Gaadi et al., 2016; Baruth et al., 2008; Groten, 1993; Kouadio et al., 2014; Zhang et al., 2010). Most of the studies were carried out by the correlation of NDVI with yield (Groten, 1993; Liu and Kogan, 2002; Rasmussen, 1997). Nessa (2005) used NDVI for rice growth monitoring and production estimation over Bangladesh by using the National Oceanic and Atmospheric Administration-Advanced Very High-Resolution Radiometer (NOAA-AVHRR) satellite data with a resolution of spectral bands greater than one km. Bala & Islam (2009) developed potato yield prediction models by using NDVI, LAI (leaf area index), and the fraction of photosynthetically active radiation (fPAR) vegetation indices for Munshiganj district of Bangladesh by using Moderate Resolution Imaging Spectroradiometer (MODIS) (with lowest resolution greater than 250 m) 8-day composite surface reflectance data. Rahman et al. (2012) used NOAA-AVHRR data for the estimation of potato yield in Bangladesh. Hansen et al. (2008) suggested that high spatial resolution for monitoring forests is required for better assessing the rates and spatial extents of forest change.

This study aims to contribute to the advancement of potato yield forecasting by harnessing the potential of satellite imagery and crop simulation modeling to address the challenges posed by climate variability. This research has employed state-of-the-art satellite imagery processing techniques to delineate potato fields accurately. An integrated satellite-derived agricultural data with the AquaCrop model, a widely acclaimed crop simulation tool that accounts for various environmental and agronomic factors affecting crop growth was proposed. The integration of satellite imagery and the AquaCrop model holds promise as a valuable tool for policymakers, agronomists, and potato farmers to enhance productivity and ensure food security in the face of an increasingly uncertain climate.

Materials and Methods

The study was conducted in Munshiganj district, the main potato growing area of Bangladesh. The district lies between 23° 22' to 23° 36' N latitude and 90° 28' to 90° 36' E longitude (Fig. 1), covering an area of 954.96 km² where 59% area is cultivable land. The study area consists of two administrative units called Upazila: Munshiganj Sadar, and Tongibari. The climate condition of this area is hot and humid in the summer (May to October) and cool and dry in the winter (November to April). Munshiganj district receives an annual average rainfall of 2376 mm, where 80% of rainfall occurs between May and October. The

maximum and minimum mean temperatures during the winter vary between 25.82 and 12.1 °C. During summer, the maximum and minimum mean temperatures vary between 34.6 and 25.6 °C. The average monthly minimum and maximum humidity vary from 70 to 84%, where the minimum humidity is observed during the dry season and the maximum humidity is observed during the summer. The soil condition of this area is dominated by heavy loam and heavy clay, while clay occupies the second and third positions respectively.

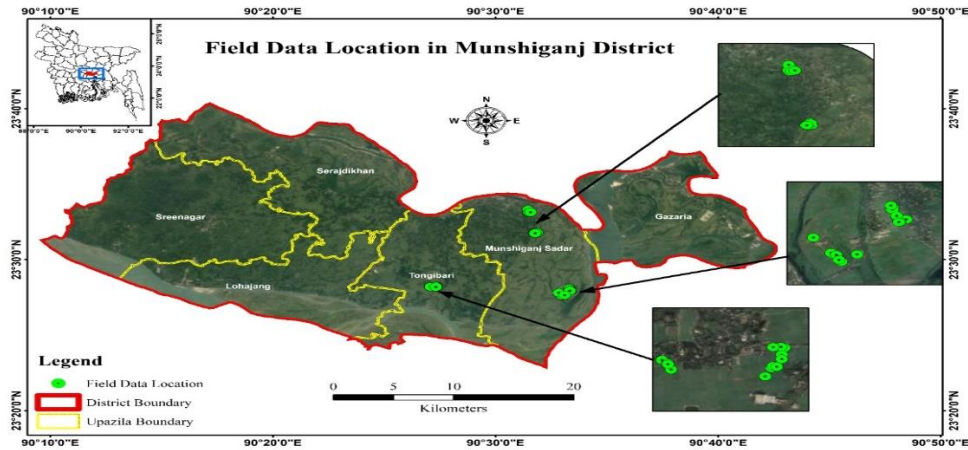


Figure 1. Map of the study area (Munshiganj district) in Bangladesh

A total of 49 potato fields were identified for the growing seasons: 2022–2023 by interviewing the farmers of selected Upazilas (sub-district) of Munshiganj district. Crop information such as field locations and yield were collected with the help of the personnel from the Department of Agricultural Extension (DAE) in Munshiganj district. The agricultural pattern of this area is characterized by two growing seasons, Rabi and Kharif. Rabi is the main growing season, which is dominated by potatoes that starts in late November or the start of December and ends in April. On the other hand, Kharif is dominated by rice, which starts in June and lasts until September. Other food grains which include wheat, maize, pepper, onion, pulses, sugarcane, and mustard are also cultivated in this area.

This study will build simple relationships between within-season spectral vegetation indices and crop yield in 2022-23. The spectral vegetation indices were acquired from Level-2 (atmospherically corrected) Sentinel-2 multispectral broadband and narrowband data (Table 1). The yield data consists of crop yield survey frames with dimensions greater than $10 \times 10 \text{m}^2$. The dimensions of the frames were chosen to account for any geographic mismatch between the frames and the spatial resolution of Sentinel-2 ($10 \times 10 \text{m}^2$).

Table 1. Summary of Sentinel-2 sensor characteristics.

Band #	Designation	Spectral Range (nm)	Spatial Resolution (m)
1	Coastal aerosol	433-453	60
2	Blue	458-523	10
3	Green	543-578	10
4	Red	650-680	10
5	Red-edge 1	698-713	20
6	Red-edge 2	733-748	20
7	Red-edge 3	773-793	20
8a	NIR	785-900	10
8b	Narrow NIR	855-875	20

9	Water vapor	935-955	60
10	SWIR-Cirrus	1360-1390	60
11	SWIR1	1565-1655	20
12	SWIR2	2100-2280	20

Analysis of vegetation and prediction of its yield is related to the identification of crop types and their agronomic variables, such as density, maturity vigor, and disease. Remote sensing can provide these types of information to a great extent. There are different types of vegetation indices (VIs) derived from different spectral reflectance that are generally used to get these types of information. The NDVI is generally used extensively around the world to monitor vegetation quality, growth, and distribution over a large area. NDVI is derived from the ratio between the surface reflectance of the NIR and RED bands of the spectrum (Taylor et al., 1997).

$$NDVI = \frac{NIR - RED}{NIR + RED}$$

Healthy plants have a high NDVI value because they are characterized by strong absorption of red energy and strong reflectance of the NIR spectrum (Islam and Bala, 2008). NDVI of a crop varies with its growth and health condition with the passage of time. There are some rain and cloud in the growing period. The study used images with less than 40% cloud coverage. Thus, images from the month of January are excluded from this study. The planting days of potato varies from mid-November to early-December. Plants are visible in 15-20 days after planting. So, the study used 5 images whose sensing date was 07-12-2022, 17-12-2022, 05-02-2023, 15-02-2023 and 25-02-2023. The study used polygon vector data of the fields and mean NDVI for those fields were calculated from the images. Figure 2 showed the flow chart of the methodology used in this study.

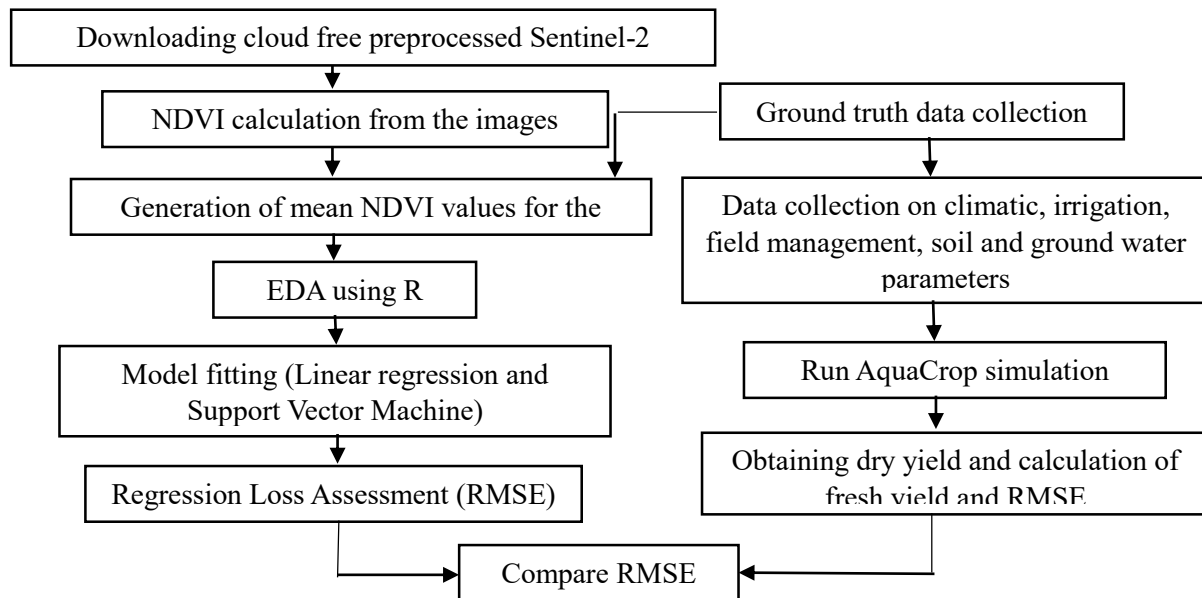


Figure 2. Methodology flow chart used in this study

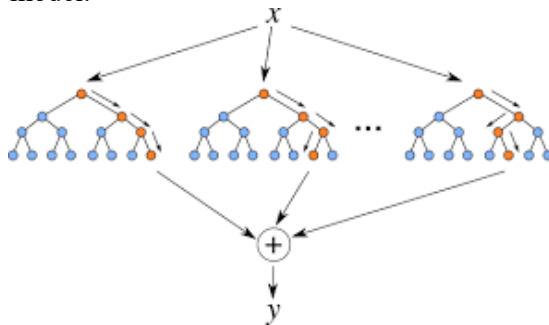
To establish the relationship, the study used several machine learning algorithms like; linear regression, support vector machine and random forest as the first-year experiment of this study suggests.

Linear Regression (LR): Linear regression algorithm shows a linear relationship between a dependent (y) and one or more independent (y) variables, hence called linear regression. Since linear regression shows the linear relationship, which means it finds how the value of the dependent variable is

changing according to the value of the independent variable. The linear regression model provides a sloped straight line representing the relationship between the variables.

Support Vector Machine (SVM): In machine learning, SVMs are supervised learning models with associated learning algorithms that analyze data used for classification and regression analysis. In SVM Regression, the straight line that is required to fit the data is referred to as hyperplane. The objective of a SVM algorithm is to find a hyperplane in an n-dimensional space that distinctly classifies the data points. The data points on either side of the hyperplane that are closest to the hyperplane are called Support Vectors. These influence the position and orientation of the hyperplane and thus help build the SVM.

Random Forest (RF) Regression: Random Forest Regression is a supervised learning algorithm that uses an ensemble learning method for regression. The ensemble learning method is a technique that combines predictions from multiple machine learning algorithms to make a more accurate prediction than a single model.



Crop growth models use plant growth processes and run these processes at multiple scales. These models help find yield during plant growth, resulting from several variables such as climate, plant density, crop management, stress factors, etc. Guerra et al. evaluate using CSMs combined with interpolation to estimate the monthly distribution of irrigation water for cotton in Georgia. The Decision Support System for Agrotechnology Transfer model has been used to simulate the phenology process for soybean crops (Mote B. et al., 2016). The Crop Environment Resource Synthesis for Wheat simulation model was calibrated for wheat yield prediction (Li H. et al., 2017). There are very few models that are being calibrated for perennial crops. The AquaCrop model has been calibrated to predict water requirements of traditional African vegetables, Amaranthus, leafy vegetables, and taro, a wetland perennial tuber crop (Walker S. et al., 2012, Bello Z. et al., 2017). The AquaCrop model was calibrated and validated for the perennial coffee crop (Vega Molina A.L. et al., 2018). The performance of the simulation model has been compared with DM techniques in the past. Hammer et al. (2020) used the Agroecological Zone simulation model and DM techniques (random forest (RF), support vector machines (SVM), and gradient boosting machine (GBM)) to predict sugarcane yield. They concluded that DM techniques are better than the Agroecological Zone model. Contrarily, there is a simple alternative to crop models in statistical methods that uses probability for crop yield prediction.

AquaCrop requires Climate, Crop, Irrigation and Field Management, Soil profile and Ground Water information to simulate the results. In the first stage, for the estimation of potato yield throughout the crop cycles, the FAO AquaCrop model was calibrated. This CSM has a mathematical approach for estimating yield. This approach considers crop development, crop transpiration, biomass production, and yield formation for yield estimation. It also considers the impact of water deficiency on yield. The collected meteorological data of Munshiganj district were minimum temperature, maximum temperature, humidity, rainfall, and wind speed obtained from the Prediction Of Worldwide Energy Resources (POWER) Project of NASA were used to estimate evapotranspiration using the FAO Penman-Monteith equation. The following information was also collected by interviewing the experts and farmers regarding soil characteristics and crop management: soil type, application of fertilizers (nitrogen, phosphorus, potassium), irrigation schedule, sowing method, planting density, and crop calendar (sowing date, days to emergence, initial canopy cover, days to maturity, days to max canopy cover, and days to harvesting).

Results and Discussion

This study used the NDVI to estimate the potato yield. Sentinel 2 images were searched for the ingestion period and 9 images were found between December 2022 to February 2023. Figure 3 showed the cloud cover (%) over the sensing period. The images from 27 December 2022 to 26 January 2023 showed high cloud coverage and the rest were low. This study used images with less than 40% cloud cover over the ingestion period. So, 5 images out of 9 were selected for further analysis.

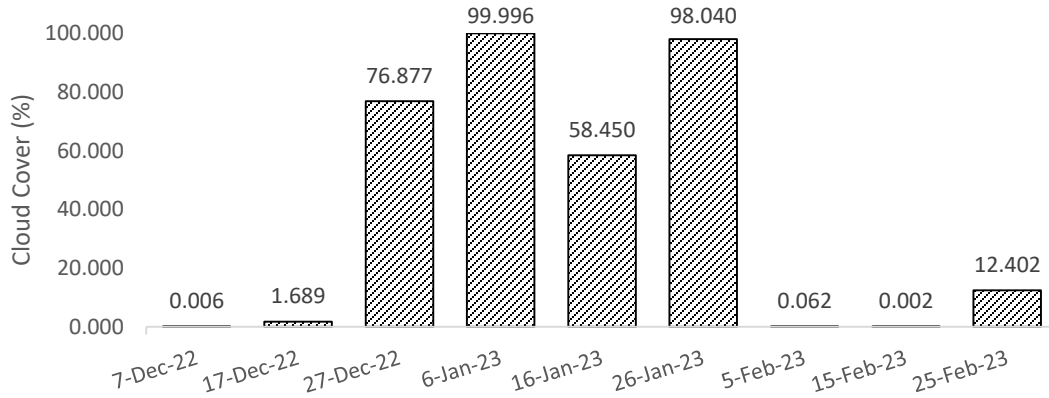
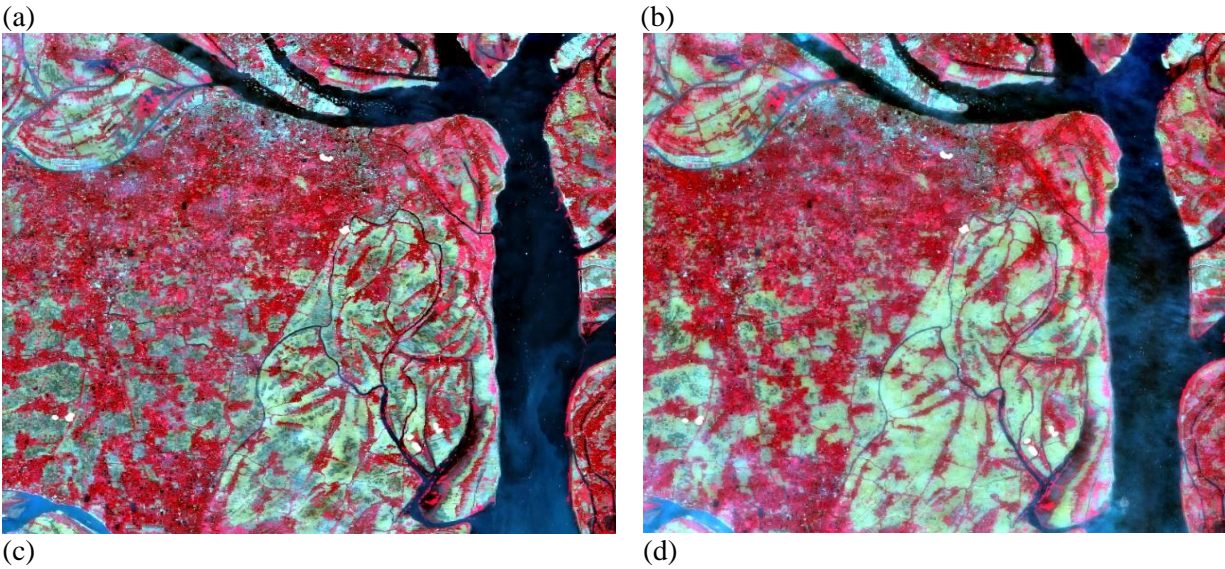


Figure 3. Cloud cover (%) over ingestion period



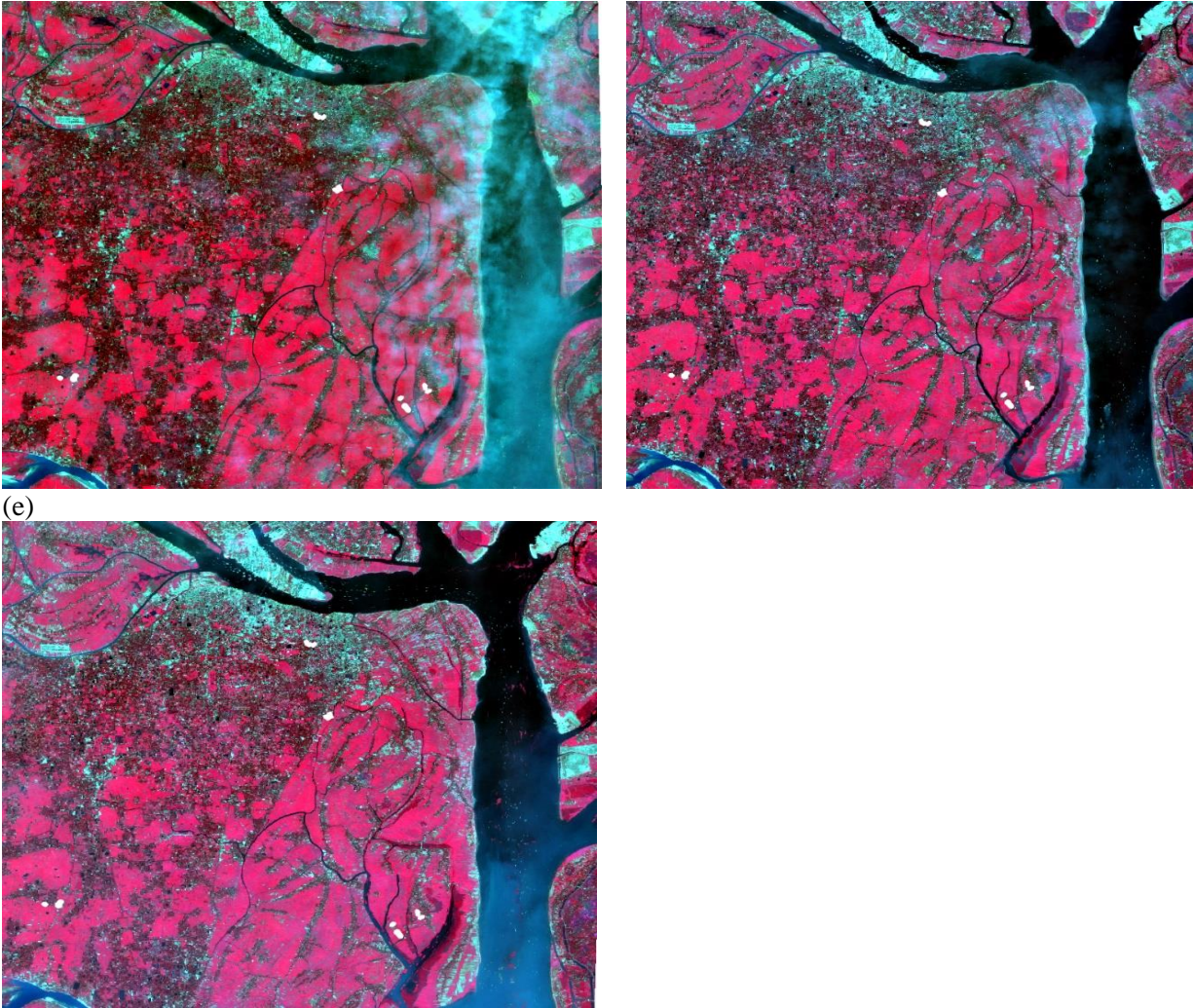


Figure 4. False color composite (RGB = Band 8, 4, 3) of study area at different dates (a) 07-12-2022, (b) 17-12-2022, (c) 05-02-2023, (d) 15-02-2023 and (e) 25-02-2023

Figure 4 showed the false color composite (RGB = Band 8, 4, 3) of the study area at different sensing dates. Near-infrared is sensitive to vegetation health and can distinguish healthy vegetation from other features. In the false-color composite, healthy vegetation would appear as bright red to pink tones. The red band primarily reflects vegetation, but it is also sensitive to urban areas and bare soil. In the false-color composite, vegetation will still appear with some brightness, but less intense than in the near-infrared channel. Urban areas and bare soil would generally appear as shades of green to brown. The green band is sensitive to the chlorophyll absorption of healthy vegetation and can differentiate different types of vegetation. In the false-color composite, vegetation would appear as shades of green, with dense and healthy vegetation showing darker green colors. Figure 4 (a) and Figure 4 (b) showed similar patterns as the sensing date are pretty much close. Figure 4 (a) showed a slightly high density of greenish areas indicating moderate to dense vegetation cover. This is due to grasslands or healthy shrubs. Bright red to pink areas represent healthy and dense vegetation, such as forests or well-maintained crops. Light green to brown areas indicates urban areas, buildings, and bare soil. Dark blue indicates water. Productivity (photosynthesis) and reflectance in the NIR is increasing in Figure 4 (b). One and a half months later, the potato fields were much redder due to the NIR band. Productivity and reflectance in the NIR continued to increase. The buildings, roads and water remain the same color. Some of the fields appear reddish as as

they were grown. Bright red to pink areas increased significantly from Figure 4 (b) to Figure 4 (c) and Figure 4 (d). This indicated the healthy vegetation of potato fields is increasing. The potato fields remain reddish but a bit darker in Figure 4 (d). The potato is now well within the reproductive phase. But again, in Figure 4 (e), it was declining a little bit indicating the senescence has started.

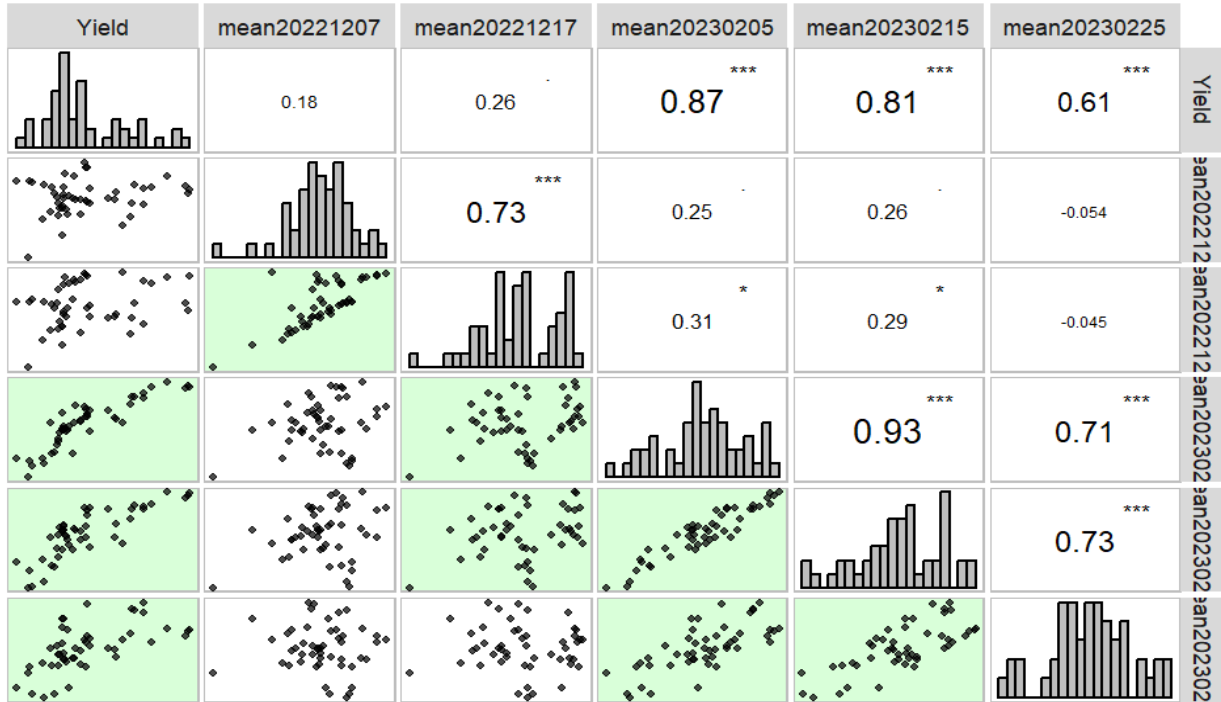
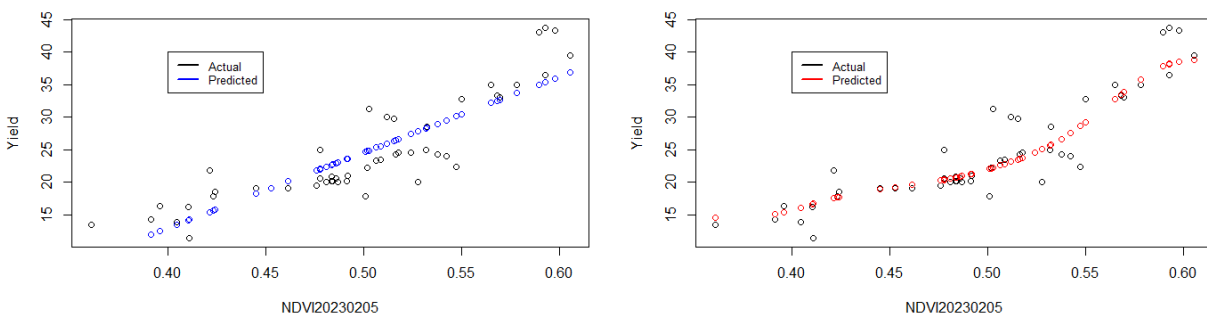


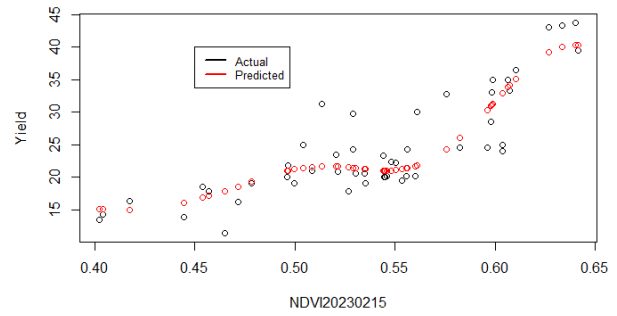
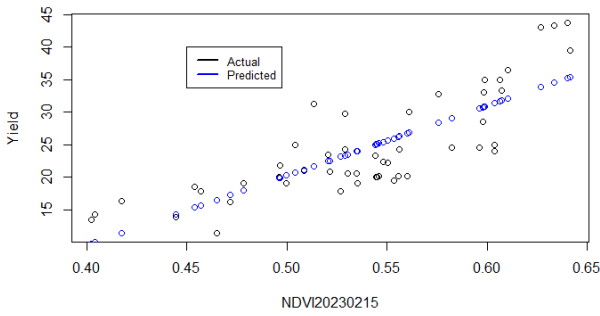
Figure 5. Exploratory Data Analysis (EDA) of Yield and NDVI

Figure 5 showed the Exploratory Data Analysis (EDA) of Yield and NDVI generated from images on different sensing dates. The diagonal elements of the matrix showed the distribution of the variable. The distribution of yield appeared to be non-normal. The Shapiro-Wilk normality test (test statistic = 0.91504, p-value = 0.001769) supported the non-normality assumption. So, fitting linear regression would be a violation of the model fitting assumption. Thus, the study will go for machine learning approach for modeling purposes. There is a highly significant correlation between yield and the NDVI generated in the month of February. The study used only those images for model fitting. And also, for comparison purposes, the study used a linear regression approach.

(a)



(b)



(c)

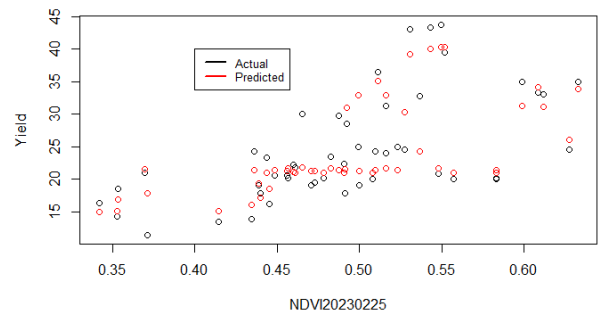
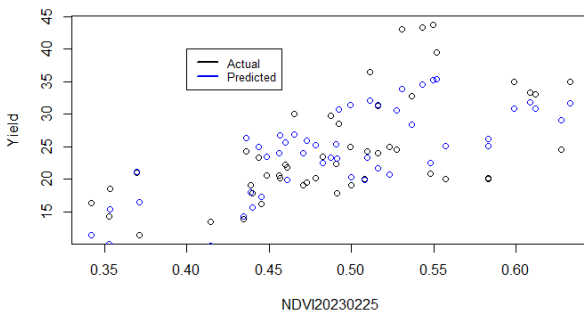
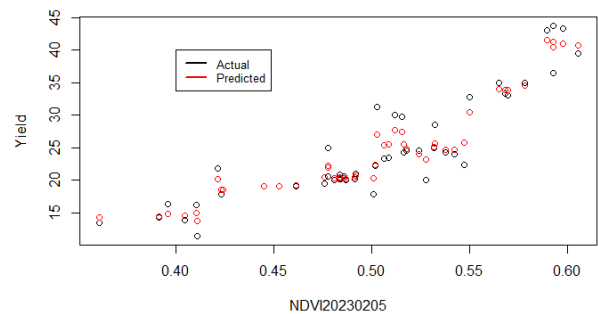
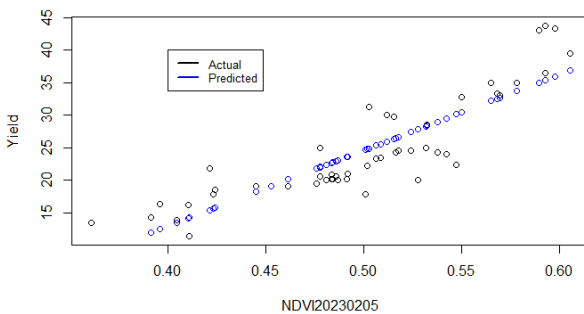


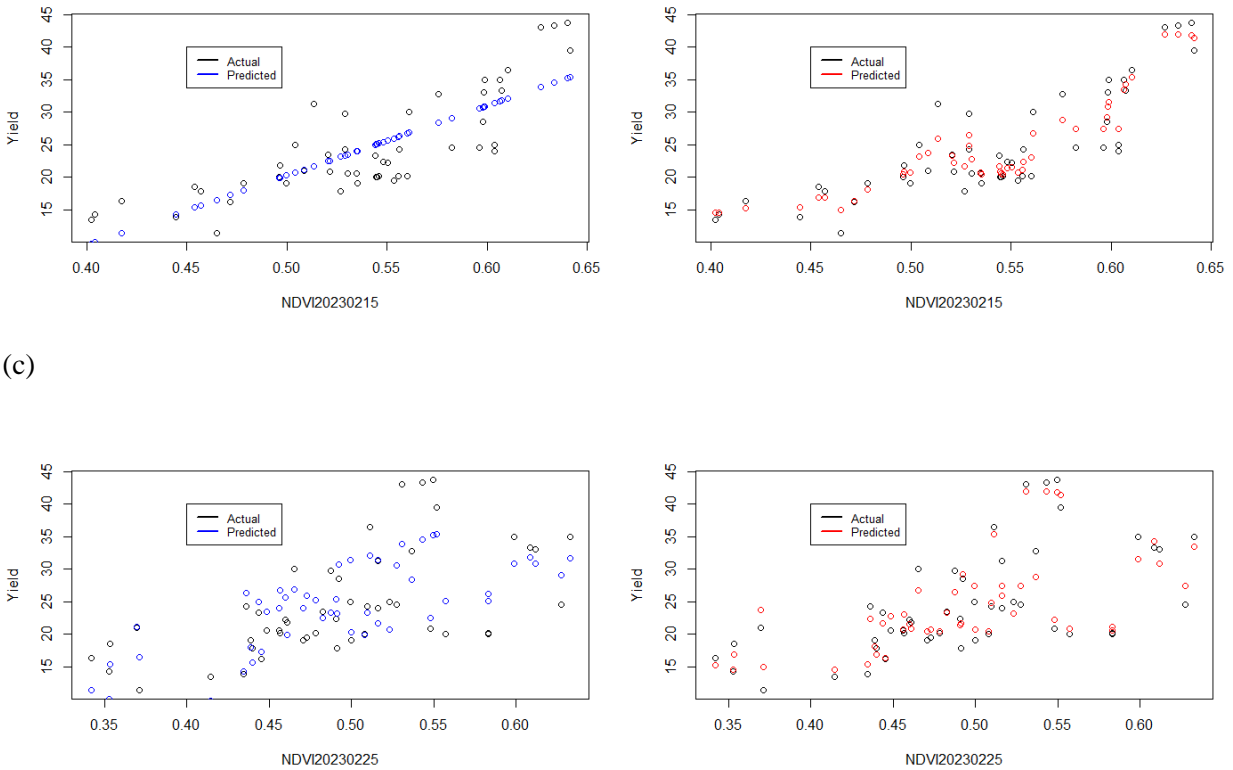
Figure 6. Scatter plots of actual and predicted points in LR vs SVM on different dates (a) 05-02-2023, (b) 15-02-2023 and (c) 25-02-2023

Figure 6 showed how well the predicted values fitted to the original values. Figure 6 (a) and Figure 6 (b) fitted very accurately compared to Figure 6 (c). As the senescence started, the NDVI values predicted the yield with less accuracy. But in the full vegetative stage, it predicted fairly well. The figure also compared the prediction using SVM to the LR. SVM was predicted with higher accuracy than LR in all three cases.

(a)



(b)



(c)

Figure 7. Scatter plots of actual and predicted points in LR vs RF on different dates (a) 05-02-2023, (b) 15-02-2023 and (c) 25-02-2023

Figure 7 also showed how well the predicted values fitted to the original values but it compares RF to LR. Figure 7 (a) and Figure 7 (b) fitted very accurately compared to Figure 7 (c). As the senescence started, the NDVI values predicted the yield with less accuracy. But in the full vegetative stage, it predicted fairly well. In the case of comparison with LR, RF predicted with higher accuracy in all three cases.

In the calibration of AquaCrop, the main parameters are related to Canopy Cover (CC), crop evapotranspiration (ETa), biomass, and yield, which need to be calibrated. For the simulation of CC, which is a very critical feature of AquaCrop, the main parameters are initial canopy cover (CCo), maximum canopy cover (CCx), Canopy Growth Coefficient (CGC), and cumulative growing degree days (CGDD) in every crop development stage. Other parameters that affected CC development have also been adjusted. For the simulation of crop ETa, the main parameter was calibrated, affecting soil evaporation and plant transpiration. This parameter is the maximum coefficient for transpiration (KcTr,x). The field location are very close, thus there is no significant variation in the climatic parameters. Also, the management practices are almost same. Plot by plot yield estimation in a very close distance is not possible using AquaCrop model. The study estimated the mean yield of Potato for Munshiganj district. The mean yield calculated from observed data is 24.50 t/ha with aligns with the official statistics of Potato yield for Munshiganj district.

Table 2. AquaCrop Simulated yield of Potato on significant sensing dates

Sl. No.	Date	Dry Yield (t/ha)	Fresh Yield (t/ha)
1	05-02-2023	1.071	5.35
2	15-02-2023	2.723	13.62
3	25-02-2023	4.880	24.40

Table 2 showed the AquaCrop Simulated yield of Potato on significant sensing dates. It follows an increasing trend. And it showed nearly the mean yield at the period of harvesting or after harvesting. At the beginning of the simulation, it under estimate the yield and it reached optimum estimate as time increases. But as time increased, it may over estimate at the end of the ingestion.

Table 3. Model comparison based on Root Mean Squared Error (RMSE).

Sl. No.	Model	RMSE		
		05-02-2023	15-02-2023	25-02-2023
1	Linear	3.86	4.62	4.62
2	SVM	3.07	3.73	3.73
3	Random Forest	1.69	2.08	2.08
4	AquaCrop	366.52	118.47	0.01

Table 3 showed the model and date comparison based on Root Mean Squared Error (RMSE). In all cases of the model, the RMSE is smaller for the NDVI generated from the image sensed on 05-02-2023. This date indicates the full vegetative stage for the potato. And the RMSE of the other two dates NDVI are the same. May be the full vegetative stage started in mid to late January and lasts until early February. The senescence period started after that. In the case of model comparison, RF performs better than SVM. As LR violates model assumption, the study ignored its performance compared to other models. As the time approaches to the maturity of the crop, the RMSE of yield from AquaCrop decreased. And, it performed better than machine learning models. But at the beginning and end, the accuracy was much lower.

Conclusions

The present study aimed to forecast potato yield using satellite imagery and the AquaCrop model, focusing on the use of the NDVI as a crucial indicator of vegetation health and productivity. The findings demonstrate the potential of remote sensing and machine learning techniques to accurately estimate potato yield and provide valuable insights into the changing agricultural landscape under the influence of climate variability. Overall, the research findings shed light on the applicability and effectiveness of remote sensing techniques in estimating potato yield. By leveraging the power of satellite imagery and machine learning models, farmers, agronomists, and policymakers can gain timely and precise information about crop health, allowing for better-informed decision-making and resource allocation. The study's outcomes hold

significant implications for agriculture, especially in regions vulnerable to climate change. With the identified peak vegetative stage offering valuable insights into the timing of optimum yield, farmers can plan their cultivation and management strategies more effectively. Furthermore, the research highlights the advantages of employing machine learning algorithms for yield forecasting over traditional linear regression methods. SVM and RF demonstrated higher accuracy and robustness, particularly during the full vegetative stage, where the dynamic growth of vegetation significantly impacts yield. The adoption of machine learning models can revolutionize agricultural forecasting, providing reliable predictions and aiding stakeholders in making strategic decisions. The AquaCrop simulated yield of potato showed an increasing trend over time, reaching close to the mean yield during the harvesting period. While the model initially underestimated yield, it improved accuracy as time progressed, demonstrating its effectiveness in capturing the growth dynamics of the crop. Notably, as the crop approached maturity, AquaCrop outperformed machine learning models in yield estimation. However, at the beginning and end of the ingestion period, the accuracy was relatively lower. The research findings hold significant potential for addressing global food security challenges and promoting climate-resilient agriculture. By advancing our understanding of crop dynamics and enhancing yield prediction capabilities, this research contributes to the broader goal of achieving sustainable and adaptive agricultural practices in a changing climate. Continued research and technological advancements will undoubtedly pave the way for an improved understanding of agricultural systems, enabling effective responses to the evolving challenges posed by climate variability.

References

- Akhand, K.; Nizamuddin, M.; Roytman, L. and Kogan, F. (2016). Using remote sensing satellite data and artificial neural network for prediction of potato yield in Bangladesh. In: Remote Sensing and Modeling of Ecosystems for Sustainability XIII (Vol. 9975, p. 997508). International Society for Optics and Photonics.
- Al-Gaadi, K. A.; Hassaballa, A. A.; Tola, E.; Kayad, A. G.; Madugundu, R.; Alblewi, B. et al. (2016). Prediction of potato crop yield using precision agriculture techniques. *PLoS One* 11(9): e0162219.
- Atzberger, C. (2013). Advances in remote sensing of agriculture: context description, existing operational monitoring systems and major information needs. *Remote Sens* 5(2): 949–981.
- Bala, S.K. and Islam, A.S. (2009). Correlation between potato yield and MODIS-derived vegetation indices. *Int J Remote Sens* 30(10): 2491–2507.
- Baruth, B.; Royer, A.; Klisch, A. and Genovese, G. (2008). The use of remote sensing within the MARS crop yield monitoring system of the European Commission. *Int. Arch Photogramm Remote Sens Spat Inf Sci* 37: 935–940.
- BBS (2022). *Yearbook of Agricultural Statistics 2015*. 27th series, Statistics and Information Division, Ministry of Planning, Dhaka, Bangladesh.
- Bello Z., Walker S. (2017). Evaluating AquaCrop model for simulating production of amaranthus (*Amaranthus cruentus*) a leafy vegetable, under irrigation and rainfed conditions. *Agric. For. Meteorol.*, 247:300–310.
- Er-Raki S., Bouras E., Rodriguez J., Watts C., Lizarraga-Celaya C., Chehbouni A. (2020). Parameterization of the AquaCrop model for simulating table grapes growth and water productivity in an arid region of Mexico. *Agric. Water Manag.* 2020;245:106585
- Groten, S. M. E. (1993). NDVI-crop monitoring and early yield assessment of Burkina Faso. *Int. J Remote Sens* 14(8): 1495–1515.
- Guerra L., Garcia A.G., Hook J., Harrison K., Thomas D., Stooksbury D., Hoogenboom G. (2007). Irrigation water use estimates based on crop simulation models and kriging. *Agric. Water Manag.*,

- 89:199–207. doi: 10.1016/j.agwat.2007.01.010.
- Hammer R.G., Sentelhas P.C., Mariano J.C. (2020). Sugarcane Yield Prediction through Data Mining and Crop Simulation Models. *Sugar Tech.* 2020;22:216–225
- Hansen, M. C.; Roy, D. P.; Lindquist, E.; Adusei, B.; Justice, C.O. and Altstatt, A. (2008). A method for integrating MODIS and Landsat data for systematic monitoring of forest cover and change in the Congo Basin. *Remote Sens Environ* 112(5): 2495–2513.
- Islam, A.S. and Bala, S.K. (2008). Assessment of potato phenological characteristics using MODIS-derived NDVI and LAI information. *GIScience Remote Sens* 45(4): 454–470.
- Kern A., Barcza Z., Marjanović H., Árendás T., Fodor N., Bónis P., Bognár P., Lichtenberger J. (2018). Statistical modelling of crop yield in Central Europe using climate data and remote sensing vegetation indices. *Agric. For. Meteorol.*,260:300–320.
- Kouadio, L.; Newlands, N.K.; Davidson, A.; et al. (2014). Assessing the performance of MODIS NDVI and EVI for seasonal crop yield forecasting at the ecodistrict scale. *Remote Sens* 6(10): 10193–10214.
- Kuwata K., Shibasaki R. (2015). Estimating crop yields with deep learning and remotely sensed data; *Proceedings of the 2015 IEEE International Geoscience and Remote Sensing Symposium (IGARSS)*; Milan, Italy. 26–31 July 2015; pp. 858–861.
- Li H., Chen Z., Liu G., Jiang Z., Huang C. (2017). Improving winter wheat yield estimation from the CERES-wheat model to assimilate leaf area index with different assimilation methods and spatio-temporal scales. *Remote Sens.*, 9:190.
- Liu, W.T. and Kogan, F. (2002). Monitoring Brazilian soybean production using NOAA/AVHRR based vegetation condition indices. *Int. J Remote Sens* 23(6): 1161–1179.
- Lobell D.B., Burke M.B. (2010). On the use of statistical models to predict crop yield responses to climate change. *Agric. For. Meteorol.*, 150:1443–1452
- Mohammad, M.I.S.; Ahmad, S. and Abdullah, A. (1994). Agriculture application of remote sensing: paddy yield estimation from Landsat-5 thematic mapper data. Internet publication. <http://www.gisdevelopment.net/aars/acrs/1994/ts1/ts1003.shtml>, published GIS Development 1994.
- Mote B., Vasani M., Ahir H., Yadav S., Pandey V. (2016). Simulation of phenology and yield attributing characters of legume crops using DSSAT and InfoCrop Model. *Adv. Life Sci.*, 5:5265–5271.
- Nessa, M. (2005). Monitoring of rice growth and production in Bangladesh using NOAA Satellite Data. MS Dissertation submitted to Bangladesh University of Engineering and Technology (BUET), Dhaka, Bangladesh.
- Rahman, A.; Khan, K.; Krakauer, N.Y.; Roytman, L. and Kogan, F. (2012). Using AVHRR-based vegetation health indices for estimation of potato yield in Bangladesh. *J Civil Environ Eng* 2:111
- Rasmussen, M.S. (1997). Operational yield forecast using AVHRR NDVI data: reduction of environmental and inter-annual variability. *Int J Remote Sens* 18(5): 1059–1077. <https://doi.org/10.1080/014311697218575>
- Reynolds, C.A.; Yitayew, M.; Slack, D.C.; et al., (2000). Estimating crop yields and production by integrating the FAO crop specific water balance model with real-time satellite data and ground-based ancillary data. *Int J Remote Sens* 21(18): 3487–3508
- Taylor, J.C.; Wood, G.A. and Thomas, G. (1997). Mapping yield potential with remote sensing. In: Stafford JV (ed) Proceedings of the first European conference on precision agriculture, Vol 2. SCI, London,

pp 713–772

- Teillet, P. M. (1986). Image correction for radiometric effects in remote sensing. *Int J Remote Sens* 7(12): 1637–1651
- Walker S., Bello Z., Mabhaudhi T., Modi A., Beletse Y., Zuma-Netshiukhwi G. (2012). Calibration of AquaCrop model to predict water requirements of traditional African vegetables; *Proceedings of the II All Africa Horticulture Congress 1007*; Skukuza, South Africa. 15–20 January 2012; pp. 943–949.
- Yadav S., Misra A., Mishra S., Pandey V. (2018). Crop growth simulation models (InfoCrop v. 2.1, DSSATv4. 5, WOFOSTv1. 5 and Cropsytv 4.19) software. *Water Energy Secur. Arena Clim. Chang.*, 34:456–469.
- You J., Li X., Low M., Lobell D., Ermon S. (2017). Deep gaussian process for crop yield prediction based on remote sensing data; *Proceedings of the Thirty-First AAAI Conference on Artificial Intelligence*; San Francisco, CA, USA. 4–9 February 2017; pp. 4559–4565
- Vega Molina A.L., Pertuz Peralta V.P., Pérez Orozco A.B., Ortiz Iglesias M.I., González Guerrero E. (2018). Calibration of the aquacrop model in special coffee (*Coffea arabica*) crops in the sierra nevada of Santa Marta, Colombia. *J. Agron.*, 17:241–250.
- Zhang, P.; Anderson, B.; Tan, B.; et al., (2010). Monitoring crop yield in USA using a satellite-based climate-variability impact index. In: Geoscience and remote sensing symposium (IGARSS), 2010 IEEE international IEEE, pp 1815–1818

BIOINFORMATIC ANALYSIS OF DICER-LIKE (DCL), ARGONAUTE (AGO), AND RNA-DEPENDENT RNA POLYMERASE (RDR) GENES AND THEIR ASSOCIATED REGULATORY ELEMENTS IN BRASSICA SPECIES (*Brassica rapa* L.)

¹ZOBAER AKOND, ² SHEIKH HASNA HABIB, ³ NURUL HAQUE MOLLAH
¹ASICT, BARI, GAZIPUR; ³ORC, BARI; ³BIOINFORMATICS LAB, DEPT. OF STATISTICS, UNIVERSITY OF RAJSHAHI.

Abstract

RNA interference (RNAi) or gene silencing in eukaryotes is a commonly occurring mechanism. It is controlled by the three main gene families called Dicer-like (DCL), Argonaute (AGO), and RNA-dependent RNA polymerase (RDR). They control gene expression at the transcriptional or post-transcriptional level and often maintain plant growth and development. They also play the important role to regulate gene expression in response to different biotic and abiotic factors. This mechanism is actually maintained by the 19-24 nt non-coding small RNA molecules (miRNA and siRNA). But how these genes function and their structures and the associated regulatory elements have not been analyzed in detail. Our analysis identified 4 *BrDCL*, 13 *BrAGO*, and 6 *BrRDR* RNAi-related genes from the *Brassica rapa* genome. Motif structure analysis showed that the predicted proteins conserve similar motif characteristics similar to their paralog RNAi genes of *Arabidopsis*. Moreover, sequence logo and relative frequency analysis showed that Lysine (K), Serine(S), Valine(V), Leucine(L), and Glutamic acid(E) were the prevalent amino acids of the predicted motifs in the identified proteins. The trans-regulatory analysis showed that the top-ranked 10 TF families (Dof, bZIP, C2H2, ERF, BBR-BPC, MICK-MADS, MYB, TCP, WRKY, and AP2) consisted of 393 (78%) regulators of which Dof 115(23%), bZIP 58(11.55%), C2H2 49(9.76%), ERF 30(6%), BBR-BPC 29(5.77%), MICK-MADS 23(4.58%), MYB, TCP and WRKY each 23 (4.58%) and AP2 regulate 21(4.18%) TFs. RNAi genes-TFs network analysis illustrated that eight key TF families were highly connected with the identified RNAi genes in *B.rapa* with some exception of ERF, MYB, TCP and ,WRKY. Overall results would therefore provide an excellent basis for in-depth molecular investigation of these genes and their regulatory elements for rapeseed-mustard crop improvement against different stressors.

Keywords: RNAi genes, *Brassica rapa*, Transcription Factor, Gene networking

Introduction

RNA interference (RNAi) also known as RNA/gene silencing is one of the special mechanisms that is highly conserved in most multicellular eukaryotic organisms. This occurs by non-coding small RNA molecules (miRNA and siRNA) to regulate gene expression at the transcription and post-transcription (PTS) level by targeting complementary RNAs and protecting cells from deadly exogenous and endogenous genetic materials (Yun and Zhang, 2023). RNAi plays a significant role in plants' various biological, molecular and cellular processes for example growth and development, epigenetic modifications, maintaining genomic stability, and different pathogenic and environmental stress responses(Qian et al., 2011; Cui et al., 2020).

Dicer-like(DCL), Argonaute(AGO), and RNA-dependent RNA polymerase(RDR) are the three major RNA-silencing machinery gene families (Cao et al., 2016). RNA silencing is first triggered by the double-stranded RNA (dsRNA) or partially double-stranded stem-loop RNA that is cleaved by the activity of RNaseIII-type DICER-LIKE proteins(DCL) into small RNA(sRNA) molecules of length 21-24 nucleotide termed as micro RNA(miRNA) and short-interfering RNA(siRNA)(Cui et al., 2020; Yun and Zhang, 2023). Secondly, one strand of these miRNAs/siRNAs is combined with AGO protein to create a pre-RNA-induced silencing complex(pre-RISC) that needs the molecular chaperone Heat shock protein 70

(Hsp70)/90(Hsp90) (Iwasaki et al., 2010; Yun and Zhang, 2023). The sRNA is merged by the function of the N-domain of AGO and only the guide RNA strand exists in the complex to produce a complete RISC (Mirzaei et al., 2014; Akond et al., 2020; Yun and Zhang, 2023). The RISC binds with complementary mRNAs led by single-stranded sRNA to restrict translation during post-transcriptional gene silencing (PTGS), RNA degradation, and creation of heterochromatin during transcriptional gene silencing (TGS), which leads to particular gene silencing. These sRNAs are produced from the targeted RNA by host cell encoded RNA-dependent RNA polymerases (RDRs) to generate more dsRNAs to process miRNAs/siRNAs and to start a new cycle of RNA silencing.

The proteins of these three families contain some particular domains which measure their important characteristics (structure and function). The proteins of the DCL family are identified for the presence of six domains, viz., a DEAD domain, a helicase conserved C-terminal (Helicase C) domain, a Dicer dimerization domain (Dicer dimer/Duf283), a PAZ (Piwi Argonaute and Zwillig) domain, a Ribonuclease III domain (Ribonuclease 3), and a double-stranded RNA-binding domain (DSRM) (Cui et al., 2020). The proteins of the AGO family are located in the RISC that cleaves the target mRNAs, and are characterized and identified for the presence of variable MID and N-terminal domains, and well-conserved PAZ and PIWI (P-element-induced wimpy testis) domains (Cui et al., 2020; Akond et al., 2022). The proteins of the RDR family are crucially important to continue the RNA silencing process. The proteins of this gene group represent a particular conserved RNA-dependent RNA polymerase (RDRP) catalytic domain (Cui et al., 2020).

So far, investigations about DCL, AGO and RDR gene families have been carried out on 18 plant species. Results showed varying number of protein members of these three groups are present among the species. For instance, the Arabidopsis, rice, maize, foxtail millet, grapevine, tomato, wheat, soybean, pepper, cucumber, barley, sugarcane, sweet orange, tea, sorghum, quinoa, tobacco and coffee possess four, five, five, eight, four, seven, seven, seven, four, five, five, four, four, five, five, eight, four and nine DCL genes; ten, 19, 18, 19, 13, 15, 39, 21, 12, seven, 11, 21, eight, 18, 14, 21, nine and 11 AGO genes; six, eight, five, 11, five, six, 16, seven, six, eight, seven, 11, four, nine, seven, 11, three and eight RDR genes, respectively (Cui et al., 2020; Akond et al., 2022).

The previous studies provided sufficient evidence that these gene families are strongly conserved in plant species with diversified characteristics and functions, but broad scale analyses of these genes are not yet done in *Brassica rapa*. For example, the Arabidopsis thaliana DCL1 (*AtDCL1*) shows the properties of miRNA biogenesis whereas *AtDCL2/DCL3/DCL4* mediate siRNA processing (Wang et al., 2016b). *AtDCL3/DCL4* are also important for RNA-directed DNA methylation of the FWA transgene, which is related to histone H3 lysine 9 (H3K9) methylation (Qian et al., 2011; Wang et al., 2016b). Although the *AtDCL2* generates siRNAs to form the defensive process against viral infection and *cis*-acting antisense transcript, but *AtDCL4* controls the vegetative period change by the generation of siRNAs from the trans-acting transcript (Deleris et al., 2006). Interestingly, *AtDCL3* choose short dsRNAs and *AtDCL4* cuts the long dsRNA substrates (Wang et al., 2016b; Akond et al., 2022). DCL genes in plants such as *AtDCL1* and *AtDCL3* increase flowering (Schmitz et al., 2007). Recently a study has identified that three proteins viz., *Pt-DCL1*, *Pt-DCL2*, and *Pt-DCL3* are strongly related to the leaf rust pathogen (*Puccinia triticina*) that is known as a very destructive disease of wheat (Dubey et al., 2020).

Argonaute proteins also play key activities during RNA-guided gene silencing process for plants' growth and development (Carbonell et al., 2012; Meng et al., 2013a). For example, the *AtAGO1* is connected to the transgene-silencing pathways (Fagard et al., 2000) and the *AtAGO4* to the epigenetic silencing (Zilberman et al., 2003). The *AtAGO7* and *AtAGO10* proteins control growth (Hunter et al., 2003) and meristem functions in plant cells (Moussian et al., 1998). Recently a study showed that some AGO genes (*TaAGO2a/2b*) of wheat is predicted to play role in wheat growth and development specifically in

grain quality improvement(Akond et al., 2022). Two AGO genes(*TaAGO1b/TaAGO4*) identified from wheat is predicted to play key role at vegetative and reproductive phase in cold environment at the vernalizing stage(Meng et al., 2013b). RDR proteins in plants (*Arabidopsis*, maize) are also engaged in RNAi-related process viz., co-suppression, protection of pathogen infection, chromatin modification, and post-transcriptional gene silencing actions(Dalmay et al., 2000; Mourrain et al., 2000; Jovel et al., 2007).

Brassica rapa L subsp. *oleifera* (syn. *Brassica campestris*) commonly known as field mustard is one of the important oilseed crops for its great source of vegetable oil for human consumption and industrial purposes. It is used as fodder, biodiesel and young leaves are also used as human food as a green vegetable. Canola oil is popular for low erucic acid and low glucosinolate content in its meal protein that is also derived from the *Brassica rapa* (Dharmendra et al., 2014). *Brassica rapa* (*B. rapa*) is a diploid species (A genome; n=10) which may have been domesticated about 3000 years ago and have experienced a whole-genome triplication since its deviation from *Arabidopsis* (Lysak et al., 2005; Xiao et al., 2014; McAlvay et al., 2021). *B. rapa* shows deep morphological variety viz., leafy vegetables, turnips, and oil types, that may have been of both genetic and epigenetic differences(Xiao et al., 2014). The genome sequencing of the *B.rapa* (283.8Mb) was explored in 2011(Xiao et al., 2014) that have allowed for in-depth investigation of the predicted genes. In Bangladesh, rapeseed-mustard is the main source of edible oil. Oilseed crops are produced in 243 thousand hectors and total oil production is nearly 203 thousand tons (<http://bari.gov.bd/site/page/Agro-Technology-Hand-Book>). The oilseed variety BARI-14 has been also derived from *Brassica rapa* species by Bangladesh Agricultural Research Institute (BARI) in Bangladesh. Studies suggested that the RNA silencing genes in plants play numerous roles to regulate growth and development as well as important biotic and abiotic stress responses. The in-depth analysis of genomic functions of these gene groups and their associated regulatory elements are little known. The current study was carried out for comprehensive *in-silico* analyses of DCL, AGO, and RDR gene families and their regulatory components in *B. rapa* using integrated bioinformatics approaches. These results will help molecular plant breeders/researchers to provide important clues for the implementation of gene silencing pathways and RNAi-mediated host immunity in different oilseed varieties for crop improvement as a whole in Bangladesh. The main objectives however of this study include:

-
- To identify and characterize the RNA silencing machinery/RNAi-related genes of the *B. rapa* genome;
- To analyze the motif structures and their diversity in these genes/proteins;
- To predict the associated regulatory transcription factors (TFs);
- To predict the gene-TF relationship via gene-network;

Materials and Methods

Data Curation

First of all, the TAIR database (<http://www.arabidopsis.org/>) was used to extract the protein sequences of DCL, AGO, and RDR gene families of *Arabidopsis thaliana* and then these peptide sequences were used in BLASTp search in the Phytozome database(<https://phytozome-next.jgi.doe.gov/blast-search>) and then cross-checked was performed in NCBI database(<https://blast.ncbi.nlm.nih.gov/Blast.cgi>) against *Brassica rapa* genome for more confirmation to predict the protein sequences of *B.rapa*. Default algorithm parameter settings were kept (E-value=0.05 and Matrix= BLOSUM62) during BLAST process. Finally, 23 best possible RNAi-related genes (4 BrDCL,13BrAGO and 6BrRDR) were predicted according to the E-value (<0.01), percentage of identity (>90.0%), maximum score and the number of domain compositions. Secondly, the gene symbol of the corresponding 4 BrDCL, 13BrAGO and 6BrRDR predicted protein sequences were recorded from the NCBI. Afterwards, the following bioinformatic analyses such as the motif structure of the genes, transcription factor (TF), gene networking and gene set enrichment analysis were carried.

Prediction of Conserved Motif Structure

A popular webserver known as Multiple Expectation Maximization for Motif Elicitation (MEME) (http://meme.sdsc.edu/meme4_3_0/cgi-bin/meme.cgi) was used to predict the conserved motifs of the predicted BrDCL, BrAGO, and BrRDR protein members. This analysis was performed using the following parameters (i) an optimum motif width as ≥ 6 and ≤ 50 ; (ii) a maximum number of motifs of 20; (iii) minimum sites per motif sites is 2 and maximum sites per motif is 8 and motif site distribution is ZOOPS. Any Motifs that did not match the structural domains in each protein family were rejected.

Identification of the transcription factors (TFs)

To predict the putative transcription factor (TF) of the identified RNAi genes of *B. rapa*, the web-based PlantTFDB (<http://plantfdb.cbi.pku.edu.cn/>) database was used. To extract the TF list from Plant Transcriptional Regulatory Map (PlantRegMap) (http://plantregmap.gao-lab.org/tf_enrichment.php) of the 4 BrDCL, 13 BrAGO and 6BrRDR genes, the gene symbols of the corresponding BrRNAi proteins were first collected from the NCBI database following BLASTp process. Then the gene symbol list for BrDCL, BrAGO and BrRDR were submitted separately to predict the TFs which possess significantly over-represented targets in the input genes.

Gene Networking Construction

To understand the plant transcriptional regulatory system and relationship with the predicted RNAi proteins—a gene network analysis between TFs and RNAi-related proteins in *B. rapa* were studied. To construct the network and to visualize it an open-source software platform Cytoscape 3.10.0 were used.

Results and Discussion

Identification of the RNAi genes from *B. rapa* genome

The best possible final set of RNA silencing genes in *B. rapa* were predicted with the help of AtDCL, AtAGO, and AtRDR protein sequences taken as query sequences for BLASTp search against the *B. rapa* genome (Brassica rapa FPsc at Phytozome v13) in the Phytozome database. We also cross checked all the gene in the NCBI database for further accurate analysis. However lastly in total 23 RNAi-related genes (4 BrDCL, 13 BrAGO, and 6 BrRDR) were finally selected for subsequent analyses. In plants and animals, some important domains such as DEXD-helicase, helicase-C, Dicer-dimmer/Duf283, PAZ, RNase III (Ribonuclease-3), and double-stranded RNA-binding (dsRB/DSRM) are well-conserved in DCL proteins (Liu et al. 2014). 4 DCL genes in *B. rapa* were also identified by considering these six domain characteristics similar to that of the structure of AtDCLs. Argonaute proteins are known as the very important RNA binding proteins characterized by the presence of PAZ and PIWI domains (Qin et al. 2018). Based on these two domain characteristics, 13 BrAGOs were also identified from the *Brassica rapa* genome in this study (Table 1). BrRDR genes are identified based on RdRp domain.

Table 1. Basic genomic information about BrDCL, BrAGO, and BrRDR protein families in *B. rapa*

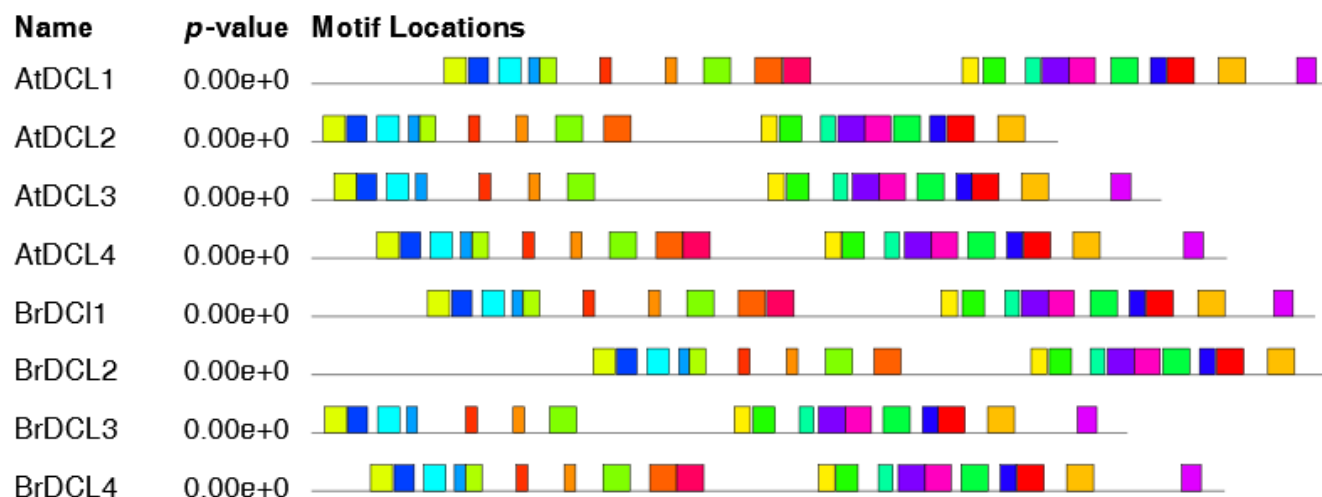
Gene no.	Gene name	Accession no. (Seq id)	Genomic location	Genome (bp)	CDS length (bp)	Number of introns	Predicted Protein		
							Length (aa)	Molecular Weight (kDa)	pI
DCL									
1	AtDCL1	AT1G01040	chr1:23146..31227	8107	5733	19	1910	213.57	5.88
2	AtDCL2	AT3G03300	chr3:767926..776214	8289	4167	21	1388	156.86	6.32
3	AtDCL3	AT3G43920	chr3:15753548..15760859	7283	4743	23	1580	177.42	5.98
4	AtDCL4	AT5G20320	chr5:6859218..6869307	10055	5109	23	1702	191.27	6.30
5	BrDCL1	Brara.J00078.1	chrA10:403438..410967	7530	5601	15	1866	208.68	5.96
6	BrDCL2	Brara.E03521.1	chrA05:27770726..27779858	9133	5685	22	1894	157.52	6.77
7	BrDCL3	Brara.F01924.1	chrA06:14081091..14087778	6688	4554	23	1517	171.30	5.93
8	BrDCL4	Brara.J01580.1	chrA10:13641433..13651196	9764	5097	24	1698	191.71	6.65
AGO									
1	AtAGO1	AT1G48410	chr1:17885633..17892596	6597	3153	20	1050	116.46	9.41
2	AtAGO2	AT1G31280	chr1:11181711..11185344	3893	3045	2	1014	113.42	9.50
3	AtAGO3	AT1G31290	chr1:11188293..11192317	4281	3585	2	1194	129.18	9.33
4	AtAGO4	AT2G27040	chr2:11536534..11542357	5890	2775	21	924	102.84	9.05

5	AtAGO5	AT2G27880	chr2:11871488..11876894	5612	2994	19	997	111.08	9.51
6	AtAGO6	AT2G32940	chr2:13971997..13977476	5606	2637	21	878	98.68	8.72
7	AtAGO7	AT1G69440	chr1:26101527..26105166	3922	2973	2	990	113.39	9.29
8	AtAGO8	AT5G21030	chr5:7139892..7144272	4456	2553	20	850	95.50	8.96
9	AtAGO9	AT5G21150	chr5:7192239..7198324	6143	2691	21	896	100.52	9.18
10	AtAGO10	AT5G43810	chr5:17610972..17616797	6164	2967	18	988	110.86	9.35
11	BrAGO1a	Brara.H00354.1	chrA08:3360453..3366384	5932	3240	21	1079	119.42	9.43
12	BrAGO1b	Brara.E01925.1	chrA05:16771472..16778000	6529	2814	18	1111	122.88	9.45
13	BrAGO2	Brara.I02739.1	chrA09:26217713..26221562	3850	3114	2	1037	115.56	9.61
14	BrAGO3	Brara.E01555.1	chrA05:10275374..10278911	3538	3033	1	1009	112.53	9.51
15	BrAGO4a	Brara.D01607.1	chrA04:14183385..14189266	5882	2769	21	922	103.03	8.87
16	BrAGO4b	Brara.E01296.1	chrA07:13646953..13652856	5904	2772	21	923	103.33	8.82
17	BrAGO5	Brara.G01334.1	chrA07:13879303..13884416	5114	2904	19	957	106.65	9.52
18	BrAGO6	Brara.C01682.1	chrA03:8198054..8203613	5560	3096	21	867	97.21	9.03
19	BrAGO7	Brara.G02481.1	chrA07:20707601..20711182	3582	2955	2	984	112.13	9.33
20	BrAGO8	Brara.B00933.1	chrA02:4415711..4421295	5585	2721	20	906	101.40	9.25
21	BrAGO9a	Brara.J01517.1	chrA10:13258763..13263399	4637	2721	21	903	102.19	9.25
22	BrAGO9b	Brara.J01515.1	chrA10:13242702..13247995	5294	2502	20	911	102.27	9.28
23	BrAGO10	Brara.F03787.1	chrA06:28583302..28588634	5333	3015	16	1004	112.84	9.42
RDR									
1	AtRDR1	AT1G14790	chr1:5093961..5098032	4310	3324	2	1107	126.21	7.92
2	AtRDR2	AT4G11130	chr4:6780522..6784440	4184	3402	3	1133	129.32	6.23
3	AtRDR3	AT2G19910	chr2:8595820..8600757	5327	2979	17	992	112.75	7.73
4	AtRDR4	AT2G19920	chr2:8602222..8606887	5011	2784	17	927	105.18	6.78
5	AtRDR5	AT2G19930	chr2:8607340..8612441	5102	2934	17	977	110.88	6.67
6	AtRDR6	AT3G49500	chr3:18349161..18353624	5280	3591	1	1196	136.92	6.82
7	BrRDR1	Brara.F01003.1	chrA06:5750710..5754363	3654	3330	2	1109	112.84	9.42
8	BrRDR2	Brara.I02558.1	chrA09:23798964..23803145	4182	3369	3	1122	127.49	6.46
9	BrRDR3	Brara.I04715.1	chrA09:40258994..40264082	5089	3000	16	999	114.27	8.41
10	BrRDR4	Brara.J01367.1	chrA10:12246526..12251483	4958	2982	17	993	112.10	8.52
11	BrRDR5	Brara.G00096.1	chrA07:745790..750606	4817	2868	16	955	108.08	6.44
12	BrRDR6	Brara.A02175.1	chrA01:13628371..13633064	4694	3597	1	1198	137.07	6.52

Motif composition analysis of the BrDCL, BrAGO and BrRDR proteins

A motif is a sequence pattern that occurs repeatedly in a group of related sequences. Motifs are called small active site of an enzyme for precise folding of the protein and molecular evolution (Akond et al., 2022). To know more about the similarities and dissimilarities of the related proteins of an organism, the motif analysis plays a key technique to explain the regulatory roles in corresponding gene expression. In this study, a well-defined motif analysis along with their consensus sequence stack with logo to indicate the sequence conservation and the relative frequency of amino acids in that sequence were recorded for the 4BrDCL, 13 BrAGO and 6BrRDR using a web-based bioinformatic tool called MEME (**Figure 1-6 and Table 2**). We predicted a maximum of 20 motifs for each protein element and compared their resemblance with that of the motif structures of the corresponding proteins obtained from *A.thaliana*. From the analysis it was observed that 4 BrDCLs contained almost all the predicted 20 motifs in the same order of AtDCL proteins (**Figure 1**). Motif 16 and 15 were absent in BrDCL2 and the motif 9,16 and 20 were absent in BrDCL3 like AtDCL2 and 3.

From the background frequency table, we observed that Alanine (A), Glutamic acid (E), Lysine(K), Serine(S) and Tryptophan(W) were the influential amino acids in the motifs of the identified protein sequences/primary (source) sequences. Presence of S was the highest nearly 9 % followed by E and K each 7% and A was 6% (**Table 2**).



Motif	Symbol	Motif Consensus
1.		CYQRLEFLGDAVLDYLIITRHLFNTYPKLPPGELTDLRSASVNNENFAQVA
2.		EVLVMTPOIILLDALRHSFJKMEMIKLLILDECHHATGKHPY
3.		TSVAEEGLDIQTCNLVIRFDLPKTVCSYIQSRGRARMPNSDYIMMVERGN
4.		LEALTTEKQCQETFSLERLELLGD AFLKYAVSRHLFLKYPTKDEGQLSRRR
5.		PKVLGDVVESIAGAJFLDSGYDLEAVWRVFEPLLDPMVTPETLQLHPVRE
6.		ESCLAGHRWLKSKSVADVVEALIGAYLVEGGKLAALHFMKWIGINVDFDP
7.		KPRKSLSI FLVPTVVLVKQQAEVIRAHNTNLKVGHYCG
8.		QNMISNSNLCRLATDKKLGQYIRDEAFEPKRWTAPGQPSVFPVDVKG
9.		YKVESTGAMVSLGSSVSLIYFYCSRLPGDEYFKPKPEFDFEKDEEPGGLI
10.		IARRYQLEVLEKAKERNTIVYLETGAGKTLIAIMLIKSLGY
11.		SGYATYAEYYKKKYGVDLNHPDQPLLKPKPIFYVHNLLHNR
12.		LLPSVMHRVESLLLAIZLKKLISASIP
13.		RPRIFGMTASPVVRKGEVSS
14.		ELESLLKYEFKKGLLVEAJTHASYPESG
15.		RGTLHEICLKKLWPMPSFDCVVEGGPAHAKFFTFGV
16.		CRJTLPANAPFEEJEGPLLPSMELAKKAVCLKAVKKLHELGVFTDFLLPD
17.		JLYCLDELGLWCAYKAAQSFL
18.		YRSEEDIRCIIFVERIITALV
19.		LENAVVYAPHSGKVYYVDEICHDLNAESPF
20.		NLAKKIHNLETLLNSKVYTVENEKELEGFV

a. **Figure 1. Location of the conserved motifs of the predicted BrDCL protein family drawn using MEME-suite (a maximum of 20 motifs are displayed). Each color represents different motifs in the predicted proteins domains**

Secondly, we also found 13-19 motifs in the 13 BrAGO proteins. It was observed from the analysis that almost all BrAGO proteins possessed similar motif characteristics to their paralogs AtAGOs. Ten BrAGO proteins however possessed 17-19 motifs. BrAGO2 and BrAGO3 contained 16 motifs. Though the BrAGO1a contained 18 motifs similar to that of AtAGO1 but BrAGO1b lacks 5 motifs (**Figure 2**). The similar motif characteristics implies that the BrAGO proteins may have roles like AtAGO proteins. The background frequency analysis showed that Glycine (G) (0.077), Lysine (L) (0.0653), Leucine(L) (0.078), Arginine(A) (0.066), Proline(P) (0.0627), Serine(S)(0.0741) and Valine (V)(0.0739) were the prevalent amino acids of the predicted motifs that exist among the identified BrAGOs (**Table 2**). Among the amino acids the contribution of Leucine was highest (7.8%) in relevant protein expression followed by Glycine (7.77%), Serine (7.41%), Valine (7.39%).



b. Figure 2. Location of the conserved motifs of the predicted BrAGO protein family drawn using MEME-suite (a maximum of 20 motifs are displayed). Each color represents different motifs in the predicted proteins domains

c.

Thirdly, we observed that the 6 BrRDR proteins also contain 10-18 motifs like their 6 AtRDR paralogs. Analysis showed that the BrRDR3/4/5 possessed the highest 18 motifs and the motifs 16 and 19 was missing for these three proteins. These two motifs however were present in BrRDR1/2/6 like their AtRDR paralogs (Figure 3). The presence of these two motifs in the above protein elements implied that they may have some specific roles in growth and development of *B. rapa*. Frequency analysis showed that six amino acids

viz., Aspartic acid(D) (0.0608), Glutamic acid (E) (0.0703), Lysine (K)(0.0755), Leucine (L)(0.0965), Serine (S) (0.0784) and Valine (V)(0.065) were the higher prevalent in motif functions of the 6 BrRDR proteins (Table 2). Among these the contribution of L was the highest (9.65%) followed by S (7.84%), K(7.55%), E(7.03%). Lysine is an important amino acid plays significant role in grain formation in crops.



Motif	Symbol	Motif Consensus
1.		NSKDCVFFPQKGPRLGBEIAGGDLGDGMYFVSRBPKLJEH
2.		VDMTGITFZQIDDIHCHDQDNNVDLKDNGKPCIHSDGTGYISEDLMRCP
3.		VKCYFIRTDSTASYDMQNPYIFSGKSIHEARMHFMHVHTLPSLANYMARF
4.		ISGDVLVYKNPGLHPGDIRVLKATYVKAL
5.		TTSNPPQPTKLNRLIALLSYLGVPDEFF
6.		MKKKCLELADJYDAVDAPKTGAKVELPYDLKPKEFPDYMERDEKPTYTS
7.		ILKBGIMVGLRRYZFLAFKDGKREKKK
8.		PPLLIQFRMFYDGYAVKGTFLNKKLPPRTVQVRPSMIKVS
9.		GRJLVTEGYILMGTVDETGELEEGZVCVI
10.		EESKTIIFDNIIRAAAKAAARYG
11.		TGTHLHKVLGDQNVLTVKFADVPRSSTYC
12.		ESANEVIQYKQEFYGAAGFEDSKKSLEELYPQALALYNIV
13.		KPSELSPEELEELFKMFLKARFNASNVIGIAADSWLTIMD
14.		PPSEISKLPCEFEDEPVPEFHMEKCGLWYENYRTEMSQAM
15.		GEVITADEIRQWKDLPMVAYEAAVWDRGLGRH
16.		PPMDYTPAPPRI LDHDTVLEEEIEEFFVDYMVNDSLGVIANAHVVHADR
17.		MILGGIPLDEPHLKDMLSILLKTZKNDLK
18.		LEWDSGKTHYYQCHVAPDGSYRFKGPLJE
19.		PSAYQIRYGGYKGVAVDPSS
20.		EFRDGGJGSI SEELALEVLRKV

d.

e. Figure 3. Location of the conserved motifs of the predicted BrRDR protein family drawn using MEME-suite (a maximum of 20 motifs are displayed). Each color represents different motifs in the predicted proteins domains

The sequence logo drawn for each of the 20 motifs illustrated the sequence conservation in that position as well as the height of each letter shows the relative frequency of the corresponding amino acid at the position of BrDCL, BrAGO and BrRDR proteins. The digits in the column named ‘Sites’ shows the repetition number of that particular motif among the total number of RNAi proteins of *B.rapa* and *A.thaliana* (Figure.4-6). The digits in the column named ‘Width’ shows the length of the corresponding motif.

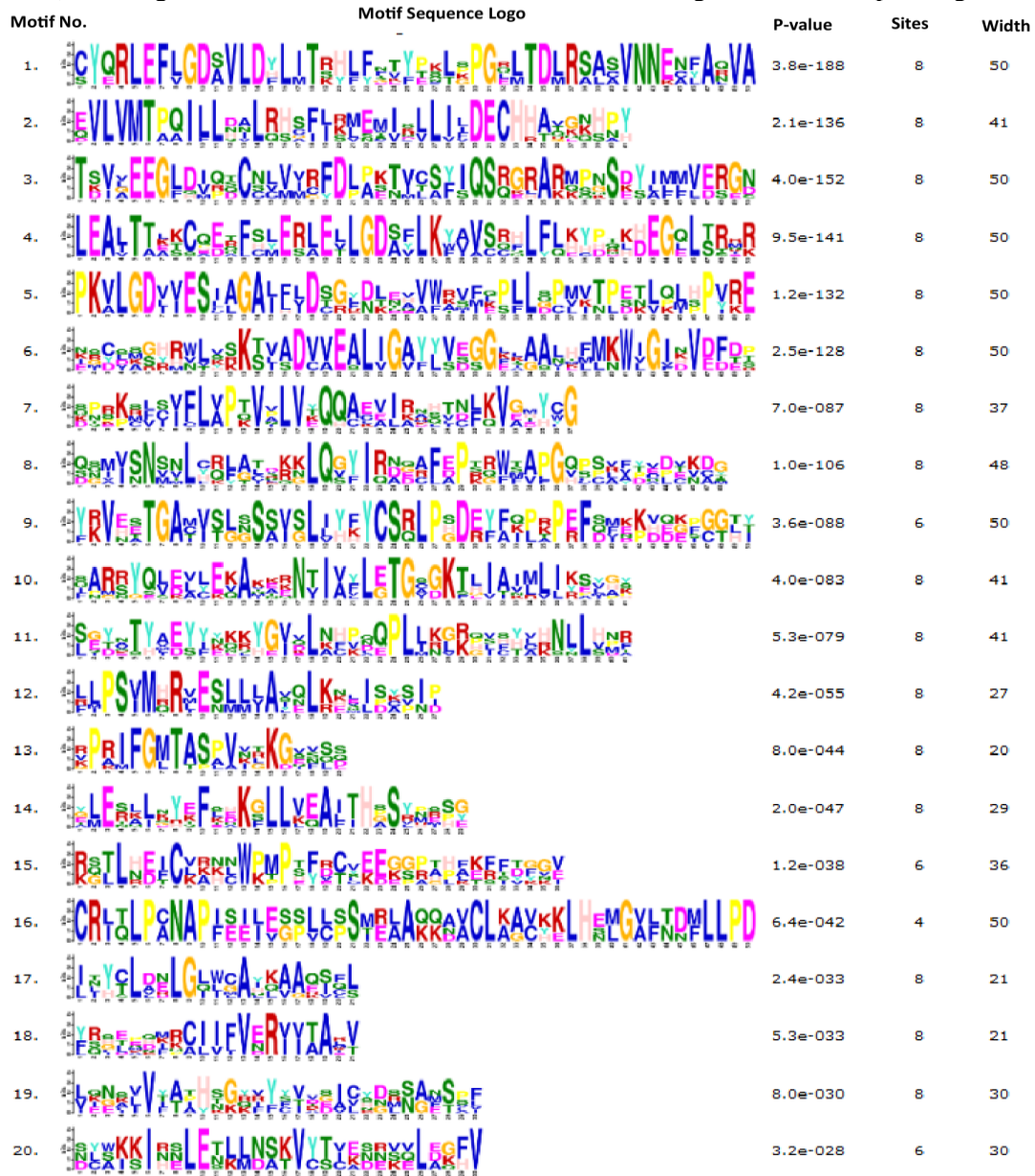


Figure 4. Sequence LOGO for the motifs found in BrDCL. The overall height of the stack indicates the sequence conservation at that position, and the height of each letter represents the relative frequency of the corresponding amino acid at that position

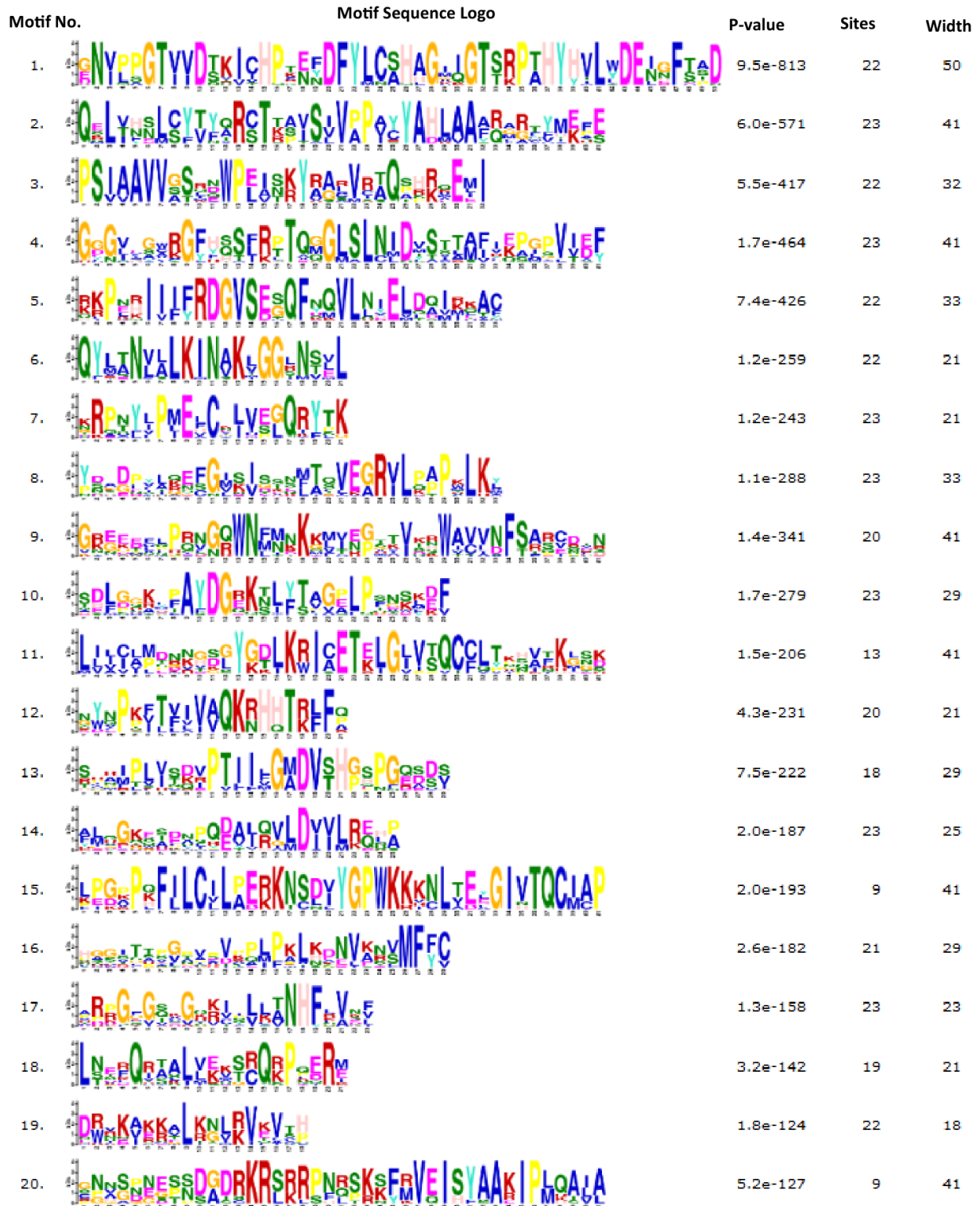


Figure 5. Sequence LOGO for the motifs found in BrAGO. The overall height of the stack indicates the sequence conservation at that position, and the height of each letter represents the relative frequency of the corresponding amino acid at that position

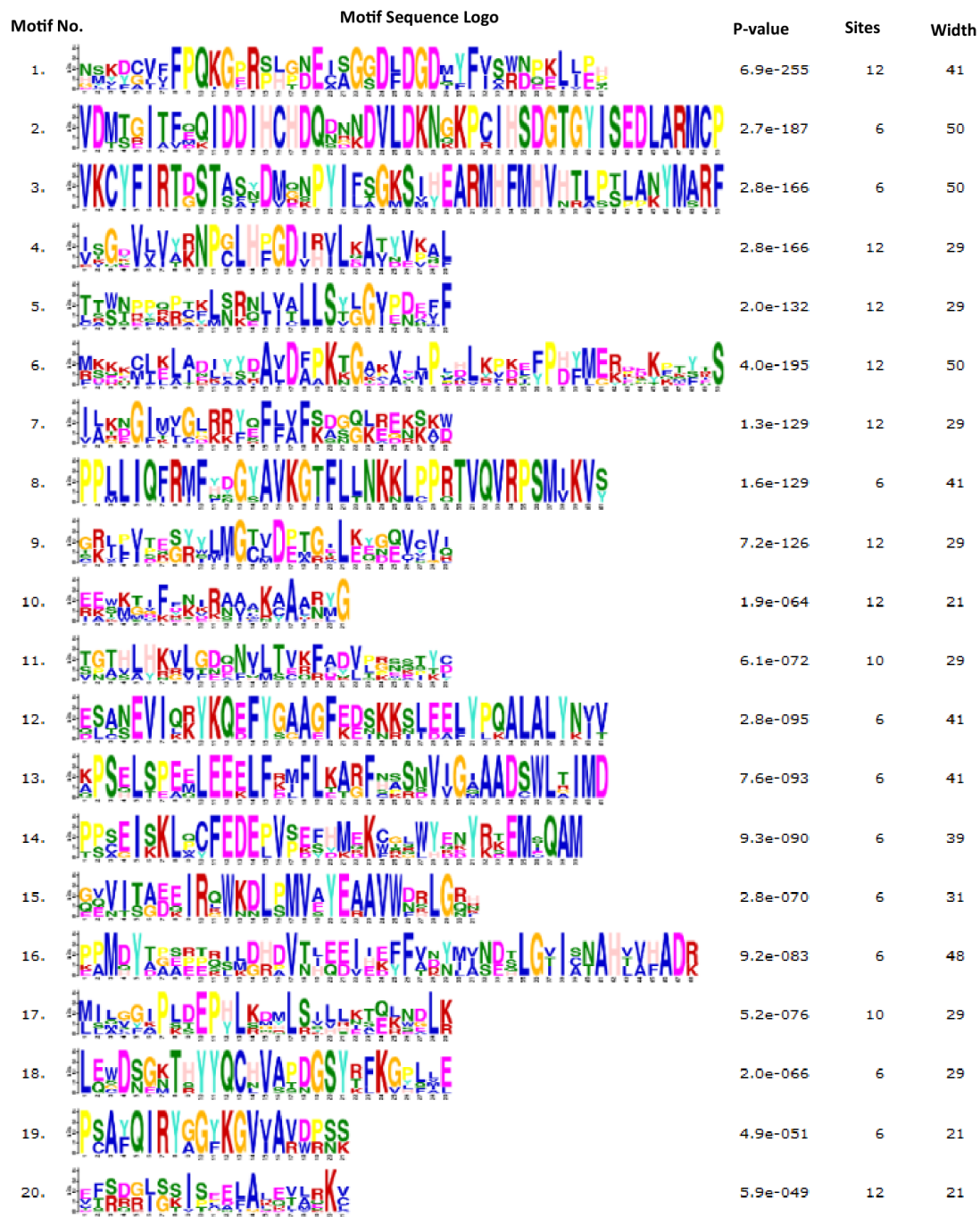


Figure 6. Sequence LOGO for the motifs found in BrRDR. The overall height of the stack indicates the sequence conservation at that position, and the height of each letter represents the relative frequency of the corresponding amino acid at that position

Table 2. List of the background frequencies built from the primary (source) sequences used by the MEME suite to tell how prevalent each letter of the motif alphabet was in the source sequences that were used to create the motifs

i. Order	Name	Freq.	Bg.	Freq.	Bg.	Freq.	Bg.
		BrDCL		BrAGO		BrRDR	
A	Alanine	0.0619	0.0619	0.0558	0.0558	0.0586	0.0586
C	Cysteine	0.0229	0.0229	0.0174	0.0174	0.0178	0.0178
D	Aspartic acid	0.0529	0.0529	0.0483	0.0483	0.0608	0.0608
E	Glutamic acid	0.0761	0.0761	0.0542	0.0542	0.0703	0.0703
F	Phenylalanine	0.0415	0.0415	0.0414	0.0414	0.0492	0.0492
G	Glycine	0.0532	0.0532	0.077	0.077	0.0572	0.0573
H	Histidine	0.0278	0.0278	0.0248	0.0248	0.0232	0.0232
I	Isoleucine	0.0494	0.0494	0.0523	0.0523	0.0519	0.0519
K	Lysine	0.0703	0.0703	0.0653	0.0653	0.0755	0.0755
L	Leucine	0.11	0.11	0.078	0.078	0.0965	0.0965
M	Methionine	0.0227	0.0226	0.0234	0.0234	0.0259	0.026
N	Asparagine	0.0412	0.0412	0.048	0.048	0.037	0.037
P	Proline	0.0406	0.0406	0.0627	0.0627	0.0488	0.0488
Q	Glutamine	0.0352	0.0352	0.049	0.049	0.03	0.03
R	Arginine	0.0484	0.0484	0.066	0.066	0.054	0.054
S	Serine	0.0886	0.0886	0.0741	0.0741	0.0784	0.0784
T	Threonine	0.047	0.047	0.0507	0.0507	0.0464	0.0464
V	Valine	0.071	0.071	0.0739	0.0739	0.065	0.065
W	Tryptophan	0.00915	0.00915	0.00691	0.00691	0.011	0.011
Y	Tyrosine	0.0302	0.0302	0.031	0.031	0.0423	0.0423

Analysis of trans-regulatory elements of the identified BrRNAi genes

Transcription factor (TF) also called *trans*-acting element combining with *cis*-acting element in the promoter region of a gene regulate the gene expression. To predict the TF for the identified gene symbols extracted from the *B. rapa* genome from NCBI database were used (**Table 2**). In this work, 502 trans factors were finally predicted for the 23 *B. rapa* RNAi genes. The predicted TFs were classified into 31 groups/families (**Table 3**). The top-ranked 10 TF families (Dof, bZIP, C2H2, ERF, BBR-BPC, MICK-MADS, MYB, TCP, WRKY and AP2) comprises of 393 (78%) regulators of which Dof 115(23%), bZIP 58(11.55%), C2H2 49(9.76%), ERF 30(6%), BBR-BPC 29(5.77%), MICK-MADS 23(4.58%), MYB, TCP and WRKY each 23 (4.58%) and AP2 regulate 21(4.18%) TFs. The DNA-binding one finger (Dof) is also a plant specific TF gene family found in green algae to higher plants which showed bifunctional binding characteristics with DNA and proteins to control transcriptional machinery in plant cells(Noguero et al., 2013; Gupta et al., 2015). Dof is involved in regulating genes related to seed maturation and germination, phytohormone and light-mediated regulation, and plant tolerance to biotic and abiotic stresses(Noguero et al., 2013; Gupta et al., 2015; Azam et al., 2018). The bZIP TF families contributed to gene regulation for development and resistance response to various environmental stressors(Zhang et al., 2015). C2H2, a zinc finger-type protein, is also one of the influential TF families that possess finger-like structures and can bind

Zn²⁺(Han et al., 2020). This TF plays a vital role in plant growth, development, and stress signal transduction (H. et al., 2014). A study showed that the genes of this TF family play a deep role in salt, osmotic, drought, cold, drought, oxidative, and high-light stress (Han et al., 2020). Some stress-associated plant hormones such as abscisic acid (ABA), salicylic acid (SA), jasmonic acid (JA), and ethylene (ET) perform a crucial role against many environmental stressors (pathogens and abiotic) mediated by C2H2 class proteins (Han et al., 2020). The TF family ERF (ethylene response factor) is one of the largest subfamilies that belong to the APETALA2/ERF family. It includes ethylene signaling and the response pathway in plants that was characterized by a single AP2 domain (Müller and Munné-Bosch, 2015). This TF family also responds to plant hormones with improved plant survival during stress conditions. For example, several AP2/ERF families respond to the plant hormones abscisic acid (ABA) and ethylene (ET) to help stimulate ABA and ET-dependent and independent stress responsive genes (Xie et al., 2019). An experimental investigation showed that an ethylene response factor (SIERF5/ERF5) helps to increase adaptation to drought and salt tolerance in tomato (Pan et al., 2012).

Table 3. List of gene symbols used in TF vs Gene networking to predict degree of interaction

No.	Gene Name	Gene Symbol	Protein ID
BrDCL			
1.	BrDCL1	LOC103844613	XP_033138117
2.	BrDCL2	LOC103855153	XP_009130358
3.	BrDCL3	LOC103873620	XP_009150277
4.	BrDCL4	LOC103845687	XP_009120817
BrAGO			
1	BrAGO1a	LOC103833004	XP_009107358
2.	BrAGO1b	LOC103868679	XP_009145006
3.	BrAGO2	LOC103840257	XP_009115003
4.	BrAGO3	LOC103849944	XP_009124901
5.	BrAGO4a	LOC103864747	XP_009140756
6.	BrAGO4b	LOC103829646	XP_009103572
7.	BrAGO5	LOC103829691	XP_009103628
8.	BrAGO6	LOC103857461	XP_009132895
9.	BrAGO7	LOC103830930	XP_009105000
10.	BrAGO8	LOC103851403	XP_009126507
11.	BrAGO9a	LOC103845607	XP_009120723
12.	BrAGO9b	LOC103845605	XP_033138521
13.	BrAGO10	LOC103827949	XP_009101761
BrRDR			
1.	BrRDR1	LOC103872274	XP_009148868
2.	BrRDR2	LOC103833901	XP_009108193
3.	BrRDR3	LOC103842618	XP_009117513
4.	BrRDR4	LOC103845422	XP_018511278
5.	BrRDR5	LOC103828268	XP_009102127
6.	BrRDR6	LOC103875370	XP_009152135

The plant-specific Barley B recombinant-basic Penta-Cysteine (BBR/BPC) TF family shows essential functions for proper plant growth and development (Shanks et al., 2018; Theune et al., 2019). The proteins of this family regulate flower development, the size of the stem cell niche, and seed development through

transcriptional regulation of homeotic transcription factor genes (Theune et al., 2019). BBR/BRP also works for brassinosteroid hormone signaling in plants such as Arabidopsis. BPC6 targets the promoters of all key brassinosteroid signaling elements(Theune et al., 2019). The MIKC-MADS family encodes the TFs for important and numerous functions connected to plant growth and development(Díaz-Riquelme et al., 2009). This TF is popular to act as a regulatory network for rapid and simultaneous functional divergence in vegetative and reproductive stages in plants for regulating gene expression in flowers, pollen, endosperm, guard cells, roots, and trichomes(Díaz-Riquelme et al., 2009). This family was also responsible for the transcription of OsRDR1 genes to increase the resistance power against the rice stripe virus (RSV) in rice (Wang et al., 2016a; Mosharaf et al., 2021). In plants, MYB TF was also found in higher numbers. In *A. thaliana*, this TF family accounts for nearly 9% of the total TFs(Cao et al., 2020). This TF was identified for its conserved MYB domain (a 52 amino acid motif) at the N-terminus and was an evolutionarily conserved domain found in almost all eukaryotes(Martin and Paz-Ares, 1997; Cao et al., 2020). The TFs of this family in plants are also linked to various biological processes, namely, the circadian rhythm, defense and stress responses, cell fate and identity, seed and floral development, and regulation of primary and secondary metabolism(Ramya et al., 2017; Cao et al., 2020). In various plant species, the WRKY family is believed to be involved in i) the modulation of antagonistic interaction between salicylic acid and jasmonic acids signaling and ii) the enhancement of defense against neurotropic pathogens. The earlier investigation also reported that both AP2 TF family contributed to gene regulation for development and resistance response to various environmental stressors (Liu et al., 2001; Zhang et al., 2015).

Table 4. Distribution of TF families those regulating RNAi genes in *Brassica Rapa* L

Gene\TF	AP2	B3	BBR- BPC	BES1	bHLH	Myb	CH2H2	CH	CAMTA	CPP	Dof	ERF	FAR1	G2-like	GATA	GRAS	HSF	LBD	MIKC- MADS	MYB	NAC	NFYB	Nin- like	RAV	SRS	TCP	Trithelix	WOX	WRKY	WABBY	ZH-HD	
BrDCL1	1	1	2		2		2				2	1				1			1													
BrDCL2			1				1				1	8			2	1		1		1								1				
BrDCL3	1	1	2				1				5				1	1			1		2		1									
BrDCL4	1	1	2				4				13				1	1			1											2		
BrAGO1a	1	1	2				22	1			9				1	1			1													
BrAGO1b	1		2		1	15	9								1	10			1													
BrAGO2	1						4				1				1	7			1												1	
BrAGO3	1		1				1	1			11						2		1		2	1										
BrAGO4a	1		2			8	1		3		8			1	1				2										1	1		
BrAGO4b	3	1	2								8			1	1				1		2											
BrAGO5	1										1	6				1		1				10				8					5	
BrAGO6		1				1	2		2	1	2							1														
BrAGO7	1	1	2				3				7				1				1													
BrAGO8	1		2	1	1		1	1			10								1		5						9		1		2	
BrAGO9a	1	1									4	7							1						2							
BrAGO9b	1		1				1				11			1					1				1									
BrAGO10	1	1	2			1	1				11	4			5	1			1				1									
BrRDR1			1				11	2			1				1	1			1								6					
BrRDR2	1		2		1		2		1		1		1	1	1	1			1													
BrRDR3	1						2				1								6			1						1				
BrRDR4	1	1	2								3				3	1			1													
BrRDR5	1	1	2				1				6	4							1		11				1							
BrRDR6							1				6	4																				
Total=502	21	12	29	1	5	58	49	2	3	4	115	30	1	2	14	15	19	2	23	23	11	2	2	1	3	23	4	1	22	1	4	

Gene networking analysis between TFs and RNAi genes of *B.rapa*

A comprehensive relationship between the predicted RNAi genes of *B. rapa* and the associated TFs were measured by means of a gene-networking technique. To construct the whole network, an open-source software Cytoscope 3.10.0 was used. The network produced 236 nodes and 502 edges between the genes and TFs. On the basis of node ‘Degree’ criteria, the relationship was build. The higher the degree the more the connection of a particular RNAi gene with the TFs. The network analysis shows that the Dof TF family is found highest number in the RNAi genes except BrAGO1b, BrRDR2 and BrRDR5 (Table 4 and Figure 7).

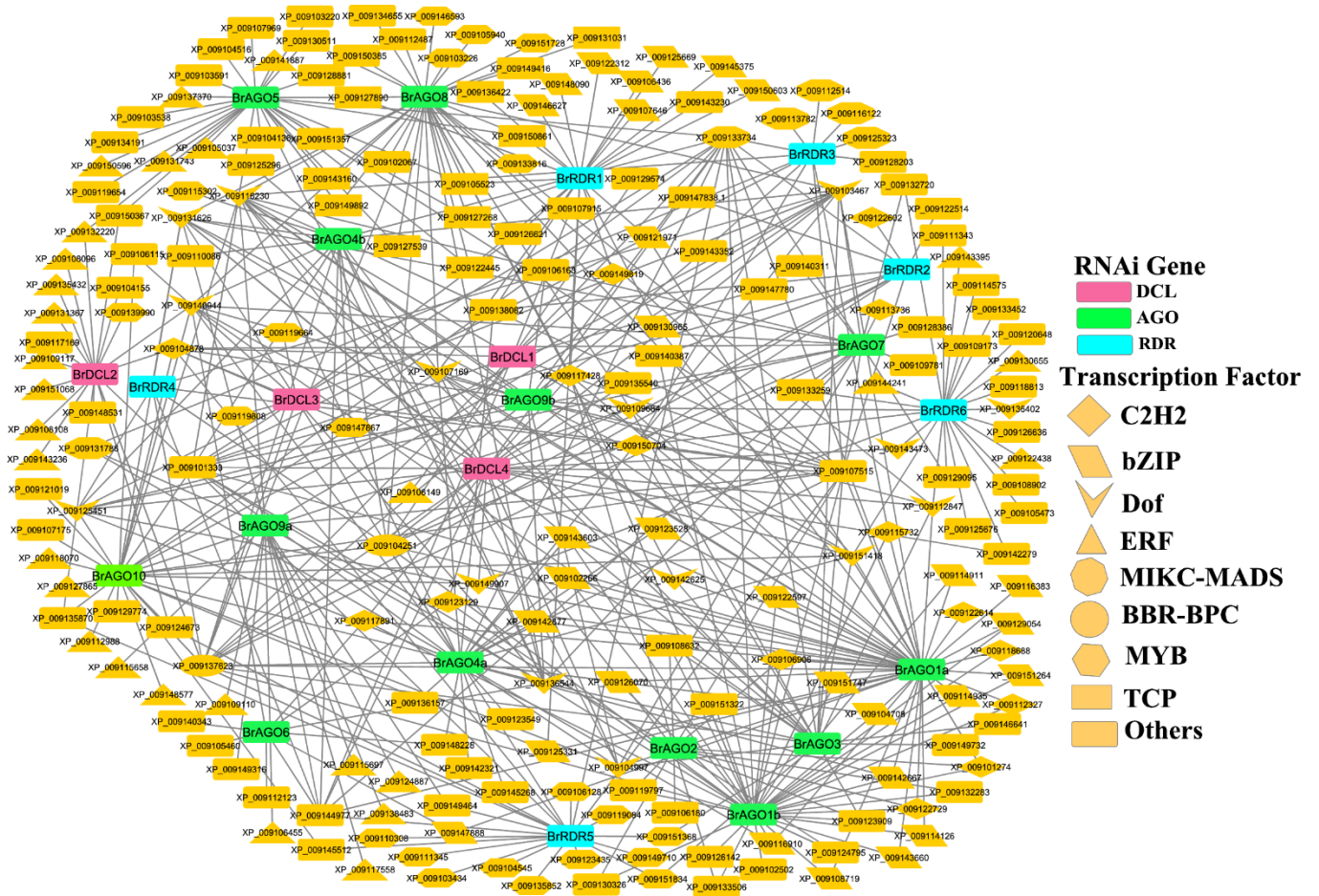


Figure 7. TF-RNAi gene interaction network. The network represents highly interconnected regions of the network. The constructed network produced 236 nodes and 502 edges. The edges define the interconnection between the RNAi genes and the TF family. Eight top-ranked TFs are symbolized with different symbols. Three groups of RNAi genes are highlighted in three distinct colors

Among the BrDCL genes BrDCL4 is linked to highest number of Dof TF family. Among the BrAGO genes, BrAGO3/4a/4b/8/9b/10 are linked with the higher number of Dof TF. Six Dof TF is associated with the BrRDR6. Interestingly, no bZIP TF was associated with the 4 BrDCLs. This TF family was only found higher number in BrAGO1a/1b/4a and BrRDR1. The C2H2 family was related to almost all RNAi genes of *B.rapa* except BrAGO4a/4b/5/9a and BrRDR4. The ERF family was associated with specific number of RNAi genes (BrDCL1/8, BrAGO5/9a/10 and BrRDR6). The analysis showed that BrAGO2/5/6/9a and BrRDR1/3/6 were not connected with any BBR-BPC TF (Table 3 and Figure 7). There was low link between the MIKC_MADS TF and all RNAi genes of *B. rapa* except BrDCL2, BrAGO2/8 and BrRDR1/6. The MYB TF was found highest number in BrRDR5 followed by BrAGO5/4b/3 and BrDCL3/2. The TCP was associated with only three RNAi genes (BrAGO5, BrAGO8 and BrRDR1). One of the important TF family AP2 was also linked to almost all RNAi genes except BrDCL2, BrAGO6, BrRDR1 and BrRDR6. The regulatory network showed that RNAi process of predicted putative genes in *B.rapa* represents a diagrammatic evolutionary model that could be explored in detail through the characterization of these predicted genes.

Conclusion

Oilseed crops are highly important source of edible oil. But these crops are often face various stresses that result in huge loss of oilseed production. Like other plants, in *B.rapa*, a number of particular RNAi genes BrDCL, BrAGO, and BrRDR play important roles against stresses to help crops for healthy and timely growth and development. In this work, several bioinformatic approaches were applied to identify, characterize and uncover the diversity of the *B.rapa* RNAi genes. The analysis results suggest that *B.rapa* genome contains 4 DCL, 13 AGO, and 6 RDR genes. The MEME motif analysis showed that the predicted proteins conserve similar motif characteristics similar to their paralog RNAi genes of *Arabidopsis*. The relative frequency analysis showed that Lysine (K), Serine(S), Valine(V), Leucine(L), and Glutamic acid(E) were the dominant amino acids of the projected motifs in the identified proteins. The TF analysis showed that the Dof, bZIP, C2H2, ERF, BBR-BPC, MICK-MADS, MYB, TCP, WRKY, and AP2 are the top 10 TF families consisted of 393 (78%) regulators out of 502. The gene-TF network analysis showed that eight key TF families were highly connected with the identified RNAi genes in *B.rapa* with some exception. Finally, it can be concluded that this genomic info will further help to investigate the in-depth analysis of these genes in *B.rapa* species for functions in controlling gene expression against different biotic and abiotic factors to improve oilseed crop production.

3.e.i.1 References

- Akond, Z., Rahman, H., Ahsan, M. A., Mosharaf, M. P., Alam, M., and Mollah, M. N. H. (2020). Bioinformatic analysis based genome-wide identification, characterization, diversification and regulatory transcription components of RNA silencing machinery genes in wheat (*Triticum aestivum* L.). *bioRxiv*. doi: 10.1101/2020.05.21.108100.
- Akond, Z., Rahman, H., Ahsan, M. A., Mosharaf, M. P., Alam, M., and Mollah, M. N. H. (2022). Comprehensive in Silico Analysis of RNA Silencing-Related Genes and Their Regulatory Elements in Wheat (*Triticum aestivum* L.). *Biomed Res. Int.* 2022. doi: 10.1155/2022/4955209.
- Azam, S. M., Liu, Y., Rahman, Z. U., Ali, H., Yan, C., Wang, L., et al. (2018). Identification, Characterization and Expression Profiles of Dof Transcription Factors in Pineapple (*Ananas comosus* L.). *Trop. Plant Biol.* doi: 10.1007/s12042-018-9200-8.
- Cao, J.-Y., Xu, Y.-P., Li, W., Li, S.-S., Rahman, H., and Cai, X.-Z. (2016). Genome-Wide Identification of Dicer-Like, Argonaute, and RNA-Dependent RNA Polymerase Gene Families in Brassica Species and Functional Analyses of Their Arabidopsis Homologs in Resistance to *Sclerotinia sclerotiorum*. *Front. Plant Sci.* 7, 1–17. doi: 10.3389/fpls.2016.01614.
- Cao, Y., Li, K., Li, Y., Zhao, X., and Wang, L. (2020). MYB transcription factors as regulators of secondary metabolism in plants. *Biology (Basel)*. doi: 10.3390/biology9030061.
- Carbonell, A., Fahlgren, N., Garcia-Ruiz, H., Gilbert, K. B., Montgomery, T. A., Nguyen, T., et al. (2012). Functional analysis of three Arabidopsis argonautes using slicer-defective mutants. *Plant Cell*. doi: 10.1105/tpc.112.099945.
- Cui, D. L., Meng, J. Y., Ren, X. Y., Yue, J. J., Fu, H. Y., Huang, M. T., et al. (2020). Genome-wide identification and characterization of DCL, AGO and RDR gene families in *Saccharum spontaneum*. *Sci. Rep.* doi: 10.1038/s41598-020-70061-7.
- Dalmay, T., Hamilton, A., Rudd, S., Angell, S., and Baulcombe, D. C. (2000). An RNA-dependent RNA polymerase gene in Arabidopsis is required for posttranscriptional gene silencing mediated by a transgene but not by a virus. *Cell*. doi: 10.1016/S0092-8674(00)80864-8.
- Deleris, A., Gallago-Bartolome, J., Bao, J., Kasschau, K. D., Carrington, J. C., and Voinnet, O. (2006). Hierarchical action and inhibition of plant dicer-like proteins in antiviral defense. *Science (80-)*. doi: 10.1126/science.1128214.
- Dharmendra, K., Neelam, M., Yashwant, K. B., Ajay, K., Kamlesh, K., Kalpana, S., et al. (2014). Alternaria blight of oilseed Brassicas: A comprehensive review. *African J. Microbiol. Res.* doi:

- 10.5897/ajmr2013.6434.
- Díaz-Riquelme, J., Lijavetzky, D., Martínez-Zapater, J. M., and Carmona, M. J. (2009). Genome-wide analysis of MIKCC-type MADS box genes in grapevine. *Plant Physiol.* doi: 10.1104/pp.108.131052.
- Dubey, H., Kiran, K., Jaswal, R., Bhardwaj, S. C., Mondal, T. K., Jain, N., et al. (2020). Identification and characterization of Dicer-like genes in leaf rust pathogen (*Puccinia triticina*) of wheat. *Funct. Integr. Genomics.* doi: 10.1007/s10142-020-00745-w.
- Fagard, M., Boutet, S., Morel, J.-B., Bellini, C., and Vaucheret, H. (2000). AGO1, QDE-2, and RDE-1 are related proteins required for post-transcriptional gene silencing in plants, quelling in fungi, and RNA interference in animals. *Proc. Natl. Acad. Sci.* doi: 10.1073/pnas.200217597.
- Gupta, S., Malviya, N., Kushwaha, H., Nasim, J., Bisht, N. C., Singh, V. K., et al. (2015). Insights into structural and functional diversity of Dof (DNA binding with one finger) transcription factor. *Planta.* doi: 10.1007/s00425-014-2239-3.
- H., Z., Y., L., F., W., D., Y., L., W., J., G., et al. (2014). A novel rice C2H2-type zinc finger protein, ZFP36, is a key player involved in abscisic acid-induced antioxidant defence and oxidative stress tolerance in rice. *J. Exp. Bot.*
- Han, G., Lu, C., Guo, J., Qiao, Z., Sui, N., Qiu, N., et al. (2020). C2H2 Zinc Finger Proteins: Master Regulators of Abiotic Stress Responses in Plants. *Front. Plant Sci.* doi: 10.3389/fpls.2020.00115.
- Hunter, C., Sun, H., and Poethig, R. S. (2003). The Arabidopsis Heterochronic Gene ZIPPY Is an ARGONAUTE Family Member. *Curr. Biol.* doi: 10.1016/j.cub.2003.09.004.
- Iwasaki, S., Kobayashi, M., Yoda, M., Sakaguchi, Y., Katsuma, S., Suzuki, T., et al. (2010). Hsc70/Hsp90 Chaperone Machinery Mediates ATP-Dependent RISC Loading of Small RNA Duplexes. *Mol. Cell* 39, 292–299. doi: 10.1016/J.MOLCEL.2010.05.015.
- Jovel, J., Walker, M., and Sanfaçon, H. (2007). Recovery of *Nicotiana benthamiana* Plants from a Necrotic Response Induced by a Nepovirus Is Associated with RNA Silencing but Not with Reduced Virus Titer. *J. Virol.* doi: 10.1128/jvi.01192-07.
- Liu, Q., Zhang, G., and Chen, S. (2001). Structure and regulatory function of plant transcription factors. *Chinese Sci. Bull.* doi: 10.1007/bf03187184.
- Lysak, M. A., Koch, M. A., Pecinka, A., and Schubert, I. (2005). Chromosome triplication found across the tribe Brassiceae. *Genome Res.* 15, 516–525. doi: 10.1101/gr.3531105.
- Martin, C., and Paz-Ares, J. (1997). MYB transcription factors in plants. *Trends Genet.* doi: 10.1016/S0168-9525(96)10049-4.
- McAlvay, A. C., Ragsdale, A. P., Mabry, M. E., Qi, X., Bird, K. A., Velasco, P., et al. (2021). Brassica rapa Domestication: Untangling Wild and Feral Forms and Convergence of Crop Morphotypes. *Mol. Biol. Evol.* 38, 3358–3372. doi: 10.1093/molbev/msab108.
- Meng, F., Jia, H., Ling, N., Xue, Y., Liu, H., Wang, K., et al. (2013a). Cloning and characterization of two Argonaute genes in wheat (*Triticum aestivum* L.). *BMC Plant Biol.* doi: 10.1186/1471-2229-13-18.
- Meng, F., Jia, H., Ling, N., Xue, Y., Liu, H., Wang, K., et al. (2013b). Cloning and characterization of two Argonaute genes in wheat (*Triticum aestivum* L.). *BMC Plant Biol.* 13, 1–10. doi: 10.1186/1471-2229-13-18.
- Mirzaei, K., Bahramnejad, B., Shamsifard, M. H., and Zamani, W. (2014). In silico identification, phylogenetic and bioinformatic analysis of argonaute genes in plants. *Int. J. Genomics.* doi: 10.1155/2014/967461.
- Mosharaf, M. P., Rahman, H., Ahsan, M. A., Akond, Z., Ahmed, F. F., Islam, M. M., et al. (2021). In silico identification and characterization of AGO, DCL and RDR gene families and their associated regulatory elements in sweet orange (*Citrus sinensis* L.). doi: 10.1371/journal.pone.0228233.
- Mourrain, P., Béclin, C., Elmayan, T., Feuerbach, F., Godon, C., Morel, J. B., et al. (2000). Arabidopsis SGS2 and SGS3 genes are required for posttranscriptional gene silencing and natural virus resistance. *Cell.* doi: 10.1016/S0092-8674(00)80863-6.
- Moussian, B., Schoof, H., Haecker, A., Jürgens, G., and Laux, T. (1998). Role of the ZWILLE gene in the regulation of central shoot meristem cell fate during Arabidopsis embryogenesis. *EMBO J.* doi:

- 10.1093/emboj/17.6.1799.
- Müller, M., and Munné-Bosch, S. (2015). Ethylene response factors: A key regulatory hub in hormone and stress signaling. *Plant Physiol.* doi: 10.1104/pp.15.00677.
- Noguero, M., Atif, R. M., Ochatt, S., and Thompson, R. D. (2013). The role of the DNA-binding One Zinc Finger (DOF) transcription factor family in plants. *Plant Sci.* doi: 10.1016/j.plantsci.2013.03.016.
- Pan, Y., Seymour, G. B., Lu, C., Hu, Z., Chen, X., and Chen, G. (2012). An ethylene response factor (ERF5) promoting adaptation to drought and salt tolerance in tomato. *Plant Cell Rep.* doi: 10.1007/s00299-011-1170-3.
- Qian, Y., Cheng, Y., Cheng, X., Jiang, H., Zhu, S., and Cheng, B. (2011). Identification and characterization of Dicer-like, Argonaute and RNA-dependent RNA polymerase gene families in maize. *Plant Cell Rep.* 30, 1347–1363. doi: 10.1007/s00299-011-1046-6.
- Ramya, M., Kwon, O. K., An, H. R., Park, P. M., Baek, Y. S., and Park, P. H. (2017). Floral scent: Regulation and role of MYB transcription factors. *Phytochem. Lett.* doi: 10.1016/j.phytol.2016.12.015.
- Schmitz, R. J., Hong, L., Fitzpatrick, K. E., and Amasino, R. M. (2007). DICER-LIKE 1 and DICER-LIKE 3 redundantly act to promote flowering via repression of FLOWERING LOCUS C in *Arabidopsis thaliana*. *Genetics.* doi: 10.1534/genetics.107.070649.
- Shanks, C. M., Hecker, A., Cheng, C. Y., Brand, L., Collani, S., Schmid, M., et al. (2018). Role of BASIC PENTACYSTEINE transcription factors in a subset of cytokinin signaling responses. *Plant J.* doi: 10.1111/tpj.13962.
- Theune, M. L., Bloss, U., Brand, L. H., Ladwig, F., and Wanke, D. (2019). Phylogenetic analyses and GAGA-motif binding studies of BBR/BPC proteins lend to clues in GAGA-MOTIF recognition and a regulatory role in brassinosteroid signaling. *Front. Plant Sci.* doi: 10.3389/fpls.2019.00466.
- Wang, H., Jiao, X., Kong, X., Hamera, S., Wu, Y., Chen, X., et al. (2016a). A signaling cascade from miR444 to RDR1 in rice antiviral RNA silencing pathway. *Plant Physiol.* doi: 10.1104/pp.15.01283.
- Wang, T., You, L., Li, R., Fu, D. Q., Zhu, B. Z., Luo, Y. B., et al. (2016b). Cloning, identification, and expression analysis of a Dicer-Like gene family from *Solanum lycopersicum*. *Biol. Plant.* doi: 10.1007/s10535-016-0620-8.
- Xiao, D., Wang, H., Basnet, R. K., Zhao, J., Lin, K., Hou, X., et al. (2014). Genetic dissection of leaf development in *Brassica rapa* using a genetical genomics approach. *Plant Physiol.* 164, 1309–1325. doi: 10.1104/pp.113.227348.
- Xie, Z., Nolan, T. M., Jiang, H., and Yin, Y. (2019). AP2/ERF transcription factor regulatory networks in hormone and abiotic stress responses in *Arabidopsis*. *Front. Plant Sci.* doi: 10.3389/fpls.2019.00228.
- Yun, S., and Zhang, X. (2023). Genome-wide identification, characterization and expression analysis of AGO, DCL, and RDR families in *Chenopodium quinoa*. *Sci. Rep.* 13, 3647. doi: 10.1038/s41598-023-30827-1.
- Zhang, L., Zhang, L., Xia, C., Zhao, G., Liu, J., Jia, J., et al. (2015). A novel wheat bZIP transcription factor, TabZIP60, confers multiple abiotic stress tolerances in transgenic *Arabidopsis*. *Physiol. Plant.* doi: 10.1111/ppl.12261.
- Zilberman, D., Cao, X., and Jacobsen, S. E. (2003). ARGONAUTE4 control of locus-specific siRNA accumulation and DNA and histone methylation. *Science (80-)*. doi: 10.1126/science.1079695.

DEVELOPMENT OF ONLINE-BASED BARI VEHICLE MANAGEMENT AND REQUISITION SYSTEM

Z AKOND¹, M.A. MONAYEM MIAH² AND M. Z. HASAN³

^{1,2}ASICT, BARI, Gazipur, ³Transport Section, BARI

Abstract

Scientists and other officials at BARI often travel intra-district and inter-district for research activities and other official purposes. But at present the vehicle management and requisition method is done manually in paper form. In line with the mission and vision of the development of digital and smart Bangladesh and APA targets, we have developed an online-based transport management and vehicle requisition system called BARI Vehicle Management System (BVMS) for the complete replacement of the high level of labor, cost, and time. In this digital system, all relevant info and data about all vehicles of BARI HQ and outer stations are recorded and stored. Moreover, a user-friendly web-based digital system has been developed to approve the required vehicle to the employee of BARI as per their choice. This digital system has been established following the previously approved BARI vehicle/transport requisition form. For accurate development of the system, an outsourcing platform was involved. MySQL database, PHP scripting language, and HTML were used for the smart and easy operation and web-enabled view. Any employee will be able to access and use this system using an internet-connected device. This digital system, however, will promote the vehicle requisition very quickly and transparently and it help to create a good operational environment for BARI vehicles for BARI authority as a whole

Introduction

BARI is one of the largest multi-crop research institutes of the NARS in Bangladesh where more than 3000 employees work including scientists, officers, and staff. They however directly and indirectly play a role in different activities related to agricultural research that promote the mission and vision of BARI as a whole in Bangladesh. We are now accessing and involving our daily works/services digitally in this globe. In Bangladesh, we are also introducing super digital benefits in terms of 4IR technologies such as IoT, AI, big data, nanotechnology, robotics, multi-omics big data, etc. Bangladesh has recently achieved its targets of transparency, accountability, and good governance by providing citizen services (Seba) with the line of Digital Vision 2021. This digital success in service providing to mass people has enabled government offices to speed up the work environment which results in lowering the time, cost, and visit (TCV). The present government has taken actions and has given complete emphasis to making all government/non-government services available to the mass people/stakeholders easily to increase transparency, accountability, no corruption, to establish the smart-governance/good governance in Bangladesh to make our society and economy smart so that will lead to fulfilling the vision of Smart Bangladesh within 2041. In line with the mission of smart Bangladesh 2041, BARI is on its way to uplifting the research activities and delivering as well as disseminating its technologies with low TCV. BARI has developed several digital/online systems to provide the required services to BARI officials and other users/stakeholders with lower TCV. In line with the objective of the APA target in the last financial year 2022-2023, the ASICT division of BARI has developed an online/digital system for vehicle management and requisition that is one of the significant services.

- Objectives: i) to develop the online/digital system of the BARI vehicle requisition
 ii) to manage the vehicles/transport system digitally

Materials and Methods

To develop the software, all required information and data are recorded and stored first. Before developing software, a framework/flowchart/steps of the work are necessary to develop. The steps may include A. information and data collection ii) accurate design iii) implementation iv) verification (trial and error) and v) maintenance (Figure 1).

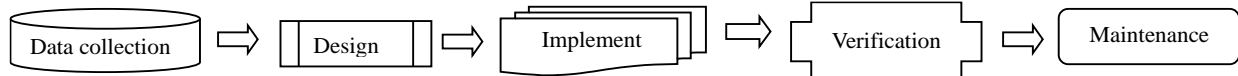


Figure 1. Steps of the software framework to be developed

Different programming languages are required to develop web-based software. We used the MySQL database in the ‘**backend**’ environment of the software and on the other hand, PHP: Hypertext Preprocessor, a widely-used open-source scripting language was used for the ‘**frontend**’ environment. PHP scripts are used because this software is executed on the server. This software has been developed by outsourcing (Techuno). This software however includes the following four key modules:

- Insertion to database module-----user-friendly input screen
- Extracting from database module---attractive output screen
- Report presentation module---list of applicants
- Search facility module---search for applicants

The software has been developed in line with the approved ‘Vehicle Requisition Form’.

Results and Discussion

The development of the software has been completed and launched before 30.06.2023 and it will be titled BARI Vehicle Management System (BVMS). This software is listed under Internal eServices at the BARI website (www.bari.gov.bd). It will be accessed via the link: <https://baripmis.org/transport/login>. It is usable if the user’s device is connected to the internet. BARI employees with his/her BARI ID will be able to ‘**log in**’ and use this online service and submit the vehicle requisition application/form to the relevant authority of BARI. This software is user-friendly, easy to access, improved storage capacity, rapid submission facility.

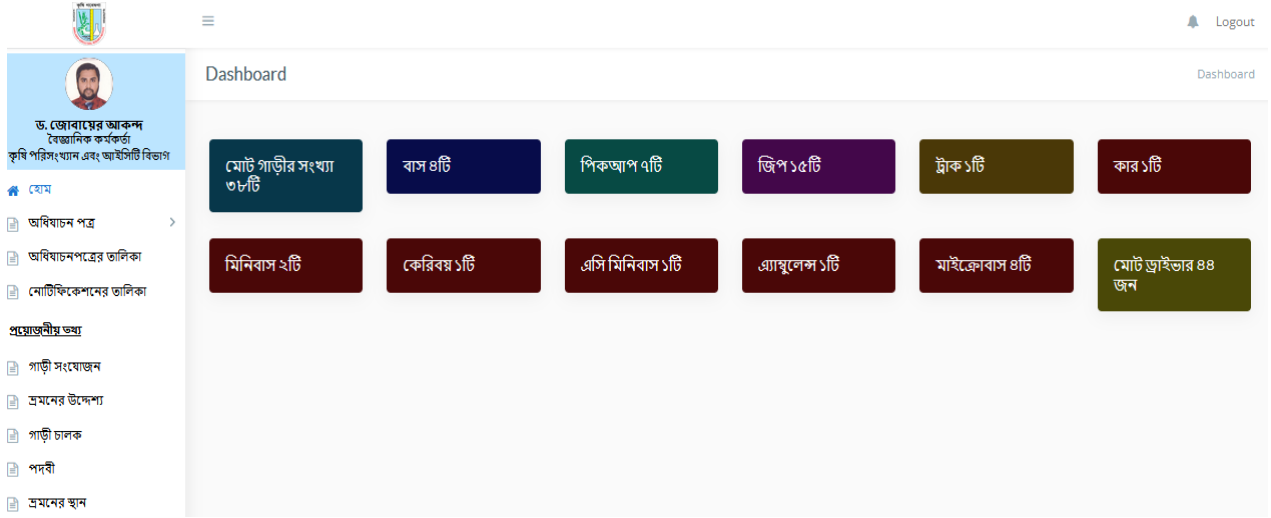
The final version of this software has been established with the line of the BARI transport requisition form and as per the requirement of the BARI transport section. The user should fill-up the following steps before the final and successful submission of the vehicle requisition form/application:

Step-1: Open the link: <https://baripmis.org/transport/login>

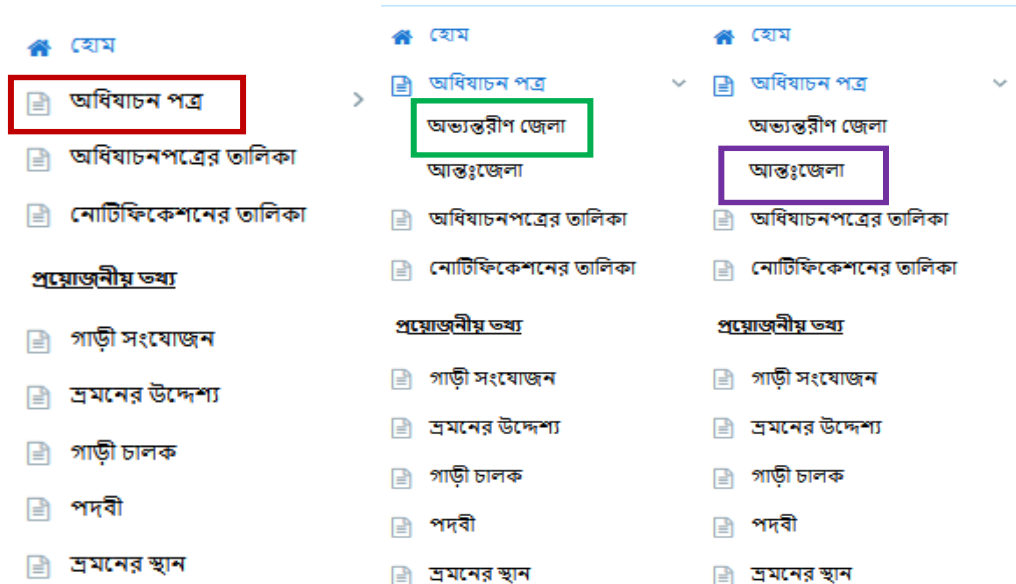
Step-2: Use BARI ID to log in to the software




Step-3: When user will log in, the following dashboard will appear.




Step-4: Click on: ‘অধিযাচন পত্র’ and then select ‘অভ্যন্তরীণ’/‘আন্তঃজেলা’



Step-5: For the ‘অভ্যন্তরীণ’ requisition the user will get the following blank form. In the form, the user’s name, designation, division, and mobile number will be displayed by default.


Application
Logout



ড. জোবায়ের আকন্দ
বৈজ্ঞানিক কর্মকর্তা
কৃষি পরিসংখ্যান এবং আইসিটি বিভাগ

- 🏠 [হোম](#)
- 📄 [অধিযাচন পত্র](#)
- অভ্যন্তরীণ জেলা
- আন্তঃজেলা
- 📄 [অধিযাচনপত্রের তালিকা](#)
- 📄 [নোটিফিকেশনের তালিকা](#)
- পর্যবেক্ষণীয় তথ্য**
- 📄 [গাড়ী সংযোজন](#)
- 📄 [শ্রমনের উদ্দেশ্য](#)
- 📄 [গাড়ী চালক](#)
- 📄 [পদবী](#)
- 📄 [শ্রমনের স্থান](#)

○ সরকারী
অভ্যন্তরীণ জেলা যানবাহন ব্যবহারের অধিযাচনপত্র
○ ব্যক্তিগত

ব্যবহারের তারিখ *

ব্যবহারের সময় *

ব্যবহারের শেষ সময় *

গাড়ী ব্যবহারকারী *

গাড়ী ব্যবহারকারী

গাড়ী ব্যবহারকারী

গাড়ী ব্যবহারকারী

গাড়ী ব্যবহারের উদ্দেশ্য (সংক্ষিপ্ত বিবরণসহ) *

গন্তব্য স্থানের নামঃ *

মোবাইল নং *

ই-মেইল

যাত্রী সংখ্যাঃ *

যানবাহনের প্রকারঃ *

যানবাহনঃ *


পুলের গাড়ী ব্যবহার করার উদ্দেশ্যঃ *


জ্বালানীর উৎসঃ *

সুপারিশকারী *

ডকুমেন্ট

Step-6: The user will fill up the form with the necessary info and attach the required documents if necessary. If one requires a vehicle from the division, select the division and submit the form. Finally, the following approved letter will get the user/employee.


Application



ড. জোব্বারের আকাশ
বেজানিক কর্মকর্তা
কৃষি পরিসংখ্যান এবং অফিসারি বিভাগ

ঘোষ

- অবিদ্যান পত্র
- অবিদ্যানপত্রের তালিকা
- নোটিফিকেশনের তালিকা

প্রয়োজনীয় ক্রম

- গাড়ী সংযোজন
- প্রমোশন উদ্দেশ্য
- গাড়ী চালক
- শপথ
- প্রমোশন স্থান

বাংলাদেশ কৃষি গবেষণা ইনস্টিটিউট
গাড়ীপুর-১৭০১

সরকারী

অত্যন্তরীণ জেলা যানবাহন ব্যবহারের অবিদ্যানপত্র

ব্যক্তিগত

 অফিস কপি
 চালকের কপি

ব্যবহারের তারিখ: ০৯-০৮-২০২৩ ব্যবহারের সময়: ০৭:৩০ AM হতে: ০৫:৩০ PM

গাড়ী ব্যবহারকারীর নাম: ড. জোব্বারের আকাশ, বেজানিক কর্মকর্তা, কৃষি পরিসংখ্যান এবং অফিসারি বিভাগ, +৮৮০১৭৯৫২২৮৫৭১

গাড়ী ব্যবহারের উদ্দেশ্য সংক্ষিপ্ত বিবরণসহ: পরিবারিক অনুরোধে ছেড়গান

পত্রব্য স্থানের নাম: Dhaka

ব্যবহারকারীর যোবাইন নং: +৮৮০১৭৯৫২২৮৫৭১ ই-মেইল: akond23@anoo.com যাত্রী সংখ্যা: ৩

যানবাহনের প্রকার: জিপ যানবাহন সরবরাহকারী: বিভাগকেন্দ্র

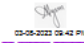
জ্ঞানানীর উৎস: ব্যক্তিগত

অবিদ্যানকারী



০৯-০৮-২০২৩ ১২:০০ AM
ড. জোব্বারের আকাশ
বেজানিক কর্মকর্তা
কৃষি পরিসংখ্যান এবং অফিসারি বিভাগ

অনুমোদনকারী



০৯-০৮-২০২৩ ০৯:৫২ AM
ড. মো. আনবুল হোসেন
মুখ্য বেজানিক কর্মকর্তা (স্বতন্ত্রাঙ্গ)
কৃষি পরিসংখ্যান এবং অফিসারি বিভাগ

নমুনাখতি :


গাড়ী অবিদ্যান সংক্রান্ত বিশেষ শর্তাবলী


১. সরকারী সভাগ/সেবায়নের ক্ষেত্রে সবার আবেদন সূচী ও স্থান অবশ্যই অবিদ্যানে উল্লেখ করতে হবে।
২. সরকারী মালমাল ব্যক্তি/পরিষদে কাজে মহাপরিচালক কর্তৃক অনুমোদিত সময়সীমার নাম উল্লেখপূর্বক কমিটির সভাপতি যানবাহনের অবিদ্যান দিবেন।
৩. সরকারীভাবে অবিদ্যানকৃত গাড়ী কোন প্রকার পরিবারিক/ব্যক্তিগত কাজে ব্যবহার করা যাবে না।
৪. অবিদ্যানে উল্লিখিত স্থান ব্যতিরিক্ত অন্য স্থানে গাড়ী নেয়া যাবে না।
৫. অবিদ্যানে উল্লিখিত ব্যক্তি ব্যতিরিক্ত অন্য কেউ গাড়ী ব্যবহার করতে পারবে না।
৬. অবিদ্যানকৃত গাড়ীতে কোন অবস্থাতেই মালকত্র এবং অন্যথা অর্ধেক রিভিনে বহন করা যাবে না।
৭. অবিদ্যানকৃত গাড়ীতে অর্ধেক মালমাল বহন করলে এর মালিকার অবিদ্যানকারীর উপর কর্তব্য।

গাড়ী অবিদ্যান পত্রের নিয়মাবলী

১. গাড়ী ব্যবহারের অঙ্কন: ২ (দুই) দিন পূর্বে গাড়ী অবিদ্যান পরিচালক (সেবা ও সরবরাহ) এর দপ্তরে পাঠাতে হবে।
২. অফিস/সেবা গাড়ী অবিদ্যানে তেজ/বিভাগীয় প্রধান এবং পরিচালক (গবেষণা) এর মুম্বিনিসহ অবিদ্যান পরিচালক (সেবা ও সরবরাহ) এর দপ্তরে পাঠাতে হবে।
৩. রিভিনসহ জন্ম, কাঠী অবিদ্যানে নেয়া হলে তদন্তকেন্দ্র অফিসারের প্রত্যাহারের পর পরিচালক (সেবা ও সরবরাহ) এর দপ্তরে পাঠাতে হবে।
৪. গাড়ী অবিদ্যানে একই দিনে একটির বেশি গাড়ী সরবরাহ করা যাবে না।
৫. ঢাকা শহর ব্যতিরিক্ত ৪০ কিঃ মিঃ এর অধিক দূরত্বে প্রমোশন জন্য ব্যক্তিগত গাড়ী অবিদ্যান অনুমোদনযোগ্য নয়।

Step-7: If one requires a vehicle from the BARI transport pool. The applicant will select the pool option and by fill-up all the necessary info like the previous steps, the application will be submitted and finally the following approved letter get the user/applicant.





ড. জোবায়ের আকন্দ
বৈজ্ঞানিক কর্মকর্তা
কৃষি পরিসংখ্যান এবং আইসিটি বিভাগ

বাংলাদেশ কৃষি গবেষণা ইনস্টিটিউট
গাজীপুর-১৭০১

সরকারী
 ব্যক্তিগত

অন্তর্জাতিক জেলা যানবাহন ব্যবহারের অধিযাচনপত্র

ব্যক্তিগত

অফিস কপি

চালকের কপি

ব্যবহারের তারিখ: ০৩-০৮-২০২৩ **ব্যবহারের সময়:** ০৭:৩০ AM **হতে:** ০৫:৩০ PM

গাড়ী ব্যবহারকারীর নাম: ড. জোবায়ের আকন্দ, বৈজ্ঞানিক কর্মকর্তা, কৃষি পরিসংখ্যান এবং আইসিটি বিভাগ, +৮৮০১৭৯৫২২৮৫৭১

গাড়ী ব্যবহারের উদ্দেশ্য সংক্ষিপ্ত বিবরণসহ: পারিবারিক অনুষ্ঠানে যোগদান

গন্তব্য স্থানের নাম: মিরপুর, ঢাকা

ব্যবহারকারীর মোবাইল নং: +৮৮০১৭৯৫২২৮৫৭১ **ই-মেইল:** akond25@yahoo.com **যাত্রী সংখ্যা:** ৪

যানবাহনের প্রকার: জিপ **যানবাহন সরবরাহকারী:** পরিবহন পুল

পুলের গাড়ী ব্যবহার করার উদ্দেশ্য: বিভাগ/কেন্দ্রের গাড়ী ফাকা না থাকায় পরিবহন পুলের গাড়ী প্রয়োজন।

জ্বালানীর উৎস: ব্যক্তিগত

অধিযাচনকারী



03-08-2023 12:00 AM
ড. জোবায়ের আকন্দ
বৈজ্ঞানিক কর্মকর্তা
কৃষি পরিসংখ্যান এবং আইসিটি বিভাগ

বিভাগীয় প্রধানের সুপারিশ



03-08-2023 09:48 PM
ড. মো. আব্দুল মোমেনিম মিয়া
মুখ্য বৈজ্ঞানিক কর্মকর্তা (ভারপ্রাপ্ত)
কৃষি পরিসংখ্যান এবং আইসিটি বিভাগ

সুপারিশসহ অগ্রদিত করা হল।

অনুমোদনকারী



03-08-2023 09:49 PM
ড. ফেরদৌসী ইসলাম
পরিচালক (সেবা ও সরবরাহ) চলতি দায়িত্ব
সেবা ও সরবরাহ উইং

অনুমোদিত।

পরিবহন কর্মকর্তা



03-08-2023 09:50 PM
মো. জোবায়ের হাসান
সহকারী কৃষি প্রকৌশলী
এফএমপিই বিভাগ

অনুমোদিত।

গাড়ী অধিযাচন সংক্রান্ত বিশেষ শর্তাবলী

১. সরকারী সভা/সমেলনের ক্ষেত্রে সভার আলোচ্য সূচী ও স্থান অবশ্যই অধিযাচনে উল্লেখ করতে হবে।
২. সরকারী যানবাহন খরিদ/পরিবহন কাজে যথাপরিচালক কর্তৃক অনুমোদিত সদস্যগণের নাম উল্লেখপূর্বক কমিটির সভাপতি যানবাহনের অধিযাচন দিবেন।
৩. সরকারীভাবে অধিযাচনকৃত গাড়ী কোন প্রকার পারিবারিক/ব্যক্তিগত কাজে ব্যবহার করা যাবে না।
৪. অধিযাচনে উল্লিখিত স্থান ব্যতিত অন্য স্থানে গাড়ী নেয়া যাবে না।
৫. অধিযাচনে উল্লিখিত ব্যক্তি ব্যতিরেকে অন্য কেউ গাড়ী ব্যবহার করতে পারবে না।
৬. অধিযাচনকৃত গাড়ীতে কোন অবস্থাতেই যাদকল্প বা ও অন্যান্য অর্থে জ্বিনিস বহন করা যাবে না।
৭. অধিযাচনকৃত গাড়ীতে অর্থে যানবাহন বহন করলে এর মাছভার অধিযাচনকারীর উপর বর্তাবে।

Step-8: If any employee is needed the vehicle for inter-district travel then he/she will have to select the ‘আন্তঃজেলা’ option for vehicle requisition but in this case, permission is a must from Director (SS) and DG (BARI) with the recommendation from the corresponding divisional head/center/sub-center. If is travel is related to research related activities, then a recommendation from Director (Research) is required. If the travel is on project-related activities, then a recommendation from Director (Planning and Evaluation) is required. For general purposes, a recommendation from Director (SS). For example, the following figure shows the vehicle-approved requisition letter/form for research purposes.



ড. জোবায়ের আকন্দ
বৈজ্ঞানিক কর্মকর্তা
কৃষি পরিসংখ্যান এবং আইসিটি বিভাগ

ঘোষ

অধিযাচন পত্র

অধিযাচনপত্রের তালিকা

নোটিফিকেশনের তালিকা

প্রয়োজনীয় তথ্য

গাড়ী সংযোজন

সমন্বয়ের উদ্দেশ্য

গাড়ী চালক

পদবী

সমন্বয়ের স্থান

বাংলাদেশ কৃষি গবেষণা ইনস্টিটিউট
গাজীপুর-১৭০১

সরকারী
 ব্যক্তিগত

আন্তঃজেলা যানবাহন ব্যবহারের অধিযাচনপত্র

অফিস কপি
 চালকের কপি

ডিউটি শুরু তারিখ: ০৩-০৮-২০২৩

যাত্রা শুরুর সময়: ০৬:৩০ AM

ডিউটির শেষ তারিখ: ০৪-০৮-২০২৩

যাত্রার শেষ সময়: ০৮:৩০ PM

গাড়ী ব্যবহারকারীর নাম: ড. জোবায়ের আকন্দ, বৈজ্ঞানিক কর্মকর্তা, কৃষি পরিসংখ্যান এবং আইসিটি বিভাগ, +৮৮০১৭৯৫২২৮৫৭১

গাড়ী ব্যবহারের উদ্দেশ্য সংক্ষিপ্ত বিবরণসহ: গবেষণা সংক্রান্ত

গন্তব্য স্থানের নাম: রাজশাহী।

যানবাহনকারীর যোগাযোগ নং: +৮৮০১৭৯৫২২৮৫৭১ ই-মেইল: akond25@yahoo.com যাত্রী সংখ্যা: ৪

যানবাহনের প্রকার: জিপ যানবাহন সরবরাহকারী: পরিবহন পুল

পুলের গাড়ী ব্যবহার করার উদ্দেশ্য: বিভাগ/কেন্দ্রের গাড়ী নষ্ট থাকায় পরিবহন পুলের গাড়ী প্রয়োজন।

যানবাহন ব্যবহারের ধরণ: গবেষণা সংক্রান্ত জ্বালানীর উৎস: পরিবহন পুল

গাড়ী চালকের নাম: মোঃ শহিদ উল্লাহ, গাড়ীচালক

গাড়ী চালকের মোবাইল নং: ০১৭১২৪৭৮৫৭৩ যানবাহন নং: জিপ, গাজীপুর-ঘ-১১-০০৩৪

আবেদনকারী	পরিচালক/কেন্দ্র/বিভাগীয় প্রধান	পরিচালক (গবেষণা) এর সুপারিশ
 03-08-2023 12:00 AM ড. জোবায়ের আকন্দ বৈজ্ঞানিক কর্মকর্তা কৃষি পরিসংখ্যান এবং আইসিটি বিভাগ	 03-08-2023 10:32 PM ড. মো. আবদুল মোনায়েম মিয়া মুখ্য বৈজ্ঞানিক কর্মকর্তা (জরুরি) কৃষি পরিসংখ্যান এবং আইসিটি বিভাগ approved	 03-08-2023 10:33 PM ড. মো. আব্দুল্লাহ ইউছুফ আখতার পরিচালক (গবেষণা) গবেষণা উইং
পরিচালক (সেবা ও সরবরাহ)	মহাপরিচালক	পরিবহন কর্মকর্তা
 03-08-2023 10:34 PM ড. ফেরদৌসী ইসলাম পরিচালক (সেবা ও সরবরাহ) (স্বাক্ষরিত) সেবা ও সরবরাহ উইং Recommended	 03-08-2023 10:35 PM ড. মোহাম্মদ শরীফ সরকার মহাপরিচালক মহাপরিচালক মহোদয়ের দপ্তর অনুমোদিত।	 03-08-2023 10:35 PM মো. জুবাইর হাসান সহকারী কৃষি প্রকৌশলী এক্সএমপিই বিভাগ অনুমোদিত।

গাড়ী অধিযাচন সংক্রান্ত বিশেষ শর্তাবলী

- সরকারী সভা/সেমিনার/কেন্দ্রে সভার আলোচ্য সূচী ও স্থান অবশ্যই অধিযাচন উল্লেখ করতে হবে।
- সরকারী খালাস/খরিদ/পরিবহন কাজে মহাপরিচালক কর্তৃক অনুমোদিত সদস্যগণের নাম উল্লেখপূর্বক কমিটির সভাপতি যানবাহনের অধিযাচন দিবেন।

Conclusion

The developed BARI Vehicle Management System (BVMS) software is an online-based system. It will be helpful for the BARI authority to manage and approve the vehicles very effectively in terms of low labor, cost, and time. If this system is implemented full scale at BARI, involvement of labor will save highly. Transparency and good management will be established. Employees will not require any paper form and they will be able to submit from any devices and from anywhere and anytime from an internet-connected devices. Hope it will be highly a user-friendly digital system to approve vehicles.

SERVICES OF THE ASICT DIVISION 2022-2023

M. A. MONAYEM MIAH
CHIEF SCIENTIFIC OFFICER, ASICT DIVISION, BARI, GAZIPUR

Introduction

Agricultural Statistics and Information & Communication Technology (ASICT) Division comprises two parts: Agricultural Statistics and ICT. Concerned scientists of both parts conduct different types of research relevant to Agricultural Statistics and ICT. In addition, the scientists of both parts are providing agricultural statistics and ICT-related support services to BARI personnel and other stakeholders of the agriculture system to facilitate agricultural research and development. Besides, this division has been working to implement the *National ICT Policy 2018* and *Digital Bangladesh 2021*. However, the ASICT division is constantly keeping its vital role for BARI as a whole.

Web Information

BARI-developed technologies and related information are being published regularly through its website (www.bari.gov.bd) and mobile apps. In addition to technologies, some important issues like tender circulars, job circulars, journal publications, annual reports, etc. are also hosted as and when necessary. The uploaded information along with their number has been shown in Table 1. The number of upload documents is 1.52% higher in 2022-23 compared to 2021-22.

Table 1. List of information uploaded in the website and mobile apps during 2022-23

Sl. No.	Type of information	Uploaded number	Type of document
1.	Office order	1087	PDF
2.	Notice	549	PDF &Text
3.	BARI-related news published in the newspapers	57	PDF
4.	Reports & publications (i.e. success stories, annual reports, Journals, leaflets, booklets, and other publications)	98	PDF
5.	Agro-technology (Handbook of agro-technology, cropping patterns, mobile apps, etc.)	112	PDF
6.	Query & answer	552	Text & PDF
7.	Scientists/Officers/Staffs/Labors	31	Text
8.	Leave order	549	PDF
9.	Job notice	33	PDF
10.	Transfer & promotion	193	PDF
11.	NOC	271	PDF
12.	Higher studies	93	PDF
13.	Training & meeting	108	PDF
14.	Photo gallery	4993	Image
15.	Videos	0	YouTube video
16.	Tender document	44	PDF
17.	Salary increment	254	PDF
18.	Loan management	693	PDF
19.	Labour database	0	PDF
20.	Labour-related officer order	52	PDF
21.	Retirement order	185	PDF
22.	Seminar/workshop	95	PDF

23	Evaluation Report	36	PDF
24	All form	13	PDF
25	GRS & Appellate officers	08	PDF
26	Monitoring & Evaluation	07	PDF
27	Focal point officer & Alternative officers	08	PDF
22.	Other information (Innovation, citizen charter, APA, NIS, project, Board of Management, policy document, budget, ADP, Centre, Division, etc.)	419	PDF &Text
Total upload		10536	-

Note: The total number of uploads in 2022-23 was 10,378

Web-based Query and Answer

BARI has started online e-agriculture services for its beneficiaries. Any stakeholder can ask agriculture-related questions with the help of online facilities of the BARI website and Mobile apps. On the other hand, it has been providing different feedback to the end users through the BARI website (www.bari.gov.bd) and Mobile apps (baritechnology.org/m). The number of queries/answers addressed by different centers/divisions during 2022-23 is 3.2% higher compared to the year 2021-22 (Table 2).

Table 2. Number of queries & answers addressed by different centers/divisions during 2022-23

Sl. No.	Name of Centre/Division	Number of queries & answers
1.	Vegetable Division, HRC	170
2.	Pomology Division, HRC	146
3.	Floriculture Division, HRC	14
4.	Tuber Crops Research Centre	26
5.	Oil Seed Research Centre	9
6.	Pulses Research Sub-station	2
7.	Regional Spices Research Centre	48
8.	Soil Science Division	8
9.	FMPE Division	5
10.	IWM Division	3
11.	Vertebrate Division	2
12.	Seed Technology Division	4
13.	Pathology Division	10
14.	Biotechnology Division	2
15.	On Farm Research Division	3
16.	Entomology Division	15
17.	Plant Breeding Division	2
18.	ASICT Division	83
Total		552

Note: The total number of queries & answers in 2022-23 was 535.

Citizen Information Service Centre

BARI has started disseminating technological information to the citizen. Any citizen can come and obtain his/her required agricultural technology-related information/services directly from Citizen Information Service Centre and/or from the respective crop Centre/research divisions at BARI. During 2022-2023, a total of **137** citizens of different professions from **13** districts visited the BARI citizen services information Centre and got services in **17** different areas.

Ensuring access to information for citizens through the Right to Information Act

BARI has appointed personnel to ensure citizens access to the information in the easiest way. During 2022-2023, the following information has been provided to the citizens (Table 3).

Table 3. Citizen's access to information in 2022-2023

S N	Name of the authority	No. of application received regarding RTI Act, 2009	No. of queries solved through providing information	No. of decisions for not providing requested information with reasons	No. of appeals against the decision of the officer in charge	No. of settlement appeals	No. of disciplinary action taken by the authorities	The amount received as the value of information as per rule 8 of the RTI Act, 2009	Details of activities taken by the authorities
1	BARI	2	2	-	-	-	-	-	-

Online-based Services to the Citizen

BARI has started providing online-based different services to the citizen since 2016-17 (Table 4). ASICT Division develops at least one online-based service each year. During 2022-23, one service entitled '*Transpiration management system*' has been developed. Any scientist from BARI Headquarters can get vehicle use permission from higher authority by filling up the online transport requisition form through the link (<https://baripmis.org/transport/>). A list of online-based services of BARI has been shown in Table 4.

Table 4. List of online-based services in BARI

Sl.No.	Service	Link	Year
1.	Krishi Projukti Bhandar	http://m.baritechnology.org/	2015-16
2.	Job application	https://bari.taletalk.com.bd	2016-17
3.	District-wise cropping pattern	https://baritechnology.org/crpt	2017-18
4.	Online APA reporting	https://baripmis.org/apa	2018-19
5.	Online loan management	baripmis.org/form-app	2018-19
6.	BARI telephone directory	https://play.google.com/store/apps/details?id=com.baridirectorey.iamsh.baridirectorey	2019-20
7.	Gene bank	http://pgrcbari.org/	2020-21
8.	Matri Kalam supply form	https://baripmis.org/sapling/	2021-22
9.	Transportation management system	https://baripmis.org/transport/	2022-23

Service Simplification to the Citizen

BARI started web-based service simplification using ICT from 2017-2018. The ASICT Division of BARI has to simplify at least one web-based service for its stakeholders each year. During 2022-23, one service titled '*BARI Vehicle Management System*' has been simplified for providing instant and easiest transport facilities to the scientists, officers, and staffs of BARI (Table 5).

Table 5. List of web-based service simplification at BARI

SN	Type	Service	Year
1.	Information centre	Citizen information services	2017-18
2.	Collection of seed and seedling	Limited collection of BARI develop variety seeds and sapling.	2018-19
3.	Collection and preservation of personal information	Collection & preservation of the information of BARI scientists/officers/staff	2019-20
4.	Online-based Query-Answer	Providing quick responses to the citizen's queries regarding the BARI developed variety and technology	2020-21
5.	Determination of pesticide residue in agri-products, foods, soil, and water	Providing the results of pesticide residue in agri-products, foods, soil, and water to the stakeholders in the quickest possible time.	2021-22
6	BARI Vehicle Management System	Providing instant and easiest transport facilities to the scientist, officers, and staffs of BARI.	2022-2023

ICT-based Innovation to the Citizen

BARI started developing ICT-based innovation services for the citizen from 2016-2017. The ASICT Division of BARI has to develop at least one ICT-based innovation for its stakeholders each year. In the year 2022-2023, ASICT Division developed an online “*Matri Kalam Form Online Registration*” for providing information on the availability of fruit saplings and registering the form for purchasing those fruit saplings (Table 6).

Table 6. List of ICT-based innovations to the citizen services at BARI

Sl. No.	Type	Innovation	Year
1.	Apps	Krishi Projukti Vander (Mobile apps)	2016-17
2.	Online service	Faster analysis of soil samples	2017-18
3.	Apps	Mobile apps for mango yield estimation	2018-19
4.	Web Apps	GeoMango: Satellite-based mango orchard mapping	2019-20
5.	Web Apps	Provision for Advisory on Necessary Irrigation	2020-21
6.	Pension System	Providing pension directly to the users bank account	2021-22
7.	Matri Kalam Form Online Registration	Providing information on the availability of fruit saplings and registering the form for purchasing those fruit saplings.	2022-2023

Social Networking (Facebook)

BARI has been publicizing its regular activities among the public through social networking. Any person can ask and interact with BARI authority regarding BARI-mandated crop varieties, improved technologies, and other agricultural information through its official Facebook page (www.facebook.com/BD.GOV.BARI). At present BARI Facebook page is followed by **21,235** Facebook users (it was **9500** in 2021-22). During 2022-23, a total of 500+ posts (in 2021-22, it was 236) and 267 public Quarry/Answer were addressed through the BARI Facebook page.

Social Networking (YouTube)

BARI disseminates its regular activities among the public through its **YouTube** channel. Any person can easily know about BARI technologies through its official YouTube channel titled ‘Bangladesh Agricultural Research Institute’ (<https://www.youtube.com/@BD.GOV.BARI>). At present BARI YouTube channel has

741 subscribers and 25 videos. During 2022-23, 154 subscribers were added to the channel with 6436 views (220.7 hours watch time).

Web-based Mail Services

BARI has its domain of email connectivity under the name “bari.gov.bd”. At present, a total of 757 web mails have been assigned under the BARI domain. It has been decided to assign email addresses to all scientists under the BARI domain gradually.

Networking and Antivirus Maintenance

ASICT Division is giving services on LAN & Antivirus maintenance, especially for the scientists and officers of BARI headquarters. Rendering 24-hour internet services at BARI headquarters. At present more than 600 computers are connected to the network and provided with a corporate version of antivirus. The number of networking and antivirus maintenance done by the ASICT Division during 2022-2023 has been stated in Table 7.

Table 7. Networking and antivirus maintenance during 2022-23

SN	Subject	Number
1.	Trouble shooting for LAN & internet connectivity	868
2.	Trouble shooting for Antivirus	38
3.	New internet connectivity	61
4.	Network connection repair	54
	Total	1021

Wi-Fi Connectivity

The ASICT division has established Wi-Fi connectivity in different places at BARI. This division is providing services on Wi-Fi & maintenance, especially for the scientists and officers of BARI headquarters. At present 932 devices are connected to the Wi-Fi network.

Statistical Analysis Service

ASICT division has been giving services on statistical analysis through computer package software such as R and SPSS. Some important analyses have been given to the scientists of different Centers/Divisions which is shown in the following Table 8.

Table 8. Statistical analysis services rendered to different centers/divisions during 2022-23

Name of Centre/ Division/RARS	Number of Experiment	Required Analysis
Plant Breeding Division	4	CRD, RCBD, Factorial, Split plot, Combined, Correlation & Regression, MVA, Error Bar, Time Series, GGE, AMMI, GIS Map, T-test, Drone Image Processing, etc.
Farm Division	6	
Agricultural Economics	4	
Entomology Division	2	
Seed Technology Division	1	
HRC	6	
PGRC	2	
TCRC	7	
ORC	24	
OFRD	1	
OFRD, Satkhira	5	
OFRD, Khulna	1	
BINA	3	
BSRI	1	
ACIAR Project	12	
Total	79	

E-Governance

(a) E-filing System

Access to Information (a2i) has been established e-filing system in BARI Headquarters (HQ), Crops Center, and RARS. ASICT division assists the e-filing system especially for the Headquarters, Crops Center, and RARS personnel. At present **187** personnel are connected with the e-filing system. The number of letters issued in BARI headquarters through the e-filing system increased 123% from 2021-22 to 2022-23 (Table 9).

Table 9. List of file and letter issued in HQ through e-filing system during 2022-23

SN.	Name of Wing/Centre/Division/Section	No. of file (2022-23)	No. of letter issued		
			2021-22	2022-23	% increase
1.	Support and Services wing	9	51	60	18
2.	Research Wing	15	34	67	97
3.	Training & Communication Wing	56	561	878	57
4.	Planning and Evaluation Wing	21	30	122	307
5.	Horticulture Research Center	83	54	509	843
6.	Oilseed Research Center	14	91	171	88
7.	Tuber Crops Research Center	80	207	350	69
8.	Plant Genetic Research Center	29	67	341	409
9.	Agronomy Division	19	58	509	778
10.	Soil Science Division	7	22	208	845
11.	Entomology Division	72	39	110	182
12.	On-Farm Research Division	191	94	163	73
13.	Agricultural Economics Division	42	54	475	780
14.	Plant Physiology Division	38	18	80	344
15.	Plant Pathology Division	18	1	95	9400
16.	Plant Breeding Division	16	125	434	247
17.	IWM Division	3	79	284	259
18.	ASICT Division	14	120	143	19
19.	Postharvest Technology Division	35	10	104	940
20.	Biotechnology Division	2	48	54	13
21.	Seed Technology Division	28	7	173	2371
22.	Vertebrate Pest Management Division	9	18	96	433
23.	FMPE Division	55	64	257	302
24.	Farm Division	84	21	307	1362
25.	Machinery Repair and Maintenance	27	40	102	155
26.	Regional Spice Research Center	10	14	131	836
27.	Pulse Research Sub-station	2	34	90	165
28.	Administration Section	267	1712	2254	32
29.	Finance and Accounts	343	508	584	15
30.	Transport Section	10	43	111	158
31.	Building and Ground Section	11	0	4	0
32.	Procurement and Store Section	24	0	24	0
33.	Common Service	3	0	110	0
Total BARI		1637	4224	9400	123

(b) E-tendering System

Central Procurement Technical Unit (CPTU) has established an e-tendering system at BARI. ASICT division assists on the e-tendering system, especially for the headquarters through two Procurement Entity

(PE) offices like Building & Ground section and Procurement & Store section. During 2022-23, a total of **167** e-tendering have been implemented through two PE offices (Table 10).

Table 10. List of E-tendering during 2022-23

Sl. No	Name of office	Number of e-tender
1.	Procurement & Store section	68
2.	Building & Ground section	99
	Total	167

(c) Labour Management Software

BARI labour management automation process is going on in full swing. At present, 53 Centre/divisions/sections and **3225** labour information are included in this automation. This automation software is divided into three parts viz, labour information, labour salary, and labour report. Each part can be operated solely and has the option to be integrated as per requirements.

(d) Salary System Software

BARI payroll management system has been developed for the BARI personnel. This system is user-friendly. Any person can use his/her own BARI ID number and prepare his/her salary statement. At present, a total of **542** scientists/officers/staff are using this system.

(e) Management Information System (MIS) Software

MIS software is divided into three separate modules viz. Personnel Management Information System (PMIS), Training Management Information System (TMIS), and Publications Management Information System. Each module can be operated solely and has the option to be integrated as per requirements.

Table 11. Present status of the three MIS software modules

MIS Software Modules	Achievement (data entry)
Personnel Management Information System (PMIS)	100 %
Training Management Information System (TMIS)	100 %
Publications Management Information System	100%

Human Resource Development

ASICT division has engaged in developing human resources through various types of training programs related to ICT. In 2022-23, ASICT Division successfully conducted seven training programs on e-governance and the Right to Information Act 2009, and two workshops on tackling the challenges of 4IR in Agriculture.

Table 12. List of training/workshops conducted at ASICT division during 2022-23

SN	Course Title	No. of training	Duration (day)	No. of participant	Venue
1.	Training on implementation of e-Governance Action Plan	4	01	80	ASICT Lab and Sujanagar Upazila, Pabna
2.	Workshop on Tackling the Challenges of 4IR in Agriculture	2	01	120	Seminar Room, BARI
3.	Training on Right to Information Act 2009	3	01	60	Biometrical Lab, ASICT Division

বার্ষিক কর্মসম্পাদন চুক্তির অগ্রগতি প্রতিবেদন ২০২২-২০২৩

কর্মসম্পাদন ক্ষেত্র	ক্ষেত্রের মান	কার্যক্রম	সূচক	সূচকের মান	লক্ষ্যমাত্রা (অসাধারণ)	একক	১ম ত্রৈমাসিক অগ্রগতি	২য় ত্রৈমাসিক অগ্রগতি	অর্ধ-বার্ষিক অগ্রগতি (১ম+২য়)	৩য় ত্রৈমাসিক অগ্রগতি	৪র্থ ত্রৈমাসিক অগ্রগতি	বার্ষিক চূড়ান্ত অগ্রগতি (১ম+২য়+৩য়+৪র্থ)	দাবীকৃত নম্বর
১	২	৩	৪	৫	৬	৭	৮	৯	১০	১১	১২	১৩	১৪
[১.১] বিভিন্ন ফসলের উচ্চ ফলনশীল জাত ও প্রযুক্তি উদ্ভাবন	২৫	[১.২] উদ্ভাবিত জাত এবং প্রযুক্তির সম্প্রসারণ	[১.২.৮] বার্ষিক গবেষণা রিপোর্ট প্রকাশিত	১০	১	সংখ্যা	০	১	১	০	০	১	১০
			[১.২.৯] লিফলেট, নিউজ লেটার, বুকলেট, জার্নাল ইত্যাদি প্রকাশিত	৫	১	সংখ্যা	০	১	১	০	০	১	৫
			[১.২.১১] আয়োজিত মেলায় অংশগ্রহণ	১০	১	সংখ্যা	০	১	১	০	০	১	১০
সর্বমোট প্রাপ্ত নম্বর = ২৫													
[১] ই-গভর্ন্যান্স ও উদ্ভাবন সংক্রান্ত কার্যক্রমের বাস্তবায়ন ও জোরদারকরণ	৩০	BARI ১.১ সেবা সহজিকরণ/ডিজিটাইজেশনের মাধ্যমে উদ্ভাবনী ধারণা বাস্তবায়ন	BARI ১.১.১ সেবা সহজিকরণ/ ডিজিটাইজেশনের মাধ্যমে ন্যূনতম একটি উদ্ভাবনী ধারণা বাস্তবায়িত	১০	০৪/০৫/২০২৩	তারিখ	০	০	০	০	০২/০৫/২৩	০২/০৫/২৩	১০
		BARI ১.২ ইতঃপূর্বে বাস্তবায়িত উদ্ভাবনী ধারণা, সহজিকৃত ও ডিজিটাইজকৃত সেবার ডাটাবেজ প্রস্তুতকরা ও সেবাসমূহ চালুরাখা	BARI ১.২.১ ইতঃপূর্বে বাস্তবায়িত উদ্ভাবনী ধারণা, সহজিকৃত ও ডিজিটাইজকৃত সেবার ডাটাবেজ প্রস্তুতকৃত	২	১৩/১০/২০২২	তারিখ	০	১২/১০/২২	১২/১০/২২	০	০	১২/১০/২২	২
			BARI ১.২.২ ইতঃপূর্বে বাস্তবায়িত উদ্ভাবনী ধারণা, সহজিকৃত ও ডিজিটাইজকৃত সেবা সমূহ চালুকৃত	৭	০৪/০৫/২০২৩	%	০	০	০	০২/০২/২৩	০	০২/০২/২৩	৭
		BARI ১.৩ ই-নথি ব্যবহার বৃদ্ধি	BARI ১.৩.১ ই-ফাইলো নোট নিষ্পত্তিকৃত	৪	৮৫%	তারিখ	৮৪.২৮% (২১.০৭%)	৮৪.৭২% (২১.১৮%)	৮৫%	৮৬.৮১% (২১.৭০%)	৯৮.২৪% (২৪.৫৬%)	৮৮.৫১%	৪
		BARI ১.৪ ৪র্থ শিল্প বিপ্লবের চ্যালেঞ্জ মোকাবেলায় আইন/পলিসি/কর্মপরিকল্পনা প্রণয়ন এবং বিষয়ভিত্তিক কর্মশালা আয়োজন	BARI ১.৪.১ ৪র্থ শিল্প বিপ্লবের চ্যালেঞ্জ মোকাবেলায় আইন/পলিসি/কর্মপরিকল্পনা প্রণীত	৪	৩১/১০/২০২২	তারিখ	০	২৭/১০/২২	২৭/১০/২২	০	০	২৭/১০/২২	৪
			BARI ১.৪.২ ৪র্থ শিল্প বিপ্লবের চ্যালেঞ্জ মোকাবেলায় বিষয় ভিত্তিক কর্মশালা আয়োজিত	৩	২	সংখ্যা	০	০	০	০	২	২	৩

কর্মসম্পাদন ক্ষেত্র	ক্ষেত্রের মান	কার্যক্রম	সূচক	সূচকের মান	লক্ষ্যমাত্রা (অসাধারণ)	একক	১ম ত্রৈমাসিক অগ্রগতি	২য় ত্রৈমাসিক অগ্রগতি	অর্ধবার্ষিক অগ্রগতি (১ম+২য়)	৩য় ত্রৈমাসিক অগ্রগতি	৪র্থ ত্রৈমাসিক অগ্রগতি	বার্ষিক চূড়ান্তঅগ্রগ তি (১ম+২য়+ ৩য়+৪র্থ)	দাবীকৃত নম্বর	
১	২	৩	৪	৫	৬	৭	৮	৯	১০	১১	১২	১৩	১৪	
[২] প্রাতিষ্ঠানিক সক্ষমতাবৃদ্ধি	২০	BARI_২.১ তথ্য বাতায়ন হালনাগাদকরণ	BARI_২.১.১ তথ্য বাতায়ন হালনাগাদকৃত (ত্রৈমাসিকভিত্তিতে)	৬	৪	সংখ্যা	১	১	২	১	১	৪	৬	
		BARI_২.২ ই- গভর্ন্যান্স ও উদ্ভাবন কর্ম পরিকল্পনা বাস্তবায়ন	BARI_২.২.১ কর্ম পরিকল্পনা বাস্তবায়ন সংক্রান্ত প্রশিক্ষণ আয়োজিত	৩	৪	সংখ্যা	০	০	০	০	০	৪	৪	৩
			BARI_২.২.২ ই-গভর্ন্যান্স কর্মপরি কল্পনা বাস্তবায়নের জন্য বরাদ্দকৃত অর্থব্যয়িত	৩	৮০%	%	০	০	০	০	৫০%	৫০%	১০০%	৩
			BARI_২.২.৩ কর্ম পরিকল্পনার অর্ধবার্ষিক স্বমূল্যায়ন প্রতিবেদন মন্ত্রিপরিষদ বিভাগে প্রেরিত	৩	১৫/০১/২৩	তারিখ	০	০	০	০	১২/০১/২৩	০	১২/০১/২৩	৩
			BARI_২.২.৪ আওতাধীন দপ্তর/সংস্থার অর্ধবার্ষিক স্বমূল্যায়ন প্রতিবেদন পর্যালোচনা পূর্বক চূড়ান্ত প্রতিবেদন মন্ত্রিপরিষদ বিভাগে প্রেরিত	২	৩১/০১/২৩	তারিখ	০	০	০	০	২৪/০১/২৩	০	২৪/০১/২৩	২
			BARI_২.২.৫ দেশে/বিদেশে বাস্তবায়িত ন্যূনতম একটি উদ্যোগ পরিদর্শনকৃত	৩	৩১/০৫/২৩	তারিখ	০	০	০	০	০৬/০৩/২৩	০	০৬/০৩/২৩	৩
সর্বমোট প্রাপ্ত নম্বর = ৫০														

কর্মসম্পাদন ক্ষেত্র	ক্ষেত্রের মান	কার্যক্রম	কর্ম সম্পাদন সূচক	সূচকের মান	লক্ষ্যমাত্রা (অসাধারণ)	একক	১ম ত্রৈমাসিক অগ্রগতি	২য় ত্রৈমাসিক অগ্রগতি	অর্ধ-বার্ষিক অগ্রগতি (১ম+২য়)	৩য় ত্রৈমাসিক অগ্রগতি	৪র্থ ত্রৈমাসিক অগ্রগতি	বার্ষিক চূড়ান্ত অগ্রগতি ১ম+২য়+৩য়+৪র্থ	দাবীকৃত নম্বর	
০১	০২	০৩	০৪	০৫	০৬	০৭	০৮	০৯	১০	১১	১২	১৩	১৪	
প্রাত্যহিক	১০	[১.১] তথ্য অধিকার আইন অনুযায়ী নির্ধারিত সময়ের মধ্যে তথ্য প্রাপ্তির আবেদন নিষ্পত্তি	[১.১.১] নির্ধারিত সময়ের মধ্যে তথ্য প্রাপ্তির আবেদন নিষ্পত্তি	০৬	১০০%	%	১০০%	১০০%	১০০%	১০০%	১০০%	১০০%	০৬	
সক্ষমতা বৃদ্ধি	১৫	[১.২] স্বতঃপ্রণোদিত ভাবে প্রকাশযোগ্য সকল তথ্য হালনাগাদ করে ওয়েবসাইটে প্রকাশ	[১.২.১] হালনাগাদকৃত তথ্য ওয়েবসাইটে প্রকাশিত	০৪	৩১/১২/২২ ও ৩০/০৬/২৩	তারিখ	০	২৭/১২/২২	২৭/১২/২২	০	২৬/০৬/২৩	২৭/১২/২২ ও ২৬/০৬/২৩	০৪	
		[১.৩] বার্ষিক প্রতিবেদন প্রকাশ	[১.৩.১] নির্ধারিত সময়ে বার্ষিক প্রতিবেদন প্রকাশিত	০৩	১৫/১০/২২	তারিখ	০	১৩/১০/২২	১৩/১০/২২	০	০	১৩/১০/২২	০৩	
		[১.৪] তথ্য অধিকার আইন, ২০০৯ এর ৫ ধারা অনুসারে যাবতীয় তথ্যের ক্যাটালগ ও ইনডেক্স তৈরি/হালনাগাদকরণ	[১.৪.১] তথ্যের ক্যাটালগ ও ইনডেক্স তৈরিকৃত/ হালনাগাদকৃত	০৩	৩১/১২/২২	তারিখ	০	২০/১২/২২	২০/১২/২২	০	০	২০/১২/২২	০৩	
		[১.৫] তথ্য অধিকার আইন ও এর বিধিবিধান সম্পর্কে জন সচেতনতা বৃদ্ধিকরণ	[১.৫.১] প্রচার কার্যক্রম সম্পন্ন	০৪	৩	সংখ্যা	০	১	১	১	১	১	৩	০৪
		[১.৬] তথ্য অধিকার আইন, ২০০৯ ও এর বিধিমালা, প্রবিধানমালা, স্বতঃপ্রণোদিত তথ্য প্রকাশ নির্দেশিকাসহ সংশ্লিষ্ট বিষয়ে কর্মকর্তা/কর্মচারীদের প্রশিক্ষণ আয়োজন	[১.৬.১] প্রশিক্ষণ আয়োজিত	০৩	৩	সংখ্যা	০	০	০	১	২	৩	৩	০৩
		[১.৭] তথ্য অধিকার সংক্রান্ত প্রত্যেকটি ত্রৈমাসিক অগ্রগতি প্রতিবেদন নির্ধারিত সময়ে ওয়েবসাইটে তথ্য অধিকার সেবা বক্সপ্রকাশ	[১.৭.১] ত্রৈমাসিক অগ্রগতি প্রতিবেদন নির্ধারিত সময়ে ওয়েবসাইটে তথ্য অধিকার সেবা বক্সপ্রকাশিত	০২	৪	সংখ্যা	১	১	১	১	১	১	৪	০২

সর্বমোট প্রাপ্ত নম্বর = ২৫

APPENDIX I**SCIENTISTS WORKING AT ASICT DIVISION, 2022-2023**

Sl. No.	Name	Designation	Discipline	Remarks
1.	Dr. M. A. Monayem Miah	CSO	Agricultural Economics	In-charge
2.	Kowshik Kumar Saha	SSO	Agril. Engineering	Deputation
3.	Moh. Mukhlesur Rahman	SO	Statistics	--
4.	Nur Mohammad	SO	Statistics	--
5.	Dr. Zobaer Akond	SO	Statistics	--
6.	Kazi Saidur Rahman	SO	Statistics	--
7.	Istiaq Ahmed	SO	Statistics	--
8.	Mohammad Rasel	SO	Statistics	--
9.	Jamila Khatun Prioty	SO	Statistics	--
10.	Jahangir Hossain,	Asst. Progr	Computer Science	--

APPENDIX II**SUPPORTING STAFF WORKING AT ASICT DIVISION, 2022-2023**

Sl. No.	Name	Designation	Remarks
1.	Nazma Islam	Computer Operator	--
2.	Md. Shajahan Morol	Computer Operator	Cashier
3.	Jebun Nahar	Computer Operator	--
4.	Mohammad Abdur Rahim	Office Assistant cum Computer Typist	Storekeeper
5.	Kawser Mahmud	Office Assistant cum Computer Typist	--
6.	Md. Reduanul Islam	Lab Technician	--
7.	Md. Sayed Khan	Statistical Assistant	--
8.	Monir Hossen	Chainman	PA to CSO
9.	Md. Delwar Hossain	Office Assistant	--

APPENDIX III**LABOUR WORKING AT ASICT DIVISION, 2022-2023**

Sl. No.	Name	Designation	Remarks
1.	Md. Topan Miah	Data Entry Operator	Regular
2.	Shamima Akhter	Photocopy Operator	Irregular
3.	Md. Parvez Mosharof	Office Assistant	Irregular
4.	Md. Ismail Hossain	Cash Assistant	Irregular
5.	Md. Azizur Rahman	Internet Technician	Irregular
6.	Suvol Vodro	Driver	Master roll
7.	Sohela Akhter Happy	Data Entry Operator	Master roll
8.	Rekha Akhter	Office Assistant	Master roll
10.	Md. Al-Amin	Electrician	Master roll

APPENDIX IV

LIST OF PUBLICATIONS 2022-2023

Scientific Journal

- Ahmed, I., Ishtiaque, S., Zahan, T., Rashed, Md. S. U., Sen, R., Hossain, Md. F., Brahma, S., Ahmed, I. M., Hossain, M. A., Ali, M. A., Jahan, A. H. S., Imtiaz, S., Naher, Q., Mujahidi, T. A., Biswas, S. and Haque, M. I. (2022). Climate change vulnerability in Bangladesh based on trend analysis of some extreme temperature indices. *Theoretical and Applied Climatology*, 149: 831-842. <https://doi.org/10.1007/S00704-022-04079-4>
- Akond, Z., Rahman, H., Ahsan, M.A., Mosharof M.P., Alam, M. and Mollah M.N.H. (2022). Comprehensive *In Silico* analysis of RNA silencing-related genes and their regulatory elements in wheat (*Triticum aestivum* L.). *BioMed Research International*, <https://ops.hindawi.com/view.manscript/bmri/4955209>
- Islam, M. S., Bell, R.W., Miah, M.A.M. and Alam, M. J. (2022). Farmers' fertilizer use gaps relative to government recommendations in the saline coastal zone of the Ganges Delta. *Agronomy for Sustainable Development*, 42:59. <https://doi.org/10.1007/s13593-022-00797-1> (IF=7.81)
- Islam, M.S., Bell, R.W., Miah, M.A.M. and Alam, M. J. (2022). Unbalanced fertilizer use in the Eastern Gangetic Plain: The influence of Government recommendations, fertilizer type, farm size and cropping patterns. *PLoS ONE*, 17(7): 1-24. DOI: [10.1371/journal.pone.0272146](https://doi.org/10.1371/journal.pone.0272146) (IF= 3.75)
- Islam, M.S., Alam, M. J., Bell, R.W., Boyd, D., Hutchison, J., and Miah, M.A.M. (2023). Fertilizer use gaps of women-headed households under diverse rice-based cropping patterns: Survey-based evidence from the Eastern Gangetic Plain, South Asia. *Heliyon* 9 e14139. <https://doi.org/10.1016/j.heliyon.2023.e14139> (IF=3.77)
- Miah, M.A.M., Rashid, M.A. and Rahman, M.S. (2022). Factors of adoption and farmers' perceptions on improved lentil variety cultivation in Bangladesh: a farm level study. *Farm Economy*, Vol-XVII, 75-89
- Miah, M.A.M.; Bell, R.W.; Haque, M.E.; Rahman, M.W.; Sarkar, M.A.R. and Rashid, M. A. (2023). Conservation agriculture practices improve crop productivity and farm profitability when adopted by Bangladeshi smallholders in the Eastern Gangetic Plain. *Outlook on Agriculture*, 1–11 DOI: [10.1177/00307270221150830](https://doi.org/10.1177/00307270221150830). (IF=3.309)
- Miah, M. S.; M. T. Uddin; H. Kabir; M.A.M. Miah and M.A. Salam (2023). Productivity gap and comparative advantage of BADC Boro rice seed production in Bangladesh. *SAARC J. Agric.*, 21(1): 115-126. DOI: <https://doi.org/10.3329/sja.v21i1.65036>

Rapporteur's Report

Internal Research Review and Program Planning Workshop 2023
Agricultural Statistics and Information & Communication Technology Division

Date: 09-08-2023

Comments and Suggestions on Research Report 2022-23

SN	Comments and Suggestions	Action Taken
1.	Assessment of cropping patterns for sustainable intensification in drought prone ecosystem using remote sensing and geospatial modeling	
	➤ How to collect data by using drones should be clearly stated in the text.	✓ It has done accordingly.
	➤ Not necessary to show more photos in the text. These photos could be added to the appendix.	✓ Unnecessary photographs are not added in the text.
2.	Forecasting onion yield by using satellite-based remote sensing technique in Bangladesh	
	➤ The sowing dates can be considered in intervals, and for plots that are considered should be as close as possible.	✓ Already mentioned in the methodology section
	➤ The effect of different sowing dates for plots should be assessed.	✓ A different study will be conducted in future.
	➤ The NDVI should be taken considering the atmospheric conditions and soil moisture.	✓ NDVI is not related to soil moisture.
3.	Bioinformatic analysis of DCL, AGO, and RNA-dependent RNA polymerase (RDR) genes and their associated regulatory elements in brassica species (<i>Brassica Rapa L.</i>)	
	➤ Specific objectives should be stated in the text.	✓ It has done accordingly.
	➤ Related crop scientists should be included in this study.	✓ One oilseed scientist is one of the co-authors of this report.
	➤ Such type of research should be conducted with the collaboration of the Biotechnology division of BARI.	✓ Collaboration will be done in future.
	➤ TCRC scientists can be involved with related works, they will provide required data.	✓ Collaboration will be done in future.
4.	Change and instability analysis in area and production of major pulses in Bangladesh	
	➤ Title should be changed to "Growth and instability analysis" instead of "Change and instability analysis".	✓ Title has been changed accordingly.
	➤ The growth model along with test procedure should be explained clearly in the report.	✓ It has already explained in the methodological section.
	➤ The reason behind declining the area of pulses cultivation in Bangladesh should be stated in the report.	✓ The reasons have already been discussed in the text.
	➤ Make some comparative tables for the growth and instability of area, production and yield of pulses in the text.	✓ It has done accordingly.
5.	Potato yield forecasting using satellite images and crop simulation model under changing climate	
	➤ Such type of research may be conducted with help of TCRC data in future.	✓ Collaboration will be done in future.
	➤ As the prediction of potato yield in 60 days is less than usual, the prediction time of yield should be clarified for which we want to predict after the sowing date.	✓ The prediction time of potato yield is clarified as 60-90 days in the text.
	➤ State the name of variety of potato for which predicted yield (24.4 t/ha) was calculated.	✓ BARI Alu-7 which has already stated in the text
	➤ Sources of data should be marked in the text.	✓ Already marked in the text
	➤ Try to calculate the total area of potato cultivation by using the image processing of satellite data.	✓ Already taken such type of study for the coming year

6.	Yield prediction of mustard crop by using satellite based remote sensing technique in Bangladesh	
	➤ Correlation between NDVI and the yields of different dates should be calculated.	✓ Will be calculated after getting 2 nd year data.
	➤ The future satellite data should be observed and explained properly during forecasting the yield.	✓ Will be done in future.
7.	Development of online-based BARI vehicle management and requisition system	
	➤ The developed online system of vehicle management can be launched for pilot observation	✓ It will be launched for pilot observation.

Overall Comments and Suggestions from the Expert Panel

SN	Comments and Suggestions	Action Taken
1.	➤ We are not getting more than 60-70% accuracy in most of the models, because the parameters (temperature, rainfall, airflow, sunshine, etc.) used in the models vary from region to region. Hence, we should develop our models so that we can use them for conducting our own researches.	✓ We are able to develop our own models in the near future.
2.	➤ An informative chatbot can be developed to deliver all types of services of the ASICT division.	✓ It will be done after recruiting ICT related personnel.
3.	➤ Different divisions and centers may collaborate with ASICT for conducting their ICT-based researches.	✓ Collaboration will be done in future.
4.	➤ ASICT division should work for meta agriculture, developing sensors, IoT, etc.	✓ This is not the mandatory work of ASICT division.
5.	➤ ICT experts should be engaged in developing sensors and IoT-based researches at BARI.	✓ Recruitment of ICT related manpower is in process.
6.	➤ Service related issues of the ASICT division should also be presented in the annual research review program.	✓ Service related issues will be presented in future.
7.	➤ ICT related personnel should be recruited as soon as possible for the ASICT division.	✓ Recruitment of ICT related manpower is in process.

Comments and Suggestions on Research Program 2023-24

SN	Comments and Suggestions	Action Taken
1.	Detection of differences in vegetation and chlorophyll content in agricultural field using unmanned aerial vehicles	
	➤ Estimate the Chlorophyll content using a Drone instead of a satellite for a specific crop.	✓ Will be done accordingly.
	➤ Study with the application of fertilizer for which the change in the crop vegetation is more visible.	✓ Such type of research may be conducted by Soil Science Division
	➤ Related crop scientist must be included in this program.	✓ Already included.
2.	Marginal analysis of different herbicides use for controlling weeds in the onion field	
	➤ Related crop scientist must be included in this program.	✓ Already included.
	➤ Dominance analysis should be done after BCR analysis.	✓ Will be done accordingly.
3.	Soil sampling and drone mapping combine to deliver better fertilizer recommendation for crop production	
	➤ Drone imageries should be used instead of Landsat Satellite.	✓ Drone imageries will be used
	➤ Program title may be changed/modified.	✓ Action taken accordingly
	➤ "What will be the depth of the soil sample" should be specified in the study.	✓ Will be specified after implementation of the study.
	➤ Specific crop name should be mentioned in the title.	✓ Specific crop name will be mentioned after conducting 1 st year experiment.
	➤ Related crop scientist must be included in this program.	✓ Will be done accordingly.
4.	Prediction of monthly heatwave and its impact on the yield of summer tomato in Bangladesh	
	➤ Heatwave forecast should be made for one specific crop.	✓ Heatwave forecast will be done for a specific crop
	➤ If possible, the program should be linked with the most heat-vulnerable crop.	-do-
	➤ Forecast model should be developed for one year and specific months, specifically from April to June.	✓ Will be done accordingly
	➤ Related crop scientist may be involved with this program to get details of the crop.	✓ One related scientist will be involved in this program
5.	Predictive modeling of climate change impacts on potato production: A statistical investigation	
	➤ Only potato growing districts should be specified for this program.	✓ Will be done accordingly
6.	GGE bi-plot analysis for yield performance and stability assessment of BARI released eggplant varieties	
	➤ Specific eggplant variety (bt-brinjal) should be mentioned in the title.	✓ Title has been changed accordingly.



Bangladesh Agricultural Research Institute

Agricultural Statistics and ICT Division

Gazipur 1701

Phone: +88-02-49270129

Email: cs.o.asict@bari.gov.bd

Website: www.bari.gov.bd